AD NUMBER

AD882806

NEW LIMITATION CHANGE

TO

Approved for public release, distribution unlimited

FROM

Distribution authorized to U.S. Gov't. agencies and their contractors; Administrative/Operational Use; FEB 1971. Other requests shall be referred to Air force Materials Lab., Wright-Patterson AFB, OH 45433.

AUTHORITY

AFML ltr, 9 Apr 1973

DEVELOPMENT OF AN IMPROVED ULTRA-HIGH STRENGTH STEEL FOR FORGED AIRCRAFT COMPONENTS

R.T. Ault
G.M. Wald
R.B. Bartolo

Vasco Vascojet

RESEARCH CENTER

TECHNICAL REPORT AFML-TR-71-27
FEBRUARY 1971

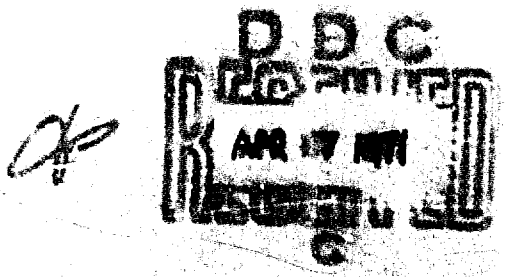

AIR FORCE MATERIALS LABORATORY
AIR FORCE SYSTEMS COMMAND
WRIGHT-PATTERSON AIR FORCE BASE, OHIO

NOTICE

When Government drawings, specifications, or other data are used for any purpose other than in connection with a definitely related Government procurement operation, the United States Government thereby incurs no responsibility nor any obligation whatsoever; and the fact that the Government may have formulated, furnished, or in any way supplied the said drawings, specifications, or other data, is not to be regarded by implication or otherwise as in any manner licensing the holder or any other person or corporation, or conveying any rights or permission to manufacture, use, or sell any patented invention that may in any way be related thereto.

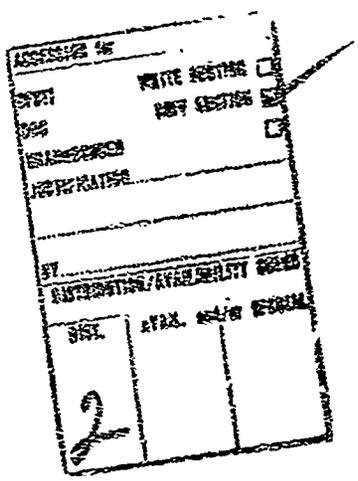

AFML-TR-71-27

Development of An Improved Ultra-High Strength Steel for Forged Aircraft Components

R. T. Ault
G. M. Waid
R. B. Bertolo

Republic Steel Corporation
Research Center

FOREWARD

This final report was prepared by the Alloy Development Section, Metallurgical Division, Research Center, Republic Steel Corporation, Cleveland, Ohio, under USAF Contract F33615-69-C-1638. The contract was initiated under Project No. 7351, Metallic Materials, and Task 735105, High Strength Metallic Materials.

The work was administered under the direction of the Air Force Materials Laboratory, Metals and Ceramic Division, LLP, with H. J. Middendorp as project engineer.

This report covers work accomplished independently by Republic Steel Corporation, Research Center, from July 20, 1966 through April 30, 1969 and work accomplished under the subject contract from May 1, 1969 to December 31, 1970. The principal participants in the research were R. T. Ault, G. M. Waid, and R. B. Bertolo.

The authors gratefully acknowledge the major assistance of Messrs. R. T. Smith, U. B. Gammon, R. R. Keck, R. E. Thompson, G. Miedl, and M. Hill in the conduct of this program. Thanks are also due to Mr. R. J. Kearney for the statistical design and analysis of the experimental alloys; Dr. P. C. Becker who performed the electron microscopy studies; and to Dr. S. J. Matas and Mr. S. W. Poole for their consultations, encouragement, and support.

The manuscript was released by the authors in January 1971 for publication as an AFML technical report.

This technical report has been reviewed and is approved.

I. Perlmutter
Chief, Metals Branch
Metals and Ceramics Division
Air Force Materials Laboratory

ABSTRACT

The objective of this program was to develop an ultra-high strength steel in the 300 to 320 ksi ultimate tensile strength range, with improved fatigue strength, fracture toughness, and stress corrosion resistance for greater reliability in forged landing gear components. Alloy development studies were conducted on two bainitic alloy systems and two martensitic alloy systems in order to develop the best combination of mechanical properties at tensile strength levels in excess of 300,000 psi. Of the four alloy systems investigated, steels from the low alloy medium carbon Ni-Cr-Mo-Si-V martensitic system developed the best combination of fracture toughness, fatigue strength and stress corrosion cracking resistance. A martensitic alloy was developed with a nominal composition of

C	Mn	P	S	Si	Ni	Cr	Mo	V
0.40	0.35	<.010	<.010	2.25	1.8	0.80	0.25	0.22

which achieves the following average longitudinal properties based on laboratory sized heats: Y.S. = 268 ksi, U.T.S. = 311 ksi, El. = 12%, R.A. = 44%, CVN = 20 ft-lbs, K_{IC} = 60 ksi $\sqrt{in.}$, K_{ISCC} = 17 ksi $\sqrt{in.}$, unnotch fatigue strength at 10^7 cycles of 170 ksi, and a notch (K_t = 3.0) fatigue strength of 80 ksi.

The stress corrosion studies demonstrated that variations in phosphorous, sulfur, silicon, chromium, and molybdenum, significantly influenced plane strain fracture toughness properties, but had essentially no effect on the K_{ISCC} stress corrosion cracking resistance parameter. The low alloy Ni-Cr-Mo-Si-V martensitic steels had greater SCC resistance than the best bainitic steel.

Processing studies conducted on two bainitic alloys and one martensitic alloy revealed that the vacuum arc remelted (VAR) steels had the highest levels of fracture toughness, and the electroslag remelted (ESR) steels had the lowest levels of fracture toughness. Investigating the influence of melting practice on fatigue properties demonstrated that for the two bainitic steels the ESR material had the highest fatigue strengths, and the VIM material the lowest fatigue strengths. For the martensitic steel the VAR material had the highest fatigue strengths followed by the ESR material and the VIM material. The experimental steels demonstrated tension-tension unnotch fatigue strengths, at 10^7 cycles, in the range of 170,000 to 210,000 psi. Notch (K_t = 3.0) fatigue strengths at 10^7 cycles of 80,000 psi were achieved. Thermal-mechanical working treatments demonstrated that the strength and toughness properties of ultra-high strength low alloy martensitic and bainitic steels are influenced only slightly by refinement of the prior austenite grain size.

Comparison of the mechanical properties of the newly developed low alloy martensitic steels with similar properties of currently used commercial ultra-high strength steels revealed that the strength-toughness and the strength-SCC resistance characteristics of the new low alloy martensitic steels are superior to those of the commercially produced steels. Both the unnotch and notch fatigue strengths of the new Ni-Cr-Mo-Si-V martensitic steels were superior to the similarly measured fatigue strengths of the commercial steels.

(iv Blank)

TABLE OF CONTENTS

LIST OF TABLES

LIST OF TABLES (cont)

LIST OF ILLUSTRATIONS

LIST OF ILLUSTRATIONS (cont)

LIST OF ILLUSTRATIONS (cont)

LIST OF ILLUSTRATIONS (cont)

LIST OF ILLUSTRATIONS (cont)

LIST OF ILLUSTRATIONS (cont)

I. INTRODUCTION

The increasingly stringent requirements, in terms of load, range, maneuverability, and performance of present and future military and commercial aircraft, places increasing demands upon the strength and reliability of the steels and other high strength materials used in these aircraft. The great need to save weight in these larger and higher performance aircraft, justifiably causes designers to look for higher and higher strength steels. The increased strength, however, must not be accompanied by decreases in fracture toughness, fatigue strength, and stress corrosion cracking resistance in order to ensure reliability in the performance of the critical load bearing components. For it is well known that very small flaws, excessive inclusion contents, or hostile environments can cause catastrophic failures at stresses well below the design level, if the material lacks sufficient fatigue strength, toughness, or stress corrosion resistance.

The objective of this program was to develop an ultra-high strength steel in the 300 to 320 ksi ultimate tensile strength range, with improved fatigue strength, fracture toughness, and stress corrosion resistance for greater reliability in forged landing gear components and related structural airframe applications. The guaranteed minimum ultimate tensile strengths of the two currently widely used low alloy steels for landing gears are 260 ksi for 4340 steel and 270 ksi for 300 M steel. An increase in the guaranteed minimum ultimate tensile strength to 300 ksi would, therefore, represent a 10 to 15% increase in ultimate tensile strength level. The approach to achieving these goals was to conduct concurrent alloy development and processing studies. The alloy development efforts included three separate approaches as follows: A. Low Alloy Bainites, B. Medium Alloy Bainites, and C. Low Alloy Martensites. The processing studies included the influence of impurities and melting practice on mechanical properties as evidenced by the effects of vacuum induction melting, electroslag remelting, and vacuum arc remelting; and the effects of thermal-mechanical working on an annealed ferrite-carbide matrix and its influence on heat treated properties of low alloy steels.

II. MATERIALS AND PROCEDURES

A. Materials

The great majority of the experimental alloys were melted in a 50 lb vacuum induction melting (VIM) furnace. The alloys were melted either as single 50 lb ingots or three-way split heats resulting in three 16 lb ingots. Fifteen heats (Heats R1 through 15) were melted in a 300 lb VIM furnace at Battelle Memorial Institute, Columbus, Ohio, as two-way split heats resulting in 50 lb ingots. Some of the earlier bainitic steels were melted in an air induction furnace and poured into 70 lb ingot molds. A prefix of the letters A, B, or C before a heat number indicate an air induction melted heat, while the letters V or Z indicate a VIM heat. All ingots were forged at 2150 F, conditioned, and rolled to 1/2-inch thick plate at 1950 F.

Three experimental alloys (C229, C230, C231) were initially air induction melted as 85 lb ingots, forged to 2-5/8-inch diameter rounds, and electroslag remelted (ESR) by Mellon Institute, Pittsburgh, Pennsylvania. The electrodes were remelted in a water cooled copper mold using AC power at a current of 2000 to 1400 amps and a voltage of 39 to 43 volts. The melting rate was 1 to 1.2 lbs/min. An automatic electrode guide mechanism kept the electrode 20 to 30 mm into the flux, using a 3-inch flux gap. The flux used contained 60-70% CaF_2, 10-15% lime, and the balance alumina. One ingot (Heat C229) had a rough surface because the furnace controls kept cutting off and the high lime flux boiled up during remelting.

The vacuum arc remelted (VAR) heats were melted at our Central Alloy District Canton, Ohio, as 350 lb electric furnace heats using a standard double slag practice and poured into 9-inch diameter electrode ingot molds. The electrode ingots were then conditioned and consumable vacuum arc remelted. The VAR ingots were then forged at 2150 F to 4-inch square bars, by length, cut into 14-inch lengths, conditioned, forged again to 1-1/2-inch thick slabs, conditioned, and rolled to 1/2-inch thick plate.

B. Test Procedures

The following general procedure was used in the processing and heat treatment of all experimental alloys. The 1/2-inch thick plate material was sectioned into rough cut 1/2-inch square tensile and Charpy coupons, gradient bars, and quenching dilatometer samples. The gradient bars were heated in a gradient furnace, with a 2200 F backwall temperature, and water quenched in order to determine the A_1, A_3 and carbide solution temperatures for subsequent heat treatment of the alloy. This ensured that each alloy was heat treated correctly, that is the austenitizing temperature was selected as the minimum temperature which ensured that all carbides were in solution (in one hour) in the austenite. All mechanical property specimens were initially normalized for 1 hour at a temperature of 100 to 150 F above the austenitizing temperature for the alloy. All heat treatments were performed in neutral salt baths and the martensitic alloys were quenched into 120 F agitated oil, and double tempered at various temperatures for 2 + 2 hours. When refrigeration treatments were used the material was refrigerated before tempering at -110 F for 1 hour. The quenching dilatometer specimens were used to determine the martensite start temperatures and if the alloy was heat treated bainitically, the TTT curve was determined metallographically. The mechanical property specimen coupons were then heat treated and subsequently finish ground. The Charpy V-notch specimens were of standard dimensions (0.394-inches square and 2.165-inches long). The tensile specimens were standard 0.252-inch diameter round specimens with a 1-inch gage length as shown in Figure 1(a). All tensile tests were performed at room temperature.

The plane-strain fracture toughness tests were performed at room temperature, in ordinary air, and at -65 F in a bath of dry ice and trichloroethylene using the notch bend specimen shown in Figure 1(b). The preparation of the test specimens consisted of cutting a 1/16-inch slot 0.230-inches deep by a grinding wheel and extending its base approximately 0.050-inches deep by electric discharge machining, using 0.003-inch thick brass shim stock which produced about a 0.004-inch wide slot. The length of the initial notch is denoted as, a_o, in Figure 1(b). The notch was further extended about

0.120-inches by fatigue precracking the specimen in a three-point bending configuration and from load measurements the maximum stress intensity (K_f max) at the crack tip during final stages of fatigue crack growth was calculated to be typically about 0.4 of K_Q for most alloys and never exceeding 60% of K_Q. The final crack length, a, was within the limits of 0.45 to 0.55 W where W is the specimen depth, nominally 0.800-inches. The plane-strain fracture toughness tests at both room temperature and -65 F were in accord with and met all of the current ASTM (E399-70T) recommendations and requirements for plane-strain fracture toughness testing (1).

The stress corrosion tests utilized the same plane-strain fracture toughness specimen, fatigue precracked in the same manner. After precracking all specimens were stored in desiccators prior to testing. All specimens were cantilever loaded "wet" (salt solution added prior to the application of load) as shown in Figure 2. The initial stress-intensity levels (K_{Ii}) were calculated according to the relationship given by Kies, et al. (2). The 3-1/2% NaCl solution was changed daily except on weekends and specimens were exposed until either the specimen failed or a minimum time of 200 hours had elapsed.

The Charpy V-notch specimens were tested at various temperatures on a 240 ft-lb capacity SATEC Impact Tester Model S1-1C, which was certified by the Army Materials and Mechanics Research Center, Watertown, Massachusetts.

Smooth and notched (K_t = 3.0) fatigue specimens were tested in tension-tension loading at an R value of +0.1 (R is the ratio of minimum stress to maximum stress). The unnotched fatigue specimens, shown in Figure 3(a), were lapped to produce a surface finish of 2 to 6 rms. The tests were performed on a Sonntag Model SF-4 fatigue testing machine cycling at 3600 cpm. The fatigue specimen and grips were surrounded with a Tygon tubing container, as shown in Figure 4, through which a flow of prepurified nitrogen gas (dewpoint of -90 F) is passed for the duration of the test in order to maintain a constant, low humidity, testing atmosphere. The alignment of the machine, loading train, and test specimen were checked thoroughly both statically and dynamically in order to minimize bending stresses.

III. RESULTS AND DISCUSSION

The results of the alloy development studies will be presented initially, and include extensive investigations on low alloy bainitic steels, medium alloy bainitic steels, and low alloy martensitic steels. The results of the stress corrosion investigations will be presented next, followed by the results of the processing studies. The processing studies include an extensive investigation of the effects of impurities and melting practice on tension-tension fatigue properties and the effects of thermal-mechanical working treatments on strength and toughness properties.

A. Alloy Development Studies

1. Low Alloy Bainitic Steels

The two decomposition products of austenite, in alloy carbon steels, which can be utilized to achieve ultra-high strength levels are lower bainite and martensite. It is now well established that for the same composition and equivalent strength levels lower bainite has toughness properties which are superior to tempered martensite (3,4,5). It was felt, therefore, that if a bainitic steel could be developed with strengths in excess of 300,000 psi ultimate tensile strength it should have toughness properties superior to those of a martensitic steel at the same strength level. One approach used to achieve this aim was to suitably alloy a steel to produce an aging response or secondary hardening upon aging subsequent to the isothermal bainitic treatment. This concept and these steels are hereafter referred to as bainaging steels. The basic alloy system chosen was a medium carbon Ni-Cr-Mo-V system. The compositions of the Ni-Cr-Mo-V bainaging alloys are presented in Table I, and the tensile and Charpy V-notch impact properties are presented in Table II. As mentioned earlier in the section on Test Procedures, for each bainitic alloy the A_1, A_3, carbide solution and M_s temperatures were determined along with the complete lower bainite portion of the TTT curve for each alloy. Therefore, the mechanical properties reported are for the optimum heat treatment for each alloy. For these low alloy bainitic steels the austenitizing temperatures ranged from 1550 F to 1750 F and the transformation times ranged from 6 hours to 48 hours to ensure that a completely bainitic structure was formed. Each alloy was isothermally transformed at a temperature of 25 F to 35 F above its M_s temperature in order to obtain maximum strength properties. The age hardening curves for these alloys indicated that if age hardening did occur, maximum hardening was observed at a temperature of approximately 950 F for an aging time of 4 hours.

The mechanical properties in Table II reveal that if the alloy overages or softens upon bainaging at 950 F the toughness generally increases, however, if the strength level remains constant or increases upon bainaging the toughness generally decreases. Thus the strength-toughness response to secondary hardening in these bainitic steels is very similar to the behavior observed in secondary hardening martensitic steels. The data in Tables I and II also reveal that for a given strength level an increase in Ni is beneficial to toughness and that increasing Cr and B are detrimental to toughness. Three of the alloys (B332, B333, and B355) had ultimate tensile strengths in excess of 300,000 psi in the as-transformed condition, while the highest strength obtained in the aged condition was 294,000 psi for alloy B346. These results indicate that in order to obtain an ultimate tensile strength of 300 ksi in these bainitic steels a minimum carbon content of 0.50% will be required. While a strength level of 301 ksi was obtained for alloy B355 with 0.45% carbon and 2.00% silicon this is not a desirable approach because of the very detrimental influence of the high silicon content on Charpy

impact toughness. Based on these results six additional compositions were vacuum induction melted, processed, and mechanical properties determined. The compositions of these alloys (Z389 through Z394) are presented in Table I, and the mechanical properties are presented in Table III. About 4% cobalt was added to all of these alloys in order to move the bainite finish curve to the left or shorter times. All of these six alloys were isothermally transformed for 6 hours.

The data in Table III reveal that all of the alloys meet the strength requirements in the as transformed condition but that significant softening occurs upon aging all alloys. As anticipated the alloy with the highest molybdenum content (Z391) demonstrated the highest retentivity of strength upon aging. As was shown by the data in Table II the elements which produce age hardening (chromium and molybdenum) cannot be raised to too high a level because a severe loss in toughness accompanies a pronounced age hardening response. The strength and toughness response of these bainitic steels as a function of chromium and molybdenum contents are shown in Figures 5 and 6. Increasing chromium content is seen to have a slight strengthening effect for all three heat treatment conditions and an inconsistent and unpronounced effect on toughness properties. Increasing molybdenum content increases strength and decreases Charpy impact toughness as shown in Figure 6. The lower strength of the as transformed bainite at the highest molybdenum level is not a real compositional effect but is probably attributed to a higher isothermal transformation temperature for alloy Z391. Alloys Z389, Z390, and Z391 were isothermally transformed to bainite for 6 hours at 495 F, 475 F, and 525 F respectively.

The strength-toughness properties of these as transformed bainitic steels are shown in Figure 7. The mechanical properties shown in Figure 7 and similar data on the other alloy systems illustrated throughout this report are plotted in this manner in order to readily compare the strength-toughness relationships of the experimental alloys with those of the currently, widely used 300 M steel. As 300 M steel is the most widely used commercial alloy for forged landing gear components it seems appropriate to compare the strength-toughness properties of the experimental alloys with the strength-toughness properties of similarly processed 50 lb VIM laboratory produced 300 M steel. When 300 M steel is vacuum induction melted and processed in the same manner as the experimental alloys, it typically achieves an ultimate tensile strength of 286 ksi with Charpy V-notch impact energy values of 19 ft-lbs at +70 F and 16 ft-lbs at -65 F when tested in the longitudinal direction. Therefore, the coordinates drawn in Figure 7 and in other figures throughout the report are drawn at a value of 286 ksi U.T.S. and 19 ft-lbs Charpy V-notch impact energy for ready comparison with the strength-toughness properties of the experimental alloys. From the data in Figure 7 it can be seen that while the desired strength levels were achieved, the Charpy impact energy values did not reach the desired levels. As the strength-toughness relationships of these low alloy bainitic steels did not look encouraging work in this alloy system was terminated.

2. Medium Alloy Bainitic Steels

At the 260 to 280 ksi ultimate tensile strength level HP 9-4-45 steel heat treated bainitically has the best combination of strength and toughness of any available commercial alloy. It's only shortcoming is that it is limited to a minimum tensile strength of about 260 ksi. Therefore, efforts were initiated to modify HP 9-4-45 steel in order to increase the strength level range of the bainitic microstructure. Initially twelve 70 lb air induction heats were made to determine if the strength level could be increased readily. After determining the TTT diagrams of the twelve alloys, four of the alloys had unsuitable TTT curves for bainitic heat treatment, therefore only eight of the alloys were heat treated for mechanical properties. The compositions of these alloys are presented in Table I and the properties are listed in Table IV. Of these eight alloys only alloy B297 showed promise toward achieving higher strength levels. It's toughness level is also very high considering that these were air melted ingots. Based on these results eleven additional medium alloy bainitic steels, with varying levels of carbon, nickel, chromium, and molybdenum were vacuum induction melted, processed and tested. The compositions of these steels (Heats Z211 through Z225) are presented in Table I and the mechanical properties are presented in Table V. Alloys Z211 through Z214 are high carbon modifications of the previous most promising medium alloy bainitic steel, (Heat B297). The data in Table V reveal that increasing the carbon content has lowered the M_s temperature sufficiently to enable the desired strength levels to be achieved in a bainitic microstructure. Each of these four alloys were isothermally transformed at both 25 and 75 F above their respective M_s temperatures. The two highest carbon heats, Z213 and Z214 achieved tensile strengths greater than 330,000 psi. The increase in strength level was, however, not without cost as the impact properties were decreased considerably. The strength-toughness relationships of these alloys are illustrated in Figure 8.

Seven heats of the medium alloy bainitic steels, Z219 through Z225, were investigated to determine the effects of varying Ni, Co, Cr, Mo, and Si levels on strength and toughness properties. Heats Z219, Z220 and Z221 (see Tables I and V) are a 0.46% C, 3.5% Ni, 2.0% Co composition with varying silicon content. As shown in Figure 9 it can be seen that increasing Si produced a modest increase in strength with a commensurate decrease in Charpy impact toughness. These alloys, however, are short of the desired strength level range. Alloys Z222, Z223, and Z224 are a modified Krupp steel with higher carbon contents for strength, and cobalt added to decrease the bainite finish times. The strength level of these bainitic steels are also marginal. The tensile strength-Charpy impact toughness relationships for these heats are also shown in Figure 8. As the strength-toughness relationships of these medium alloy bainitic steels did not look promising, work in this alloy system was stopped.

3. Low Alloy Martensitic Steels

a. Medium Carbon Ni-Cr-Mo-W-V System

The low alloy martensitic steel approaches involved two alloy systems, and the first alloy system investigated was the medium carbon Ni-Cr-Mo-W-V system. As evidence existed indicating that tungsten enhances the toughness of medium carbon martensitic steels (6) as well as the toughness of tool steels (7) it was decided to thoroughly explore the influence of tungsten on toughness in low alloy ultra-high strength steels. The composition and properties of the initial heats in the Ni-Cr-Mo-W-V system (Heats V707 through Z79) are presented in Tables I and VI respectively. Alloys Z75, Z77, Z78, and Z79 are remake heats of V710, V748, V750 and V751 respectively, because of missed compositions. These alloys were designed statistically using a 1/3 replicate of a 3^3 factorial experiment, confounding using the W(ABC) aliases. The mechanical property data in Table VI were analyzed statistically and the results of regression analyses for the 400 F temper data are shown below:

$$\text{U.T.S., ksi} = +65.5 + 468.5\,(\%C) + 13.1\,(\%Cr) + 5.9\,(\%Mo) + 6.9\,(\%W)$$

$$R^2 = 0.85 \qquad \text{Standard Error} = 6.8 \text{ ksi}$$

$$\text{CVN, ft-lbs} = +41.1 - 8.6\,(\%Cr) - 22.3\,(\%Mo) - 8.7\,(\%W) + 2.9\,(\%Cr^2) + 7.0\,(\%Mo^2) + 2.0\,(\%W^2)$$

$$R^2 = 0.74 \qquad \text{Standard Error} = 3.5 \text{ ft-lbs}$$

R^2 is the multiple correlation coefficient which measures the fraction of total variation about the average of the dependent variable, which has been explained by the regression equation. R^2 can range between 0 and 1, values close to 1 meaning that most of the variation in the dependent variable has been explained by the regression equation. Values near 0 indicate that the regression equation has explained little of the variation in the dependent variable. The standard error or standard error of estimate is a measure of the goodness of fit of the regression equation. The smaller the standard error of estimate the better the regression line fits the data. The strength-toughness relationships of these alloys are illustrated in Figure 10. Based on these results a second set of fifteen heats were statistically designed and processed. The design of these alloys (Z95 through Z111) employed a 2^3 factorial experiment, augmented by star and center points. The compositions of these heats are presented in Table I and the properties are given in Table VII. It can be seen from Table I that the composition range of Cr, Mo and W was broadened considerably in heats Z95 through Z111, compared to the earlier V707 series of heats. This was done with the intention of achieving ultimate tensile strengths in excess

of 290 ksi at tempering temperatures in the neighborhood of 1000 F. This is a very difficult goal to achieve and still maintain adequate toughness. The idea was to add sufficient alloy carbide formers to produce a moderate degree of secondary hardening to achieve the desired strength levels at high tempering temperatures. A pronounced secondary hardening response was to be avoided, because of its well known embrittling effect. It can be seen from Table VII that alloy Z106 did achieve an U.T.S. of 270 ksi when tempered at 1000 F, however the toughness level was low.

The strength-toughness relationships for these alloys are shown in Figure 11, and the results of the regression analyses for the 400 F temper condition are given below:

$$\text{U.T.S., ksi} = + 311.3 + 4.5\,(\%Cr) - 6.6\,(\%Mo) - 1.0\,(\%W) + 2.3\,(\%Mo^2) - 2.5\,(\%W \times \%Mo)$$

$R^2 = 0.94$ Standard Error = 1.8 ksi

$$\text{CVN, ft-lbs} = + 29.2 - 6.05\,(\%Cr) - 5.9\,(\%Mo) - 9.09\,(\%W) + 2.7\,(\%Cr \times \%W) + 1.80\,(\%W \times \%Mo)$$

$R^2 = 0.51$ Standard Error = 1.8 ft-lbs

In addition to these statistically designed Ni-Cr-Mo-W-V alloys a series of classically designed alloys was VIM and processed in order to determine the optimum levels of manganese, silicon and vanadium in this alloy system. The compositions of these alloys (heats Z112 through Z120) are given in Table I and the mechanical properties are listed in Table VII. The data on the manganese series of heats (Z112, Z113, Z114) reveal that manganese does not have a significant effect on either strength or toughness. The data for the vanadium series (heats Z118, Z19, and Z120) indicates that increasing vanadium from 0.10% to 0.19% has a beneficial effect on Charpy impact toughness with no further increase in toughness when vanadium is increased to 0.31%. The effect of silicon, as shown by heats Z115, Z116 and Z117, is to markedly increase both yield and ultimate tensile strength, with a sacrifice in toughness at the highest silicon level. Based on these results three additional compositions were melted, processed, and mechanical properties determined. The compositions of these alloys are listed in Table I (Z386, Z387, Z388) and the mechanical properties are listed in Table VIII. The strength and toughness properties for the 600 F tempering temperature are shown as a function of tungsten content in Figure 12. The data reveal that tungsten has a negligible effect on both strength and toughness properties, and therefore it appears that the addition of the element tungsten to these low alloy martensitic steels is not beneficial. While this combination of strength and toughness (312 ksi and 17 ft-lbs) does not need to be apologized for, it is not as promising as some of the alloys in the Ni-Cr-Mo-Si-V low alloy martensitic system, therefore work was

stopped at this point on the Ni-Cr-Mo-W-V alloy system.

b. Medium Carbon Ni-Cr-Mo-Si-V System

The second approach for the low alloy martensitic steels was the medium carbon Ni-Cr-Mo-Si-V alloy system. Initially fifteen VIM heats (Z43 through Z60) were processed and evaluated and their compositions and properties are given in Tables I and IX respectively. Unless noted otherwise all of the alloys in this alloy system were refrigerated for 1 hour at -100 F prior to double tempering for 2 + 2 hours at the indicated tempering temperature. The effect of silicon content on strength and toughness properties is shown in Figures 13 and 14. In both series of alloys increasing silicon markedly increased both yield and ultimate tensile strength. In the Z43 alloy series increasing silicon also increased the room temperature Charpy impact toughness slightly, while in the Z58 alloy series increasing silicon decreased toughness slightly. The effect of silicon content on the Charpy impact energy-transition temperature curves for these six alloys is illustrated in Figures 15, 16, 17 and 18. The data in these figures illustrate that generally as silicon is increased and hence strength level is increased that the Charpy impact energy is decreased for a given test temperature. The data in Figure 16 however demonstrate the opposite effect and it is seen that as silicon content is increased toughness increases at all test temperatures. This is an important observation and indicates that further exploration of the effect of silicon content on toughness is necessary and also its possible interaction with chromium and molybdenum as the only difference in the Z43 series and the Z58 series of heats is the chromium and molybdenum levels. The data presented in Figures 17 and 18 also reveal the importance of tempering temperature in evaluating toughness properties when silicon content is a variable. These data reveal that at the 600 F tempering temperature the low silicon (0.[illegible]% Si) alloy does not have superior toughness properties even though the alloy is much less strong than the two higher silicon alloys. This is because at a tempering temperature of 600 F the low silicon steel (Z58) is right in the middle of the tempered martensite embrittlement trough as illustrated in Figure 19. Because of the well known effect of silicon in retarding the kinetics of cementite precipitation the tempered martensite embrittlement range has been shifted to the right about 200 F to 700 F and 800 F for the higher silicon levels compared to the usual 500 F and 600 F range for the lower silicon levels The influence of increasing silicon upon retarding the degredation of strength properties with increasing tempering temperature is also illustrated in Figure 19. Similar observations are made for the Z43 series of alloys in Figure 20.

The effect of chromium on strength and toughness properties is illustrated in Figure 21 for both the Z46 and Z49 three-way-split series of heats. The Charpy impact-transition temperature curves for these six alloys are shown in Figures 22 and 23. For the Z49

series zero chromium appeared to be the best level, while for the Z46 series about 0.9% chromium appeared to give the best combination of properties. The influence of cobalt and vanadium on toughness properties is illustrated in Figures 24 and 25. The data in Figure 24 reveal that 1% cobalt is detrimental to toughness properties and has no effect on strength properties in these low alloy martensitic steels. Increasing vanadium content from 0.10% to 0.20% is seen to be beneficial to toughness properties as shown in Figure 25. The strength-toughness relationships for alloys Z43 through Z60 are compared to similar properties for laboratory produced 300 M steel in Figures 26 and 27. It is noted from these figures that for test temperatures of both +70 F and -65 F that many of these alloys look promising from a strength-toughness viewpoint. The mechanical properties on this first series of heats, in the Ni-Cr-Mo-Si-V alloy system, have demonstrated, therefore, that increasing vanadium content from 0.10% to 0.20% is beneficial to impact toughness, that 1% cobalt is detrimental to impact toughness, and that the optimum levels of Si, Cr, and Mo warrant further detailed investigation.

In order to determine the optimum levels of Si, Cr, and Mo in this alloy system, as well as any possible interaction effects between these elements, a set of fifteen statistically designed heats were vacuum induction melted and processed. In addition to these statistically designed alloys a series of classical design single compositional variable alloys were melted and processed in order to determine the optimum levels of Ni, Mn, and V in these Ni-Cr-Mo-Si-V low alloy martensitic steels. The results of the single variable experiments will be discussed first.

OPTIMUM LEVELS OF NICKEL, MANGANESE, AND VANADIUM

In addition to determining the optimum levels of Ni, Mn, and V in these low alloy martensitic steels, the effect of columbium on strength and toughness was also investigated. The use of Cb as a strengthener and grain refiner in hot rolled, high strength low alloy (HSLA) steels is well known, however its effect on structure and properties in medium carbon martensitic steels has not previously been reported. The element vanadium is usually used for this purpose in quenched and tempered ultra-high strength steels. The compositions and mechanical properties of the Cb series of heats (Z332-Z334) are listed in Tables I and X respectively. These data illustrated in Figure 28 reveal that strength properties are independent of columbium content, but that Charpy impact toughness increases with Cb content. The effect of Cb is therefore, similar to the effect of vanadium in enhancing toughness, however, as will be shown later vanadium has a more pronounced effect than columbium.

The compositions of the nickel series of heats are listed in Table I and the mechanical properties are listed in Table X and illustrated in Figure 29. The influence of nickel was investigated in two sets of three-way-split heats (Heats Z273, Z274,

Z275 and Z329, Z330, and Z331), and therefore the data points from the two separate sets of heats are not connected in Figure 29. The strength is generally higher and the toughness generally lower in the higher nickel series of heats because these heats had about a 0.40% carbon content compared to a 0.38% carbon content for the lower nickel level series of heats. The effect of nickel level on strength properties is not straight forward, but should probably be interpreted as having essentially no effect on strength properties. In the 2 to 3% Ni range the toughness properties seem to be independent of nickel level. In the lower nickel range the Charpy impact energies significantly increase when nickel increases from 0.52 to 1.66%. In addition the data in Table X reveal that the reduction in area values increase considerably (from 20% to 40%) over this same range of nickel contents. These data indicate that for 0.40% carbon martensitic steels there is no improvement in toughness when Ni is increased from 2 to 3% and that the optimum nickel content should probably be in the range from 1.5 to 2.0%.

The mechanical properties for the vanadium series of heats (Z276, Z277, and Z278) shown in Figure 30 demonstrate that as the vanadium content is increased from 0.10% to 0.20% there is a slight increase in yield strength, no change in ultimate tensile strength, but a substantial increase in notch impact toughness. When the vanadium level increases from 0.20 to 0.29% there is essentially no change in strength, but a further slight increase in toughness. Specimens from these three heats were examined metallographically in order to explain the improvement in toughness with increasing vanadium content. Figure 31 shows the microstructures of the three vanadium alloys at a magnification of 100X. Measurements of the prior austenite grain size revealed that Heat Z276 with 0.10% V had an ASTM grain size of 5.4, and Heats Z277 (0.20% V) and Z278 (0.29% V) had ASTM grain sizes of 8.4 and 8.7 respectively. The information in Figure 30 also indicates that the percent reduction in area (% RA) increases in a parallel manner to toughness with increasing vanadium content. It is well known that % RA is grain size dependent and therefore, it is clear that the refinement of grain size by the addition of vanadium up to 0.20% is responsible for the large improvement in toughness and RA but that a further increase in vanadium content causes only slight further grain refinement and thus only a slight further improvement in toughness and reduction in area. These three alloys were also examined by transmission electron microscopy in order to determine if other factors besides grain refinement were responsible for the improvement in mechanical properties. This investigation indicated that all three alloys had similar structures of tempered martensite and plates of Fe_3C, and no significant differences were found; therefore, it is believed that the major effect of vanadium on the improvement of mechanical properties is due to grain refinement.

The results of the manganese series of heats (Z270, Z271, and Z272) presented in Table X and Figure 32 demonstrate that as the Mn content is increased, the Y.S. and U.T.S. remain essentially constant, but the toughness decreases substantially. As these

low alloy martensitic steels are not lacking in hardenability, and the finding that increasing manganese is detrimental to toughness it would appear prudent to add only sufficient manganese to tie up about 0.010% maximum sulfur; about 0.30% Mn would therefore appear to be about optimum. In order to understand the reason for decreasing Charpy impact energy with increasing manganese, these alloys were examined by transmission electron microscopy. The results of this examination indicate that the precipitation of carbides during tempering was similar in all three alloys, the carbide in this case (600 F temper) being essentially Fe_3C. The only difference that could be discerned was that alloy Z272 with the highest Mn level had a greater number of microtwinned martensite plates than did the lower Mn alloy Z270. Figures 33 and 34 show typical regions of alloys Z270 and Z272 respectively. Although, Heat Z272 was not heavily microtwinned it did contain substantially more twins than Heat Z270.

It has been well established that microtwinned martensite has inherently less toughness than dislocated martensite (8,9) and that the lowering of the M_s temperature increases the tendency towards twinned martensite (10). Manganese lowers the M_s temperature in steels and therefore by increasing the Mn content there is a greater tendency towards the production of lower toughness, twinned martensite. It is a little surprising however, that an increase of approximately 0.50% Mn would be enough to produce a substantial difference in the toughness of the martensite if twinning were the only explanation. Therefore, it is felt that twinning does play a role in lowering the toughness of the higher manganese alloy but in addition, some subtle effect of Mn may be operative which as yet cannot be detected. Structure-property correlations in medium carbon martensitic steels are at best elusive.

OPTIMUM LEVELS OF SILICON, CHROMIUM, AND MOLYBDENUM

In order to determine the proper levels of Si, Cr, and Mo, and possible interaction effects between these elements, a set of fifteen statistically designed heats were vacuum induction melted as two-way split heats resulting in 50 lb ingots. The composition of these heats (Heats R1 through 15) are listed in Table I and the mechanical properties are shown in Table XI. The prefix R before heats 1 through 8 stands for remake as the compositions were missed the first time on the first eight heats and hence were remade. These 50 lb heats provided sufficient material to determine fracture toughness and stress corrosion properties in addition to tensile and Charpy impact properties. In order to determine mechanical property-composition prediction equations and possible interaction effects between the elements Si, Cr, and Mo, Heats R1 through 15 were designed statistically utilizing a 2^3 factorial experiment, augmented by star and center points. The prediction equations for ultimate tensile strength, plane strain fracture toughness at both room temperature and -65 F, and

Charpy impact energy resulting from the regression analyses for the composition and mechanical properties shown in Tables I and XI are presented below:

$$\text{U.T.S., ksi} = 322.5 - 90.2\,(\%\,Si) + 76.6\,(\%\,Cr) + 24.6\,(\%\,Si^2) - 23.1\,(\%\,Cr^2) + 12.8\,(\%\,Mo)$$

$$R^2 = 0.92 \qquad \text{Standard Error} = 2.9 \text{ ksi}$$

$$K_{IC}, \text{ ksi}\sqrt{\text{in.}} \text{ at } +70 \text{ F} = -35.7 + 119.9\,(\%\,Si) - 39.1\,(\%\,Cr) + 31.5\,(\%\,Mo) - 29.6\,(\%\,Si^2) - 19.8\,(\%\,Mo^2) - 19.8\,(\%\,Cr \times \%\,Mo) + 16.1\,(\%\,Cr^2)$$

$$R^2 = 0.97 \qquad \text{Standard Error} = 1.5 \text{ ksi}\sqrt{\text{in.}}$$

$$K_{IC}, \text{ ksi}\sqrt{\text{in.}} \text{ at } -65 \text{ F} = 20.46 + 38.0\,(\%\,Si) - 36.7\,(\%\,Cr) - 11.9\,(\%\,Mo) - 14.8\,(\%\,Si^2) + 10.7\,(\%\,Cr^2)$$

$$R^2 = 0.94 \qquad \text{Standard Error} = 1.4 \text{ ksi}\sqrt{\text{in.}}$$

$$\text{CVN, ft-lbs at } +70 \text{ F} = -4.5 + 29.4\,(\%\,Si) - 7.0\,(\%\,Si^2) - 5.5\,(\%\,Mo) - 3.3\,(\%\,Cr)$$

$$R^2 = 0.68 \qquad \text{Standard Error} = 1.3 \text{ ft-lbs}$$

From the values of the multiple correlation coefficient (R^2) and the values of the standard error of estimate, it can be seen that both the U.T.S. and K_{IC} equations should have a high degree of predictability. The multiple correlation coefficients measure the fraction of total variation about the average of the dependent variable which has been explained by the regression equation (values close to 1 meaning that most of the variation in the dependent variable has been explained by the regression equation). The standard error of estimate is a measure of the goodness of fit of the regression equation. However, for the CVN equation, only 68% of the variation in average measured toughness is explained by the variations in Si, Cr, and Mo. This observation is not too surprising as it is well known that fracture initiation tests such as the Charpy V-notch impact test, the reduction in area, and fatigue properties are far more sensitive to inclusion content than are crack propagation tests such as fracture toughness. Hence, the CVN values will be reflecting the content and distribution of other microstructural features in addition to the intended compositional variables Si, Cr, and Mo far more than the fracture toughness values. At these strength levels, it is clear that a crack propagation test such as K_{IC} is a better toughness parameter for screening compositional variables than is the Charpy V-notch impact test. Only the +70 F K_{IC} - composition equation indicates an interaction effect between elements as shown by the negative % Cr x % Mo term. It is noted that the -65 F K_{IC} - composition equation differs from the +70 F K_{IC} - composition equation in that it does not contain either a Mo^2 or a Cr x Mo term. It is not unexpected that a toughness-composition response curve is different both qualitatively and quantitatively at different test temperatures.

The mechanical property-composition prediction equations for U.T.S. and K_{IC} are expressed graphically in Figures 35, 36, 37. The dependence of ultimate tensile strength upon silicon content illustrated in Figure 35 reveals that strength is essentially constant until the Si level is approximately 2.1% at which point the ultimate tensile strength (U.T.S.) increases rapidly. At the same silicon level both K_{IC} expressions reach a maximum and the fracture toughness decreases above about 2.1% Si as strength increases. From these data it would appear that the optimum silicon level is about 2.1%. The influence of chromium level upon K_{IC} and U.T.S. illustrated in Figure 36 discloses that U.T.S. increases sharply with increasing Cr, until about 1.7% Cr when a maximum is reached and U.T.S. begins to decrease with a further increase in chromium. The +70 F K_{IC} equation indicates that K_{IC} decreases until about 1.5% Cr at which point K_{IC} reaches a minimum and with a further increase in Cr, K_{IC} increases again. The -65 F K_{IC} equation indicates that K_{IC} decreases until about 1.7% Cr and then a slight upturn in K_{IC} is observed with increasing Cr. It is believed that the -65 F K_{IC} versus chromium response curve is the more valid one and although fracture toughness does increase again at high Cr levels it probably never reaches the level observed at the lowest Cr contents (about 0.75%). From a fracture toughness standpoint, therefore, it would seem that a lower Cr level (about 0.75%) would be most desirable. The mechanical property versus molybdenum expressions shown in Figure 37 disclose that as Mo is increased over the range from 0.25% to 1.0% strength increases linearly and fracture toughness decreases. It would appear advisable therefore, to keep the Mo level low and only add sufficient Mo (about 0.25%) to meet hardenability requirements. The -65 F K_{IC} - composition prediction equation is illustrated in three dimensions in Figure 38. This figure discloses that to achieve maximum fracture toughness silicon should be maintained at about 2.1%, and that molybdenum and chromium should both be limited to the lowest levels investigated which is about 0.25% and 0.75% respectively. It should be noted that the use of prediction equations to extrapolate beyond the compositional limits of the alloy design is an unwise practice.

In a further attempt to understand the influence of, and proper level of Cr and Mo from a fracture toughness viewpoint several correlations of fracture toughness with Cr and Mo parameters are presented in Figures 39, 40, and 41. Data for these figures were taken from heats which had a silicon level in the range from 1.78% to 2.15% which produced an ultimate tensile strength range of 297 ksi to 315 ksi. The data in Figure 39 reveal that the ratio of the carbide forming elements (Cr + Mo) to carbon should be kept as low as possible for maximum fracture toughness. As shown in Table I all of these low alloy martensitic steels had a carbon content of about 0.40%. The variation of fracture toughness with combined chromium and molybdenum content shown in Figure 40 demonstrates again that Cr plus Mo should be held to the lowest possible levels for maximum fracture toughness. The

data presented in Figure 41 indicate that the Cr to Mo ratio does not significantly affect fracture toughness at either +70 F or -65 F.

Based on this analysis of the statistically designed alloys and the results of the single variable experiments to determine the optimum levels of Ni, Mn, and V, two additional heats were vacuum induction melted and processed. As discussed previously the optimum Ni, Mn, and V levels were determined to be about 1.8%, 0.30%, and 0.25% respectively. The results from the statistically designed heats indicated that the optimum silicon and molybdenum levels should be about 2.1% and 0.25% respectively and that chromium should be low, probably at about 0.75%. In order to further clarify the differences in slope of the +70 F K_{IC}, and the -65 F K_{IC} response curve as a function of chromium content (Figure 36) it was decided advisable to melt a high Cr level heat in addition to the lower Cr level heat. The higher Cr level heat would also present an opportunity to validate the predictability of the ultimate tensile strength equation as well. The compositions and mechanical properties of these two heats (Z525 and Z551) along with the composition and properties of laboratory produced 300 M steel (Heat Z449) are presented in Tables I and XII. It can be seen from the data in Table XII that the lower chromium heat Z551 (0.82% Cr) achieved an excellent combination of strength and toughness properties with an ultimate tensile strength of 311 ksi, 19 ft-lbs Charpy impact energy, and a K_{IC} of 60 ksi $\sqrt{in.}$ at +70 F and 45 ksi $\sqrt{in.}$ at -65 F. As expected the higher chromium heat Z525 (1.90% Cr) produced a higher strength level (318 ksi) and a lower toughness level (14 ft-lbs, and 49 ksi $\sqrt{in.}$). These experimental results are compared to the predicted results in Table XIII, utilizing the mechanical property-composition prediction equations presented earlier. This comparison reveals that the prediction equations should not be used to provide accurate quantitative estimates of mechanical properties, but that they are of value in indicating mechanical property-compositional trends qualitatively.

The Charpy impact properties of Heats Z525, Z551, and R1 through 15 are compared to the impact energies of laboratory produced 300 M steel (Heat Z449) in Figures 42 and 43. Considering the generally observed relationship of rapidly decreasing toughness with increasing strength at these ultra-high strength levels, the strength-toughness relationships of these medium carbon (about 0.40% carbon) Ni-Cr-Mo-Si-V martensitic steels are considered quite attractive. The plane strain fracture toughness properties of these alloys are compared to those of 300 M steel in Figures 44 and 45. These comparisons reveal that at both room temperature and -65 F the ultimate tensile strength-fracture toughness relationships for the new experimental martensitic steels are considerably improved compared to 300 M steel. Considering the fracture toughness properties of the alloy with the optimum composition (Z551) it is seen that the tensile strength level has been increased by about 25,000 psi

while maintaining the same level of fracture toughness as in 300 M steel. As shown by the laboratory heat of 300 M steel in Figures 44 and 45 and as demonstrated by all of our experience with the HP 9Ni-4Co steels the fracture toughness properties obtained from billet stock from large diameter vacuum arc remelted ingots are almost always greater than those obtained on 4-1/2-inch diameter VIM laboratory ingots. It is, therefore, anticipated that the fracture toughness levels of the experimental martensitic steels will be improved by about 10 to 20% when they are made commercially by electric furnace-vacuum arc remelt practice. A more detailed comparison of the mechanical properties of these new low alloy martensitic steels with similar properties of other commercially available ultra-high strength steels will be made in the final section of this report.

FRACTURE TOUGHNESS - CHARPY IMPACT CORRELATIONS

The availability of a relatively large amount of well documented fracture toughness and Charpy impact data generated in this program provided the opportunity to attempt correlations between fracture toughness and Charpy impact energy values. Even though previous attempts to correlate K_{IC} with Charpy impact energy values have proven unsuccessful (11), the large economic and time saving convenience of the Charpy impact test compared to the plane strain fracture toughness test was sufficient motive for another attempt to determine a statistically valid correlation between K_{IC} and CVN toughness parameters. It is clear from the average CVN and K_{IC} values for Heats R1 through 15, shown in Figure 46, that there is not a simple linear relationship between K_{IC} and CVN. A total of 47 separate K_{IC}, CVN, and Y.S. observations were programed in a variety of forms in an attempt to determine a valid correlation between K_{IC} and CVN parameters. The most valid correlation found is given below as equation (a):

Eqn. (a)

$$\left(\frac{K_{IC}}{YS}\right)^2 = -0.18 + \frac{46.3}{YS} + \frac{0.75\ CVN}{YS}$$

$$R^2 = 0.91 \qquad \text{Standard Error} = 0.0049$$

or

$$K_{IC} = YS\left[-0.18 + \frac{46.3}{YS} + \frac{0.75\ CVN}{YS}\right]^{1/2}$$

$$R^2 = 0.66 \qquad \text{Standard Error} = 4.87\ \text{ksi}\sqrt{\text{in.}}$$

A second correlation not as statistically valid, but one that can be plotted in two dimensions is presented below as equation (b):

Eqn. (b)

$$\left(\frac{K_{IC}}{YS}\right)^2 = -0.045 + 1.37\ \left(\frac{CVN}{YS}\right)$$

$$R^2 = 0.82 \qquad \text{Standard Error} = 0.0068$$

$$\text{or} \quad K_{IC} = YS\ [-0.045 + 1.37\ \left(\frac{CVN}{YS}\right)]^{1/2}$$

$$R^2 = 0.66 \qquad \text{Standard Error} = 4.87\ \text{ksi}\sqrt{\text{in.}}$$

This equation (b) is expressed graphically in Figure 47, and the large amount scatter observed would indicate that this is not a reliable relationship to use. One of the problems in determining a statistically valid correlation between K_{IC} and CVN is that it is not possible to obtain a good independent estimate of CVN and YS because YS and CVN are highly correlated. The expression given in equation (a) is significantly better than equation (b) as can be seen by the values of R^2 and the standard error of estimate. Even equation (a), however, will not be a good predictive equation because there is too much scatter about the line as indicated by the standard error of estimate. In summary equation (a) is certainly the best equation to use to estimate K_{IC} values from CVN values, however, even equation (a) is only of value for a "ball park" estimate of K_{IC} and unfortunately the experimentalist will still have to perform the fracture toughness test in order to determine a meaningful and valid K_{IC} number. Both of these expressions were obtained from data on low alloy martensitic steels which had yield strengths in the range of 234 to 267 ksi, ultimate tensile strengths in the range of 281 to 332 ksi, K_{IC} values in the range of 34 to 70 ksi $\sqrt{\text{in.}}$, and CVN values in the range of 11 to 21 ft-lbs.

B. Stress Corrosion Studies

In addition to enhancing the strength-toughness relationships in ultra-high strength steels one of the aims of this program was to improve the stress corrosion cracking (SCC) resistance of ultra-high strength steels. Toward this aim two approaches were taken; (1) to lower the impurity elements phosphorous and sulfur to the lowest possible levels, and (2) investigate systematically the influence of the elements silicon, chromium and molybdenum on SCC resistance.

INFLUENCE OF PHOSPHOROUS AND SULFUR

The influence of the impurities phosphorous and sulfur on the toughness of high strength steels has been investigated widely, however, little work has been done concerning the effects of these impurities on the SCC resistance of high strength steels. To investigate this effect a series of six 35 pound heats of 9-4-45 steel were vacuum induction melted (VIM) with varying phosphorous and sulfur levels and subsequently forged and rolled to 1/2" thick plate material. Tensile, Charpy impact, fracture toughness, and stress corrosion specimens from each heat were subsequently heat treated to both bainitic and martensitic microstructures. The bainitic specimens were normalized, austenitized, and isothermally transformed at 465 F for six hours. The martensitic specimens were normalized, austenitized, oil quenched, refrigerated at -110 F and tempered at 500 F for 2 + 2 hours. The fatigue cracked stress corrosion specimens were cantilever loaded in a 3-1/2% NaCl solution which was changed daily, except on weekends, and the K_{ISCC} values were determined after specimens had run out for 500 hours. K_{ISCC} stands for the plane strain stress intensity, under SCC conditions, above which cracking is observed. The compositions and properties of the six heats (V723-V746) are shown in Table I and Table XIV. The stress corrosion curves for two of the alloys are shown in Figures 48 and 49 and curves summarizing the influence of phosphorous and sulfur levels on CVN, K_{IC} and K_{ISCC} properties are illustrated in Figures 50 through 55. The complete delayed failure curves for all six alloys were presented in the Second Quarterly Progress Report on this contract. The stress corrosion curves in Figures 48 and 49 illustrate the severe degradation in load carrying capacity of ultra-high strength steels when fatigue cracked samples are stressed in an aqueous environment. For all phosphorous and sulfur levels the bainitic microstructure exhibited greater stress corrosion cracking resistance than the martensitic microstructure.

The effect of phosphorous content on K_{IC} and K_{ISCC} for sulfur levels of .009% and .010% is shown in Figure 50. For this sulfur level it is seen that both fracture toughness and SCC resistance are essentially independent of phosphorous level over the range of .004 to .020%. The effect of sulfur content on K_{IC} and K_{ISCC} is illustrated in Figure 51 for phosphorous contents less than .004%. It can be seen that increasing sulfur level significantly decreases fracture toughness of both the bainitic and martensitic microstructures, while there is apparently no effect of sulfur on the K_{ISCC} levels. The effect of phosphorous plus sulfur content on these two parameters is shown in Figure 52 and reveals a pronounced detrimental effect on K_{IC} and a slightly detrimental effect

on K_{ISCC}. With respect to toughness it can be seen from Table XIV that for the same total P + S content (0.029% for alloys V726 and V727) that sulfur is the more detrimental of the two elements. The effect of phosphorous, sulfur, and phosphorous plus sulfur on Charpy impact properties is shown in Figures 53, 54, and 55 respectively. It is evident from these figures that sulfur is far more detrimental to toughness than phosphorous. We have seen, therefore, that while increasing phosphorous and sulfur levels are detrimental to toughness properties of both bainitic and martensitic 9-4-45 steel that these impurity elements had essentially no effect on SCC resistance as characterized by K_{ISCC}. It should be noted that only the trends of this impurity element study should be considered, and not the absolute magnitude of the toughness numbers, as these properties were obtained on small laboratory heats of 9-4-45 steel and not commercially produced vacuum arc remelted material.

INFLUENCE OF SILICON, CHROMIUM, AND MOLYBDENUM

The influence of silicon, chromium and molybdenum on SCC resistance in low alloy martensitic steels was investigated by means of the fifteen statistically designed heats (R1 through 15) in order to determine the compositional dependence of the stress corrosion resistance parameter K_{ISCC}. The K_{ISCC} values were determined from specimens which had not failed after 200 hours in a 3-1/2% NaCl solution which was changed daily except on weekends. The stress corrosion curves for all fifteen alloys were reported in the Sixth Quarterly Progress Report on this contract and three of these stress corrosion curves are shown in Figures 56, 57, and 58. The general shape of the stress intensity-time to failure curves was the same for all fifteen heats. As shown in Figures 56, 57, and 58, and by the K_{ISCC} data in Table XI the variations in Si, Cr, and Mo produced significant changes in plane strain fracture toughness, however, the SCC resistance parameter K_{ISCC} was essentially uneffected by these compositional variations. The K_{ISCC} values for all fifteen alloys were in the range of 16 to 19 ksi $\sqrt{in.}$ and hence the stress corrosion resistance of these 0.40% carbon martensitic steels is independent of the intended variations in Si, Cr, and Mo; 1.78 to 2.75% Si, 0.80 to 1.75% Cr, and 0.26 to 1.02% Mo (compositions listed in Table I). These same variations in Si, Cr, and Mo produced a change in fracture toughness values ranging from 40 to 64 ksi $\sqrt{in.}$ (Table XI), indicating that K_{ISCC} and K_{IC} are in no way simply related. The often made generalization that if a material's fracture toughness is increased its stress corrosion resistance will also be increased is shown here not to be either a good or valid generalization.

While the K_{ISCC} threshold stress intensity values were independent of composition it can be seen from the stress intensity - time to failure curves in Figures 56 through 58, from the portion of the curve where the stress intensity decreases rapidly at essentially constant time, that this essentially constant time to failure over a varying stress range shifts significantly from alloy to alloy. A regression analysis was run to determine if there was a significant composition dependence of the time to failure at an applied stress intensity equal to 60% of the alloy's K_{IC} value. The results of this regression analysis are given below:

Time to Failure, Minutes = 488.8 +60.3 (% Si) -735 (% Cr)
at $K_{Ii} = 0.60\ K_{IC}$ + 256.8 (% Cr^2)

$R^2 = 0.73$ Standard Error = 24.0 Minutes

The equation indicates that at this applied stress level the time to failure or stress corrosion resistance is independent of molybdenum content, linearly dependent upon silicon content, and quadratically dependent upon chromium content. For certain compositions this equation is expressed graphically in Figures 59 and 40. Neither the significance nor the reason for the complex dependence of time to failure upon Cr content is known. The increased time to failure at this stress level, with increasing silicon content, is somewhat more understandable as Carter (12) has shown that increasing Si content in 4340 type steels decreases the crack growth rate in K_{ISCC} tests. In agreement with the current results, he also found that increasing silicon did not influence the K_{ISCC} threshold stress intensity level even though it did decrease the crack growth rate. This indicates that in 0.40 carbon, low alloy martensitic steels, composition can and does influence the rate of subcritical flaw growth under stress corrosion cracking conditions even though it does not influence the stress intensity level at which rapid mechanical crack propagation begins. This stress intensity level at which the slowly moving crack reaches a critical length under SCC conditions and rapid mechanical crack propagation begins is known to be higher than the K_{IC} value for the alloy in these types of steels (12,13), therefore, indicating that some type of crack blunting mechanism is operative. In steels at these ultra-high strength levels, the extent of subcritical slow crack growth is relatively short in terms of both time and crack length; therefore, not much reliance can be placed on finding a subcritical flaw during periodic inspections and, hence, the decreased crack growth rate with increasing silicon content is of no practical import. For comparison purposes, the K_{ISCC} value of 300 M steel (VIM Heat Z449) was determined to be 13 ksi $\sqrt{in.}$ (Figure 61). The increase in strength level from about 286 ksi for 300 M steel to about 315 ksi for the experimental Ni-Cr-Mo-Si-V martensitic steels, therefore, has not produced a degradation in stress corrosion cracking resistance. A more detailed comparison of the K_{ISCC} values of these experimental low alloy martensitic high strength steels with K_{ISCC} values of several commercial high strength steels will be made in the final section of this report.

As the fatigue testing portion of this program included the fatigue testing of bainitic steels as well as martensitic steels it was decided to determine the K_{ISCC} values of an experimental bainitic steel in both the VIM and VAR conditions. The stress corrosion behavior of medium alloy bainitic steel Z411 and the same composition in the VAR condition (Heat 3838800) (compositions listed in Table I) are shown in Figures 62 and 63. The K_{ISCC} value of this medium alloy bainitic steel is seen to be independent of melting practice. While the K_{ISCC} value of

13 ksi $\sqrt{in}$. seems quite low for a bainitic microstructure, the carbon content of this steel is relatively high (about 0.50% carbon) and it is felt that if this same composition was heat treated to a martensitic microstructure the K_{ISCC} value would be lower than 13 ksi $\sqrt{in}$.

From an alloy development standpoint it was disappointing to find that the basic stress corrosion resistance of low alloy martensitic steels was independent of the variations in Si, Cr, and Mo contents, thereby closing the door on one more possible avenue of improving the stress corrosion resistance of low alloy martensitic steels from a compositional point of view. It was also disappointing to learn that lowering the levels of phosphorous and sulfur down to .003% P and .002% S did not provide any enhancement in K_{ISCC} for either bainitic or martensitic ultra-high strength steels. Paxton has investigated the effect of several impurities at different impurity levels on the stress corrosion cracking resistance of 300 grade maraging steel and demonstrated that impurity levels had little effect on K_{ISCC} values with the total range of K_{ISCC} values varying from 7 to 15 ksi $\sqrt{in}$. (14). This work on the influence of impurities on the stress corrosion resistance of 18% Ni maraging steel has recently been verified on a commercial scale by the evaluation of a high purity 18% Ni (300) (5-ton heat, .003% C, .001% N, .004% S, .002% P) maraging steel forging where the K_{ISCC} level was determined to be 7 ksi $\sqrt{in}$. (15). Thus, from an impurity level standpoint, it appears that the stress corrosion cracking resistance cannot be improved for either the 18% Ni maraging steels or the low alloy martensitic or bainitic steels. From a microstructural point of view, bainitic structures have greater stress corrosion cracking resistance than martensitic structures; however, at strength levels above 300 ksi, the strength-toughness relationships of bainitic steels are no longer attractive as was demonstrated earlier in this report. The influence of grain refinement has been studied for 4340 steel and it was found that K_{ISCC} values ranged from 14-16 ksi $\sqrt{in}$. independent of prior austenite grain size variations from ASTM 7 to 12 (16). It was observed, however, that the crack growth rates decreased with decreasing prior-austenite grain size. From a compositional standpoint, the only work to date on low alloy martensitic steels which has shown that stress corrosion cracking resistance can be improved by alloying is the work of Sandoz which demonstrated that K_{ISCC} increases for decreasing C and Mn levels in 4340 type steels (17). These steels, however, were heat treated to a relatively low strength level (about 170 to 195 ksi yield strength) and it is not clear that the same compositional dependence would be observed at strength levels near 300 ksi.

It appears, therefore, that at strength levels in the neighborhood of 300,000 psi, low alloy steels have greater stress corrosion cracking resistance than 18% Ni maraging steels; however, these levels of resistance are not inherently high and appear to be largely independent of compositional, microstructural, and impurity variables. Thus, metallurgical means for improving the inherent stress corrosion cracking resistance of ultra-high strength steels is not immediately apparent and, therefore, the present means of successful utilization of steels at these strength levels such as shot peening, cadmium plating, and painting will continue to be necessary for the foreseeable future.

C. Processing Studies

The processing studies include the investigation of the effects of three different melting practices; electroslag remelting, vacuum induction melting, and vacuum arc remelting on strength and toughness, and tension-tension fatigue properties. In addition the effect of thermal-mechanical treatments on the mechanical properties of both bainitic and martensitic steels was investigated.

1. Influence of Melting Practice on Strength and Toughness Properties

The influence of melting practice on mechanical properties was investigated for a low alloy bainitic steel, a medium alloy bainitic steel, and a low alloy martensitic steel. The three experimental alloys were selected from the preliminary alloy development results and vacuum induction melted (VIM), electroslag remelted (ESR), and vacuum arc remelted (VAR) to the lowest possible levels of impurities. The compositions of these three alloys do not necessarily represent the optimum composition in each alloy system, as the compositions had to be selected early in the program in order to be processed by the different melting practices. The compositions of the three experimental steels with the three different melting practices are presented in Table I. The low alloy bainitic steel was not vacuum arc remelted. The VIM heats (Z409, Z411, Z412) were melted as 50 lb ingots. The ESR heats (C229, C230, C231) were initially air induction melted as 85 lb ingots, forged to 2-5/8-inch diameter rounds, and electroslag remelted by Mellon Institute. The VAR heats (3838800, 3888808, 3888811) were melted initially at our Central Alloy District (Canton, Ohio) as 350 lb electric furnace heats using a standard double slag practice and poured into 9-inch diameter electrode ingot molds. These electrode ingots were then conditioned and consumable vacuum arc remelted.

The mechanical properties of these alloy melted by VIM, ESR, and VAR techniques are compared in Table XV. The VIM and VAR low alloy martensitic alloys have essentially the same strength and toughness properties; however, the ESR material (Heat C229) has high side strength properties and low side toughness properties due to a high side carbon content of 0.44 percent. Metallographic examination of specimens from Heats Z409, C229, and 3888808 revealed that there were no significant differences in the degree of microcleanliness of these three steels, and that all three were very clean. The low K_{IC} and percent reduction in area values for ESR Heat C229 cannot be totally explained by the higher carbon content, and as the alloy appeared to have a high degree of microcleanliness, the low K_{IC} and % R.A. values are most probably due to the localized segregation of non-metallic inclusions. Electron metallographic examination of extraction replicas from the fracture surfaces of the tensile samples of the ESR C229 alloy revealed that an unusually large number of both globular and angular particles were present of the fracture surface. Electron diffraction analysis of these particles tentatively identified the globular particles as SiO_2 and the angular particles as $CaAl_2O_4$. This localized segregation condition is most probably

due to the problems encountered during the electroslag remelting of this heat as previously described in the section on Materials and Procedures. The three medium alloy bainitic steels (Z411, C230, 3888800) have essentially the same strength properties, with the VAR heat having the highest level of fracture toughness and the ESR heat the lowest level of fracture toughness. The two low alloy bainitic heats both have high strength levels for a bainitic microstructure; however, the fracture toughness level of both the VIM and ESR materials is quite low.

2. Influence of Melting Practice on Fatigue Properties

As fatigue strength is one of the most important design parameters for the successful utilization of ultra-high strength steels for landing gears, an extensive fatigue study was conducted. The influence of composition, microstructure, and melting practice on the tension-tension fatigue properties of various experimental steels was investigated. Both notched and unnotched fatigue tests were conducted at an R value (ratio of minimum stress to maximum stress) of +0.10.

UNNOTCH FATIGUE TESTS

The maximum stress versus cycles to failure (S-N) curves for the three VIM steels are shown in Figures 64, 65, and 66 and the comparison S-N curves for the ESR alloys are shown in Figures 67, 68, and 69. With the exception of alloy Z412, the degree of scatter in the fatigue data is typical and not excessively large for specialty ultra-high strength steels. The reason for the unusually high number of thread failures in alloy Z412, Figure 66 is not known. The fatigue behavior of the low alloy martensitic steel produced by vacuum arc remelting (Heat 3888811) is shown in Figure 70. The fatigue behavior of the medium alloy bainitic steel produced by vacuum arc remelting (Heat 3888800) is shown in Figure 71.

The influence of melting practice on the fatigue strengths of these three alloys is illustrated in Figures 72, 73, and 74. The fatigue behavior of the low alloy martensitic steels illustrated in Figure 72 demonstrates that the VAR material had the highest fatigue strengths, and that the VIM material had the lowest fatigue strengths. The comparison S-N curves for the medium alloy bainitic steels (Figure 73) reveal that the ESR material had the highest fatigue strengths and that the VIM had the lowest fatigue strengths. The comparison S-N curves for the low alloy bainitic steels again demonstrate that the ESR material had superior fatigue life compared to the VIM material. The low alloy bainitic steel composition was not vacuum arc remelted. As melting practice has been shown to have a pronounced influence on fatigue properties for a given composition and strength level, a quantitative analysis of the inclusion contents was performed. It is well known that if environmental effects are eliminated the two primary factors controlling the fatigue behavior of high strength steels are strength level and inclusion content. It will be mentioned later that microstructure

due to the problems encountered during the electroslag remelting of this heat as previously described in the section on Materials and Procedures. The three medium alloy bainitic steels (Z411, C230, 3898800) have essentially the same strength properties, with the VAR heat having the highest level of fracture toughness and the ESR heat the lowest level of fracture toughness. The two low alloy bainitic heats both have high strength levels for a bainitic microstructure; however, the fracture toughness level of both the VIM and ESR materials is quite low.

2. Influence of Melting Practice on Fatigue Properties

As fatigue strength is one of the most important design parameters for the successful utilization of ultra-high strength steels for landing gears, an extensive fatigue study was conducted. The influence of composition, microstructure, and melting practice on the tension-tension fatigue properties of various experimental steels was investigated. Both notched and unnotched fatigue tests were conducted at an R value (ratio of minimum stress to maximum stress) of +0.10.

UNNOTCH FATIGUE TESTS

The maximum stress versus cycles to failure (S-N) curves for the three VIM steels are shown in Figures 64, 65, and 66 and the comparison S-N curves for the ESR alloys are shown in Figures 67, 68, and 69. With the exception of alloy Z412, the degree of scatter in the fatigue data is typical and not excessively large for specialty ultra-high strength steels. The reason for the unusually high number of thread failures in alloy Z412, Figure 66 is not known. The fatigue behavior of the low alloy martensitic steel produced by vacuum arc remelting (Heat 3888811) is shown in Figure 70. The fatigue behavior of the medium alloy bainitic steel produced by vacuum arc remelting (Heat 3888800) is shown in Figure 71.

The influence of melting practice on the fatigue strengths of these three alloys is illustrated in Figures 72, 73, and 74. The fatigue behavior of the low alloy martensitic steels illustrated in Figure 72 demonstrates that the VAR material had the highest fatigue strengths, and that the VIM material had the lowest fatigue strengths. The comparison S-N curves for the medium alloy bainitic steels (Figure 73) reveal that the ESR material had the highest fatigue strengths and that the VIM had the lowest fatigue strengths. The comparison S-N curves for the low alloy bainitic steels again demonstrate that the ESR material had superior fatigue life compared to the VIM material. The low alloy bainitic steel composition was not vacuum arc remelted. As melting practice has been shown to have a pronounced influence on fatigue properties for a given composition and strength level, a quantitative analysis of the inclusion contents was performed. It is well known that if environmental effects are eliminated the two primary factors controlling the fatigue behavior of high strength steels are strength level and inclusion content. It will be mentioned later that microstructure

also plays a role in affecting fatigue strength, but it is a secondary role compared to inclusion content. It now has been well demonstrated that the size, number, shape, and location of inclusions has a pronounced influence on the fatigue properties of steel (18, 19, 20, 21, 22, 23, 24, 25, 26, 27, 28). Oxides and silicates in particular have been found to be most deleterious (20, 22, 24-27), while sulfides have generally been found to have little harmful effect on fatigue properties (18, 20, 24, 26, 27). For this study, as composition and strength level were held essentially constant for a given alloy system, it seemed most likely that the fatigue behavior as influenced by melting practice could most likely be explained by variations in inclusion contents, size, shape or distribution. Standard metallographic examination for microcleanliness for all six alloys (shown in Figures 72, 73, and 74) was performed and no apparent differences were observed. All six heats were very clean. Alloys Z411, C230, and 3888800 of the medium alloy bainitic steel series were selected for detailed quantitative analysis. The quantitative analysis was performed on an AMEDA instrument which is an Automatic Microscopic Electronic Data Accumulator manufactured by Femco Corporation of Irwin, Pennsylvania. The AMEDA was used to determine total volume percentage of inclusions for all inclusion types. The AMEDA also was used to determine the size distribution of sulfide inclusions, but these data were not correlatable to fatigue strength data as sulfides are not responsible for the initiation of fatigue cracks. Unfortunately from an analysis standpoint the oxide inclusions were too small in these vacuum melted and ESR steels for size distribution data to be determined on the AMEDA. Point counting was used in a few selected instances to verify the volume percent numbers being determined on the AMEDA. Point counting was performed at a magnification of 320X, using 125 fields per specimen, with an eye piece containing a grid with 81 intersections.

The volume percent inclusion data obtained on both the AMEDA instrument and by point counting for the VIM, ESR, and VAR medium alloy bainitic steels are shown in Table XVI. Initially the volume percent measurements were determined on longitudinal sections of the threaded grip end of the failed fatigue specimen. These data reveal that the VAR alloy 3888800 has by far the lowest level of inclusions, and that the VIM melted alloy Z411 has the next highest volume percentage and the ESR alloy C230 has the highest level of inclusion content. The volume percent inclusions determined by point counting reveal the same order of rating the three alloys in terms of microcleanliness. Unfortunately these volume percent inclusion numbers do not correlate with the rating of the fatigue strengths as shown in Figure 73. The ESR alloy C230 had the highest fatigue strength but it also had the highest volume percent of inclusions. As these data were not correlateable it was thought that counting the inclusion contents adjacent to the fracture surface would be more meaningful than counting them in the threaded grip region of the specimen. The volume percent inclusion data obtained near the fracture surface region of the specimen reveal that the VIM and ESR materials have about the same percentage of inclusions and that again the VAR material has a significantly lower percentage of inclusions.

These data, however, also do not explain the relative fatigue strengths of the three alloys. The reason for the lack of correlation between the volume percent inclusion measurements and the fatigue strengths of the three alloys is thought to be due to the relatively small volume percentage of inclusions for all three alloys. Because all three heats were really quite clean it is felt that the inclusion size and distribution at the region of initiation of the first fatigue crack is a very localized situation which is not accurately represented by an average volume percentage of inclusions. It is felt that the factor which most probably controls the fatigue life of these very clean steels is the size or orientation of the oxide or silicate inclusion located in the maximum stress region of the fatigue specimen. Unfortunately, experimentally verifying this belief was not possible. Fatigue studies by Johnson and Sewell (20) and Murray and Johnson (27) support this argument by demonstrating that for the same total number of inclusions (in clean steels) the fatigue life varied over a considerable range.

A limited number of transverse fatigue tests were performed. A detailed study of transverse fatigue properties was not conducted because it was believed that the degree of anisotropy exhibited by 1/2-inch thick plate would have little relevance to the degree of anisotropy usually found in forgings or forging billet stock. The transverse fatigue properties were determined on the low alloy martensitic steel composition in both the VIM and ESR conditions. The longitudinal and transverse fatigue properties of VIM alloy 2351 are presented in Figures 75 and 76, and compared in Figure 77. Alloy 2351 is an additional heat of the same nominal composition as Heat 2409 and the composition is listed in Table I. As shown in Figure 77 a normal amount of anisotropy was observed with the 10^7 cycle fatigue strength decreasing from 170 ksi for the longitudinal direction to 140 ksi for the transverse direction. Similar data are presented in Figures 78 and 79 for the ESR low alloy martensitic composition. In this case the observed anisotropy is minimal with the transverse fatigue strengths nearly equaling the longitudinal strengths. Metallographic examination for inclusion contents, size and distribution did not provide an explanation for the different degree of anisotropy between the VIM and ESR materials.

The unnotched fatigue properties of laboratory produced 300 M steel (VIM heat 2449) are presented in Figure 80. A 10^7 cycle fatigue strength of about 175,000 psi was obtained. The fatigue properties of the two VAR steels, medium alloy bainitic steel 3888800, and low alloy martensitic steel 3888811, are compared in Figure 81. It can be seen that the fatigue strengths of the bainitic steel are slightly greater than those of the martensitic steel. Further comparison of the fatigue properties of bainitically heat treated steels is made by the data presented in Table XVII which compares the 10^7 cycle fatigue strength to ultimate tensile strength ratio (Fatigue Ratio) of the experimental steels in this program to the Fatigue Ratios of several commercial ultra-high strength steels. As fatigue strengths increase significantly with increasing R values these comparisons are only made for tension-tension fatigue tests with an R value of either +0.06 or +0.10. Concerning the experimental alloys

of this investigation it can be seen that the bainitic steels generally hav' a much higher Fatigue Ratio than the martensitic steels. Although the reason for the lower fatigue strength and Fatigue Ratio of VIM bainitic alloy Z411 is not known, it is felt that the fatigue properties of this heat are not representative of the alloy. This can be seen by comparing the Fatigue Ratios of the same composition in the VAR condition (Heat 3888800) and the ESR condition (Heat C230). The 10^7 cycle fatigue strengths of about 200,000 psi for bainitic steels VAR 3888800, and ESR C230 and C231 are noted to be considerably superior to these obtained on the commercially available martensitic steels such as 4340, 300 M and 18 Ni maraging. Other investigators have also demonstrated that the fatigue properties of lower bainite structures are superior to those of tempered martensite (33). It can also be seen from the information in Table XVII that the Fatigue Ratios of the experimental martensitic steels are quite commendable.

NOTCH FATIGUE TESTS

The notch fatigue strengths of two experimental steels are shown in Figures 82, 83, and 84. Notch fatigue tests were only performed on the VAR steels as there was insufficient plate material to obtain both unnotched and notched fatigue specimens from the VIM and ESR heats. The comparison S-N curves shown in Figure 84 reveal that the notch fatigue strengths of these two alloys come together to a common value of about 80,000 psi at 10^7 cycles. This is a commonly observed behavior, that while there may be differences in fatigue properties between alloys at $K_t = 1$, the notch fatigue properties of different high strength steels tend to be very similar. At similar R values the 10^7 cycle notch fatigue strengths of 80,000 psi for alloys 3888800 and 3888811 compare to a value of 60,000 psi for 300 M steel (30) and 40,000 psi for high-purity 18 Ni maraging steel (15).

3. Thermal-Mechanical Working Treatments

An investigation was conducted to determine the effects of deformation of an annealed ferrite-carbide matrix, upon the mechanical properties of a subsequently conventionally heat treated low alloy martensitic and bainitic steel. The genesis of this work was the work of Webster (34) which demonstrated that the deformation of an annealed or tempered martensitic structure for both AFC-77, a martensitic stainless steel, and 300 M steel, produced microscopic voids at the carbide-matrix interfaces, and that these voids were metastable in austenite at high temperatures and resulted in considerable refinement of austenite grain size by acting as barriers to grain growth. A series of thermal-mechanical treatments were given to commercial 300 M steel, an experimental low alloy martensitic steel, and an experimental low alloy bainitic steel in order to effect refinement of the prior austenite grain size and subsequent mechanical properties.

The first material investigated was commercial 300 M steel, which was processed by the following six thermal-mechanical treatments:

a. Spheroidize anneal and deform 50% at 1200 F at the completion of the annealing cycle.

b. Spheroidize anneal, cool to room temperature and deform 50%.

c. Spheroidize anneal, cool to room temperature, heat to 1200 F and deform 50%.

d. Temper quenched material at 1200 F and deform 50% at 1200 F.

e. Temper quenched material at 1200 F, cool to room temperature and deform 50%.

f. Temper quenched material at 1200 F, cool to room temperature, heat to 800 F and deform 50%.

The 300 M steel processed as shown above was austenitized at various temperatures and examined metallographically to determine prior austenite grain size. These results are shown in Table XVIII. The data indicate that austenitization must take place at least 50 F below the conventional austenitizing temperature of 1575 to 1600 F in order for significant grain refinement to take place. The hardness data on the oil quenched samples indicate that apparently all carbides are dissolved at temperatures as low as 1475 F. Material processed by each of the six processes was then austenitized for 1/2 hour at 1475 and 1525 F, oil quenched and tempered for 2 + 2 hrs at 600 F. The resulting tensile and Charpy impact properties are shown in Table XIX. For both the spheroidized annealed and tempered martensitic structures rolling at 1200 F versus rolling at room temperature did not significantly effect either strength or toughness properties. For a given deformation treatment the spheroidized microstructures produced a finer grain size than the tempered martensite microstructures.

Comparing the mechanical properties of the conventionally austenitized, quenched and tempered 300 M steel to these of the grain refined thermal-mechanically processed 300 M steel it can be seen that the yield and tensile strengths were increased generally by 3 to 6%; that the reduction in area values decreased by 9 to 30%; that the elongation values decreased by 8 to 25%, and that the Charpy impact energy values varied irregularly from an increase of 5% to a decrease of 30%. These results indicate that the reduction in prior austenite grain size from about ASTM number 9 to ASTM number 13, for 300 M steel, as a result of these thermal-mechanical treatments is not warranted from a mechanical property standpoint.

The experimental low alloy martensitic steel (Alloy 2350 with the same nominal composition as Alloys 2409 and 245) was processed with the following thermal-mechanical treatment cycles:

a. Spheroidize anneal and deform 50% by rolling at 1100 F at the completion of the annealing cycle and air cool after rolling.

b. Spheroidize anneal, air cool to room temperature, heat to 1100 F and deform 50%; air cool.

c. Austenitize, oil quench, temper at 1200 F, deform 50% at 1200 F; air cool.

d. Austenitize, oil quench, temper at 1200 F, air cool to room temperature, heat to 800 F and deform 50%; air cool.

The A350 alloy (composition shown in Table I), processed as shown above, was austenitized at various temperatures and examined metallographically to determine prior austenite grain size. These results are shown in Table XX. The data indicate that austenitization must take place at least 50 F below the conventional austenitizing temperature of 1675 to 1700 F for this alloy in order for significant grain refinement to take place. The hardness data on the oil quenched samples indicate that apparently all carbides are dissolved at temperatures as low as 1575 F. Material processed by each of the four processes was then austenitized for 1 hour at 1600 F, oil quenched and tempered for 2 + 2 hours at 600 F. The resulting tensile and Charpy impact properties are presented in Table XXI. There does not seem to be a significant difference between the four thermal-mechanical treatments and the degree of grain refinement. Compared to the conventionally quenched and tempered material, the thermal-mechanically processed material achieved a small and varying increase in yield strength; the ultimate tensile strength increased about 3.5%, the % El. values were essentially unaffected, and the % R.A. values were increased by about 20%, while the CVN values were increased by about 15%.

In order to determine if a bainitic structure would respond in a different fashion to grain refinement treatments, low alloy bainitic steel Z412 received the following processing cycles:

a. Spheroidize anneal and deform 50% by rolling at 1200 F at the completion of the annealing cycle and air cool after rolling.

b. Spheroidize anneal, air cool to room temperature, heat to 1290 F and deform 50%; air cool.

c. Austenitize, oil quench, temper at 1200 F, deform 50% at 1200 F, and air cool.

After processing as shown above, the material was austenitized at two different temperatures (1600 F and 1650 F) and then isothermally transformed at 475 F for six hours to a fully bainitic structure. The resulting tensile and Charpy impact properties are presented in Table XXII. For all three processing treatments the lower austenitizing temperature produced a finer grain size which resulted in an increase in yield strength. It did not significantly affect any of the other tensile properties. There seemed to be some trend, but perhaps not a significant one, of decreasing Charpy impact toughness with increased yield strength and finer grain size produced

by the lower austenitizing temperature. For a given austenitizing temperature there did not seem to be any significant difference in mechanical properties as a function of the thermal-mechanical process, nor was there any significant difference when compared to the conventionally heat treated bainitic material. A Hall-Petch plot of the yield strength and grain size data is shown in Figure 85 along with the data for the martensitic steels. Least-square fit lines have been drawn through the data points for each alloy and the dotted lines indicate the 90 percent confidence limits. It can be seen that for the limited range of grain sizes obtained, that grain refinement had a greater effect in increasing yield strength for the bainitic steel than for the martensitic steels. Grain refinement appears to be an ineffective means of strengthening medium carbon martensitic steels. In addition toughness properties are not significantly changed and, as was mentioned previously, it has been shown that grain refinement does not improve the K_{ISCC} values for 4340 steel (16).

IV. COMPARISON OF EXPERIMENTAL MARTENSITIC STEELS WITH COMMERCIAL HIGH STRENGTH STEELS

The alloy development studies discussed previously in Section III demonstrated that of the two bainitic alloy systems and two martensitic alloy systems investigated, the best strength and toughness properties were obtained on alloys in the medium carbon Ni-Cr-Mo-Si-V low alloy martensitic system. In addition the stress corrosion studies demonstrated that the low alloy Ni-Cr-Mo-Si-V martensaitic steels had higher SCC resistant, K_{ISCC}, values than the best bainitic steel. It is the purpose of this section, therefore, to compare the properties of the laboratory produced experimental Ni-Cr-Mo-Si-V martensitic steels with similar properties of currently used commercially produced ultra-high strength steels.

PLANE-STRAIN FRACTURE TOUGHNESS

Thick section landing gear components are sufficiently large such that the state of stress around most flaws, if present, would be plane strain. The conditions, therefore, that would lead to brittle fracture will be determined by the plane-strain fracture toughness parameter, K_{IC}. A summary of the plane-strain fracture toughness data for H-11, 4340, 300 M, HP 9-4-45, and 18 Ni maraging steels at room temperature and -65 F are illustrated in Figures 86, and 87 respectively. To the extent that was possible all of the K_{IC} data used to comprise Figures 86, and 87 were judged to be valid K_{IC} data. The K_{IC} data for 4340 steel were obtained from references (28, 35, and 36). The data for H-11 were obtained from references (35, 36, and 37). The data for HP 9-4-45 steel were obtained from references (37 and 38), for 300 M steel references (28, 37, 39, and 15); for 18 Ni maraging steel references (15, 37, 38, 40, and 41).

The room temperature fracture toughness data shown in Figure 86, reveal the usual trend of decreasing toughness with increasing strength level for all steels. At the 260 to 280 ksi strength level HP 9-4-45 steel heat treated

in the bainitic condition has the highest fracture toughness values. The drawback of the HP 9-4-45 bainitic alloy is that in thick sections the highest strength that can be guaranteed is 260 ksi. The strength-toughness relationships for the 18 Ni maraging steels are seen to be very good, however, the 18 Ni maraging steels have not been used for aircraft landing gear components because of problems with thermal embrittlement in thick sections, low notch fatigue properties, and a low strain hardening exponent. The other three steels, H-11, 4340, and 300 M have all been used in production for aircraft landing gear forgings and, of course, the 300 M alloy is used extensively today in current aircraft. It can be seen from the fracture toughness data at both temperatures (Figures 86 and 87) that the strength-fracture toughness relationships for the new low alloy Ni-Cr-Mo-Si-V martensitic steels are considerably superior to the strength-toughness relationships of 4340, H-11, and 300 M steels. It should be noted that the fracture toughness data on the experimental-laboratory martensitic steels are thought to be conservative or low side fracture toughness values. Our experience with both 300 M steel and the HP 9Ni-4Co steels has indicated that for the same composition the fracture toughness properties obtained on production material, from large ingots using electric furnace air melt-vacuum arc remelt practice, are superior to those obtained on small laboratory VIM ingots. The fracture toughness properties of the experimental steels are, therefore, expected to increase by 10 to 15 percent when determined from production VAR material. The strength-toughness relationships in Figures 86 and 87 reveal that the strength level of the new low alloy martensitic steels has been increased by about 25,000 psi (from about 250 ksi to 310 ksi) while maintaining the same level of fracture toughness.

The crack propagation resistance of these steels can be compared in terms of critical crack size rather than the absolute magnitude of K_{IC}. Fracture mechanics analyses demonstrate that fracture will occur when

$$K_{IC} = 1.1\,\sigma\sqrt{\pi C}\ \frac{1}{\sqrt{Q}} \qquad (1)$$

where:

σ = gross area applied stress
C = critical crack depth
Q = geometric flaw shape parameter

In airframe design, the applied stress is often limited to a fraction of the material ultimate tensile strength (σ_μ); i.e.,

$$\sigma = f\,\sigma_\mu \qquad (2)$$

where f is a design parameter. Therefore, equation (1) can be written as:

$$K_{IC} = 1.1\,f\,\sigma_\mu\sqrt{\pi C}\ \frac{1}{\sqrt{Q}} \qquad (3)$$

or:

$$C = \frac{Q}{1.21\,\pi f^2}\left(\frac{K_{IC}}{\sigma_\mu}\right)^2 \qquad (4)$$

The critical crack size is therefore proportial to $(K_{IC}/\sigma_\mu)^2$. Using the room temperature ultimate tensile strengths and K_{IC} values from Figure 86, the critical crack size parameter $(K_{IC}/\sigma_\mu)^2$ was calculated and are compared in Figure 88. This comparison of critical flaw size parameters reveals that the new Ni-Cr-Mo-Si-V martensitic steels at a tensile strength level of about 310 ksi have the same critical crack size as 300 M steel at 280 ksi, 4340 at 260 ksi and H-11 at 240 ksi. In other words the new experimental steels have the same flaw size tolerance as the commercial H-11, 4340, and 300 M steels at considerably higher strength levels.

CHARPY IMPACT DATA

The room temperature Charpy impact data for the new experimental martensitic steels are compared to similar data for commercial high strength steels in Figure 89. There were insufficient CVN data on commercial steels at -65 F to make a comparison at this test temperature. All of the CVN data are from longitudinally oriented specimens and the data for the commercial steels were taken from references (15, 28, 38, and 42). The data in Figure 89 reveal that a rather large degree of scatter exists for 300 M steel, however, this is not unexpected as the Charpy impact test is known to be more sensitive to inclusion contents than the plane-strain fracture toughness test. The data also reveal that for a given strength level the Charpy impact energy values for the 18 Ni maraging steels are rather low compared to 4340, HP 9-4-45, and 300 M steels. This is now a commonly observed behavior that while the 18 Ni maraging steels have high fracture toughness, they have relatively low CVN energy values. This characteristic of 18 Ni maraging steels is probably a result of the ease of plastic instability in this material. It can be seen from Figure 89 that the strength-Charpy impact toughness relationships of the new martensitic steels are significantly superior to all of the commercial steels.

STRESS CORROSION RESISTANCE

It is well known that ultra-high strength steels are very susceptible to stress corrosion cracking. To avoid stress corrosion cracking in ultra-high strength landing gear components ective treatments such as cadmium plating and painting have been ap d, and shot peening has been used to induce residual surface compressive stresses in order to suppress crack initiation. In recent years the SCC resistance of high strength materials has been determined by the use of fatigue cracked fracture toughness specimens, which have the two-fold advantage of reducing the inherent appreciable scatter incurred with the use of unnotched specimens, and providing a SCC resistance parameter which is quantitative and provides the possibility of use in design.

The threshold stress intensity values, K_{ISCC}, for the Ni-Cr-Mo-Si-V martensitic steels are compared to the K_{ISCC} values for the commercial high strength steels in Figure 90. The K_{ISCC} values for the commercial steels were obtained from references (12, 15, 16, 43, 44, and 45). The data reveal that in the strength level range of 260 to 280 ksi, 4340, 300 M, and H-11 steels have K_{ISCC} values in the range of 10 to 20 ksi $\sqrt{in}$. At strength levels in the vicinity of 300 ksi, however, the maraging steels SCC resistance decreases to K_{ISCC} values of 7 to 12 ksi $\sqrt{in}$. The new low alloy martensitic steels at much higher strength levels (298 to 332 ksi) have K_{ISCC} values in the range

of 16 to 19 ksi $\sqrt{in}$. The strength - SCC resistance relationships of the newly developed martensitic steels have, therefore, been improved compared to both 18 Ni maraging and 4340, 300 M, and H-11 steels. Even with this improvement, however, these levels of SCC resistance are not inherently high and therefore these steels will not be able to be applied from an engineering reliability standpoint by means of the fracture mechanics approach utilizing the knowledge of the stress state, defect size and periodic nondestructive inspection techniques. These new ultra-hign strength low alloy steels will, therefore, have to be utilized in the same manner that the present high strength steels have been so successfully utilized from a SCC resistance standpoint, by means of plating, painting, and shot peening.

FATIGUE PROPERTIES

The complete notch and unnotch fatigue properties of both experimental bainitic and martensitic steels were presented and discussed previously in section C-2. In Figure 91 the unnotch fatigue properties of the Ni-Cr-Mo-Si-V martensitic steels are compared to similar fatigue properties for several commercial steels. All of the data shown in Figure 91 are for tension-tension fatigue tests at R values of either +0.06 or +0.10. The rather large body of rotating-beam (R = -1.0) fatigue data on high strength steels could not be utilized for such a comparison. The fatigue data on the commercial steels were obtained from references (15, 30, 31, 32, and 38). The comparison reveals that the experimental martensitic steels have considerably higher fatigue strengths than the commercial steels. The experimental martensitic steels demonstrated 10^7 cycle fatigue strengths in the range of 170 to 190 ksi while the commercial steels exhibited 10^7 cycle fatigue strengths in the range of 90 to 130 ksi. Both groups of steels seem to have a trend of decreasing fatigue strength with increasing tensile strength level. This effect has been observed previously (46), however, neither the reason or the significance of this trend is understood at the present time. It is believed that the reason the experimental martensitic steels have greater fatigue strengths than the commercial steels is a higher degree of microcleanliness in the experimental steels. Except as it effects tensile strength level, composition is known to have little effect on fatigue properties of ultra-high strength steels. This basic difference between the laboratory produced steels and the commercially produced steels can be seen by comparing the fatigue strengths of laboratory produced 300 M steel versus commercially produced 300 M steel. It is anticipated, therefore, that the new low alloy martensitic steel when melted by commercial steelmaking practice, in large ingot sizes, will have fatigue strengths in the range of 130 to 150 ksi, when tested under similar conditions.

V. SUMMARY AND CONCLUSIONS

Exhaustive and detailed alloy development and processing investigations were conducted in order to develop an ultra-high strength steel in the 300 to 320 ksi ultimate tensile strength range, with improved fatigue strength, fracture toughness, and stress corrosion resistance for greater reliability in forged landing gear components. Two bainitic alloy systems and two martensitic alloy systems were thoroughly investigated in order to develop the best combination of mechanical properties at tensile strength levels in

excess of 300,000 psi. Of the four alloy systems investigated, steels from the low alloy medium carbon Ni-Cr-Mo-Si-V martensitic system developed the best combination of fracture toughness, fatigue strength and stress corrosion cracking resistance.

The stress corrosion st[illegible] demonstrated that while lowering phosphorous and sulfur levels is beneficial to toughness properties it has essentially no effect on SCC resistance, as indicated by the K_{ISCC} parameter, for either high strength bainitic or martensitic steels. Similar studies in low alloy martensitic steels demonstrated that variations in silicon, chromium, and molybdenum significantly effected plane strain fracture toughness properties, while having no effect on K_{ISCC} values. The low alloy Ni-Cr-Mo-Si-V steels had higher SCC resistance than the best medium alloy bainitic steel.

The processing studies conducted on two bainitic alloys and one martensitic alloy revealed that the vacuum arc remelted steels had the highest level of fracture toughness, while the electroslag remelted materials had the lowest level of fracture toughness with the vacuum induction melted material being intermediate in toughness properties. Considering the influence of melting practice on fatigue properties, for the two bainitic steels the ESR material had the highest fatigue strengths, and the VIM material the lowest fatigue strengths. For the martensitic steel the VAR material had the highest fatigue strengths followed by the ESR material and then the VIM material. The experimental steels demonstrated unnotch 10^7 cycle fatigue strengths in the range of 170,000 to 210,000 psi. The notch (K_t = 3.0) fatigue strengths of the VAR bainitic steel and the VAR martensitic steel were essentially the same (80,000 psi) at 10^7 cycles. Thermal-mechanical working treatments demonstrated that the strength and toughness properties of ultra-high strength low alloy martensitic and bainitic steels are little influenced by refinement of the prior austenite grain size.

Comparison with similar properties of currently used and commercially melted ultra-high strength steels, revealed that the strength-toughness properties of the new low alloy martensitic steels were superior to the strength toughness properties of the commercially produced steels. Comparison of the threshold stress intensity (K_{ISCC}) SCC resistance parameter indicated that the new martensitic steels had higher K_{ISCC} values than the current commercial steels at a considerably higher strength level. The tension-tension (R = +0.10) unnotch fatigue strengths at 10^7 cycles were in the range of 170 to 190 ksi for the newly developed martensitic steels compared to 90 to 130 ksi for the commercial steels.

From the alloy development and processing studies a new improved ultra-high strength martensitic steel with a nominal composition of

C	Mn	P	S	Si	Ni	Cr	Mo	V
0.40	0.35	<.010	<.010	2.25	1.8	0.80	0.25	0.22

has been developed. When heat treated by normalizing, austenitizing, oil quenching, refrigerating, and double tempering at 600 F the alloy develops the following average longitudinal, room temperature properties based on laboratory sized heats:

U.T.S., ksi	311
Y.S., ksi	268
Elongation, %	12
Reduction of area, %	44
CVN, ft-lbs	20
K_{IC}, ksi $\sqrt{in.}$	60
K_{ISCC}, ksi $\sqrt{in.}$	17
Axial fatigue strength at 10^7 cycles, $K_t = 1$, ksi	170
Axial fatigue strength at 10^7 cycles, $K_t = 3.0$, ksi	80

REFERENCES

1. "Tentative Method of Test for Plane-Strain Fracture Toughness of Metallic Materials", 1970 Annual Book of ASTM Standards, Part 31, July, 1970, p. 911.

2. J. A. Kies, H. L. Smith, H. E. Romine, and H. Bernstein, "Fracture Testing of Weldments", Fracture Toughness Testing And Its Applications, ASTM STP-381, 1965, p. 328.

3. R. F. Hehemann, V. J. Luhan, and A. R. Troiano, "The Influence of Bainite on Mechanical Properties", Trans. ASM, 49, 1957, p. 409.

4. J S. Pascover, and S. J. Matas, "Relationships Between Structure and Properties in the 9Ni-4Co Alloy System", ASTM STP-370, 1965.

5. D. W. Smith, W. Richardson, and R. F. Hehemann, Phase Transformations and Structure-Property Relationships, Progress Report to Office of Naval Research, July, 1968, Contract No. ONR No. N0014-67-A-0404-0001.

6. A. R. Elsea, F. J. Borone, and W. R. Warke, United States Patent No. 3,293,028, Dec. 20, 1966.

7. ASM Metals Handbook, 8th Edition, Vol. 1, 1961, p. 637.

8. P. M. Kelly, and J. Nutting, "The Morphology of Martensite", JISI, 197, March, 1961, p. 199.

9. S. K. Das, and G. Thomas, "Structure and Mechanical Properties of Fe-Ni-Co-C Steels", Trans. ASM, 62, 1969, p. 45.

10. P. M. Kelly, and J. Nutting, "The Martensite Transformation in Carbon Steels", Proc. Roy. Soc., A, 259, 1960, p. 45.

11. W. F. Brown, Jr., and J. E. Srawley, "Commentary on Present Practice", Review of Developments in Plane Strain Fracture Toughness Testing, ASTM STP-463, 1970, p. 216.

12. C. S. Carter, "The Effect of Silicon on the Stress Corrosion Resistance of Low Alloy, High Strength Steels", Corrosion-NACE, October, 1969, Vol. 25, No. 10, pp. 423-431.

13. C. S. Carter, "Crack Extension in Several High Strength Steels Loaded in 3.5% Sodium Chloride Solution", Boeing Document D6-19770, 1967 (available from Defense Documentation Center).

14. A. J. Stavros and H. W. Paxton, "Stress-Corrosion Cracking Behavior of an 18 Pct Ni Maraging Steel", Met. Trans., Vol. 1, No. 11, November 1970, pp. 3049-3055.

15. C. S. Carter, "Evaluation of a High-Purity 18% Ni (300) Maraging Steel Forging, AFML-TR-70-139, June, 1970, Air Force Materials Laboratory, Wright-Patterson Air Force Base.

16. R. P. M. Proctor and H. W. Paxton, "The Effect of Prior-Austenite Grain Size on the Stress-Corrosion Cracking Susceptibility of AISI 4340 Steel", ASM Trans. Quart., 62, December, 1969, 989.

17. G. Sandoz, ARPA Coupling Program on Stress-Corrosion Cracking (Thirteenth Quarterly Report), NRL Memorandum Report 2101, March, 1970.

18. Robert F. Thomson, "Fatigue Behavior of High-Carbon High-Hardness Steels", ASM Trans. Vol. 56, 1963, pp. 803-833.

19. M. Atkinson, "The Influence of Non-Metallic Inclusions on the Fatigue Properties of Ultra-High-Tensile Steels", Journal of the Iron and Steel Institute, Vol. 195, May, 1960, pp. 64-75.

20. R. F. Johnson and J. F. Sewell, "The Bearing Properties of 1% C-Cr Steel as Influenced by Steelmaking Practice", Journal of the Iron and Steel Institute, Vol. 196, December, 1960, pp. 414-444.

21. William C. Stewart and W. Lee Williams, "Effects of Inclusions on the Endurance Properties of Steels", Journal of the American Society of Naval Engineers, Vol. 60, 1948, pp. 475-504.

22. H. N. Cummings, F. B. Stulen, and W. C. Schulte, "Tentative Fatigue Strength Reduction Factors for Silicate-Type Inclusions in High-Strength Steels", Proceedings of the ASTM, Vol. 58, 1958, pp. 504-514.

23. H. N. Cummings, F. B. Stulen, and W. C. Schulte, "Relation of Inclusions to the Fatigue Properties of SAE 4340 Steel", ASM Trans., Vol. 49, 1957, pp. 482-516.

24. Roland Kiessling, "The Influence of Non-Metallic Inclusions on the Properties of Steel", Journal of Metals, Vol. 22, No. 10, October, 1969, pp. 48-54.

25. W. E. Duckworth and E. Ineson, "The Effects of Externally Introduced Alumina Particles on the Fatigue Life of En 24 Steel", The Iron and Steel Institute Special Report 77, 1963, pp. 87-103.

26. L. O. Uhrus, "Through-Hardening Steels for Ball Bearings-Effect of Inclusions on Endurance", The Iron and Steel Institute Special Report 77, 1963, pp. 104-109.

27. J. D. Murray and R. F. Johnson, "The Effect of Inclusions on the Properties of 1% C-Cr Bearing Steels", The Iron and Steel Institute Special Report 77, 1963, pp. 110-118.

28. J. J. Hauser, and M. G. H. Wells, "Inclusions in High Strength Steels, Their Dependence on Processing Variables and Their Effect on Engineering Properties", AFML-TR-69-339, February, 1970, Air Force Materials Laboratory, Wright-Patterson Air Force Base.

29. Metallic Materials and Elements for Aerospace Vehicle Structures, MIL-HDBK-5A, February 8, 1966.

30. C. L. Harmsworth, "Low Cycle Fatigue Evaluation of Titanium 6Al-6V-2Sn and 300 M Steel for Landing Gear Applications", AFML-TR-69-48, June, 1969, Air Force Materials Laboratory, Wright-Patterson Air Force Base.

31. R. L. Jones and F. C. Nordquist, "An Evaluation of High-Strength Steel Forgings", RTD-TDR-63-4030, May, 1964, Air Force Materials Laboratory, Wright-Patterson Air Force Base.

32. T. P. Groeneveld, R. C. Simon, and D. P. Moon, "High Strength Steel 9Ni-4Co", DMIC Processes and Properties Handbook, 1969.

33. F. Borik, and R. D. Chapman, "The Effect of Microstructure on the Fatigue Strength of a High Carbon Steel", Trans. ASM, 53, 1961, p. 447.

34. Donald Webster, "The Effect of Deformation Voids on Austenite Grain Growth in Steels", Trans. ASM, 62, June, 1969, p. 470.

35. E. A. Steigerwald, "Plane Strain Fracture Toughness for Handbook Presentation", AFML-TR-67-187, July, 1967, Air Force Materials Laboratory, Wright-Patterson Air Force Base.

36. E. T. Wessel, W. G. Clark, and W. K. Wilson, "Engineering Methods for Design and Selection of Materials Against Fracture", Contract DA-30-067-AMC-602(T), Westinghouse Research Laboratories Report, 1966.

37. D. F. Bullock, T. W. Eichenberger, and J. L. Guthrie, "Evaluation of the Mechanical Properties of 9Ni-4Co Steel Forgings", AFML-TR-68-57, Air Force Materials Laboratory, Wright-Patterson Air Force Base.

38. J. Wolf, and W. F. Brown, Jr., Aerospace Structural Metals Handbook, Vol. 1, Ferrous Alloys, 1970, AFML-TR-68-115, Air Force Materials Laboratory, Wright-Patterson Air Force Base.

39. S. L. Pendleberry, "Fracture-Toughness and Crack-Propagation Properties of Several High Strength Steels for Aircraft Structure", paper presented at AIAA/ASME 11th Structures, Structural Dynamics, and Materials Conference, Denver, April, 1970.

40. I. Perlmutter, and V. DePierre, "Steels for Solid-Propellant Rocket-Motor Cases", AFML-TR-64-356, January, 1965, Air Force Materials Laboratory, Wright-Patterson Air Force Base.

41. A. F. Hoenie et al., "Determination of Mechanical Property Design Values for 18NiCoMo 250 and 300 Grade Maraging Steels", AFML-TR-65-197, July, 1965, Air Force Materials Laboratory, Wright-Patterson Air Force Base.

42. R. F. Decker, C. J. Novak, and T. W. Landig, "Developments and Projected Trends in Maraging Steels", Journal of Metals, 19, 1967.

43. W. D. Benjamin, and E. A. Steigerwald, "Stress Corrosion Cracking Mechanisms in Martensitic High Strength Steels", AFML-TR-67-98, April, 1967, Air Force Materials Laboratory, Wright-Patterson Air Force Base.

44. W. D. Benjamin, and E. A. Steigerwald, "Environmentally Induced Delayed Failures in Martensitic High Strength Steels", AFML-TR-68-80, April, 1968, Air Force Materials Laboratory, Wright-Patterson Air Force Base.

45. J. H. Mulherin, "Stress-Corrosion Susceptibility of High-Strength Steel in Relation to Fracture Toughness", paper 65-MET 5, ASME, April, 1966.

46. George E. Dieter, Jr., Mechanical Metallurgy, McGraw-Hill Book Company, Inc., New York, 1961, p. 330.

TABLE I

CHEMICAL COMPOSITIONS OF EXPERIMENTAL ALLOYS

Heat No.	C	Mn	Si	P	S	Ni	Cr	Mo	W	V	Al	Co	B	Remarks
B332	0.55	0.81	0.27	<.010	<.010	1.07	0.95	0.54	-	0.10	-			Ni-Cr-Mo-V
B333	0.54	0.79	0.25			2.90	0.94	0.55	-	0.10	-			Bainaging
B334	0.48	0.80	0.27			1.13	1.07	0.54	-	0.10	-			Steels
B335	0.48	0.77	0.24			3.00	1.06	0.55	-	0.10	-			
B336	0.48	0.90	0.30			1.10	1.05	1.02	-	0.10	-	-		
B337	0.48	0.90	0.30			1.10	2.05	1.05	-	0.10	-	-		
B338	0.45	0.85	0.22			1.05	1.00	0.52	-	0.10	-	-		
B339	0.43	0.76	0.17			2.95	1.00	0.54	-	0.10	-	-		
B340	0.44	0.79	0.26			1.20	1.03	1.06	-	0.10	-	-		
B341	0.44	0.70	0.20			1.18	2.05	1.08	-	0.10	-	-		
B342	0.45	0.80	0.26			0.86	3.20	1.10	-	0.10	-	-		
B343	0.43	0.74	0.24			0.85	3.10	2.05	-	0.10	-	-		
B344	0.45	0.77	0.26			3.00	2.15	1.85	-	0.10	-	-		
B345	0.44	0.72	0.23			3.05	2.10	2.05	-	0.10	-	-	.0029	
B346	0.44	0.91	1.40			1.20	2.10	1.17	-	0.10	-	-		
B347	0.44	0.88	1.35			1.20	2.10	1.17	-	0.41	-	-		
B348	0.34	0.81	1.45			1.21	2.10	1.13	-	0.10	-	-		
B349	0.34	1.30	1.35			1.16	2.10	1.13	-	0.10	-	-		
B350	0.33	0.80	0.21			3.05	2.10	1.15	-	0.10	-	-		
B351	0.31	0.73	0.20			3.08	2.10	1.10	-	0.09	-	-	.0030	
B352	0.33	0.70	0.21			3.20	2.10	1.10	-	0.09	-	4.70		
B353	0.41	0.90	0.16			3.20	2.10	1.10	-	0.10	-	4.70		
B354	0.34	0.90	0.26			3.20	1.90	1.10	-	0.10	1.10	-		
B355	0.45	1.50	2.00			1.30	2.00	1.10	-	0.12	-	-		
B356	0.43	0.91	0.27			3.07	1.90	1.00	-	0.10	1.10	-		
B357	0.32	0.82	0.25			3.08	3.00	1.90	-	0.11	-	-		
Z389	0.50	0.73	0.31	<.002	.006	2.85	1.0	1.00	-	0.19	-	3.75		
Z390	0.48	0.74	0.31	<.002	.007	2.85	1.0	1.40	-	0.19	-	3.85		
Z391	0.49	0.75	0.31	<.002	.005	2.85	1.0	1.90	-	0.19	-	3.85		
Z392	0.49	0.78	0.28	<.002	<.005	3.07	-	1.40	-	0.22	-	4.00		

TABLE I (Continued)

CHEMICAL COMPOSITIONS OF EXPERIMENTAL ALLOYS

Heat No.	C	Mn	Si	P	S	Ni	Cr	Mo	W	V	Al	Co	Remarks
Z393	0.49	0.74	0.28	<.002	.006	2.90	0.35	1.43	-	0.21	-	3.85	Ni-Cr-Mo-V
Z394	0.50	0.74	0.28	<.002	.006	2.90	0.75	1.48	-	0.21	-	3.85	Bainaging Steels
B266	0.42	0.33	0.81	<.010	<.010	10.40	0.16	0.15	-	0.084	-	5.85	Medium Alloy
B267	0.41	0.33	0.60			10.21	0.36	0.25	-	0.087	-	5.90	Bainitic
B268	0.44	0.33	0.21			9.75	0.16	0.15	-	0.081	-	5.90	Steels
B270	0.46	0.32	0.20			8.10	0.35	0.33	-	0.080	-	3.93	
B272	0.47	0.33	0.18			9.90	0.17	0.15	-	0.086	-	5.90	
B273	0.46	0.30	0.15			10.11	0.35	0.31	-	0.084	-	7.90	
B297	0.50	0.32	0.20			8.55	0.33	0.35	-	0.086	-	3.93	
B299	0.41	0.30	0.16			9.80	0.33	0.34	-	0.086	-	5.90	
Z211	0.55	0.17	0.08	.003	.002	7.1	0.27	0.28	-	0.10	-	3.8	Medium Alloy
Z212	0.57	0.15	0.08	.003	.002	6.9	0.27	0.26	-	0.10	-	3.8	Bainitic
Z213	0.64	0.15	0.07	.003	.003	7.4	0.27	0.26	-	0.10	-	6.6	Steels
Z214	0.68	0.15	0.07	.003	.003	7.1	0.27	0.26	-	0.10	-	6.6	
Z219	0.46	0.24	0.11	<.010	<.010	3.6	0.25	0.25	-	0.11	-	2.0	
Z220	0.45	0.24	0.76			3.6	0.25	0.25	-	0.11	-	1.9	
Z221	0.47	0.24	1.56			3.4	0.25	0.25	-	0.10	-	2.0	
Z222	0.49	0.40	0.28			4.0	1.50	-	-	-	-	1.0	
Z223	0.47	0.40	0.28			4.0	1.50	-	-	-	-	2.1	
Z224	0.46	0.39	0.28			4.0	1.45	-	-	-	-	3.1	
Z225	0.46	0.25	0.10			3.8	1.00	0.50	-	0.11	-	2.0	
V707	0.39	0.71	0.33	<.010	<.010	1.95	0.48	0.48	0.54	0.09	-	-	Ni-Cr-Mo-W-V
V707	0.42	0.75	0.32			1.95	0.90	0.48	1.05	0.10	-	-	Martensitic
V709	0.40	0.79	0.25			2.05	2.00	0.53	2.10	0.10	-	-	Steels
V710	0.42	0.75	0.33			2.05	0.43	0.90	2.10	0.09	-	-	
V711	0.41	0.79	0.31			2.05	0.98	0.95	0.56	0.09	-	-	
V712	0.40	0.74	0.23			1.97	0.48	0.48	0.53	0.09	-	-	
V713	0.38	0.70	0.25			1.82	0.45	0.45	1.03	0.09	-	-	
V714	0.37	0.91	0.31			1.95	0.55	1.95	2.10	0.11	-	-	
V715	0.37	0.91	0.31			1.9	2.10	1.95	0.53	0.11	-	-	

TABLE I (Continued)

CHEMICAL COMPOSITIONS OF EXPERIMENTAL ALLOYS

Heat No.	C	Mn	Si	P	S	Ni	Cr	Mo	W	V	Al	Co	Remarks
V716	0.37	0.80	0.30	<.010	<.010	1.92	0.97	0.97	-	0.10	-	-	Ni-Cr-Mo-W-V
V717	0.37	0.80	0.30			1.97	0.97	-	1.05	0.10	-	-	Martensitic
V748	0.46	0.82	0.26			1.90	2.05	1.00	1.15	0.09	-	-	Steels
V749	0.41	0.80	0.26			1.90	0.46	1.96	1.15	0.09	-	-	
V750	0.43	0.91	0.27			1.85	1.00	1.97	2.15	0.09	-	-	
V751	0.43	0.90	0.29			1.88	-	1.00	1.15	0.10	-	-	
Z75	0.43	0.77	0.27	.002	.006	1.82	0.49	0.95	2.05	0.11	-	-	Ni-Cr-Mo-W-V
Z77	0.43	0.76	0.26	.002	.006	1.85	2.05	1.00	1.03	0.11	-	-	Martensitic
Z78	0.43	0.78	0.31	.002	.007	1.86	1.08	1.95	2.05	0.11	-	-	Steels
Z79	0.43	0.78	0.27	.002	.005	1.81	0.01	0.95	1.05	0.10	-	-	
Z95	0.42	0.74	0.27	.003	.003	1.83	1.24	1.15	1.26	0.09	-	-	
Z96	0.41	0.72	0.26	.005	.003	1.75	1.22	1.15	2.75	0.09	-	-	
Z97	0.43	0.73	0.30	.002	.002	1.76	1.23	2.67	1.26	0.09	-	-	
Z98	0.43	0.71	0.30	.005	.006	1.73	1.23	2.67	2.75	0.09	-	-	
Z99	0.43	0.73	0.27	.002	.002	1.75	2.63	1.15	1.26	0.09	-	-	
Z100	0.43	0.71	0.27	.007	.002	1.75	2.63	1.15	2.77	0.09	-	-	
Z101	0.42	0.73	0.27	.002	.003	1.80	2.65	2.70	1.29	0.09	-	-	
Z102	0.43	0.71	0.27	.003	.003	1.80	2.65	2.70	2.80	0.09	-	-	
Z105	0.41	0.73	0.25	.002	.002	1.80	2.00	2.00	2.10	0.11	-	-	
Z106	0.42	0.75	0.25	.002	.002	1.80	3.25	1.95	2.15	0.11	-	-	
Z107	0.42	0.75	0.24	.003	.002	1.80	1.95	0.74	2.20	0.10	-	-	
Z108	0.41	0.74	0.24	.003	.002	1.85	2.00	3.10	2.05	0.10	-	-	
Z109	0.42	0.74	0.26	.002	.002	1.85	1.95	1.85	1.95	0.11	-	-	
Z110	0.41	0.72	0.26	.006	.003	1.85	1.95	1.90	3.30	0.11	-	-	
Z111	0.42	0.75	0.29	.006	.003	1.90	0.70	1.85	2.10	0.10	-	-	
Z112	0.41	0.29	0.27	.005	.002	1.90	0.98	-	1.02	0.10	-	-	
Z113	0.40	0.50	0.26	.004	.002	1.90	0.97	-	1.02	0.10	-	-	
Z114	0.42	0.75	0.27	.006	.002	1.89	0.98	-	1.02	0.10	-	-	
Z115	0.41	0.75	0.26	.003	.003	1.90	0.98	-	1.02	0.10	-	-	
Z116	0.42	0.72	1.62	.004	.002	1.80	0.96	-	1.02	0.10	-	-	
Z117	0.42	0.72	2.51	.002	.002	1.80	0.97	-	1.02	0.10	-	-	

TABLE I (Continued)

CHEMICAL COMPOSITIONS OF EXPERIMENTAL ALLOYS

Heat No.	C	Mn	Si	P	S	Ni	Cr	Mo	W	V	Al	Co	Remarks
Z118	0.42	0.74	0.26	.003	.002	1.89	0.98	-	1.02	0.10	-	-	Ni-Cr-Mo-W-V
Z119	0.43	0.74	0.26	.003	.002	1.90	1.02	-	1.02	0.19	-	-	Martensitic
Z120	0.44	0.75	0.26	.003	.002	1.90	1.05	-	1.02	0.31	-	-	Steels
Z386	0.39	0.53	2.18	<.002	<.005	1.72	1.00	0.25	-	0.19	-	-	
Z387	0.40	0.53	2.11	<.002	<.005	1.70	1.02	0.25	0.34	0.19	-	-	
Z388	0.40	0.53	2.19	<.002	<.005	1.70	1.00	0.25	0.75	0.19	-	-	
Z43	0.38	0.34	1.05	.004	.005	2.00	0.60	0.25	-	0.21	.010	-	Ni-Cr-Mo-Si-V
Z44	0.38	0.34	1.70	.004	.005	1.80	0.60	0.26	-	0.21	.012	-	Martensitic
Z45	0.38	0.35	2.65	.004	.005	1.80	0.60	0.26	-	0.21	.013	-	Steel
Z46	0.39	0.36	1.65	.006	.006	2.15	0.62	0.29	-	0.20	.011	0.97	
Z47	0.39	0.36	1.65	.004	.007	2.10	0.89	0.29	-	0.20	.011	1.01	
Z48	0.39	0.36	1.65	.004	.006	2.05	1.60	0.29	-	0.20	.011	1.01	
Z49	0.39	0.36	1.65	.005	.006	3.00	0.01	0.53	-	0.21	.011	1.06	
Z50	0.36	0.36	1.65	.006	.006	3.00	0.67	0.54	-	0.21	.018	1.06	
Z51	0.38	0.37	1.65	.006	.006	3.00	1.60	0.55	-	0.20	.018	1.06	
Z55	0.39	0.36	0.31	.005	.006	2.20	0.92	0.39	-	0.10	.011	-	
Z56	0.37	0.36	1.60	.004	.006	2.10	0.95	0.41	-	0.10	.026	-	
Z57	0.37	0.36	2.55	.004	.005	2.05	0.95	0.42	-	0.10	.032	-	
Z58	0.38	0.35	0.33	.007	.006	2.10	0.97	0.42	-	0.20	.012	-	
Z59	0.38	0.36	1.65	.004	.005	2.05	0.97	0.41	-	0.20	.024	-	
Z60	0.37	0.36	2.65	.004	.005	2.00	0.98	0.43	-	0.20	.033	-	
												Cb	
Z332	0.41	0.34	2.55	<.002	.007	2.00	0.72	0.27	-	-	-	-	Cb-Series
Z333	0.40	0.33	2.50	<.002	.007	2.08	0.72	0.26	-	-	-	.039	Martensitic
Z334	0.40	0.35	2.40	<.002	.008	1.98	0.70	0.25	-	-	-	.070	Steels
Z273	0.41	0.36	2.55	<.002	.008	2.23	0.84	0.26	-	0.21	-	-	Ni-Series
Z274	0.39	0.36	2.55	<.002	.008	2.65	0.84	0.26	-	0.21	-	-	Martensitic
Z275	0.40	0.36	2.55	<.002	.008	3.05	0.84	0.26	-	0.21	-	-	Steels
Z329	0.38	0.34	2.55	<.002	.008	0.52	0.77	0.30	-	0.19	-	-	
Z330	0.38	0.34	2.55	<.002	.009	1.11	0.77	0.25	-	0.19	-	-	
Z331	0.38	0.34	2.60	<.002	.009	1.66	0.77	0.26	-	0.20	-	-	

TABLE I (Continued)

CHEMICAL COMPOSITIONS OF EXPERIMENTAL ALLOYS

Heat No.	C	Mn	Si	P	S	Ni	Cr	Mo	W	V	Al	Co	Remarks
Z276	0.38	0.26	2.60	<.002	.006	1.90	0.78	0.28	-	0.10	-	-	V-Series
Z277	0.38	0.26	2.60	<.002	.006	1.95	0.81	0.28	-	0.20	-	-	Martensitic
Z278	0.38	0.25	2.60	<.002	.006	1.90	0.83	0.28	-	0.29	-	-	Steels
Z270	0.42	0.26	2.55	.002	.008	1.98	0.75	0.26	-	0.20	-	-	Mn-Series
Z271	0.39	0.57	2.67	.002	.008	2.05	0.80	0.26	-	0.21	-	-	Martensitic
Z272	0.39	0.78	2.60	.002	.008	2.05	0.80	0.26	-	0.21	-	-	Steels
R 1	0.39	0.36	1.82	.007	.005	2.00	1.00	0.43		0.22			Ni-Cr-Mo-Si-V
R 2	0.41	0.36	1.78	.004	.005	2.00	1.01	0.84		0.22			Martensitic
R 3	0.42	0.37	1.81	.002	.005	2.00	1.77	0.43		0.22			Steels
R 4	0.41	0.37	1.80	.002	.005	2.00	1.58	0.78		0.22			
R 5	0.42	0.38	2.30	.002	.005	2.15	1.05	0.45		0.23			
R 6	0.41	0.37	2.50	.002	.005	2.15	1.05	0.80		0.23			
R 7	0.40	0.32	2.20	.006	.005	2.15	1.65	0.45		0.18			
R 8	0.40	0.31	2.20	.002	.005	2.00	1.55	0.80		0.18			
9	0.44	0.38	[illegible]	.002	.005	2.02	1.40	0.64		0.20			
10	0.42	0.38	2.75	.002	.005	2.05	1.38	0.68		0.20			
11	0.43	0.35	2.11	.006	.008	2.05	1.75	0.68		0.21			
12	0.40	0.35	2.15	.006	.007	2.07	0.80	0.65		0.21			
13	0.39	0.33	2.02	.002	.005	1.97	1.34	0.26		0.21			
14	0.40	0.33	2.02	.002	.007	2.00	1.35	1.02		0.21			
15	0.39	0.32	2.05	.002	.007	2.07	1.37	0.66		0.22			
Z525	0.41	0.32	2.10	.005	.003	1.80	1.90	0.33		0.24			
Z551	0.39	0.35	2.25	.002	.009	2.00	0.82	0.25		0.20			
Z449	0.39	0.71	1.50	.005	.005	1.72	0.73	0.40		0.06			300 M

TABLE I (Continued)

CHEMICAL COMPOSITIONS OF EXPERIMENTAL ALLOYS

Heat No.	C	Mn	Si	P	S	Ni	Cr	Mo	V	Al	Co	O	N	Remarks
VIM Analysis														
2409	0.39	0.39	2.60	.002	<.005	1.75	0.76	0.28	0.19	.08	-			Low Alloy Martensite
2411	0.52	0.20	0.06	.002	<.005	6.75	0.36	0.24	0.10	.04	4.45			Medium Alloy Bainite
2412	0.49	0.74	0.29	.002	<.002	2.75	0.99	1.36	0.17	.04	4.00			Low Alloy Bainite
Air Melt Analysis														
C229	0.45	0.48	2.67	.002	.014	1.93	0.78	0.26	0.21	-	-	.007	.008	Low Alloy Martensite
C230	0.52	0.37	0.14	.002	.008	6.80	0.38	0.27	0.10	-	4.95	.005	.004	Medium Alloy Bainite
C231	0.53	0.79	0.34	.002	.012	2.90	1.05	1.50	0.20	-	3.80	.006	.011	Low Alloy Bainite
Electroslag Remelt Analysis														
C229	0.44	0.50	2.47	<.005	<.002	1.90	0.86	0.26	0.21	-	-	<.002	.004	Low Alloy Martensite
C230	0.50	0.25	0.03	<.005	.003	6.90	0.34	0.24	0.09	-	5.20	.009	.003	Medium Alloy Bainite
C231	0.51	0.80	0.28	<.005	.004	2.90	1.05	1.52	0.20	-	4.10	.002	.010	Low Alloy Bainite
VAR Analysis														
3888808	0.38	0.53	2.57	.009	<.005	1.70	0.80	0.27	0.22	.08	-	.002	.004	Low Alloy Martensite
3888800	0.49	0.25	0.01	.008	<.005	7.10	0.39	0.36	0.07	.02	5.20	.004	.004	Medium Alloy Bainite
3888811	0.35	0.38	2.13	.005	.009	1.67	1.80	0.34	0.24	.05	-	.003	.005	Low Alloy Martensite
2351	0.40	0.37	2.60	.005	.007	2.00	0.76	0.26	0.20	-	-			Low Alloy Martensite
2350	0.42	0.39	2.63	.005	.007	2.00	0.77	0.27	0.20	-	-			Low Alloy Martensite

TABLE I (Continued)

CHEMICAL COMPOSITIONS OF EXPERIMENTAL ALLOYS

Heat No.	C	Mn	Si	P	S	Ni	Cr	Mo	V	Al	Co	Remarks
V723	0.41	0.27	0.10	.003	.002	8.55	0.28	0.33	0.09	-	4.36	9-4-45 (P + S)
V724	0.42	0.23	0.09	.013	.020	8.41	0.36	0.40	0.09	-	4.30	Steels
V725	0.44	0.27	0.05	.022	.025	8.34	0.30	0.34	0.08	-	4.30	↓
V726	0.42	0.27	0.09	.004	.025	8.30	0.30	0.33	0.09	-	4.22	
V727	0.42	0.25	0.08	.020	.009	8.20	0.28	0.40	0.09	-	4.17	
V746	0.44	0.27	0.06	.004	.010	7.97	0.31	0.32	0.07	-	4.20	

TABLE II

MECHANICAL PROPERTIES OF LOW ALLOY BAINAGING STEELS

	Isothermally Transformed Lower Bainite					Bainaged 950 F, 4 Hrs				
Heat No.	Y.S. ksi	U.T.S. ksi	El. %	R.A. %	CVN ft-lb	Y.S. ksi	U.T.S. ksi	El. %	R.A. %	CVN ft-lb
B332	264	312	9	21	9	216	229	12	31	13
B333	246	304	10	29	15	214	227	12	33	14
B334	246	293	10	35	14	213	223	12	35	16
B335	226	272	12	44	17	205	218	14	43	17
B336	244	293	11	37	11	229	242	14	39	14
B337	214	286	12	41	9	214	253	12	33	12
B338	223	262	14	49	16	201	212	15	31	18
B339	205	252	13	45	18	197	209	15	46	19
B340	220	265	12	42	14	218	230	14	45	17
B341	206	274	12	42	8	209	244	14	43	12
B342	193	286	14	37	16	200	270	11	28	10
B343	226	286	13	33	16	213	276	10	23	10
B344	151	286	13	33	20	199	284	11	29	9
B345	175	273	15	37	10	202	276	12	29	9
B346	214	294	14	28	17	178	294	7	6	7
B347	219	281	15	37	20	197	293	8	12	9
B348	182	243	17	43	24	194	264	12	39	13
B349	157	244	17	41	23	165	272	12	24	10
B350	148	232	14	41	26	179	232	15	44	17
B351	175	236	14	42	20	178	228	15	44	19
B353	201	266	14	44	18	217	257	13	38	8
B354	158	222	18	46	30	134	262	14	35	12
B355	157	301	7	6	7	139	295	3	0	3
B356	180	245	15	41	21	157	279	9	12	7
B357	122	253	15	34	18	185	279	14	33	13

Average longitudinal, room temperature properties of air melted heats.

TABLE III

MECHANICAL PROPERTIES OF LOW ALLOY BAINAGING STEELS

Heat No.	As Transformed					Aged at 950 F					Aged at 1100 F				
	Y.S. ksi	U.T.S. ksi	El. %	R.A. %	CVN ft-lbs	Y.S. ksi	U.T.S. ksi	El. %	R.A. %	CVN ft-lbs	Y.S. ksi	U.T.S. ksi	El. %	R.A. %	CVN ft-lbs
2389	252	311	11	39	14.5	221	235	16	50	15	217	227	13	41	12.5
	250	309	12	41	13.5	221	235	14	47	15	216	229	12	39	14
2390	247	313	11	35	14.5	226	241	12	38	13	219	233	11	39	13
	251	313	11	38	13.5	226	243	12	42	12.5	217	232	11	33	12
2391	229	305	11	36	12.5	233	261	11	34	11	227	251	8	17	10.5
	228	304	12	35	13.5	233	261	12	38	11	226	251	8	17	9.5
2392	258	299	11	43	14.5	233	233	12	38	12.5	223	223	12	33	12
	258	297	12	36	11.5	231	231	9	21	12.5	224	224	10	24	9
2393	262	306	11	47	9	238	239	12	39	13	226	229	12	38	12
	262	305	11	38	12.5	241	242	12	44	14	228	231	12	36	12
2394	261	315	12	40	12.5	236	243	13	43	13	226	234	12	33	8.5
	262	313	10	30	12.5	236	244	14	44	12	226	232	12	31	8

Longitudinal, room temperature properties
Aging time, 4 hours

TABLE IV

MECHANICAL PROPERTIES OF MEDIUM ALLOY BAINITIC STEELS

Heat No.	Y.S. ksi	U.T.S. ksi	El. %	R.A. %	CVN ft-lbs
B266	204	264	12	32	8
	197	264	12	32	8
B267	181	268	15	46	14
	182	267	15	44	14
B268	221	266	10	36	12
	222	265	10	40	13
B270	228	279	11	45	18
	229	271	11	43	18
B272	234	277	12	43	16
	234	277	12	41	16
B273	237	277	11	45	18
	235	277	12	50	18
B297	217	285	12	40	22
	218	283	12	41	20
B299	216	256	13	52	19
	213	256	13	54	24

Room temperature properties of air melted heats tested in longitudinal direction

TABLE V

MECHANICAL PROPERTIES OF MEDIUM ALLOY BAINITIC STEELS

Heat No.	Isothermal-Transformation Temperature, °F	Y.S. ksi	U.T.S. ksi	El. %	R.A. %	CVN ft-lbs
Z211	445	260	301	13	44	11
	495	238	272	11	45	16
Z212	415	266	316	11	39	15
	465	251	290	11	38	15
Z213	435	288	332	7	16	7
	485	268	303	6	11	7
Z214	415	288	336	7	23	7
	465	280	318	8	24	9
Z219	540	232	261	14	51	20
	590	208	232	15	56	29
Z220	540	247	284	13	50	18
	590	218	254	14	55	23
Z221	520	239	286	13	42	16
	570	221	263	13	45	17
Z222	445	218	285	12	41	16
	495	206	265	12	45	17
Z223	470	225	283	12	44	13
	520	207	264	13	46	16
Z224	490	223	281	12	40	11
	540	205	262	11	42	20
Z225	490	231	284	11	40	15
	540	212	264	12	45	15

Average longitudinal, room temperature properties

TABLE VI

MECHANICAL PROPERTIES OF MEDIUM CARBON Ni-Cr-Mo-W-V MARTENSITIC STEELS

		400 F Temper					600 F Temper				
Heat No.	Test Dir.	Y.S. ksi	U.T.S. ksi	El. %	R.A. %	CVN ft-lbs	Y.S. ksi	U.T.S. ksi	El. %	R.A. %	CVN ft-lbs
V707	L	203	257	14	52	27	204	235	14	57	24
	T	207	254	13	48	24	204	235	13	48	20
V708	L	215	290	11	36	10	215	262	11	41	10
	T	220	285	11	31	15	211	259	11	41	10
V709	L	225	286	11	28	13	219	270	12	40	13
	T	218	296	11	26	11	213	267	11	30	10
V710	L	226	279	10	34	14	242	263	11	44	12
	T	222	285	8	[illegible]	11	240	260	8	31	10
V711	L	213	274	12	[illegible]	15	211	258	12	44	11
	T	213	273	9	27	12	207	254	9	27	10
V712	L	221	263	13	45	21	216	246	14	54	19
	T	222	268	11	42	18	216	246	12	47	17
V713	L	213	271	12	45	22	215	246	13	53	20
	T	216	261	12	40	18	214	245	12	48	18
V714	L	230	284	8	21	8	234	271	10	36	9
	T	228	293	6	15	7	229	270	8	26	8
V715	L	213	286	11	32	13	212	266	11	38	11
	T	225	283	10	32	11	210	265	11	40	12
V716	L	195	267	13	40	21	196	242	12	43	16
	T	205	270	15	41	19	198	243	13	41	15
V717	L	201	265	13	45	23	198	241	13	53	17
	T	202	265	12	44	21	197	237	12	51	16
V748	L	217	310	8	18	12	218	282	11	37	12
	T	226	307	8	15	12	220	279	8	17	9
V749	L	231	283	10	26	12	237	267	11	40	11
	T	229	294	11	25	9	238	269	11	35	10
V750	L	235	300	8	18	9	255	282	9	31	10
	T	247	304	8	16	6	250	278	7	18	8
V751	L	236	290	10	34	12	244	264	11	47	12
	T	238	287	10	37	11	245	265	10	40	10
Z75	L	242	300	11	30	13	242	267	10	38	12
Z77	L	211	307	12	30	16	207	274	9	27	14
Z78	L	230	301	9	22	14	236	277	9	34	9
Z79	L	228	294	10	35	13	231	261	10	44	9

Average (2 specimens per condition) room temperature properties
Heats Z75 through Z79 are re-make heats of V710, V748, V750 and V751 respectively

TABLE VII

MECHANICAL PROPERTIES OF MEDIUM CARBON Ni-Cr-Mo-W-V MARTENSITIC STEELS

Heat No.	400 F Temper						500 F Temper						600 F Temper					
	Y.S. ksi	U.T.S. ksi	El. %	R.A. %	CVN, ft-lbs +70 F	CVN, ft-lbs -65 F	Y.S. ksi	U.T.S. ksi	El. %	R.A. %	CVN, ft-lbs +70 F	CVN, ft-lbs -65 F	Y.S. ksi	U.T.S. ksi	El. %	R.A. %	CVN, ft-lbs +70 F	CVN, ft-lbs -65 F
Z95	248	308	10	32	13	12	249	294	9	29	11	-	234	275	10	41	12	10
Z96	259	303	9	25	5	10	271	297	7	24	8	-	253	281	9	34	10	-
Z97	257	306	9	27	8	8	260	292	7	20	7	-	247	275	10	31	11	7
Z98	251	294	7	19	6	8	254	284	7	18	6	-	243	275	8	29	9	6
Z99	245	313	9	23	8	7	235	297	9	29	6	-	237	284	10	29	8	9
Z100	260	309	8	22	8	9	249	297	7	17	4	-	245	285	10	31	10	6
Z101	250	310	-	-	5	3	242	294	-	-	7	-	241	287	9	25	6	5
Z102	245	303	7	15	7	5	241	289	8	21	6	-	240	283	9	26	8	4
Z105	243	304	9	23	9	6	230	287	9	24	10	-	244	290	8	23	9	6
Z106	243	308	9	19	7	6	232	292	8	18	4	-	244	293	10	31	6	6
Z107	248	313	11	33	11	10	246	301	10	36	12	-	245	284	11	39	10	4
Z108	252	299	7	20	8	4	245	285	-	-	8	-	239	281	9	28	7	3
Z109	254	310	12	31	11	8	235	289	10	33	10	-	238	281	11	36	13	4
Z110	256	298	9	25	10	5	251	286	8	25	12	-	241	276	12	30	10	8
Z111	254	296	9	26	10	8	263	283	-	-	10	-	249	270	9	35	10	4
Z112	234	288	13	44	14	10	234	270	11	41	12	-	227	257	11	44	15	10
Z113	231	287	12	45	20	20	228	271	10	37	12	-	218	254	13	50	15	12
Z114	222	283	13	42	20	18	226	267	10	37	14	-	218	252	11	43	13	7
Z115	232	287	12	46	18	15	228	270	10	41	4	-	220	257	11	43	14	10
Z116	252	311	12	37	20	14	255	308	10	32	12	-	258	303	12	39	13	10
Z117	261	323	11	32	12	10	270	319	9	24	10	-	278	323	10	36	12	10
Z118	239	293	12	40	15	10	234	273	11	37	8	-	222	259	11	39	13	7
Z119	241	294	12	40	16	16	237	274	11	40	14	-	236	264	12	47	14	13
Z120	243	290	11	39	18	16	239	275	11	36	14	-	238	262	11	46	14	12

Average longitudinal properties

TABLE VII (Continued)

MECHANICAL PROPERTIES OF MEDIUM CARBON Ni-Cr-Mo-W-V MARTENSITIC STEELS

Heat No.	800 F Temper						1000 F Temper					
	Y.S. ksi	I.T.S. ksi	El. %	R.A. %	CVN, ft-lbs +70 F	CVN, ft-lbs -65 F	Y.S. ksi	U.T.S. ksi	El. %	R.A. %	CVN, ft-lbs +70 F	CVN, ft-lbs -65 F
Z95	227	260	10	35	14	-	218	246	11	36	13	-
Z96	239	257	9	26	12	-	222	240	11	34	11	-
Z97	232	255	9	23	8	-	221	246	9	27	6	-
Z98	228	251	9	26	8	-	222	246	9	25	8	-
Z99	229	272	10	28	10	-	213	255	11	34	10	-
Z100	234	272	9	15	11	-	218	253	9	32	10	-
Z101	234	276	8	15	9	-	217	260	8	23	7	-
Z102	230	270	8	19	8	-	218	262	9	19	9	-
Z105	230	267	9	22	10	-	220	261	10	26	9	-
Z106	233	272	9	16	9	-	221	270	10	29	9	-
Z107	231	264	10	30	11	-	212	243	12	35	14	-
Z108	227	262	10	21	9	-	220	256	9	22	7	-
Z109	230	269	8	29	12	-	219	259	12	37	12	-
Z110	235	262	10	24	11	-	217	244	10	27	10	-
Z111	232	245	8	29	12	-	227	239	10	31	12	-

Average longitudinal properties

TABLE VIII

MECHANICAL PROPERTIES OF Ni-Cr-Mo-W-V MARTENSITIC STEELS

Heat No.	Tempering Temperature °F	Y.S. ksi	U.T.S. ksi	El. %	R.A. %	CVN ft-lbs +70 F	CVN ft-lbs -65 F
Z386	500	270	317	11	38	18	-
	550	269	313	10	38	18	-
	600	268	308	12	42	16	15
	650	269	304	11	44	16	
	700	268	299	11	41	16	12
Z387	500	272	317	11	41	18	-
	550	270	312	10	40	17	-
	600	269	312	13	43	17	13
	650	271	309	11	41	17	-
	700	269	303	12	38	16	13
Z388	500	268	319	11	37	16	-
	550	268	315	10	31	15	-
	600	271	313	10	39	16	12
	650	272	310	11	35	15	-
	700	271	304	11	35	14	12

Average, longitudinal, properties

TABLE IX

MECHANICAL PROPERTIES OF MEDIUM CARBON
Ni-Cr-Mo-Si-V MARTENSITIC STEELS

Heat No.	Tempering Temperature °F	Y.S. ksi	U.T.S. ksi	El. %	R.A. %	Charpy Impact Energy, ft-lbs +70 F	0 F	-65 F	-200 F
Z43	400	243	298	11	46	20	20	20	14
	500	248	291	12	50	19	-	-	-
	600	243	284	9	45	17	16	12	7
	700	228	263	12	50	14	-	-	-
	800	207	232	11	44	22	-	-	-
Z44	400	247	305	11	44	22	21	18	16
	500	254	299	12	47	21	-	-	-
	600	258	298	10	44	20	19	16	10
	700	247	278	13	53	16	-	-	-
	800	216	245	12	50	15	-	-	-
Z45	400	260	317	11	44	22	20	17	10
	500	263	310	11	47	19	-	-	-
	600	263	307	11	45	21	19	17	9
	700	264	298	11	48	17	-	-	-
	800	232	268	13	50	13	-	-	-
Z46	400	258	311	11	42	20	20	19	11
	500	263	306	11	45	19	-	-	-
	600	261	299	10	39	16	16	13	9
	700	257	285	12	51	15	-	-	-
	800	225	250	12	47	14	-	-	-
Z47	400	256	307	10	40	21	20	16	10
	500	261	306	10	42	19	-	-	-
	600	266	306	11	41	19	16	13	10
	700	254	278	11	51	15	-	-	-
	800	221	242	11	45	14	-	-	-
Z48	400	246	313	10	40	20	20	16	7
	500	255	307	11	42	18	-	-	-
	600	256	305	6	16	16	13	12	7
	700	251	291	11	45	12	-	-	-
	800	220	266	12	40	10	-	-	-
Z49	400	256	311	13	42	21	20	14	13
	500	263	301	11	41	20	-	-	-
	600	266	301	11	46	18	16	16	12
	700	251	285	11	48	16	-	-	-
	800	219	251	10	37	14	-	-	-
Z50	400	235	293	11	45	20	18	18	13
	500	242	288	11	43	19	-	-	-
	600	256	297	11	41	14	15	13	11
	700	-	289	12	47	15	-	-	-
	800	222	261	12	40	12	-	-	-

TABLE IX (Continued)

MECHANICAL PROPERTIES OF MEDIUM CARBON
Ni-Cr-Mo-Si-V MARTENSITIC STEELS

Heat No.	Tempering Temperature °F	Y.S. ksi	U.T.S. ksi	El. %	R.A. %	Charpy Impact Energy, ft-lbs +70 F	0 F	-65 F	-200 F
Z51	400	250	261	12	40	12	-	-	-
	500	251	308	10	38	18	17	16	9
	600	256	305	11	39	16	14	14	8
	700	255	300	11	39	13	-	-	-
	800	226	273	11	34	11	-	-	-
Z55	400	230	283	13	50	22	16	16	10
	500	222	264	12	48	18	-	-	-
	600	218	255	12	48	18	16	16	11
	700	209	235	12	50	19	-	-	-
	800	199	218	13	51	23	-	-	-
Z56	400	240	305	10	37	18	18	15	10
	500	246	298	11	39	17	-	-	-
	600	246	295	10	36	16	14	12	6
	700	243	286	11	39	11	-	-	-
	800	210	251	11	39	12	-	-	-
Z57	400	256	316	10	35	18	17	15	7
	500	255	310	11	39	17	-	-	-
	600	261	307	10	41	16	15	13	6
	700	259	299	11	41	14	-	-	-
	800	226	272	11	38	8	-	-	-
Z58	400	235	286	13	50	22	21	21	16
	500	224	264	13	53	18	-	-	-
	600	220	253	12	51	19	16	16	12
	700	209	233	13	56	19	-	-	-
	800	203	221	13	53	23	-	-	-
Z59	400	248	301	11	43	21	20	15	11
	500	244	296	11	39	20	-	-	-
	600	236	294	11	48	19	15	16	10
	700	245	281	11	45	17	-	-	-
	800	216	252	11	41	14	-	-	-
Z60	400	256	312	11	40	20	17	15	8
	500	255	308	10	39	16	-	-	-
	600	263	306	10	42	18	17	13	9
	700	261	300	11	40	17	-	-	-
	800	234	275	13	46	11	-	-	-

Average, longitudinal properties

TABLE X

MECHANICAL PROPERTIES OF Ni-Cr-Mo-Si-V
MARTENSITIC STEELS (Ni, Mn, V, Cb SERIES)

Heat No.	Y.S. ksi	U.T.S. ksi	El. %	R.A. %	CVN ft-lbs +70 F	CVN ft-lbs -65 F	Remarks
Z332	265	310	10	31	11.5	9.5	Columbium Series
	268	312	11	33	13	9.5	
Z333	267	311	11	38	15.5	11	
	268	310	10	38	16	12	
Z334	264	306	12	35	17	14.5	
	266	310	11	38	17	13.5	
Z273	273	317	11	40	16	12	Nickel Series
	271	319	11	37	14	13	
Z274	282	324	11	40	14	13	
	281	325	11	40	14	13	
Z275	279	324	11	40	16	14	
	279	324	12	43	16	13	
Z329	264	311	8	19	13	10.5	
	265	310	8	20	12.5	10.5	
Z330	263	306	10	31	15	12.5	
	261	306	11	37	14.5	11	
Z331	262	303	12	39	18.5	15	
	263	305	11	40	18.5	14.5	
Z276	264	312	8	27	13	11	Vanadium Series
	264	312	9	29	14	11	
Z277	268	310	11	43	16	15	
	-	-	-	-	20	17	
Z278	264	306	11	44	20	16	
	267	307	12	45	20	17	
Z270	271	313	10	38	19	15	Manganese Series
	271	314	12	44	19	14	
Z271	269	315	10	36	16	13	
	267	315	10	34	15	12	
Z272	266	316	11	33	15	12	
	268	315	10	33	14	10	

Longitudinal properties, 600 F tempering temperature

TABLE XI

MECHANICAL PROPERTIES OF STATISTICALLY DESIGNED
Ni-Cr-Mo-Si-V MARTENSITIC STEELS

Heat No.	Y.S. ksi	U.T.S. ksi	El. %	R.A. %	CVN, ft-lbs +70 F	CVN, ft-lbs -65 F	K_{IC}, ksi√in. +70 F	K_{IC}, ksi√in. -65 F	K_{ISCC} ksi √in.
R 1	261	299	11	47	18.5	18	59.8	45.4	18
	256	296	11	44	22	21	62.7	46.2	
					20.5	19	64.3		
R 2	266	307	11	39	16.5	15.5	55.6	42.2	17
	261	303	11	40	15.5	16	60.0	39.0	
					14.5	17	58.9		
R 3	263	309	11	41	18	20.5	61.4	40.3	16
	261	306	11	39	19	19.5	60.0	40.7	
					20	17.5	62.4		
R 4	269	316	9	31	15.5	17	49.6	36.3	16
	268	312	8	25	17	14.5	48.2	37.8	
					17	15.5	49.9		
R 5	269	311	10	36	17	17.5	58.8	42.6	18
	261	301	11	38	20.5	15	59.3	40.7	
					19.5	17.5	58.7		
R 6	271	315	11	36	15	16	49.8	35.5	18
	267	311	11	35	18	15	50.7	35.5	
					16	15	50.5		
R 7	266	315	8	28	16	16.5	58.9	36.0	18
	264	313	10	40	17	13	57.6	38.1	
					19	14.5			
R 8	272	321	12	37	17	17	52.6	36.8	17
	274	321	9	26	18	15.5	49.7	32.2	
					17	14	52.0		
9	273	314	10	29	15	13.5	48.0	35.0	16
	270	312	8	23	16.5	15.5	47.6	35.0	
					14.5	12	48.0		
10	284	333	8	34	16	12	40.5	31.4	16
	286	332	9	31	17.5	11	40.4	29.6	
					15.5	9	40.1		
11	265	311	11	40	16	16.5	54.7	37.6	18
	257	309	9	25	14	17.5	54.2	40.2	
					16.5	16	57.8		
12	263	300	10	42	22	21	66.0	46.3	18
	261	299	10	37	22.5	20.5	64.4	46.2	
					19.5	19	65.0		
13	264	307	11	40	21	17	62.0	44.8	18
	262	307	11	42	19	18	61.4	45.1	
					20	15	60.9		
14	273	316	11	35	17	14.5	47.5	34.1	19
	268	312	10	35	18	9	46.7	36.8	
					18.5	10	46.1		
15	269	310	10	36	19.5	14.5	56.0	40.7	17
	261	306	10	34	19	16.5	56.6	39.2	
					-	18.5	58.8		

Longitudinal properties, 600 F tempering temperature

TABLE XII

MECHANICAL PROPERTIES OF Ni-Cr-Mo-Si-V MARTENSITIC STEELS AND 300 M STEEL

Heat No.	Y.S. ksi	U.T.S. ksi	El. %	R.A. %	CVN, ft-lbs +70 F	CVN, ft-lbs -6 F	K_{IC}, ksi $\sqrt{in.}$ +70 F	K_{IC}, ksi $\sqrt{in.}$ -65 F
Z525	269	315	9.5	40	14.3	13.8	49.6	34.4
	271	316	9.5	42	14.2	9.5	49.1	35.6
Avg.	270	318	9.5	41	14.3	10.7	49.4	35.2
Z551	267	310	11	43	19	16	60.5	45.6
	269	312	12	44	20	17	59.6	44.5
Avg.	268	311	11.5	43.5	19.5	16.5	60.0	45.0
Z549	240	285	10	42	18	15	67.9	48.2
(300M)	246	287	10	43	20	17	63.3	43.0
Avg.	243	286	10	42.5	19	16	65.6	45.6

Longitudinal properties, 600 F tempering temperature

TABLE XIII

COMPARISON OF EXPERIMENTAL AND PREDICTED MECHANICAL PROPERTIES FOR HEATS Z525 AND Z551

	Experimental Results				Predicted Results			
Heat No.	U.T.S. ksi	K_{IC} +70 F	K_{IC} -65 F	CVN ft-lbs	U.T.S. ksi	K_{IC} +70 F	K_{IC} -65 F	CVN ft-lbs
Z525	318	49	35	14	308	65	42	18
Z551	311	60	45	19	292	67	51	22

TABLE XIV

TENSILE, CHARPY, FRACTURE TOUGHNESS, AND STRESS CORROSION PROPERTIES OF 9-4-45 STEEL WITH PHOSPHORUS AND SULFUR ADDITIONS

Heat No.	Microstructure	Test Direction	Y.S. ksi	U.T.S. ksi	El. %	R.A. %	CVN ft-lbs	K_{IC} ksi $\sqrt{in.}$	K_{ISCC} ksi $\sqrt{in.}$	P %	S %
V723	Martensite	L	239	276	10	41	15	61.1	14	.003	.002
	"	T	239	271	10	40	14	-	-		
	Bainite	L	216	267	15	53	25	91.1	16		
	"	T	216	266	12	43	22	-	-		
V724	Martensite	L	246	280	9	34	12	42.3	11	.013	.020
	"	T	245	280	9	33	11	-	-		
	Bainite	L	210	269	11	43	17	64.8	15		
	"	T	210	268	11	36	12	-	-		
V725	Martensite	L	243	283	3	3	8	40.0	11	.022	.025
	"	T	243	285	2	2	5	-	-		
	Bainite	L	215	269	9	34	14	54.0	13		
	"	T	216	266	8	29	11	-	-		
V726	Martensite	L	249	288	7	22	11	43.0	12	.004	.025
	"	T	249	285	6	21	9	-	-		
	Bainite	L	215	269	10	38	13	53.0	18		
	"	T	215	270	9	27	11	-	-		
V727	Martensite	L	241	277	10	44	14	54.0	13	.020	.009
	"	T	240	277	9	41	11	-	-		
	Bainite	L	215	269	12	51	21	71.5	16		
	"	T	214	268	11	47	18	-	-		
V746	Martensite	L	244	277	10	47	14	55.0	11	.004	.010
	"	T	243	282	9	37	12	-	-		
	Bainite	L	215	267	13	50	22	77.0	17		
	"	T	213	268	11	41	20	-	-		

Average room temperature properties

TABLE XV

MECHANICAL PROPERTY COMPARISON OF VIM, ESR, AND VAR EXPERIMENTAL BAINITIC AND MARTENSITIC STEELS

Heat No.	Y.S. ksi	U.T.S. ksi	El. %	R.A. %	CVN, ft-lbs +70 F	CVN, ft-lbs -65 F	K_{IC}, ksi $\sqrt{in.}$ +70 F	K_{IC}, ksi $\sqrt{in.}$ -65 F	Remarks
Z409	270	312	10	41	15	14	55.4	39.0	VIM - Low Alloy Martensite
C229	287	332	7.5	25	11	8	34.3	27.7	ESR - Low Alloy Martensite
3888808	263	309	9	34	17	15	56.2	42.0	VAR - Low Alloy Martensite
Z411	246	299	10	39	13	11	62.0	47.0	VIM - Medium Alloy Bainite
C230	243	290	12	45	16	15	58.8	41.5	ESR - Medium Alloy Bainite
3888800	235	290	13	48	19	12	67.2	49.8	VAR - Medium Alloy Bainite
Z412	260	318	10	33	14	8	34.5	31.9	VIM - Low Alloy Bainite
C231	264	321	10	33	12	7	29.8	23.8	ESR - Low Alloy Bainite

Average, longitudinal properties

TABLE XVI

VOLUME PERCENT INCLUSION DATA ON VIM, ESR, AND VAR MEDIUM ALLOY BAINITIC STEELS

Volume % Inclusions

Alloy	Sample	Threaded Area		Fracture Area	
		AMEDA	Point Counting	AMEDA	Point Counting
Z411	1	.034	.040	-	-
"	3	.047	-	-	-
"	6	.056	-	.028	-
"	8	.038	-	.054	-
"	13	.034	-	-	-
"	Average	.042			
Z411	10	-	-	.072	.058
"	14	-	-	.044	-
				Average .050	
C230	4A	.070	-	-	-
"	4B	.047	-	-	-
"	5A	.048	-	-	-
"	5B	.063	-	-	-
"	11	.047	-	.052	-
"	Average	.055			
C230	12	-	.099	-	-
"	1	-	-	.061	.107
"	10	-	-	.048	-
				Average .054	
3808800	4	-	-	.013	-
"	7	-	-	.015	-
"	9	.018	-	.005	.050
"	10	.004	.020	-	-
				Average .011	

TABLE XVII

COMPARISON OF FATIGUE PROPERTIES OF EXPERIMENTAL STEELS WITH COMMERCIAL HIGH STRENGTH STEELS

Alloy	Melting Practice	Product Form	Test Dir.	R	U.T.S. ksi	10^7 Cycle Fatigue Strength ksi	Fatigue Ratio (10^7 Strength/ U.T.S.)	Micro-structure	Reference
4340	VAR	Billet	-	+0.06	~270	105	.39	Martensite	15
"	"	-	-	"	266	110	.41	"	29
300 M	VAR	Forging	L	+0.10	294	~90	.31	Martensite	30
"	"	-	-	+0.06	~285	118	.39	"	15
"	"	-	-	"	290	120	.41	"	15
H-11	VAR	Billet	T	+0.10	265	130	.49	Martensite	31
18 Ni Maraging	VIM-VAR	Forging	L	+0.06	307	118	.38	Martensite	15
(300 Grade)	VIM-VAR	"	T	"	306	115	.38	"	15
"	VAR	"	L	"	288	118	.41	"	15
"	VAR	"	T	"	289	108	.37	"	15
"	VAR	"	L	0.10	285	113	.40	"	31
"	VAR	"	T	"	283	98	.35	"	31
HP 9-4-45	VAR	Plate	T	+0.10	270	140	.52	Bainite	32
"	VAR	-	L	+0.10	268	134	.50	Martensite	31
"	VAR	Forging	T	"	268	130	.49	"	31
Z351	VIM	1/2" Plate	L	+0.10	321	170	.53	Martensite	THIS Investigation
"	"	"	T	"	312	140	.45	"	"
Z409	"	"	L	"	312	138	.44	"	"
Z411	"	"	"	"	299	~125	.42	Bainite	"
Z412	"	"	"	"	317	160	.51	Bainite	"
Z449 (300 M)	"	"	"	"	286	175	.61	Martensite	"

TABLE XVII (Continued)

COMPARISON OF FATIGUE PROPERTIES OF EXPERIMENTAL STEELS WITH COMMERCIAL HIGH STRENGTH STEELS

Alloy	Melting Practice	Product Form	Test Dir.	R	U.T.S. ksi	10^7 Cycle Fatigue Strength ksi	Fatigue Ratio (10^7 Strength/ U.T.S.)	Micro-structure	Reference
3868900	VAR	1/2" Plate	L	+0.10	290	195	.67	Bainite	THIS Investigation
3868911	"	"	"	"	307	190	.62	Martensite	"
C229	ESR	1/2" Plate	L	+0.10	332	170	.51	Martensite	THIS Investigation
"	"	"	T	"	332	170	.51	"	"
C230	"	"	L	"	290	207	.71	Bainite	"
C231	"	"	"	"	321	210	.66	Bainite	"

R is the ratio of minimum stress to maximum stress

TABLE XVIII

GRAIN SIZE AND HARDNESS OF THERMAL-MECHANICALLY PROCESSED 300M STEEL

Process	Austenitizing Temperature* 1475 F G.S.	1475 F R_c	1500 F G.S.	1500 F R_c	1525 F G.S.	1525 F R_c	1550 F G.S.	1550 F R_c	1575 F G.S.	1575 F R_c	1600 F G.S.	1600 F R_c
a. Spheroidal Anneal Rolled at 1200 F	13.5	55.0	12.2	53.5	11.8	58.5	11.2	57.0	10.7	58.0	10.2	58.5
b. Spheroidal Anneal Rolled at Room Temp.	14.5	56.5	13.7	55.0	12.6	58.0	11.5	56.0	11.5	58.0	11.0	56.5
c. Spheroidal Anneal Cooled to Room Temp. Rolled at 1200 F	14.0	57.0	13.2	57.5	12.4	58.7	11.7	56.0	11.1	58.0	10.4	57.5
d. Quenched and Tempered Rolled at 1200 F	12.8	55.5	12.2	57.3	11.8	57.5	11.0	57.5	10.7	55.5	10.1	57.0
e. Quenched and Tempered Rolled at Room Temp.	12.9	57.3	12.1	58.5	11.3	58.5	11.2	54.5	11.0	58.0	10.4	56.0
f. Quenched and Tempered Cooled to Room Temp. Rolled at 800 F	12.3	57.0	11.9	58.3	10.7	58.0	10.6	57.0	10.5	57.3	10.4	56.0

G.S. = ASTM Number
*Austenitized for 1/2 hour and oil quenched

TABLE XIX

MECHANICAL PROPERTIES OF THERMAL-MECHANICALLY PROCESSED 300M STEEL

Sample No.	Process	Aust. Temp.	ASTM G.S.	Y.S. (ksi)	U.T.S. (ksi)	R.A. (%)	El. (1")	CVN (ft-lbs)
1-1	Sph. Anneal	1475 F	13.5	261.0	293.2	29.3	9.0	14
1-2	Roll at 1200 F			259.0	289.2	30.5	9.0	14
Avg.				260.0	291.2	29.9	9.0	14
1-3		1525 F	11.8	253.0	288.2	29.9	10.0	17
1-4				253.0	288.2	36.3	10.0	17
Avg.				253.0	288.2	33.1	10.0	17
2-1	Sph. Anneal	1475 F	14.5	258.0	289.2	36.9	9.0	15
2-2	Roll at R.T.			260.5	290.2	32.5	10.0	17
Avg.				259.2	289.7	34.7	9.5	16
2-3		1525 F	12.6	253.0	288.2	39.6	10.0	18
2-4				251.5	288.2	38.4	10.0	16
Avg.				252.2	288.2	39.0	10.0	17
3-1	Sph. Anneal	1475 F	14.0	267.1	293.2	32.5	9.0	15
3-2	Cool to R.T.			267.1	293.2	31.1	9.0	16
Avg.	Roll at 1200 F			267.1	293.2	31.8	9.0	15.5
3-3		1525 F	12.4	257.0	291.2	31.1	10.0	19
3-4				256.5	291.2	31.9	10.0	19
Avg.				256.7	291.2	31.5	10.0	19
4-1	Tempered Mart.	1475 F	12.8	253.5	289.2	35.7	12.0	19
4-2	Roll at 1200 F			252.0	290.2	33.7	11.0	19
Avg.				252.7	289.7	34.7	11.5	19
4-3		1525 F	11.8	248.0	288.2	36.9	11.0	20
4-4				247.0	288.2	39.6	12.0	22
Avg.				247.5	288.2	38.2	11.5	21
5-1	Tempered Mart.	1475 F	12.9	249.0	291.0	39.0	11.0	20
5-2	Roll at R.T.			251.0	291.2	40.2	11.0	20
Avg.				250.0	291.1	39.6	11.0	20
5-3		1525 F	11.6	248.0	290.2	41.4	12.0	20
5-4				249.5	290.2	40.2	12.0	20
Avg.				248.7	290.2	40.6	12.0	20
6-1	Tempered Mart.	1475 F	12.3	253.0	293.2	40.8	11.0	19
6-2	Roll at 800 F			252.0	293.2	35.7	12.0	20
Avg.				252.5	293.2	38.7	11.5	19.5
6-3		1525 F	10.7	251.0	291.2	38.4	11.0	20
6-4				251.0	291.0	40.2	11.0	22
Avg.				251.0	291.1	39.3	11.0	21
Avg.	Conventional Processing and Heat Treatment	1600 F	9.4	241.6	282.3	44.7	12.0	30

All material tempered at 600 F for 2 + 2 hours

TABLE XX

GRAIN SIZE AND HARDNESS OF THERMAL-MECHANICALLY PROCESSED LOW ALLOY MARTENSITIC STEEL (Z350)

	1575 F		1600 F		1625 F		1650 F		1675 F		1700 F	
	G.S.	R_c	G.S.	R_c	G.S.	R_c	G.S.	R_c	G.S.	R_c	G.S.	R_c
a. Spheroidize Anneal, Rolled at 1100 F	12.6	57.7	11.5	56.7	11.0	55.7	10.6	55.0	10.0	56.0	9.6	55.7
b. Spheroidize Anneal, Cooled to Room Temp. Rolled at 1100 F	11.8	55.7	10.6	56.0	9.9	55.0	9.7	55.7	9.3	53.0	9.0	53.7
c. Quenched and Tempered, Cooled to Room Temp, Rolled at 1200 F	11.0	57.0	10.3	55.7	10.1	56.0	9.6	54.7	9.9	55.5	9.7	53.0
d. Quenched and Tempered, Cooled to Room Temp, Rolled at 800 F	12.0	57.0	11.5	55.0	10.8	55.0	10.1	55.7	10.0	56.0	9.1	55.7

G.S. = ASTM number
*Austenitized for 1 hour and oil quenched

TABLE XXI

MECHANICAL PROPERTIES OF THERMAL-MECHANICALLY PROCESSED LOW ALLOY MARTENSITIC STEEL (2350)

Sample No.	Process	Aust. Temp	ASTM G.S.	Y.S. ksi	U.T.S. ksi	R.A. %	El. (1") %	CVN (ft-lbs)
1-1	Sph. Anneal	1600 F	11.5	288.2	316.2	35.1	9.0	17.0
1-2	Roll at 1100 F			291.2	321.3	36.9	10.0	19.0
Avg.				289.7	318.7	36.0	9.5	18.0
3-1	Sph. Anneal	1600 F	10.6	284.1	316.2	33.7	9.0	16.5
3-2	Cool to R.T.			282.1	317.2	34.5	9.0	17.0
Avg.	Roll at 1100 F			283.1	316.7	34.1	9.0	16.7
4-1	Tempered Mart.	1600 F	10.3	276.1	315.2	39.0	11.0	16.0
4-2	Cool to R.T.			278.9	318.7	35.7	9.0	17.5
Avg.	Roll at 1200 F			277.5	316.9	37.3	10.0	16.7
6-1	Tempered Mart.	1600 F	11.5	280.1	316.2	40.2	11.0	16.5
6-2	Cool to R.T.			281.4	318.7	41.4	9.0	17.0
Avg.	Roll at 800 F			280.7	317.4	40.8	10.0	16.7
350-1	Conventional	1700 F	8.4	278.1	305.6	29.3	9.0	14.0
350-2	Processing and			279.1	305.8	26.5	9.0	15.0
Avg.	Heat Treatment			278.6	305.7	27.9	9.0	14.5

All material tempered at 600 F for 2 + 2 hours, longitudinal direction

TABLE XXII

MECHANICAL PROPERTIES OF A THERMAL-MECHANICALLY PROCESSED LOW ALLOY BAINITIC STEEL (2412)

Sample No.	Process	Aust. Temp*	ASTM G.S.	Y.S. ksi	U.T.S. ksi	R.A. %	El. (1") %	CVN ft-lbs
1-1	Sph. Anneal	1600 F	11.5	242.0	304.2	33.1	10.0	11.8
1-2	Rolled at 1200 F			241.0	303.2	28.5	10.0	12.0
Avg.				241.5	303.7	30.8	10.0	11.9
1-3		1650 F	11.0	225.9	300.2	30.5	11.0	14.2
1-4				236.9	304.2	31.1	11.0	11.5
Avg.				231.4	302.2	30.8	11.0	12.8
2-1	Sph. Anneal	1600 F	12.4	251.0	306.2	35.1	11.0	12.5
2-2	Cool to R.T.			252.0	306.2	-	9.0	14.0
Avg.	Rolled at 1200 F			251.5	306.2	35.1	10.0	13.2
2-3		1650 F	11.7	230.9	301.2	36.9	9.0	15.2
2-4				228.9	301.2	31.1	11.0	14.5
Avg.				229.9	301.2	34.0	10.0	14.8
3-1	Quenched and	1600 F	11.9	248.5	306.2	32.5	11.0	14.2
3-2	Tempered			245.0	306.2	36.3	11.0	10.6
Avg.	Rolled at 1200 F			246.7	306.2	34.4	11.0	12.4
3-3		1650 F	11.1	232.5	303.2	39.0	12.0	15.0
3-4				229.9	303.2	39.6	12.0	15.0
Avg.				231.2	303.2	39.3	12.0	15.0
412-1	Conventional	1650 F	10 6	228.9	305.2	38.4	13.0	15.0
412-2	Processing and			235.9	305.2	37.6	12.0	14.2
-	Heat Treatment							13.2
Avg.				232.4	305.2	38.0	12.9	14.1

*Austenitized at temperature for one hour and isothermally transformed at 475 F for six hours

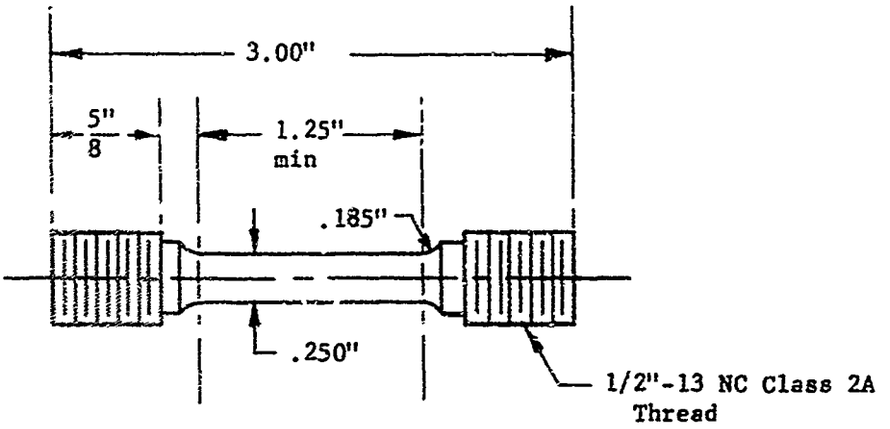

(a) Tensile Specimen

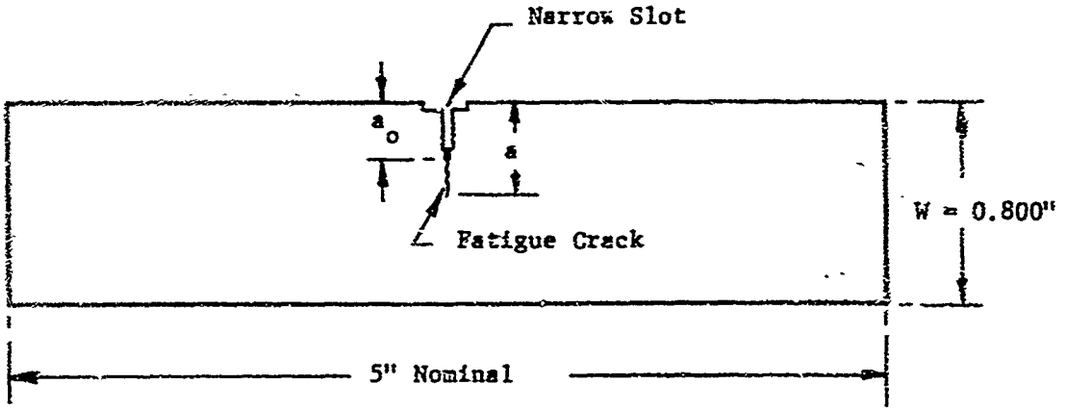

Thickness, B = 0.400"
Span, S = 4W
$a_o \cong 0.280"$
$\frac{a}{W}$ = .45-.55

(b) Slow Bend Fracture Toughness Specimen (Three Point Loading)

Figure 1. Dimensions of Tensile and Fracture Toughness Specimens

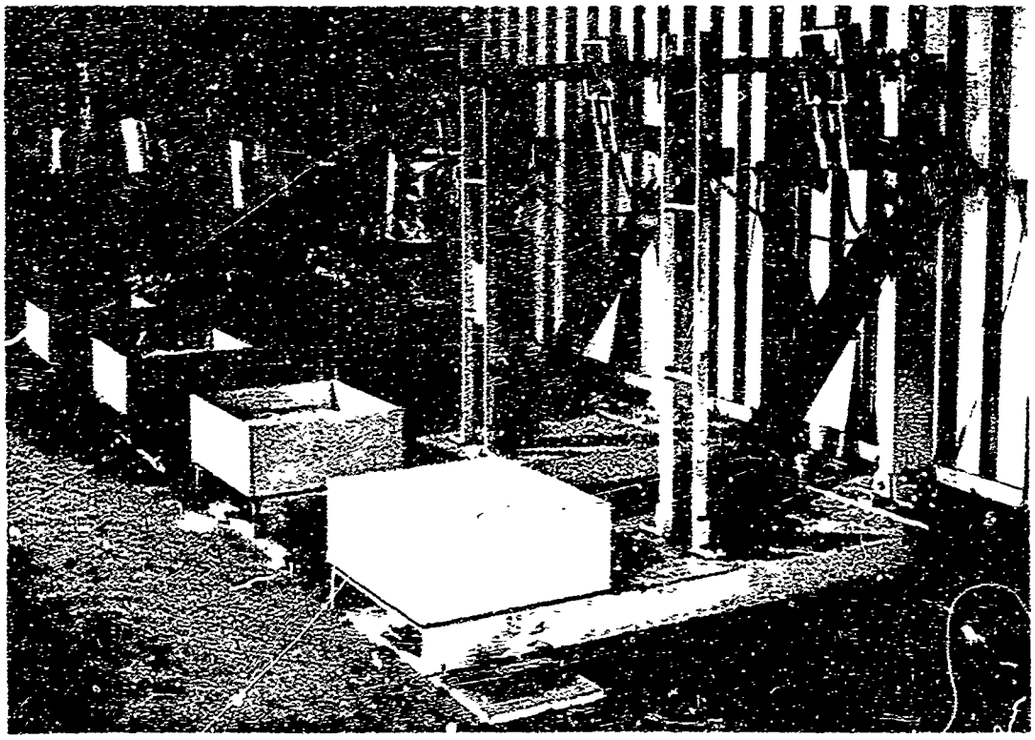

Figure 2. Cantilever Beam Stress Corrosion Test Frames

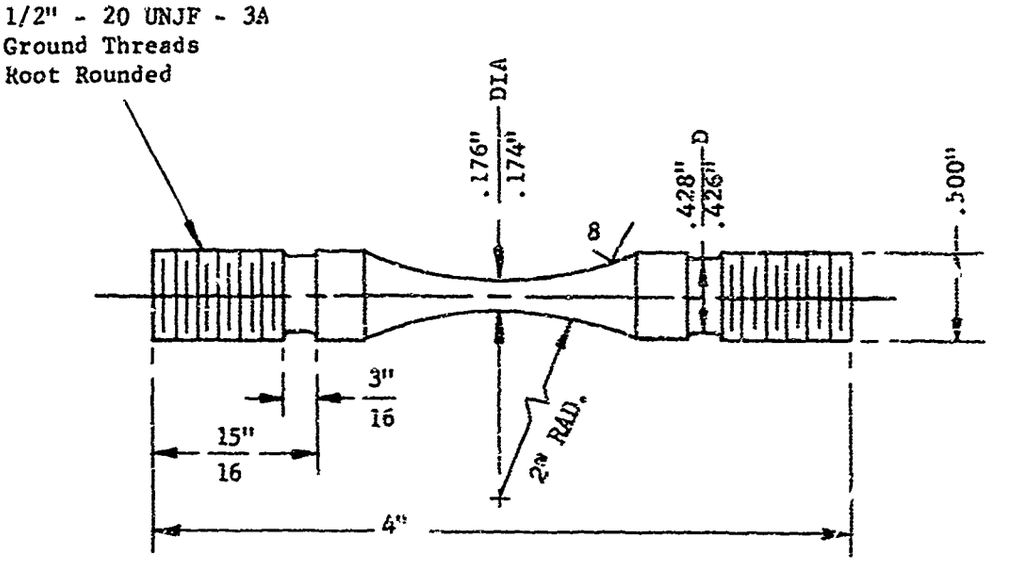

(a) Unnotched Fatigue Specimen

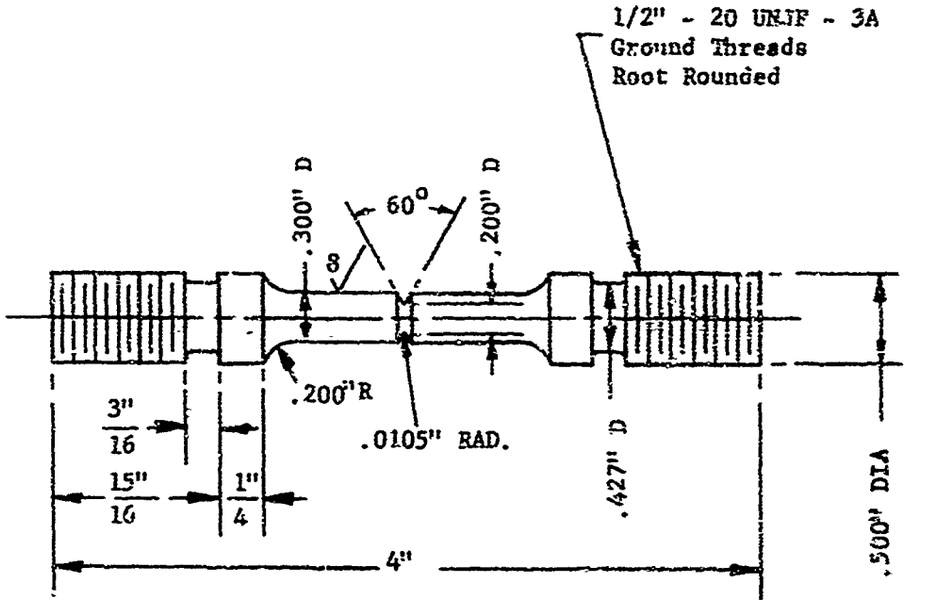

(b) Notched Fatigue Specimen

Figure 3. Unnotched and Notched Fatigue Specimens

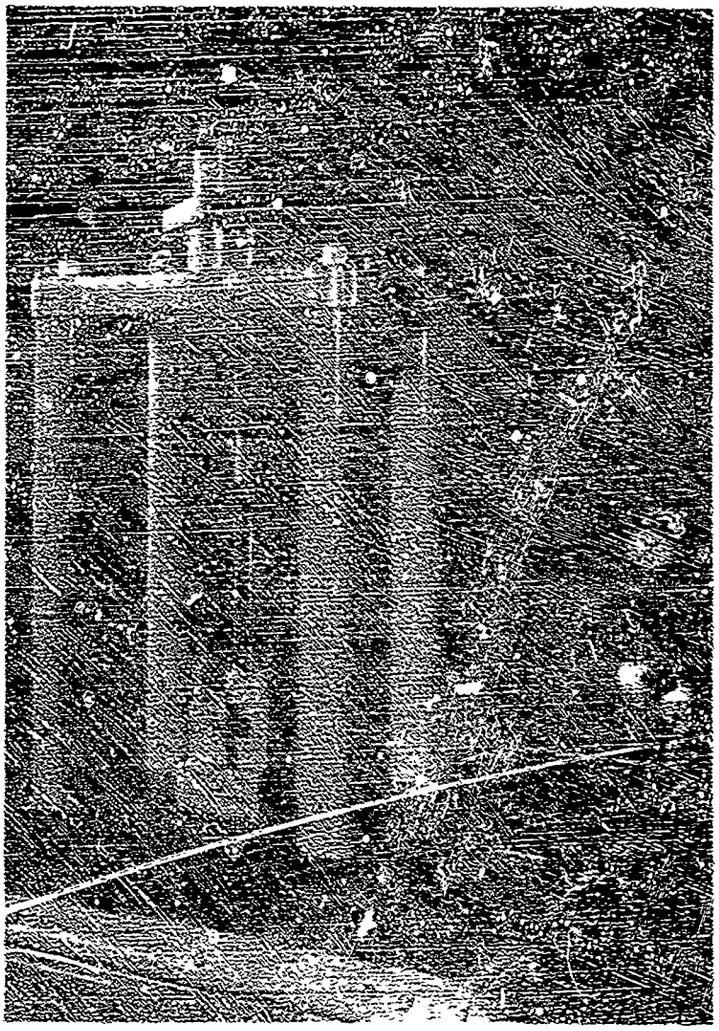

Figure 4. Fatigue Testing Apparatus

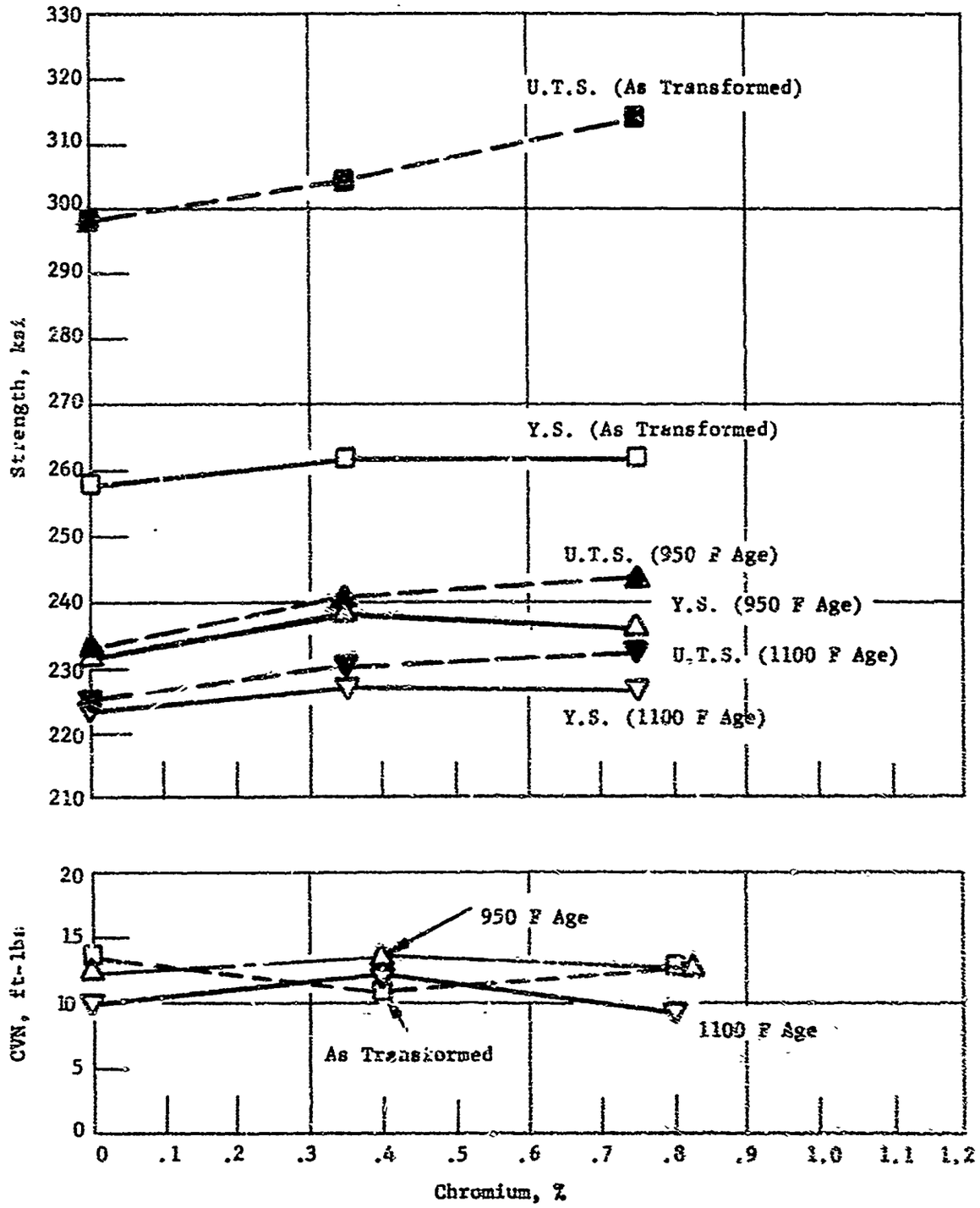

Figure 5. The Effect of Chromium on Strength and Toughness in Low Alloy Bainaging Steels

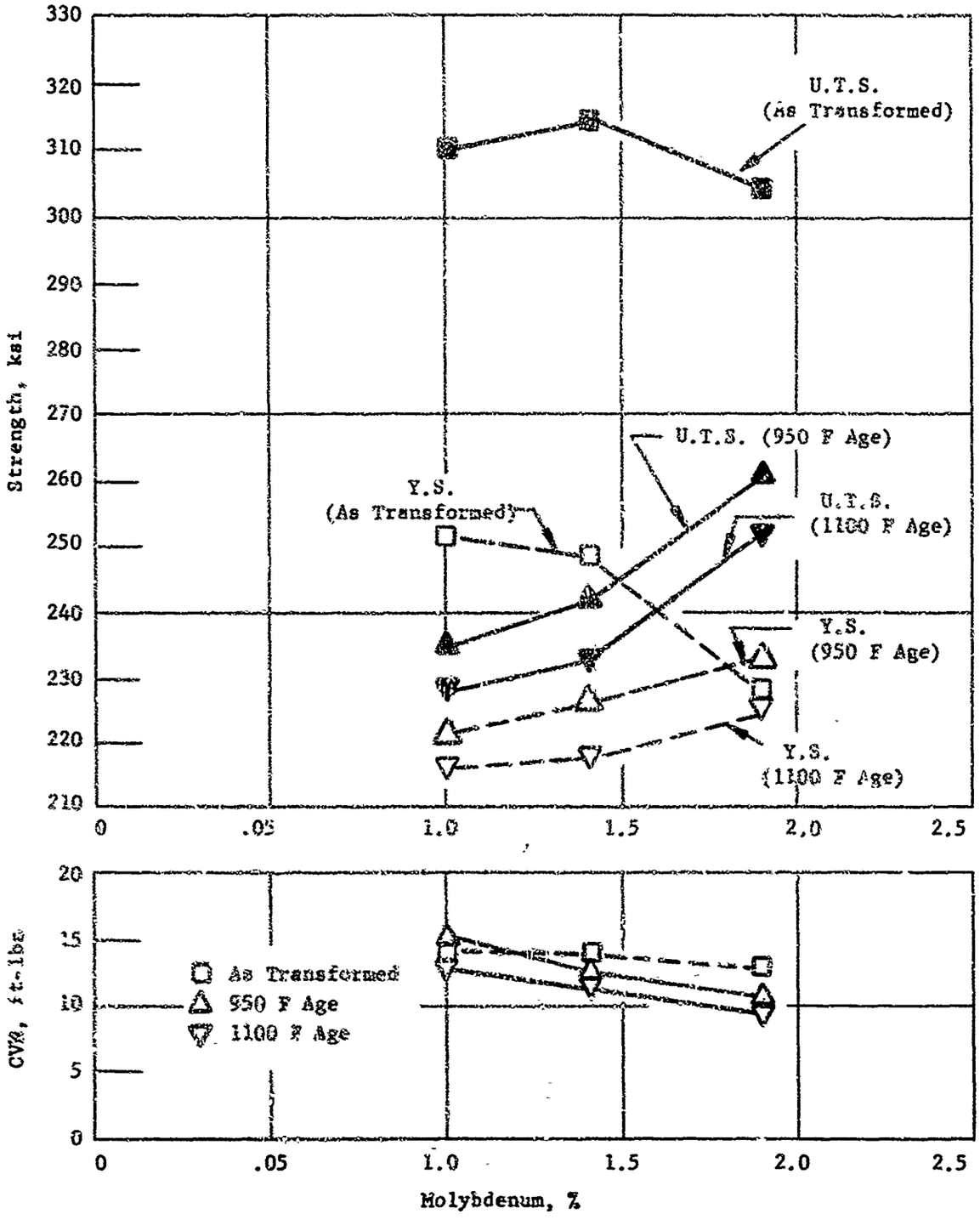

Figure 6. The Effect of Molybdenum on Strength and Toughness in Low Alloy Bainaging Steels

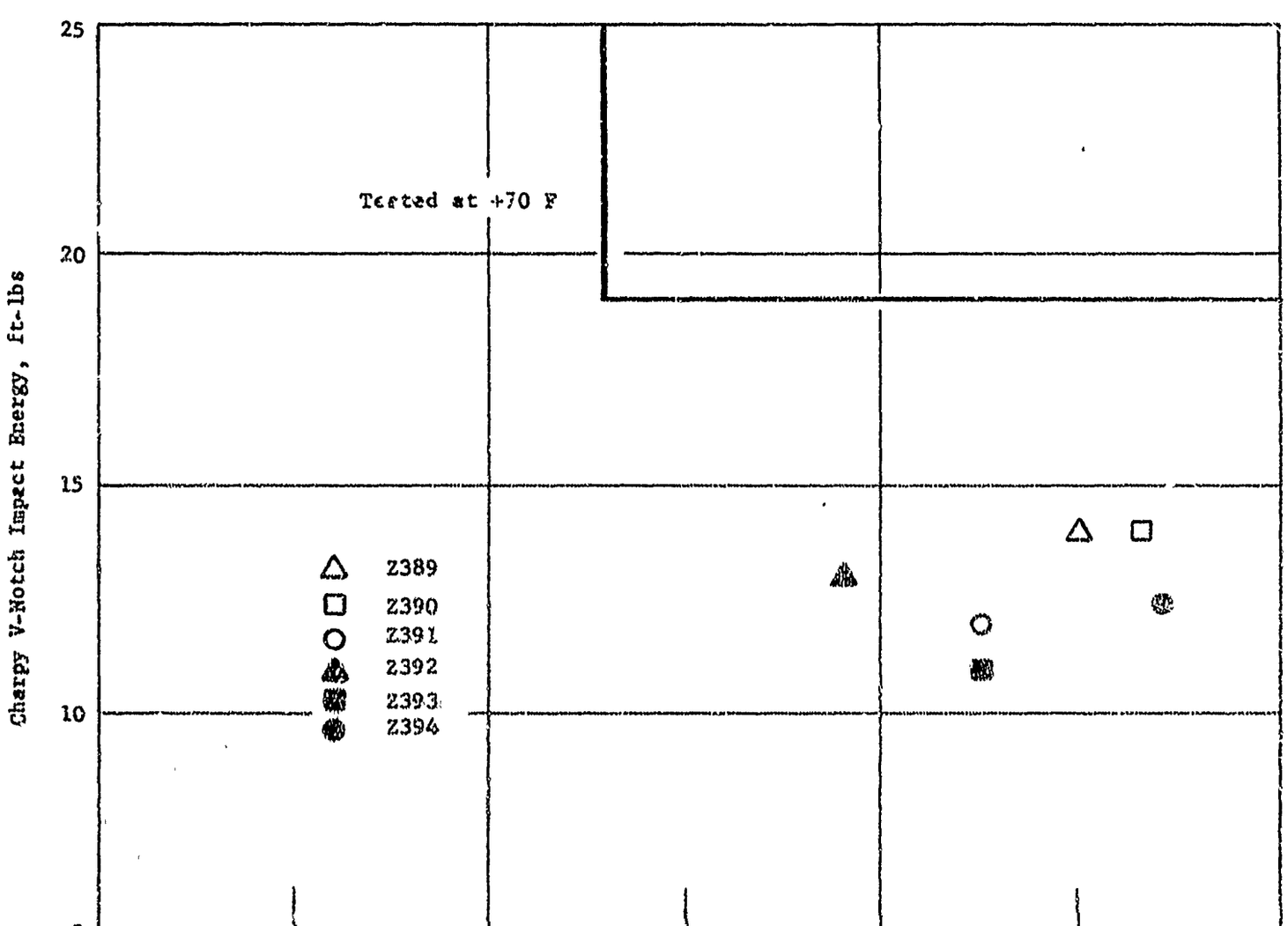

Figure 7. Strength-Toughness Relationships for Low Alloy Bainuging Steels

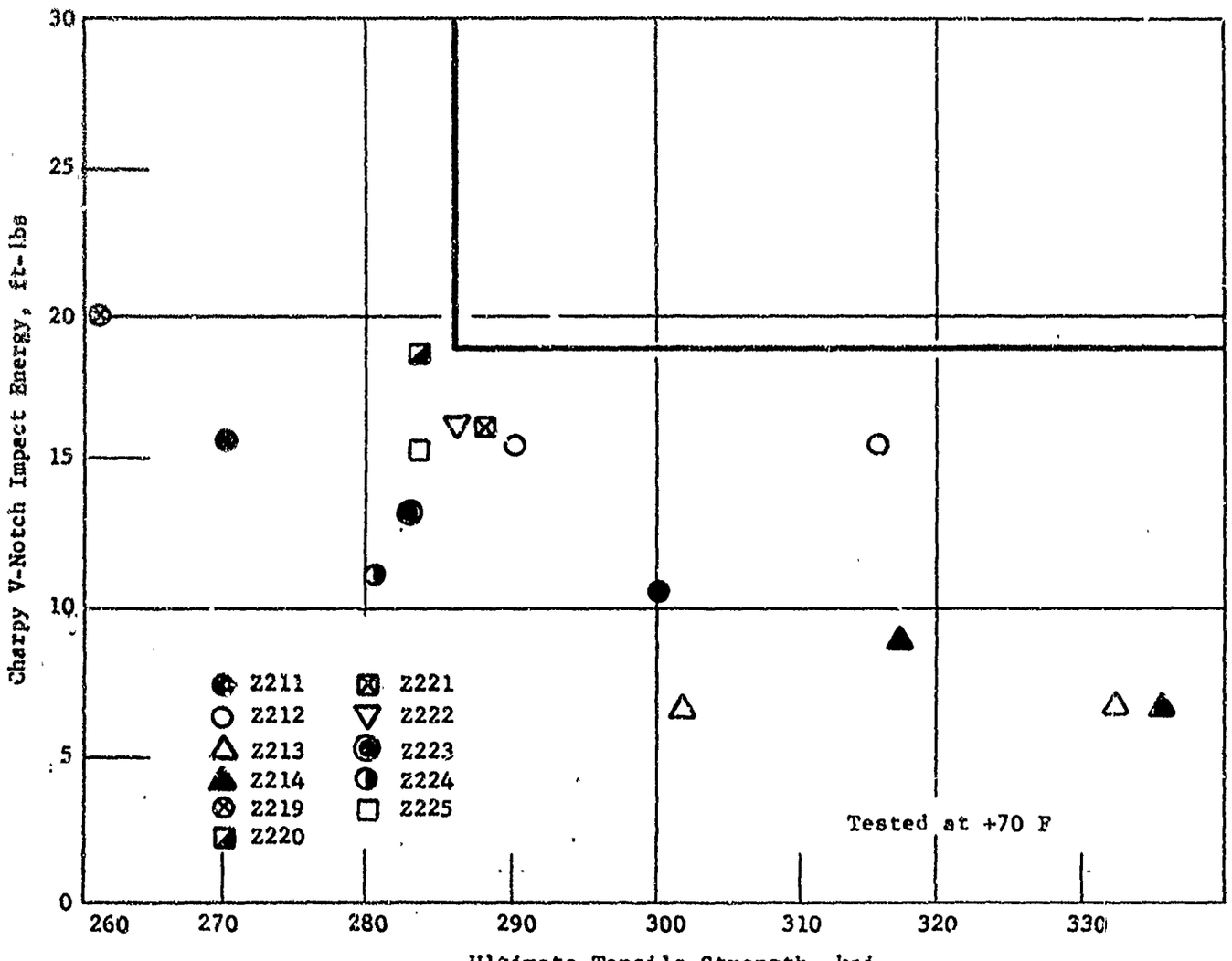

Figure 8. Strength-Toughness Relationships for Medium Alloy Bainitic Steels

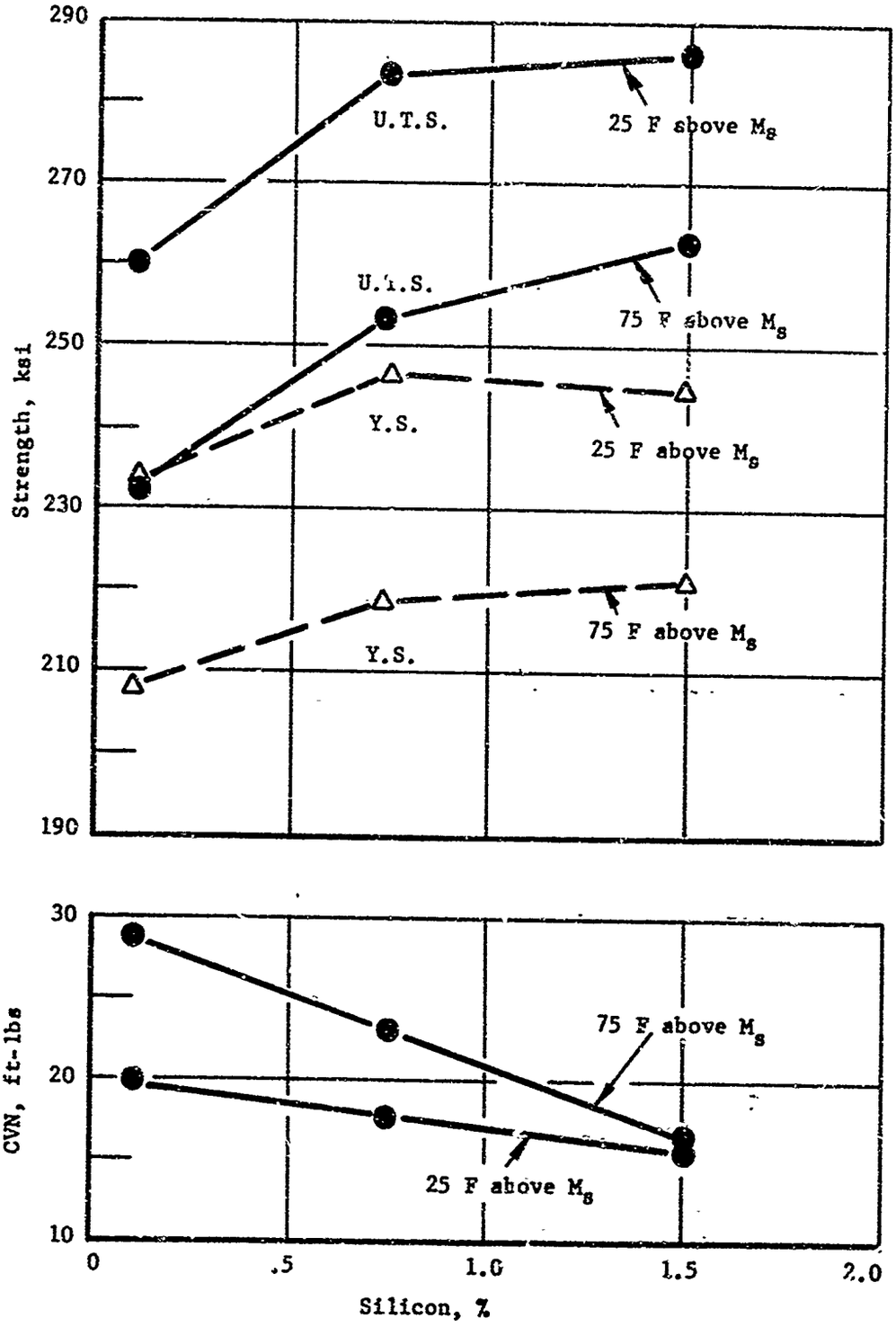

Figure 9. The Effect of Silicon on Strength and Toughness in Medium Alloy Bainitic Steels (Z219, Z220, Z221)

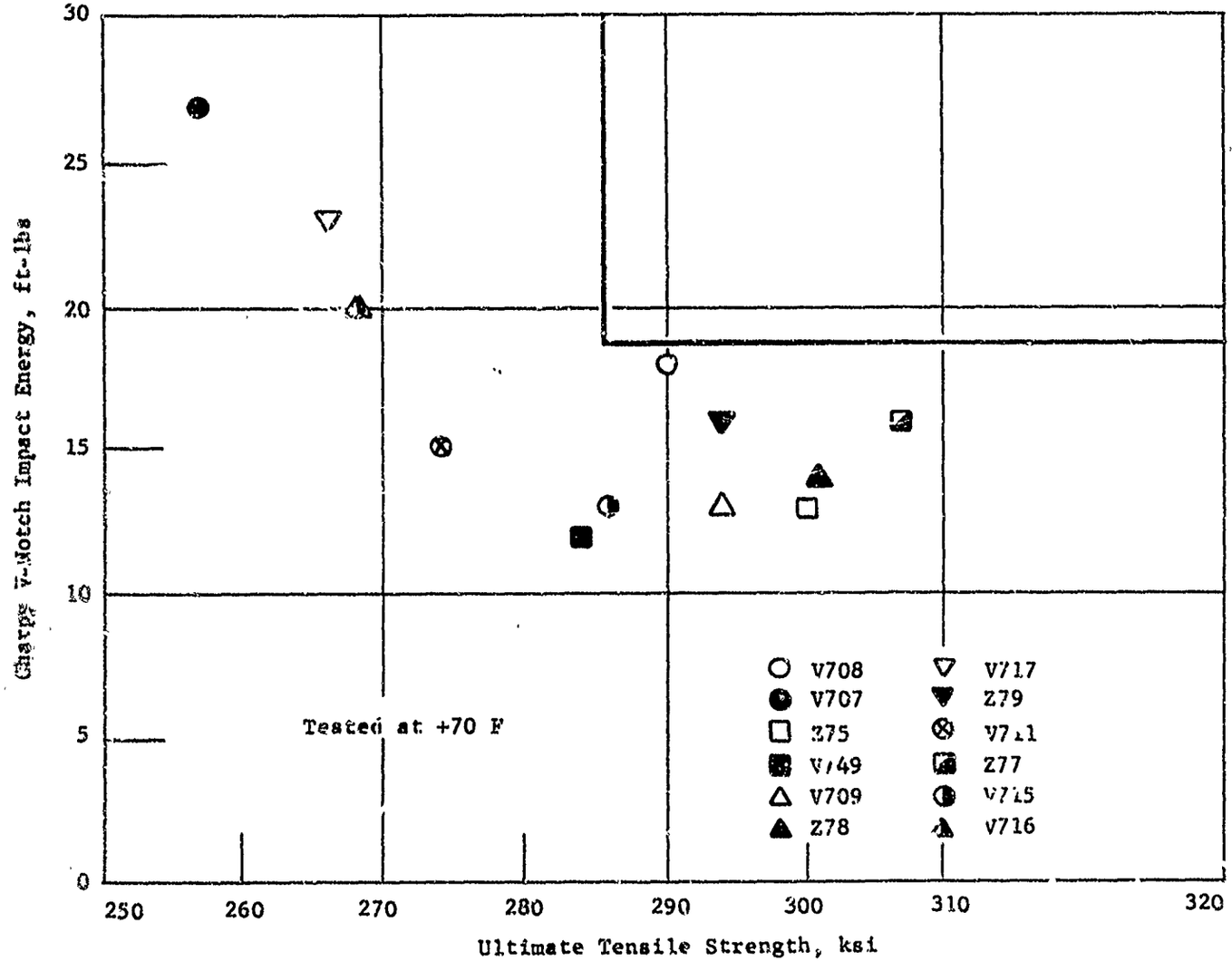

Figure 10. Strength-Toughness Relationships for Ni-Cr-Mo-W-V Martensitic Steels (400 F Temper)

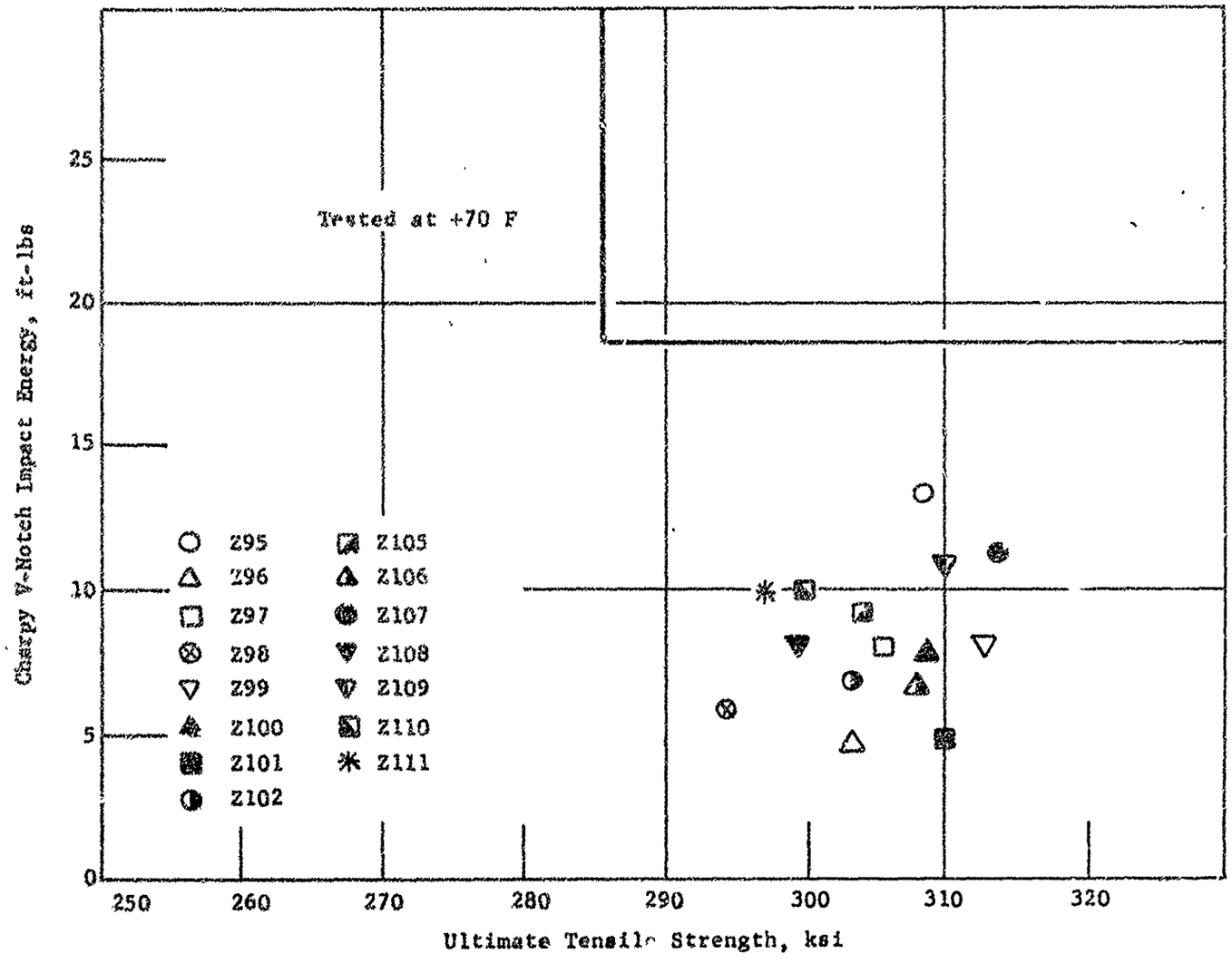

Figure 11. Strength-Toughness Relationships for Ni-Cr-Mo-W-V Martensitic Steels (Z95 through Z111) (400 F Temper)

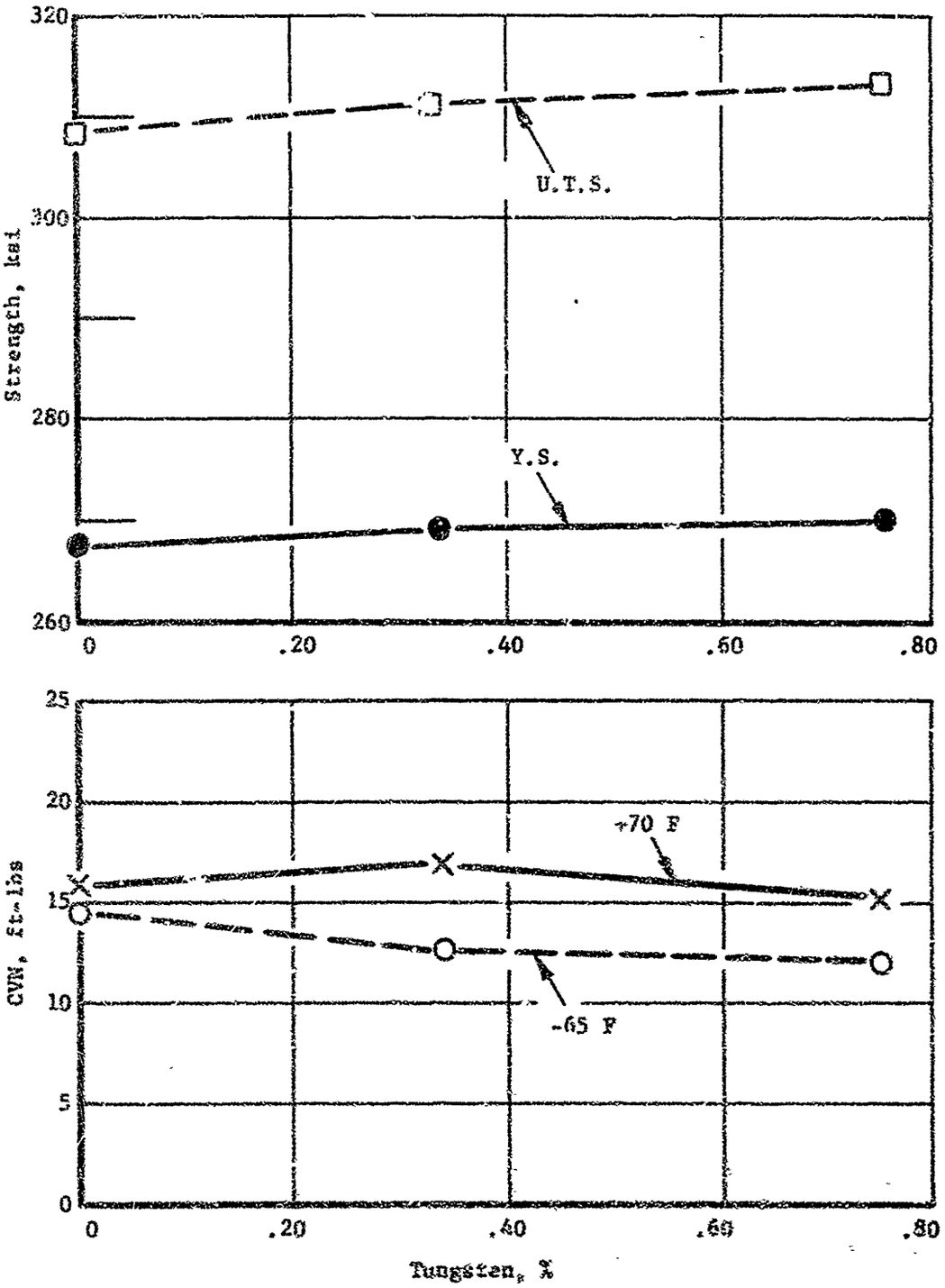

Figure 12. The Effect of Tungsten on Strength and Toughness in Ni-Cr-Mo-W-V Martensitic Steels

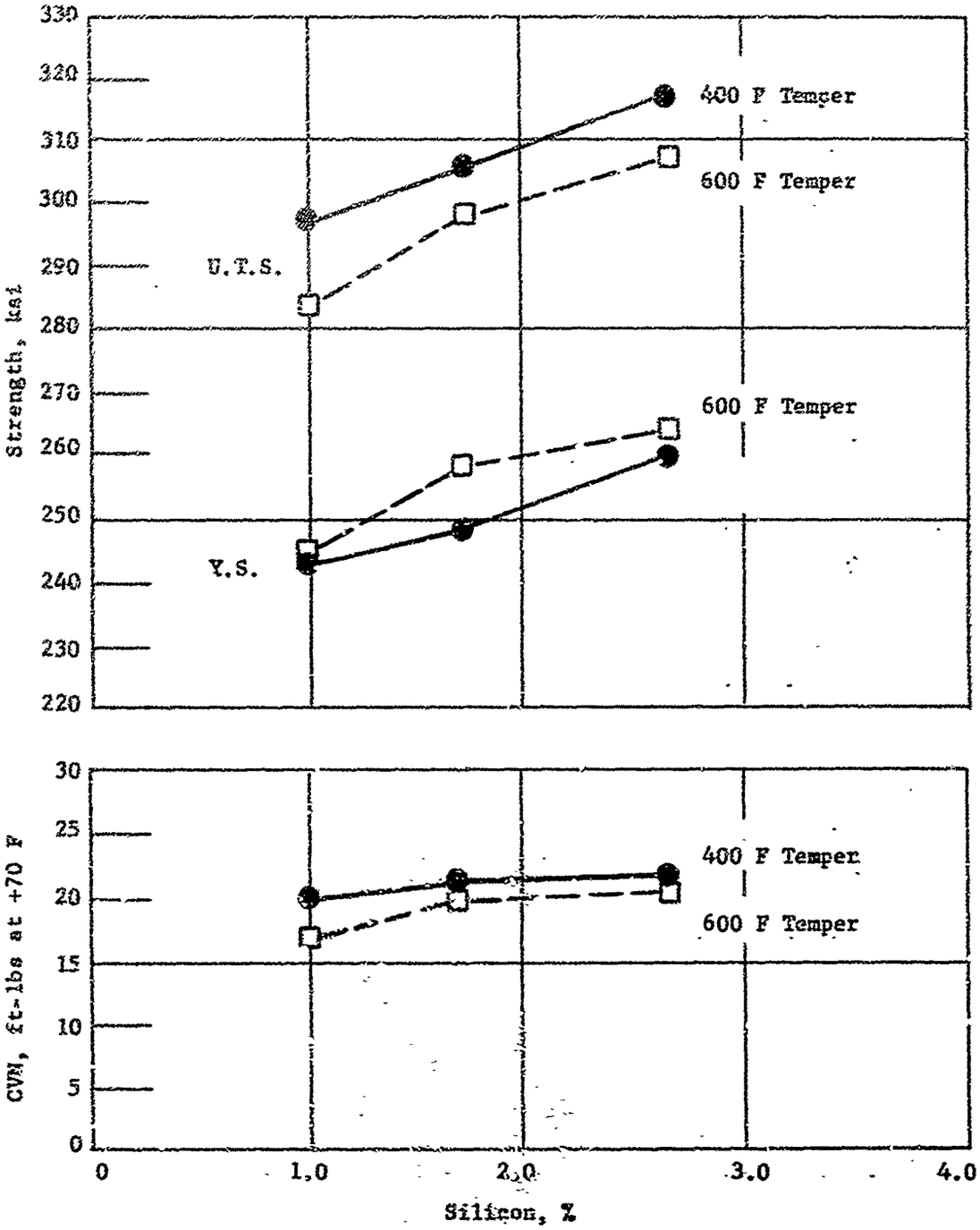

Figure 13. The Effect of Silicon on Strength and Toughness in Ni-Cr-Mo-Si-V Martensitic Alloys (Z43, Z44, Z45)

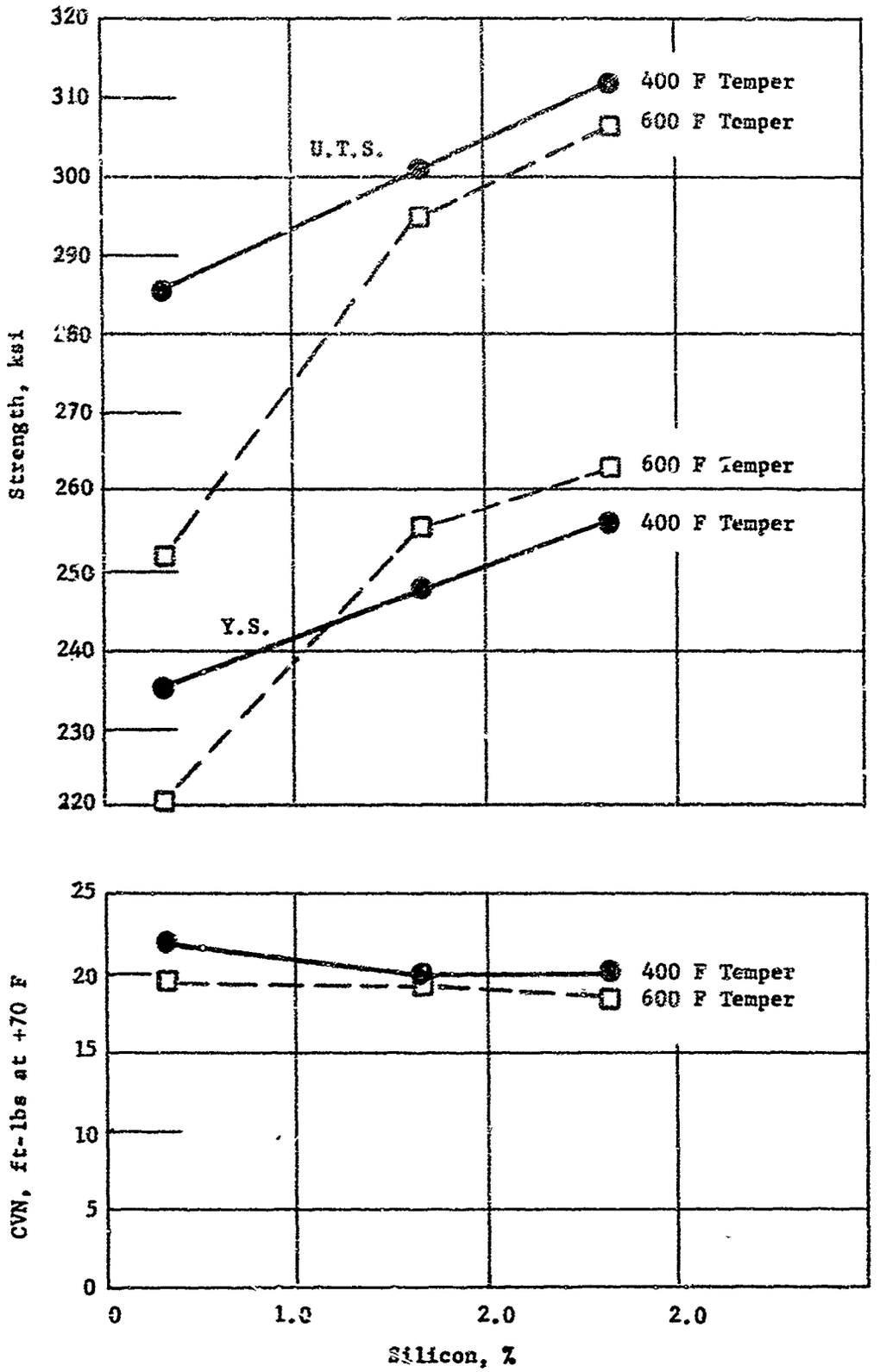

Figure 14. The Effect of Silicon on Strength and Toughness in Ni-Cr-Mo-Si-V Martensitic Alloys (Z58, Z59, Z60)

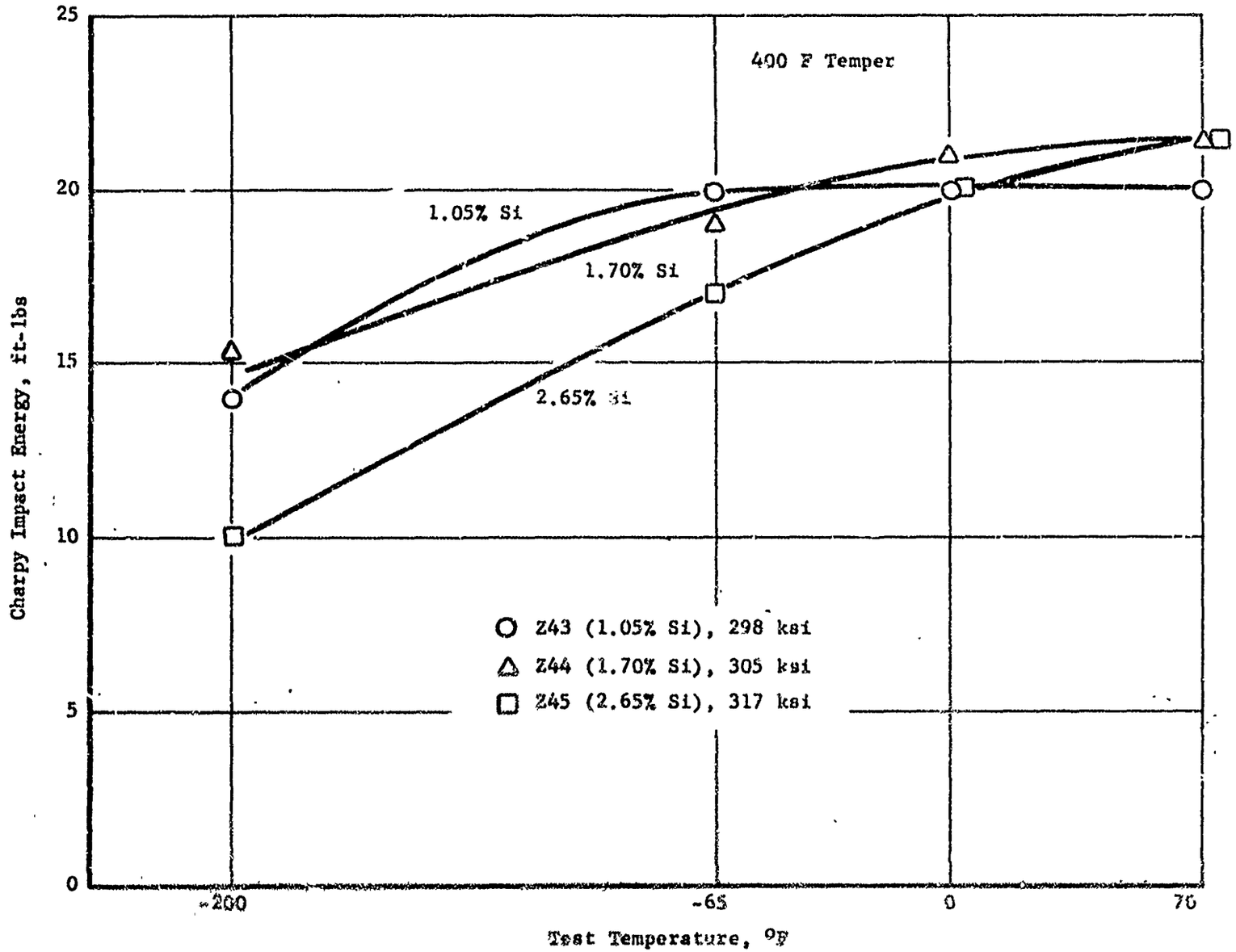

Figure 15. Effect of Silicon on Charpy Impact-Transition Curves for Heats Z43, Z44, and Z45 (400 F Temper)

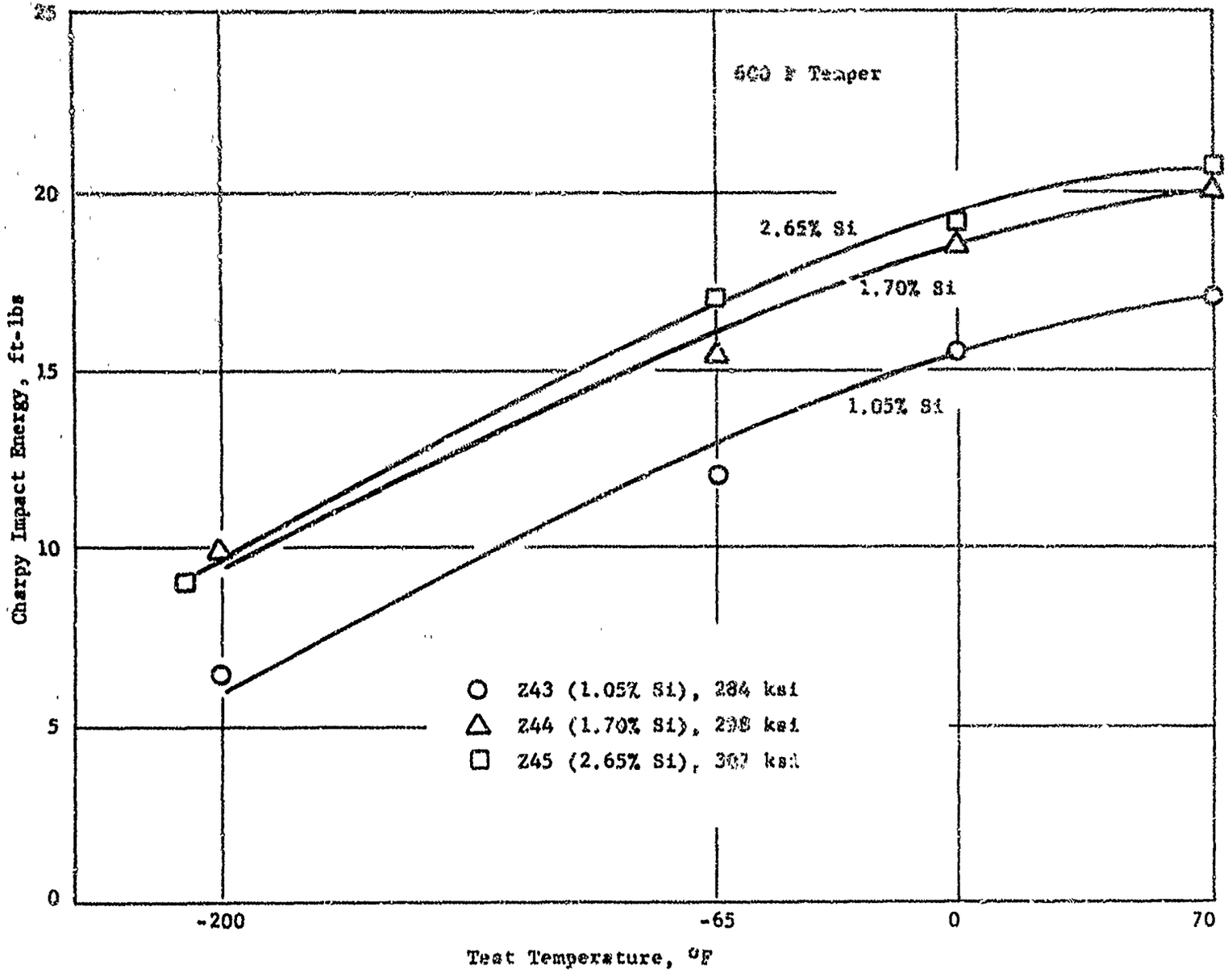

Figure 16. Effect of Silicon on Charpy Impact-Transition Curves for Heats Z43, Z44, Z45 (600 F Temper)

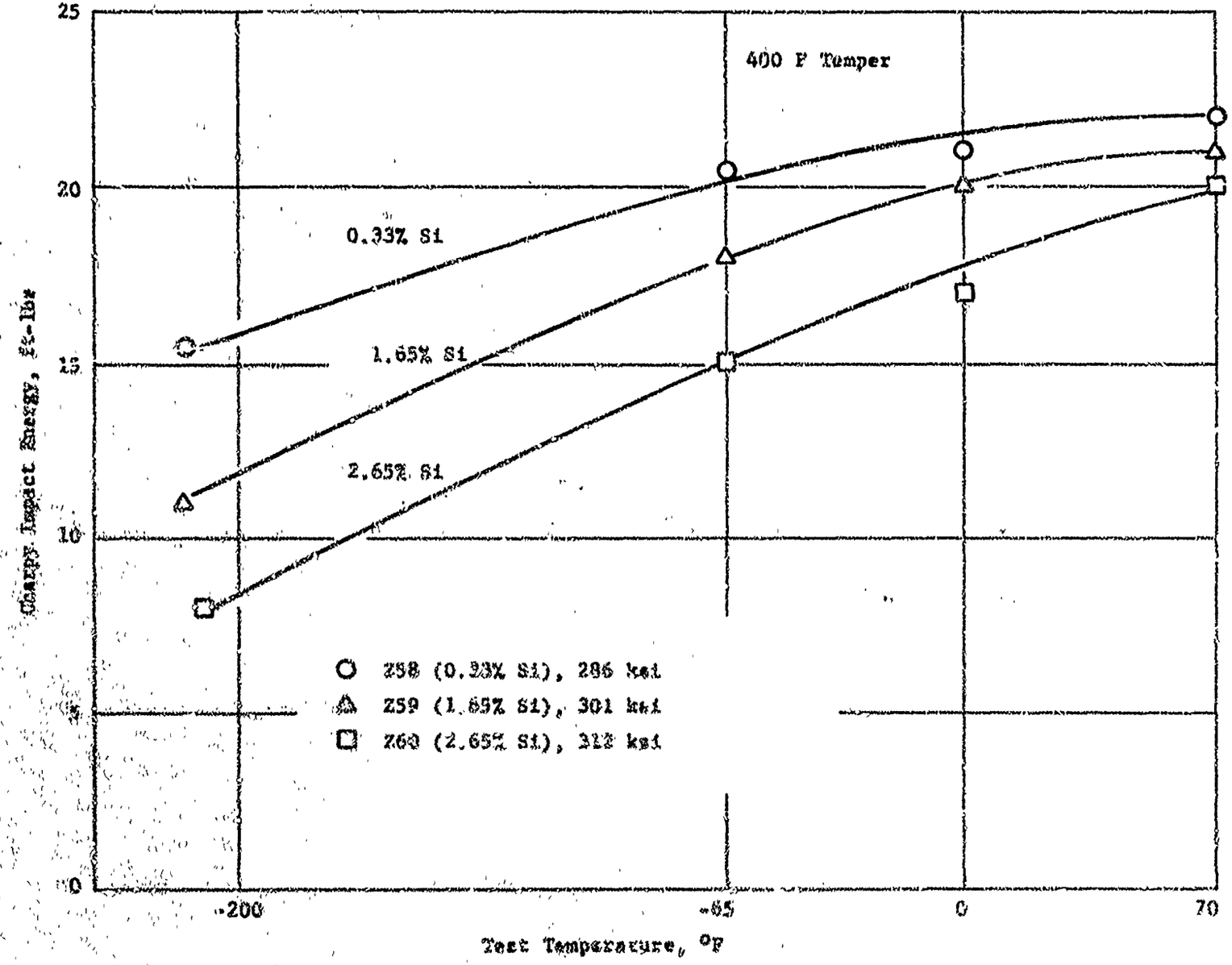

Figure 17. Effect of Silicon on Charpy Impact-Transition Curves for Heats Z58, Z59, Z60 (400 F Temper)

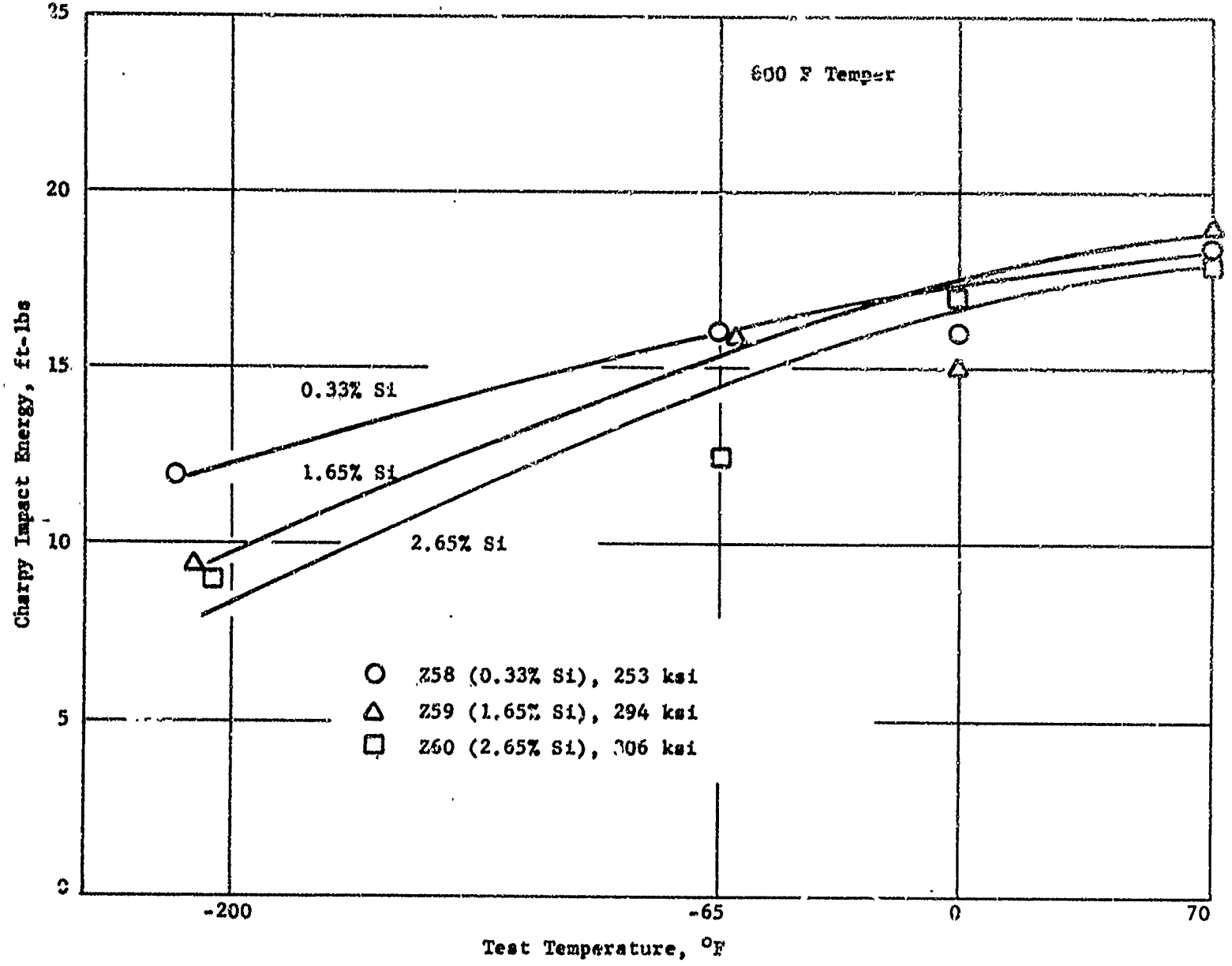

Figure 18. Effect of Silicon on Charpy Impact-Transition Curves for Heats Z58, Z59, Z60 (600 F Temper)

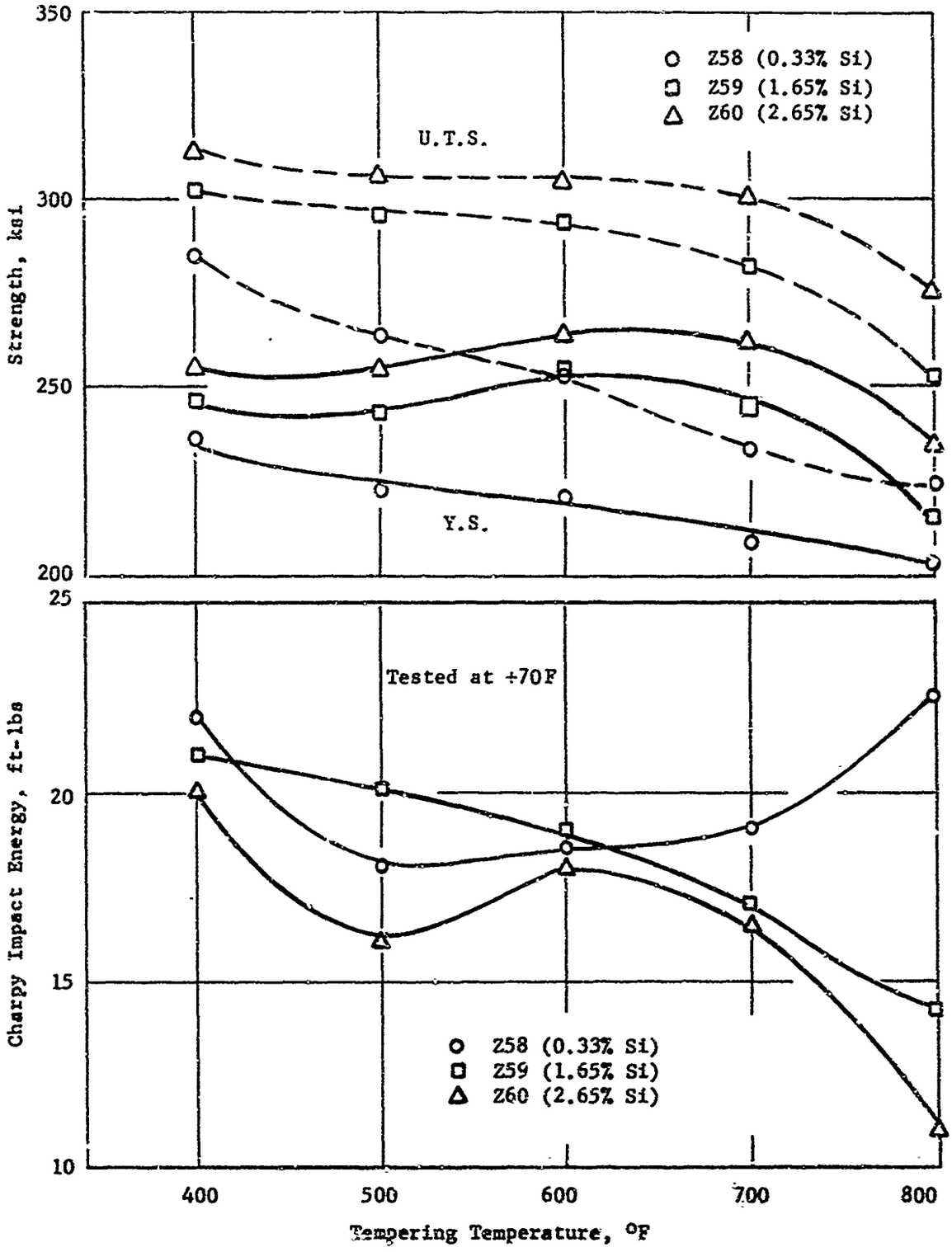

Figure 19. The Influence of Tempering Temperature on Strength and Toughness Properties of Alloys Z58, Z59, and Z60

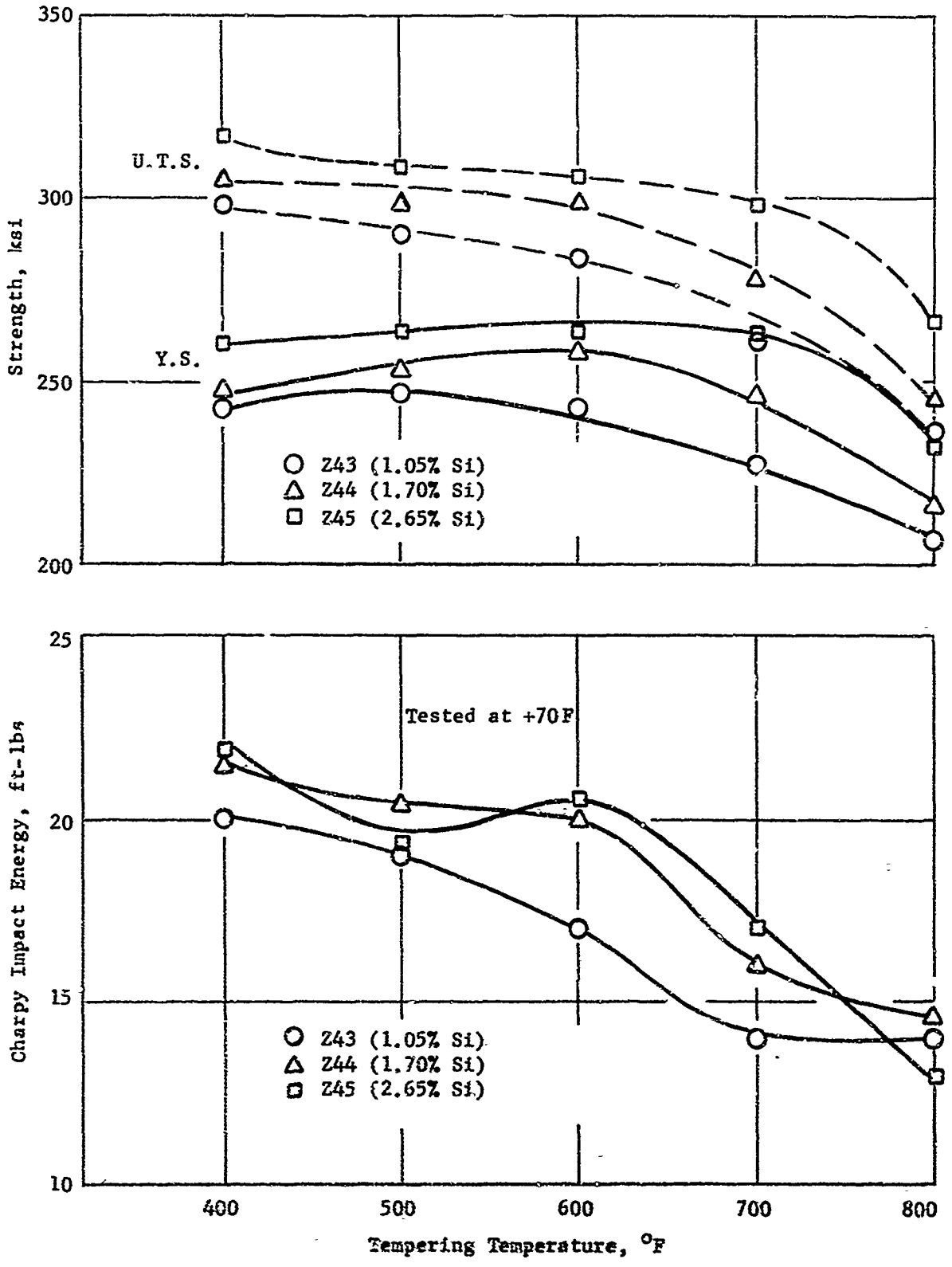

Figure 20. The Influence of Tempering Temperature on Strength and Toughness Properties of Alloys Z43, Z44, and Z45

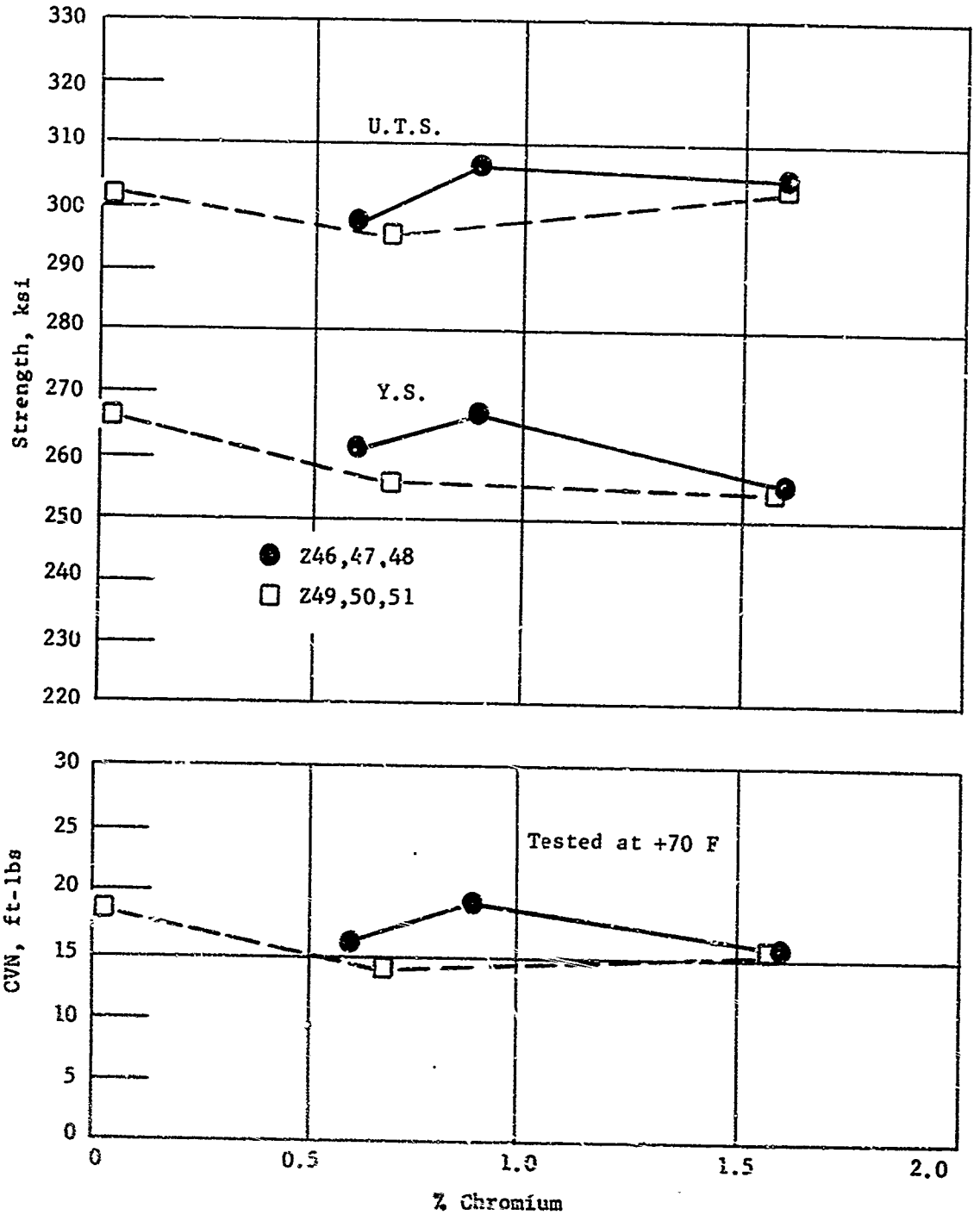

Figure 21. The Effect of Chromium on Strength and Toughness in Ni-Cr-Mo-Si-V Martensitic Steels

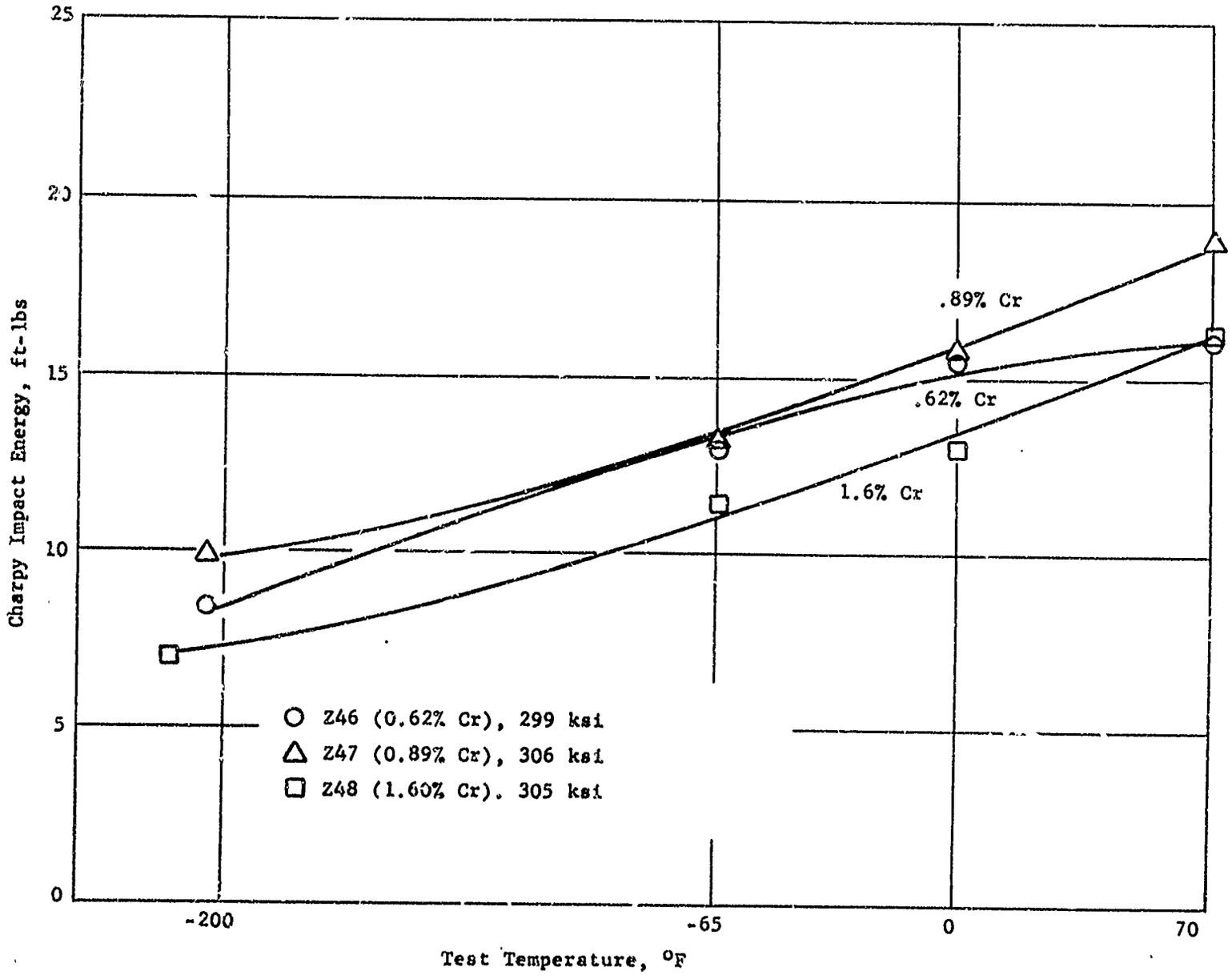

Figure 22. Effect of Chromium on Charpy Impact-Transition Curves for Heats Z46, Z47, and Z48 (600 F Temper)

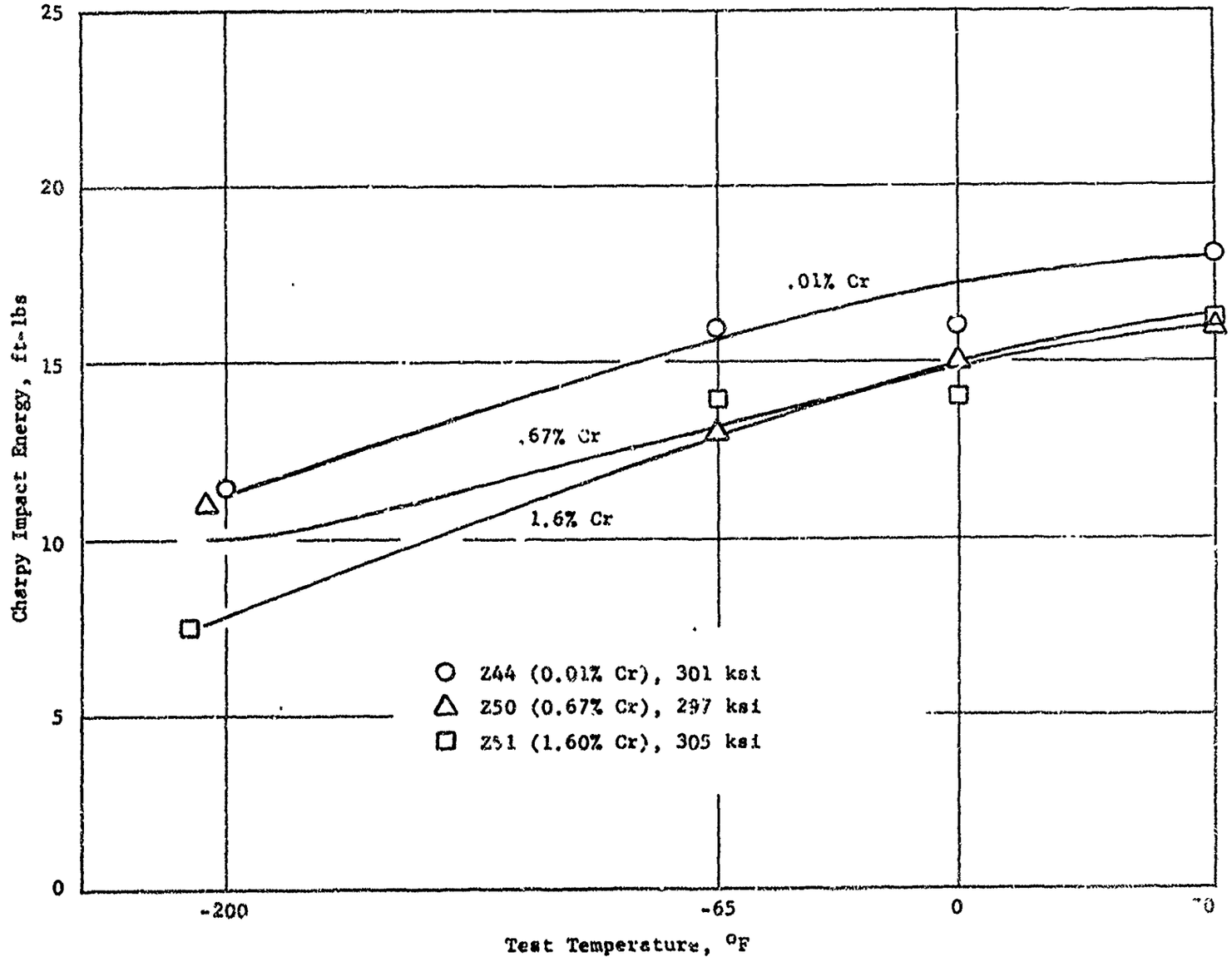

Figure 23. Effect of Chromium on Charpy Impact-Transition Curves for Heats Z49, Z50, and Z51 (600 F Temper)

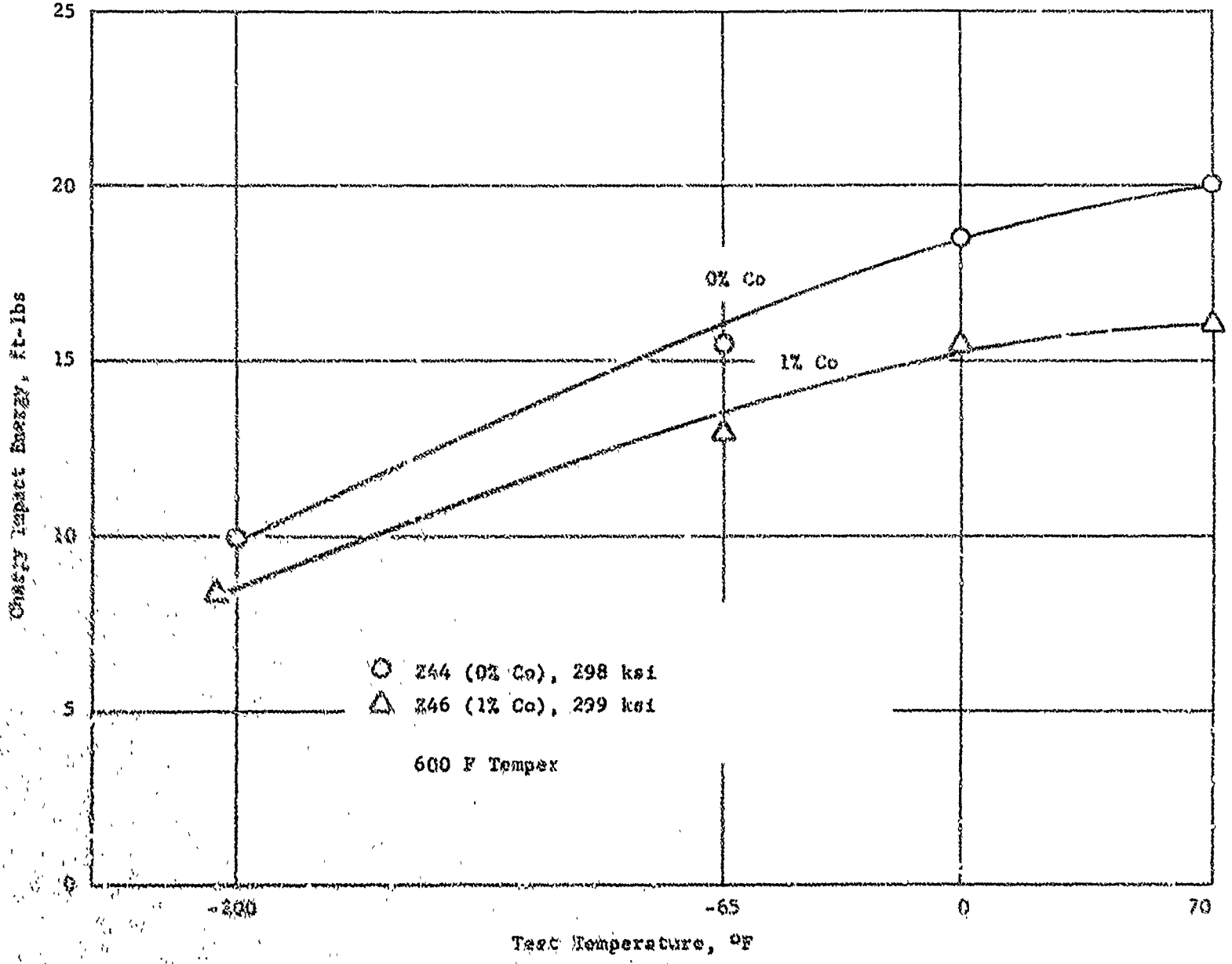

Figure 24. Effect of Cobalt on Charpy Impact-Transition Curves for Ni-Cr-Mo-Si-V Martensitic Steels

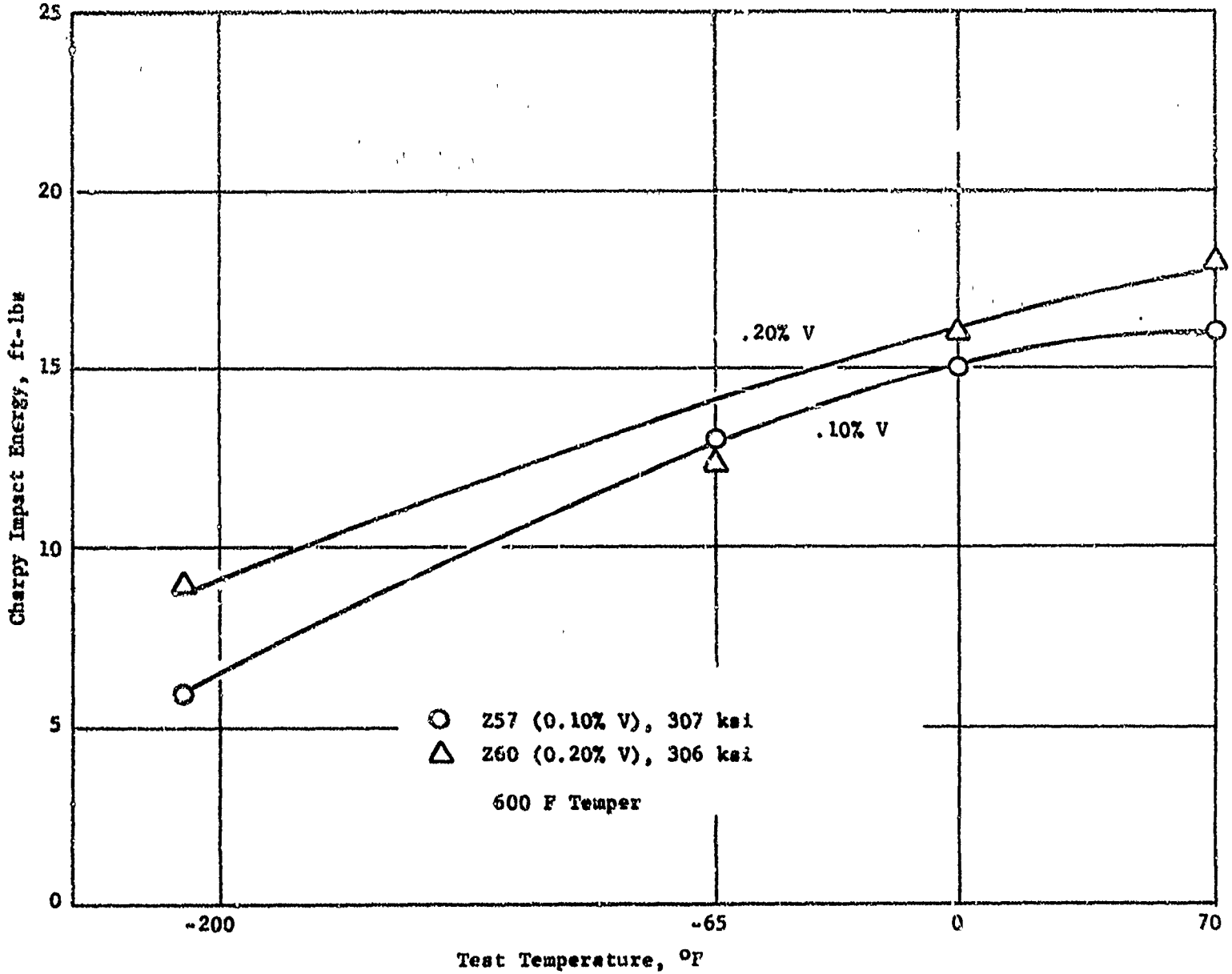

Figure 25. Effect of Vanadium on Charpy Impact-Transition Curves for Ni-Cr-Mo-Si-V Martensitic Steels

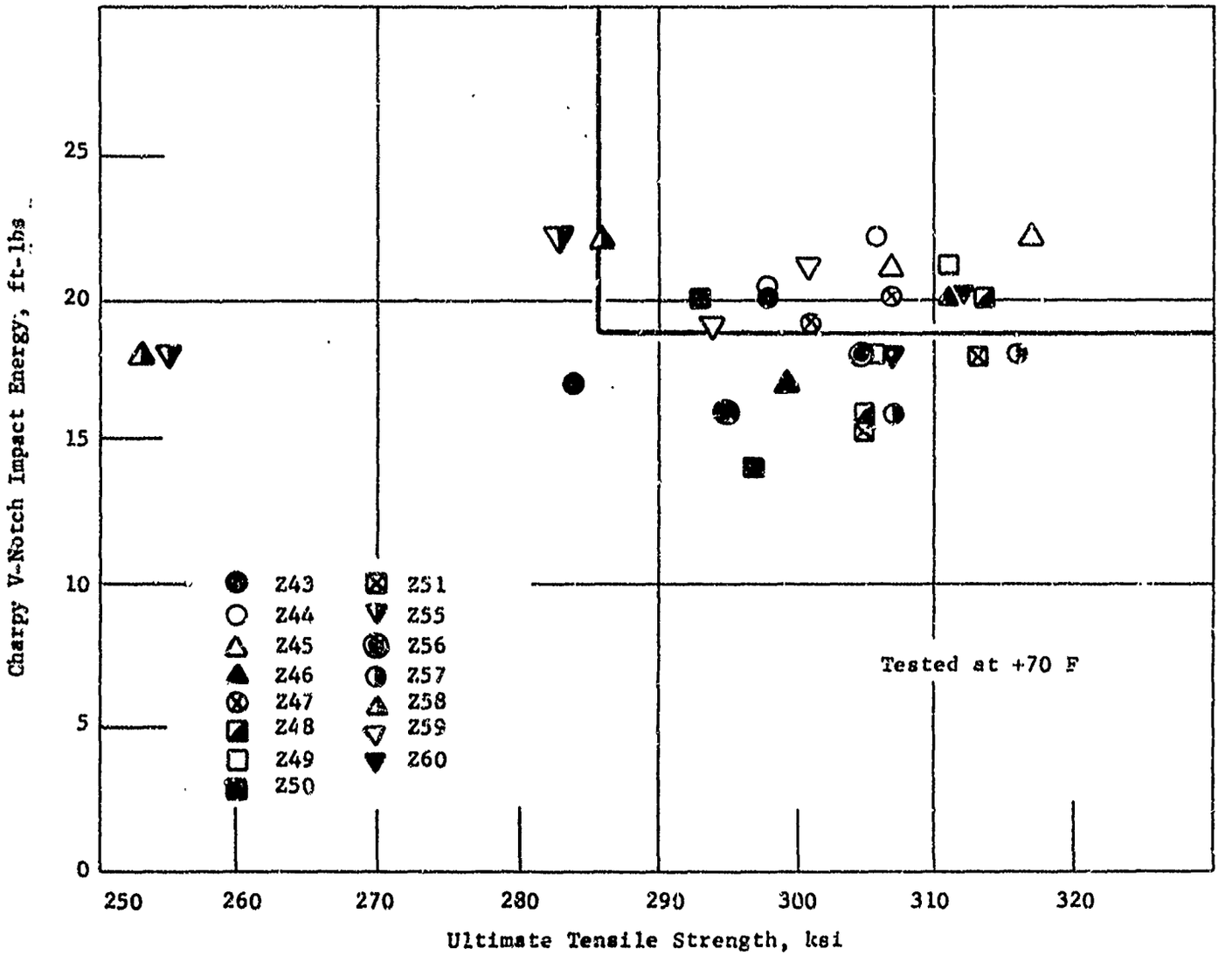

Figure 26. Strength-Toughness Relationships for Ni-Cr-Mo-Si-V Martensitic Steels (400 F and 600 F Temper)

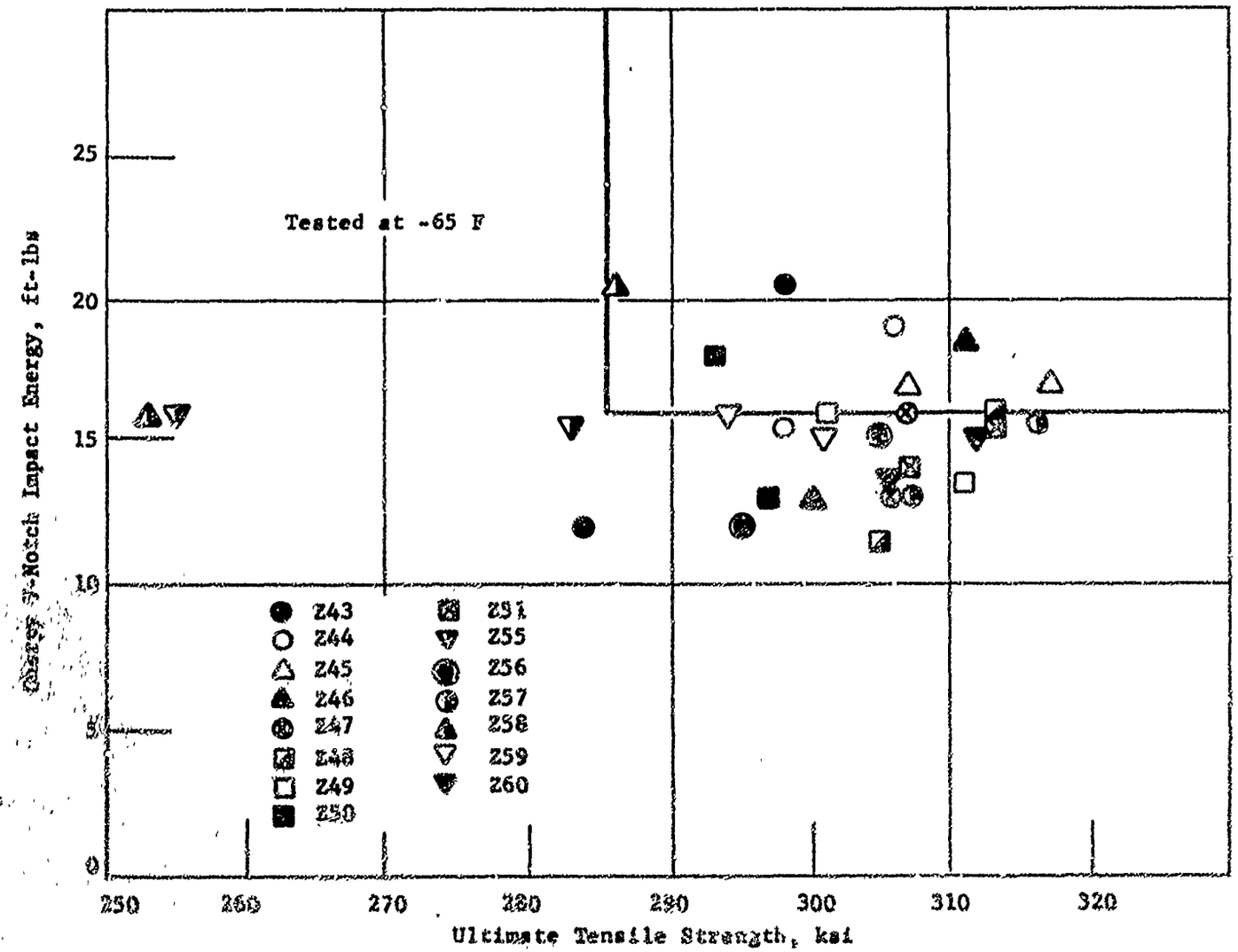

Figure 27. Strength-Toughness Relationships for Ni-Cr-Mo-Si-V Martensitic Steels (400 F and 600 F Temper)

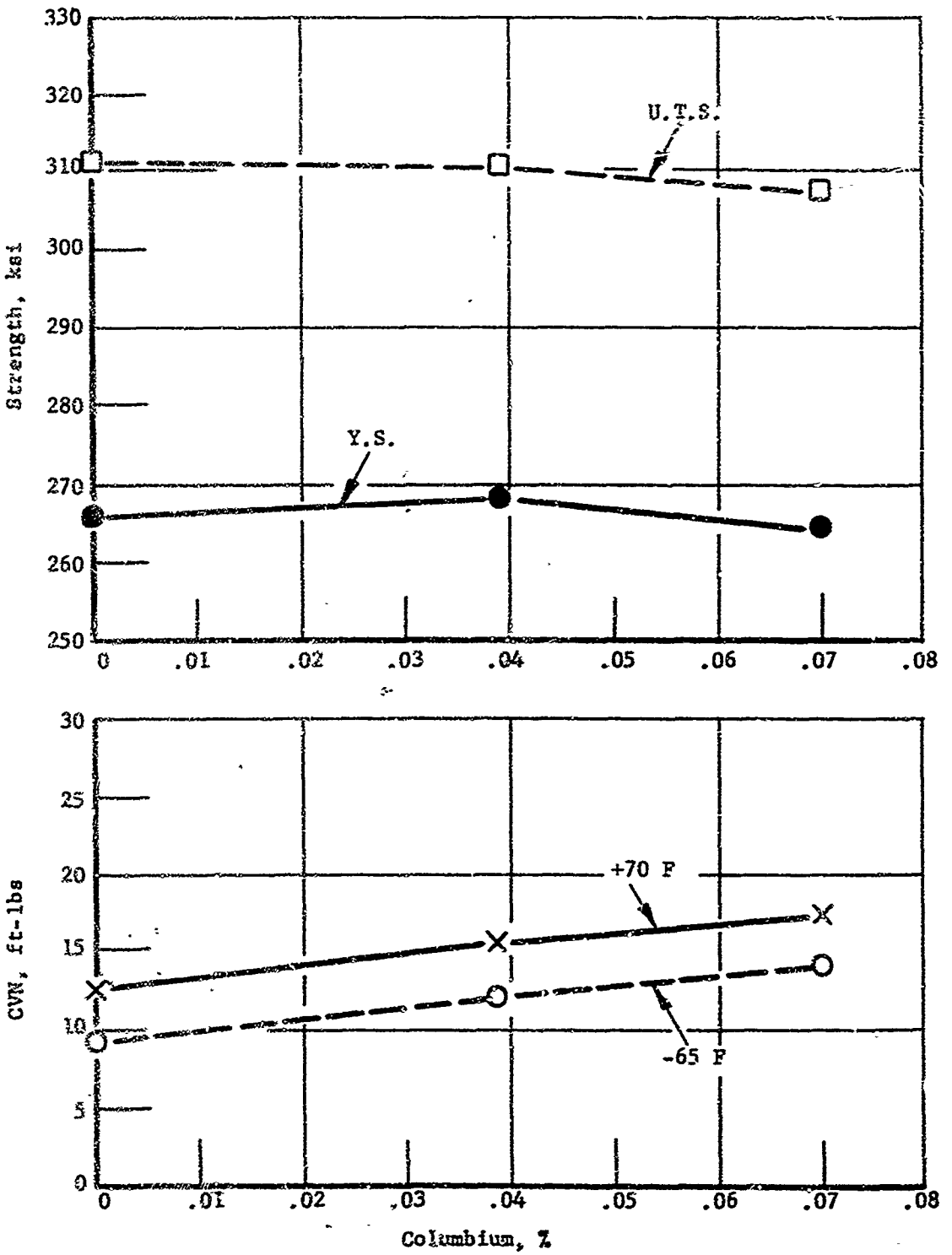

Figure 28. The Influence of Cb on Strength and Toughness in a Ni-Cr-Mo-Si Martensitic Steel

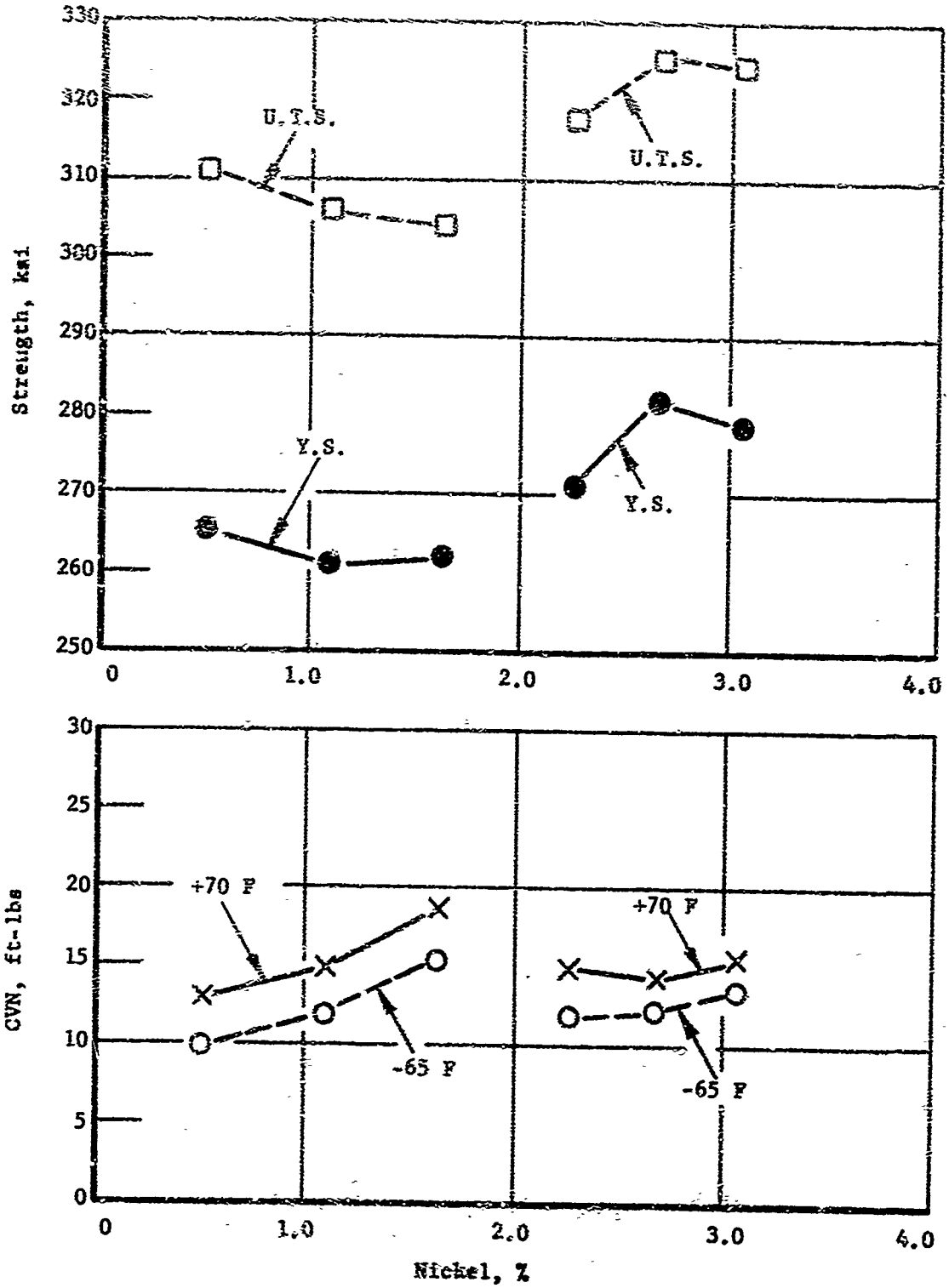

Figure 25. The Influence of Ni on Strength and Toughness in a Ni-Cr-Mo-Si-V Martensitic Steels

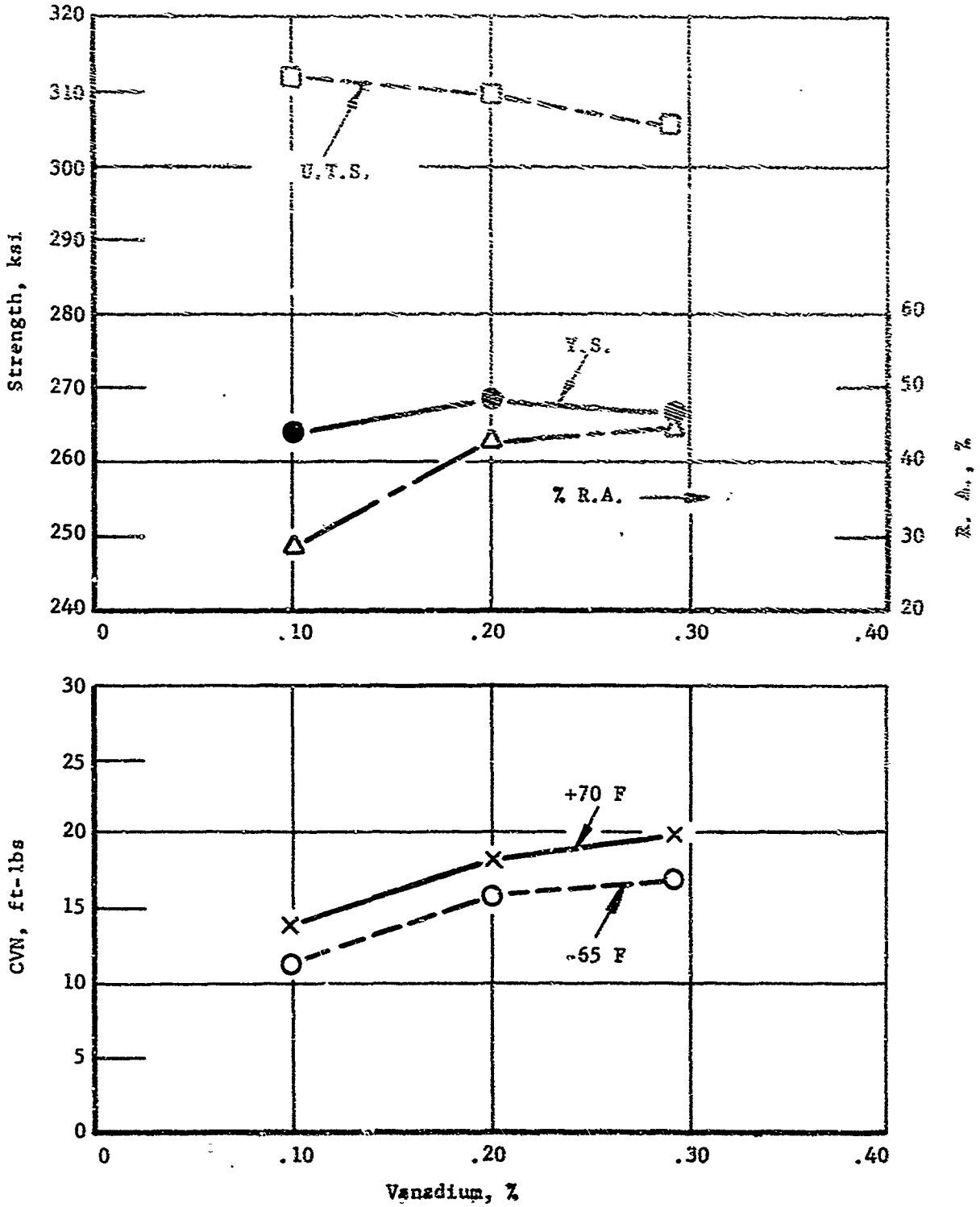

Figure 30. The Influence of V on Strength and Toughness in a Ni-Cr-Mo-Si-V Martensitic Steels

(a) Heat Z276, 0.1% V
ASTM G.S. 5.4, 100X

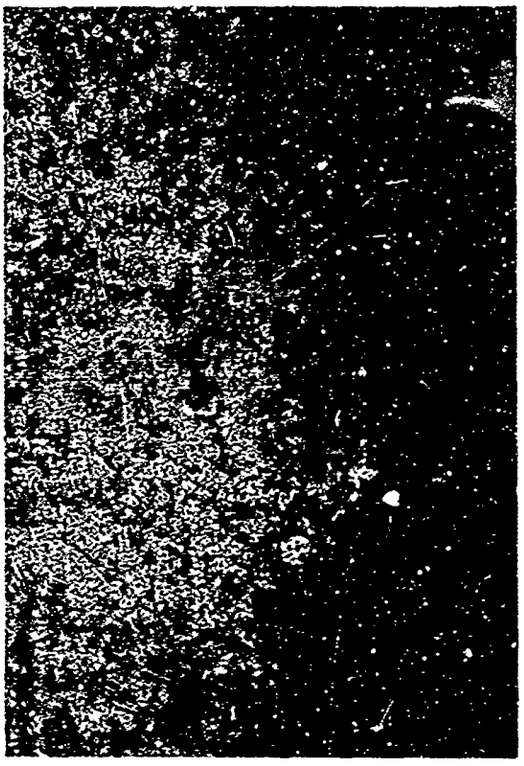

(b) Heat Z277, 0.2% V
ASTM G.S. 8.4, 100X

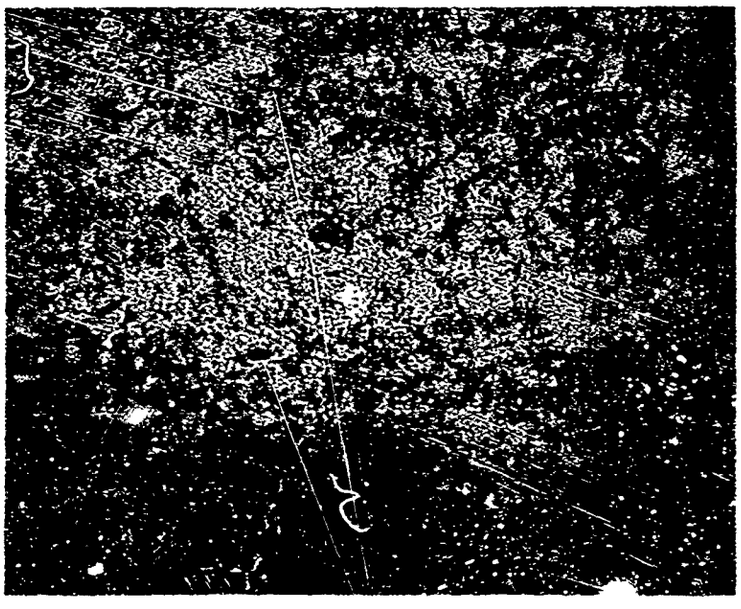

(c) Heat Z278, 0.29% V
ASTM G.S. 8 7, 100X

Figure 31. Microstructures of Vanadium Series of Ni-Cr-Mo-Si-V Martensitic Steels

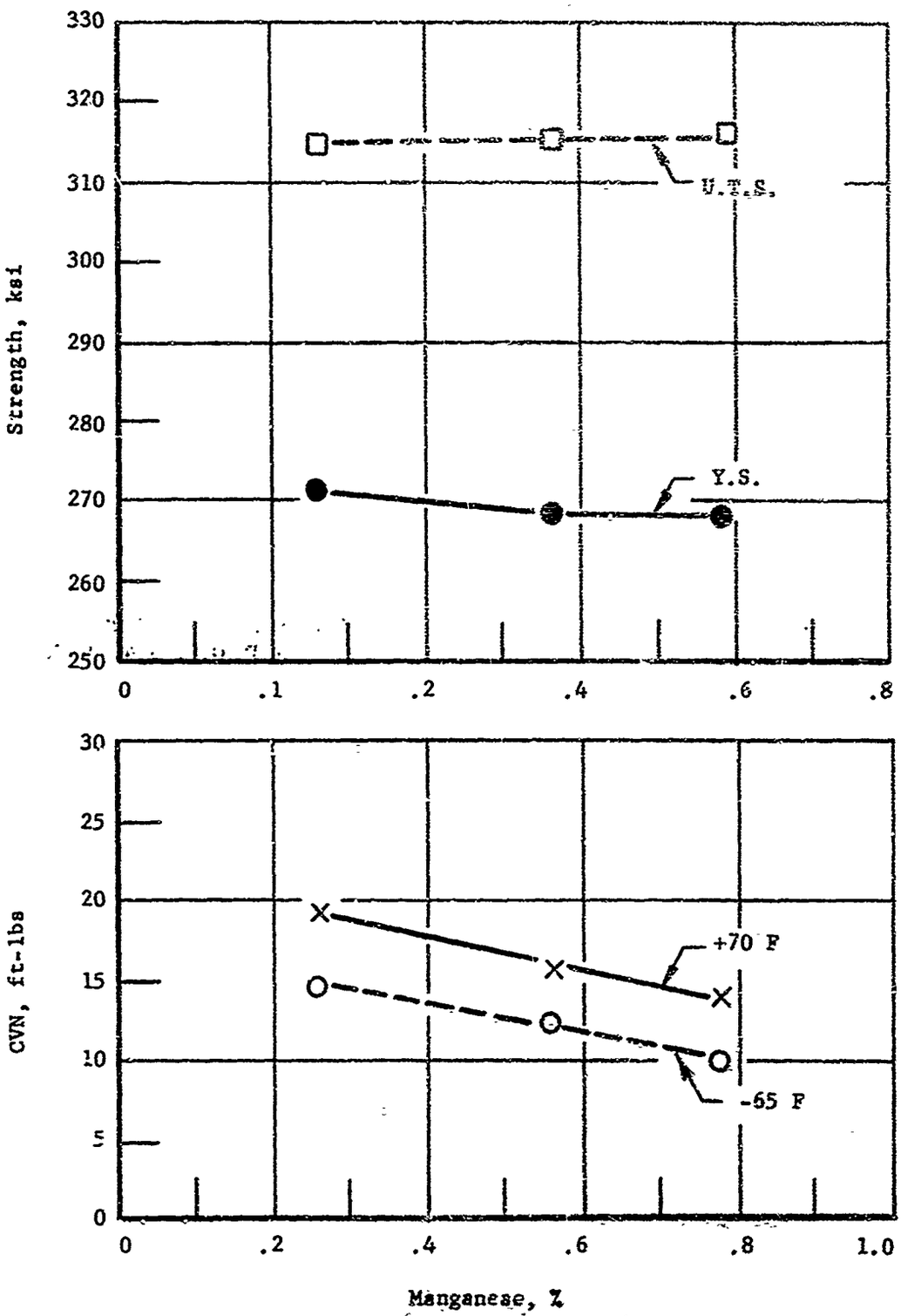

Figure 32. The Influence of Mn on Strength and Toughness in a Ni-Cr-Mo-Si-V Martensitic Steels

Figure 33. Transmission Electron Micrograph of Heat Z270, Containing 0.26% Mn, Showing Short Microtwins in Some of the Martensite Plates

20,000X

Figure 34. Transmission Electron Micrograph of Heat Z272, Containing 0.78% Mn, Showing Long Microtwins in the Martensite Plates

26,000X

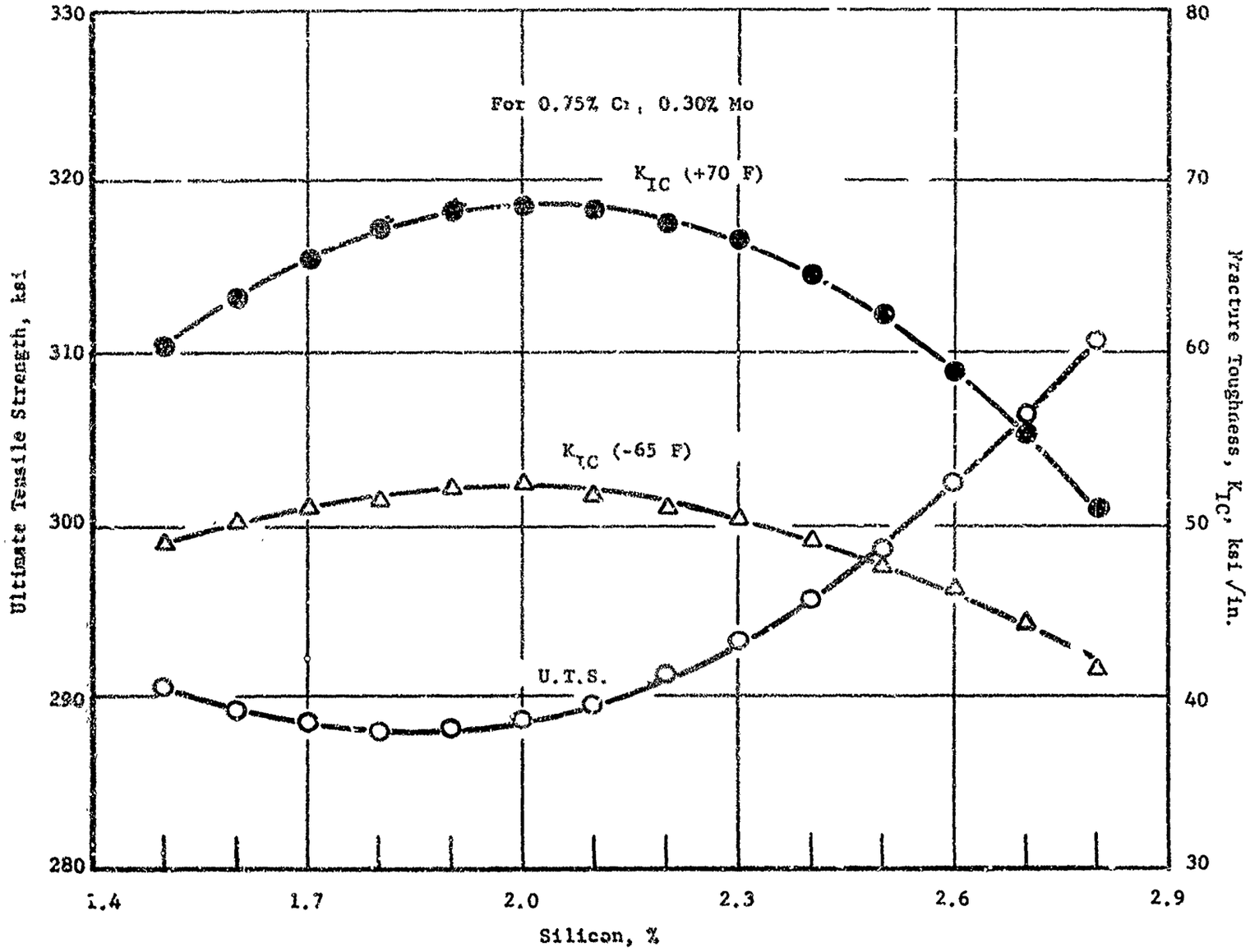

Figure 35. Graphical Representation of Mechanical Property-Composition (% Silicon) Prediction Equations for Heats R1 Through 15

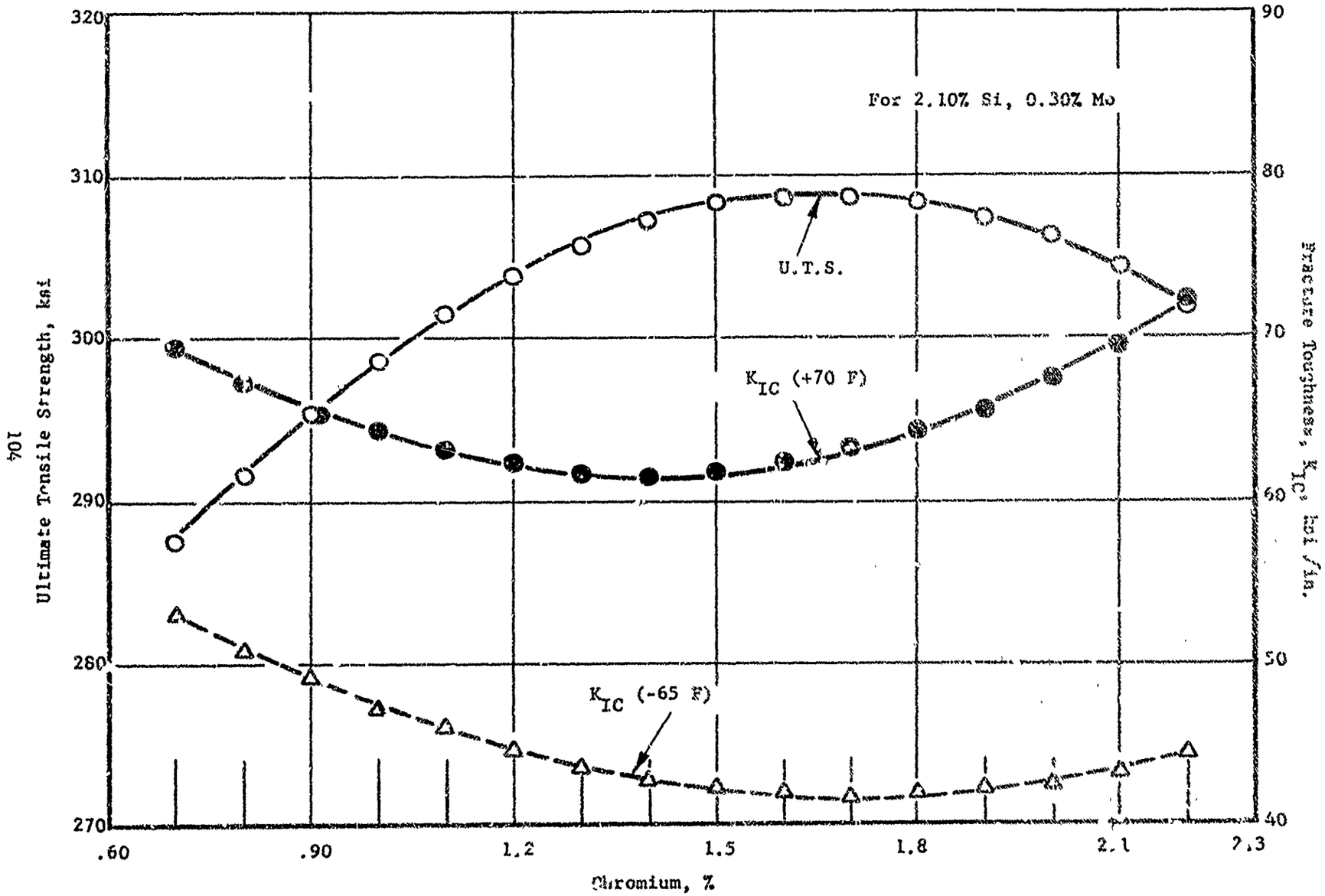

Figure 36. Graphical Representation of Mechanical Property-Composition (Chromium) Prediction Equations for Heats R1 Through 15

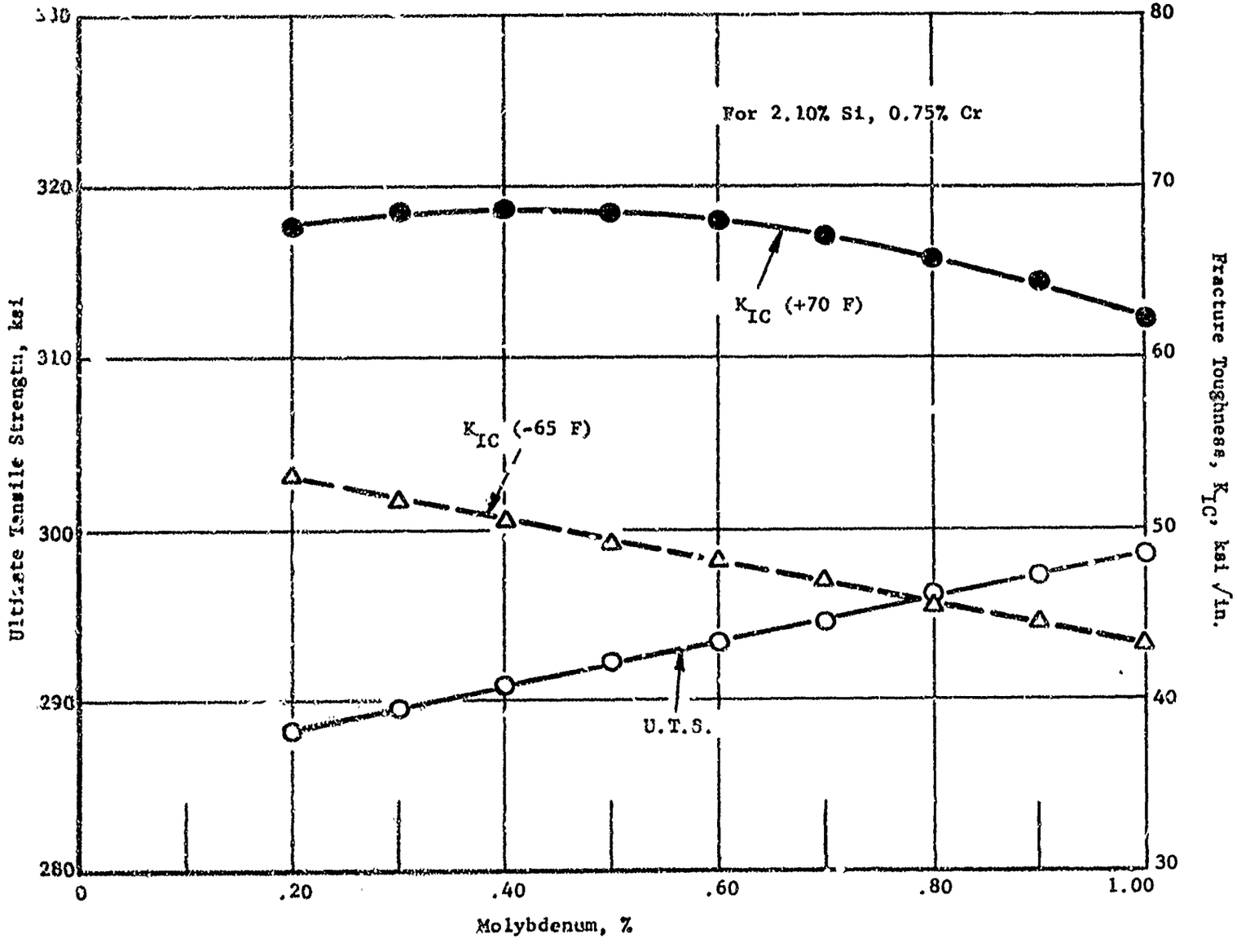

Figure 37. Graphical Representation of Mechanical Property-Composition (Molybdenum) Prediction Equations for Heats R1 Through 15

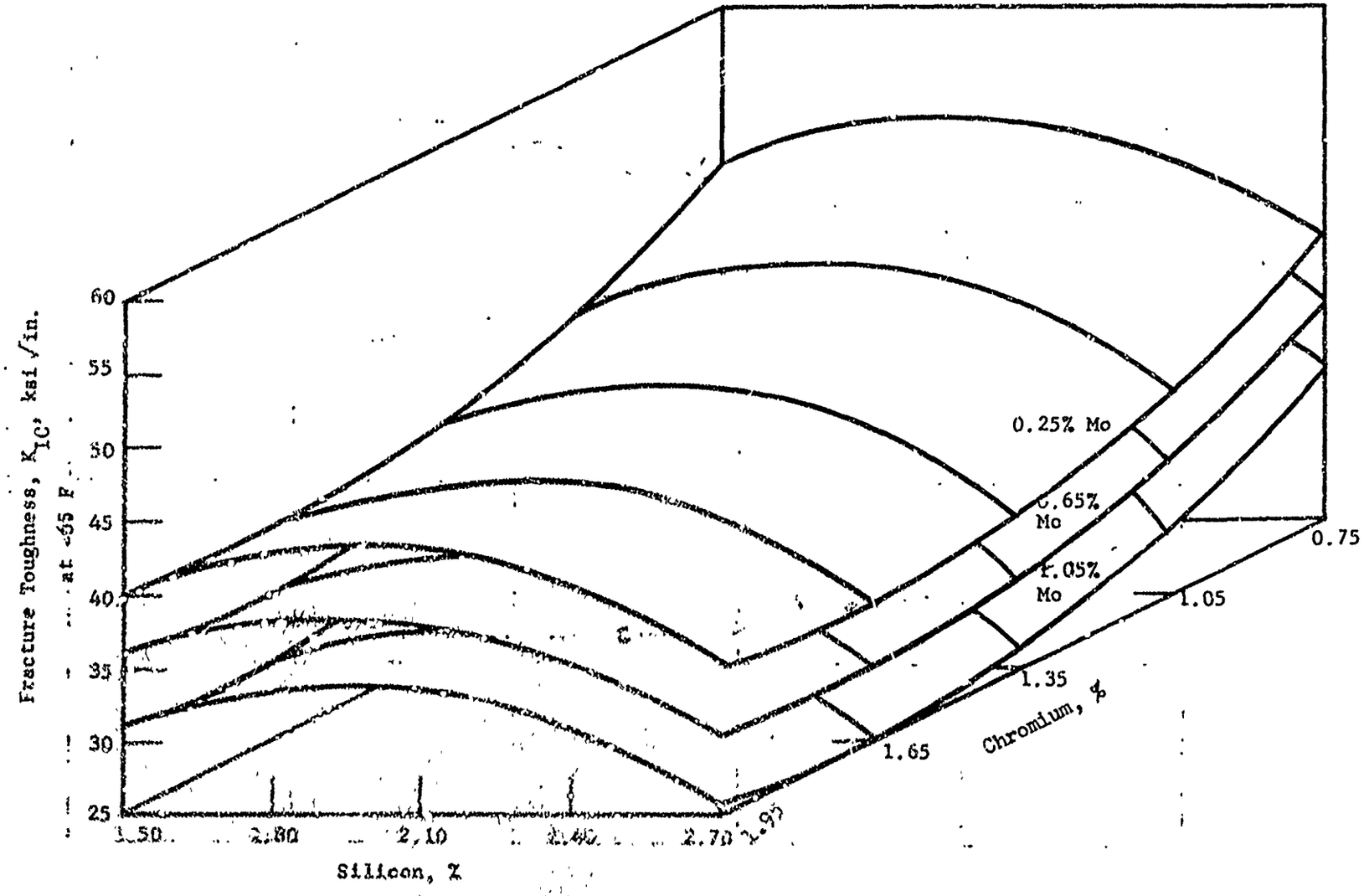

Figure 38. Three Dimensional Representation of the -65 F K_{IC} - Composition Prediction Equation for Heats K1 Through 15

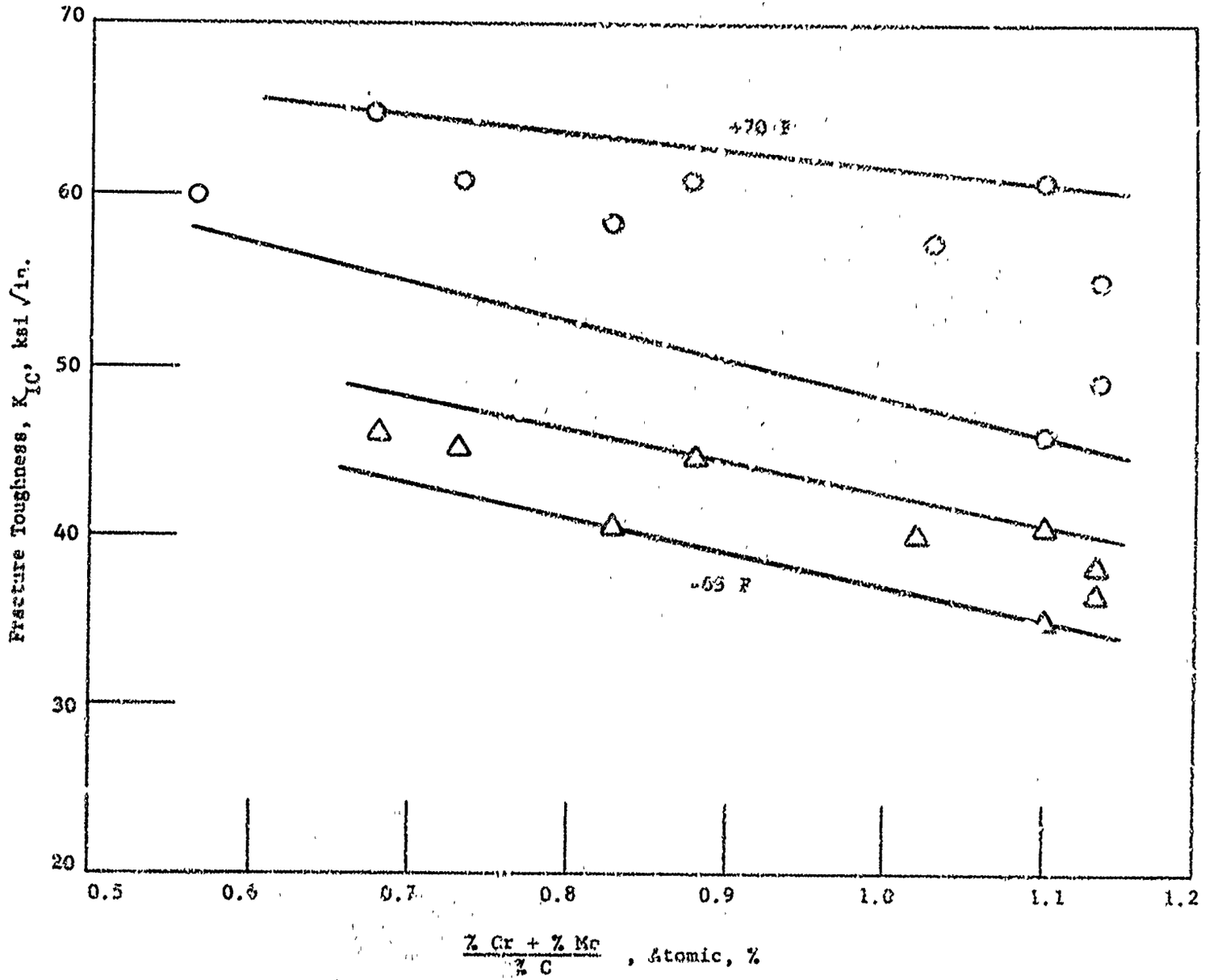

Figure 39. The Influence of Cr + Mo to Carbon Ratio on Fracture Toughness in Ni-Cr-Mo-Si-V Martensitic Steels

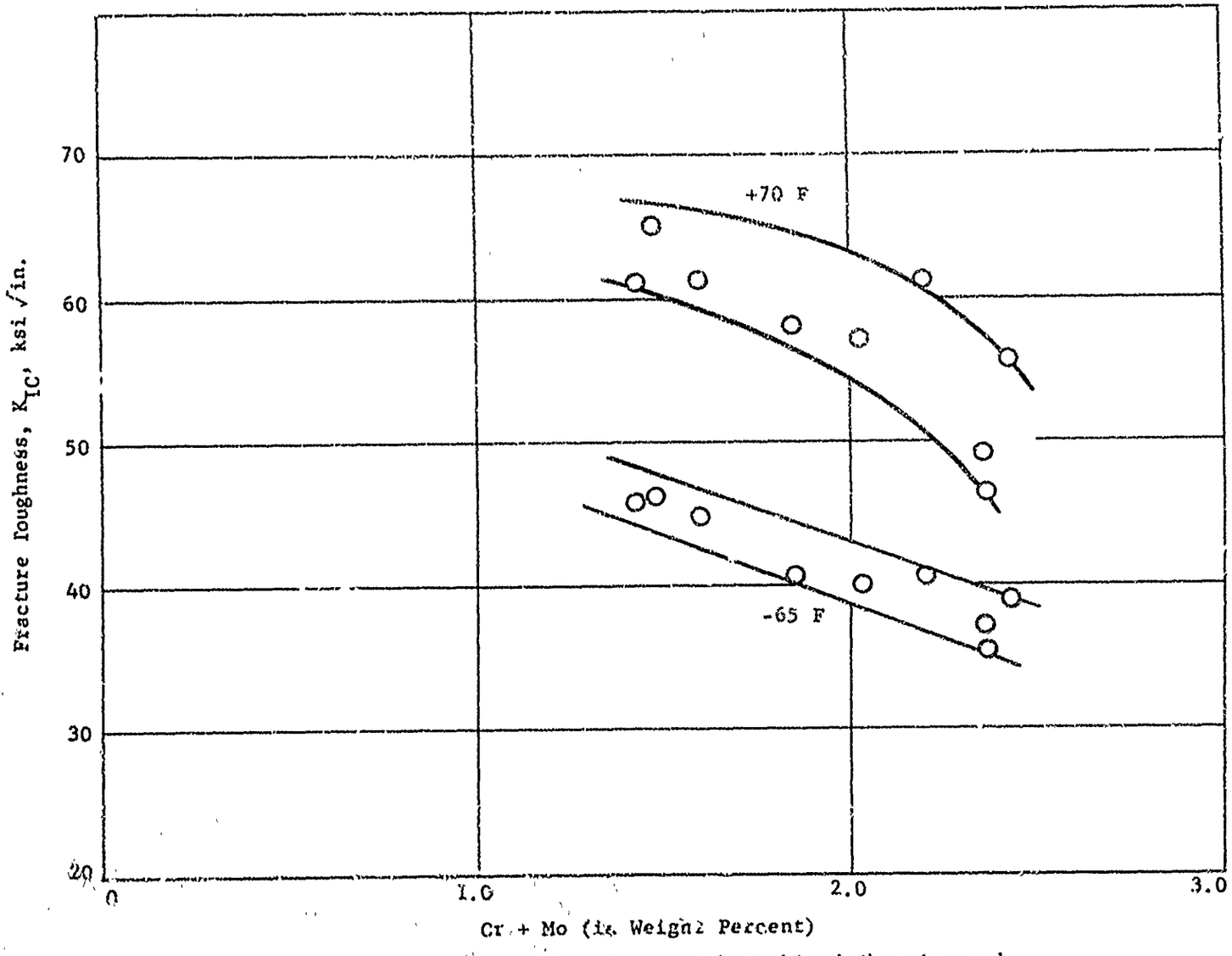

Figure 40. Variation of Fracture Toughness with Combined Chromium and Molybdenum Content

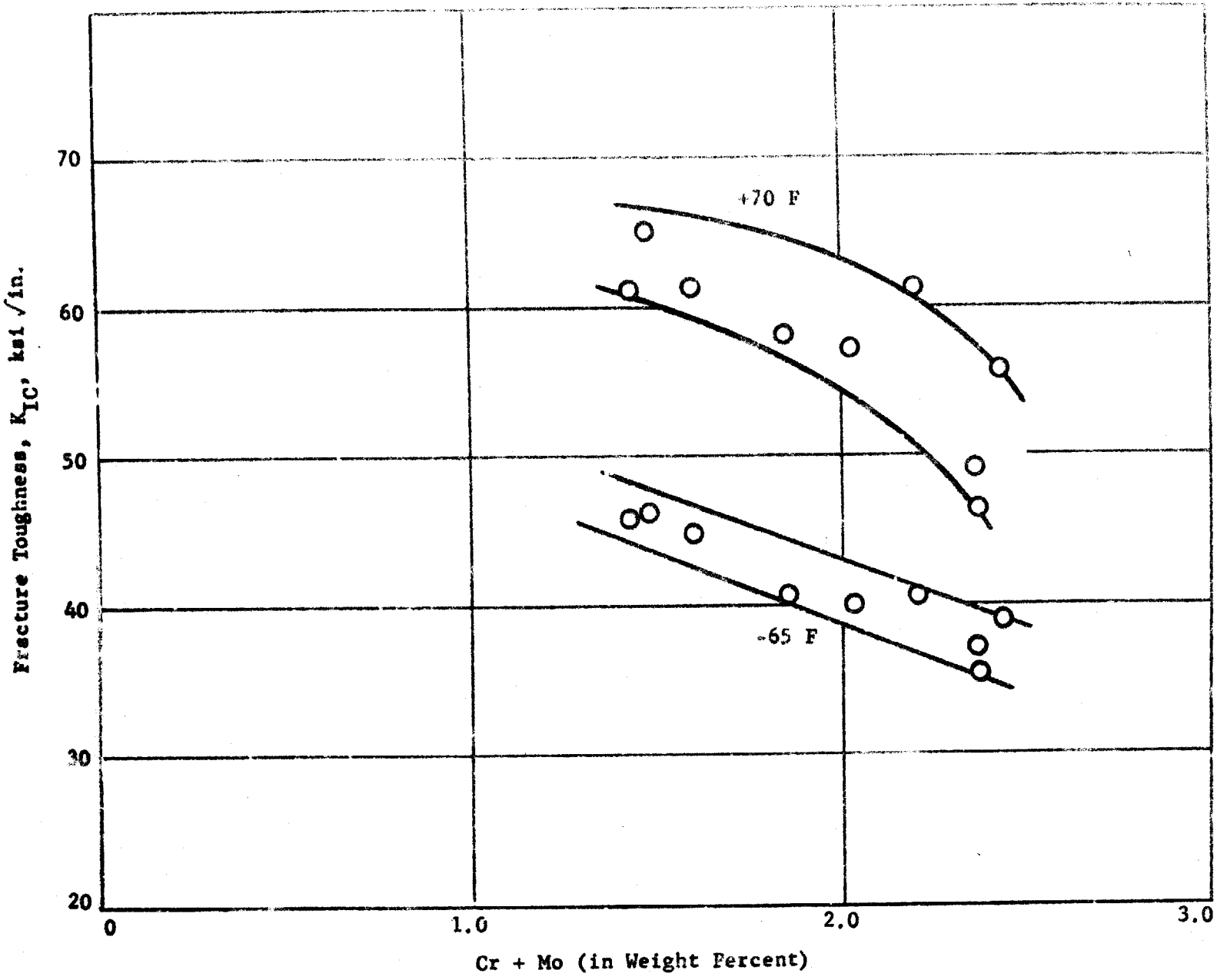

Figure 40. Variation of Fracture Toughness with Combined Chromium and Molybdenum Content

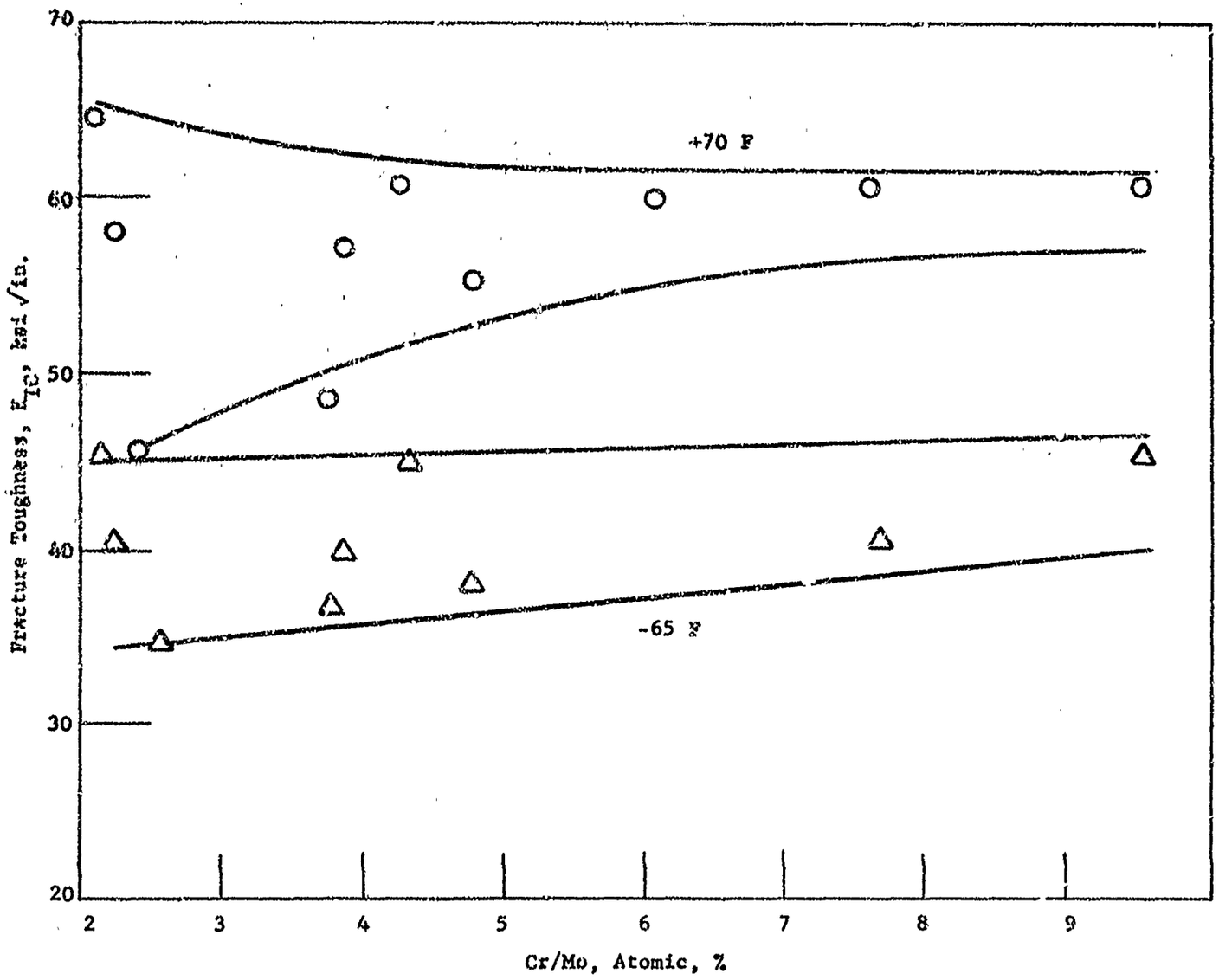

Figure 41. Variation of Fracture Toughness with Chromium to Molybdenum Ratio

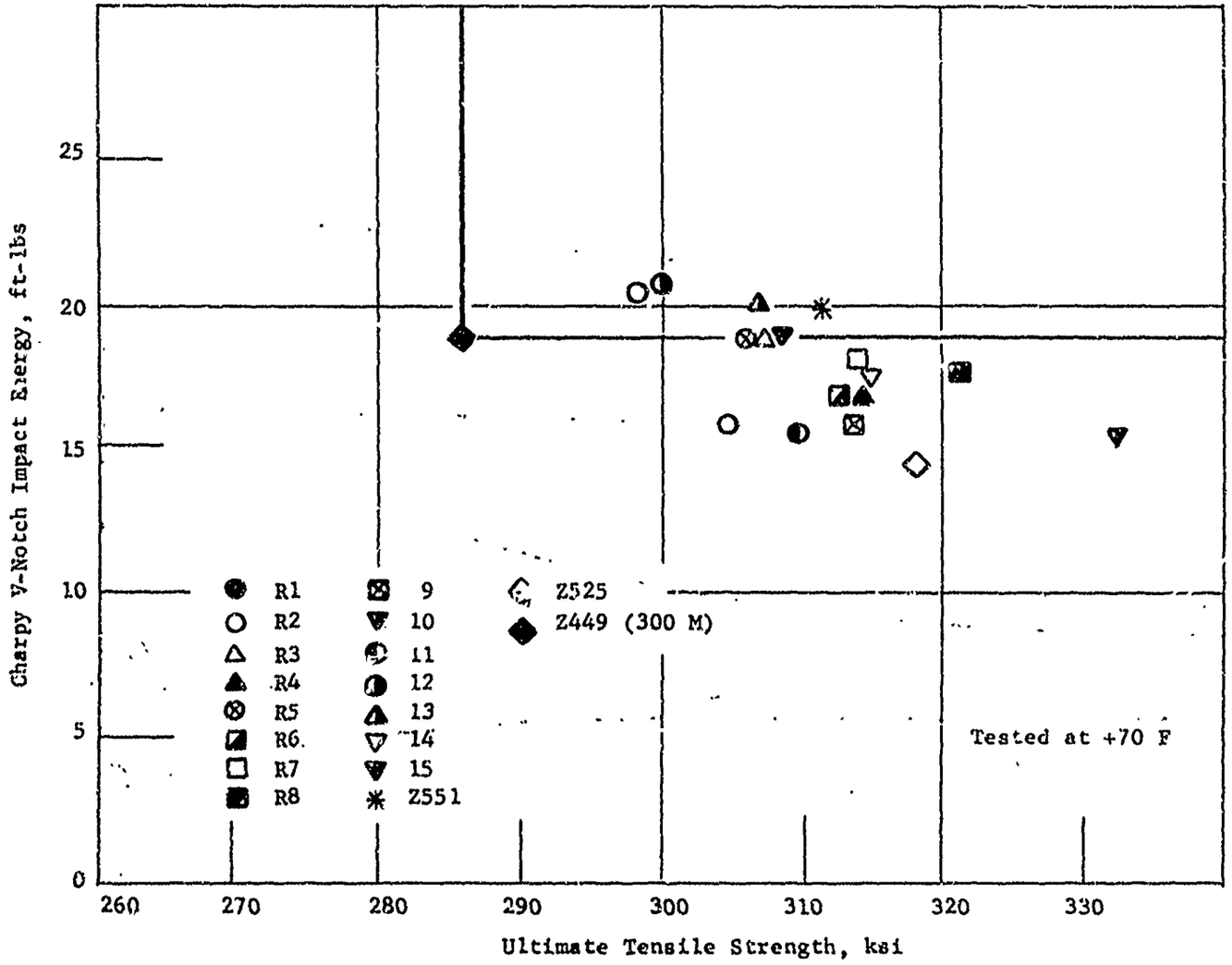

Figure 42. Strength-Toughness Relationships for Ni-Cr-Mo-Si-V Martensitic Steels Tested at +70 F

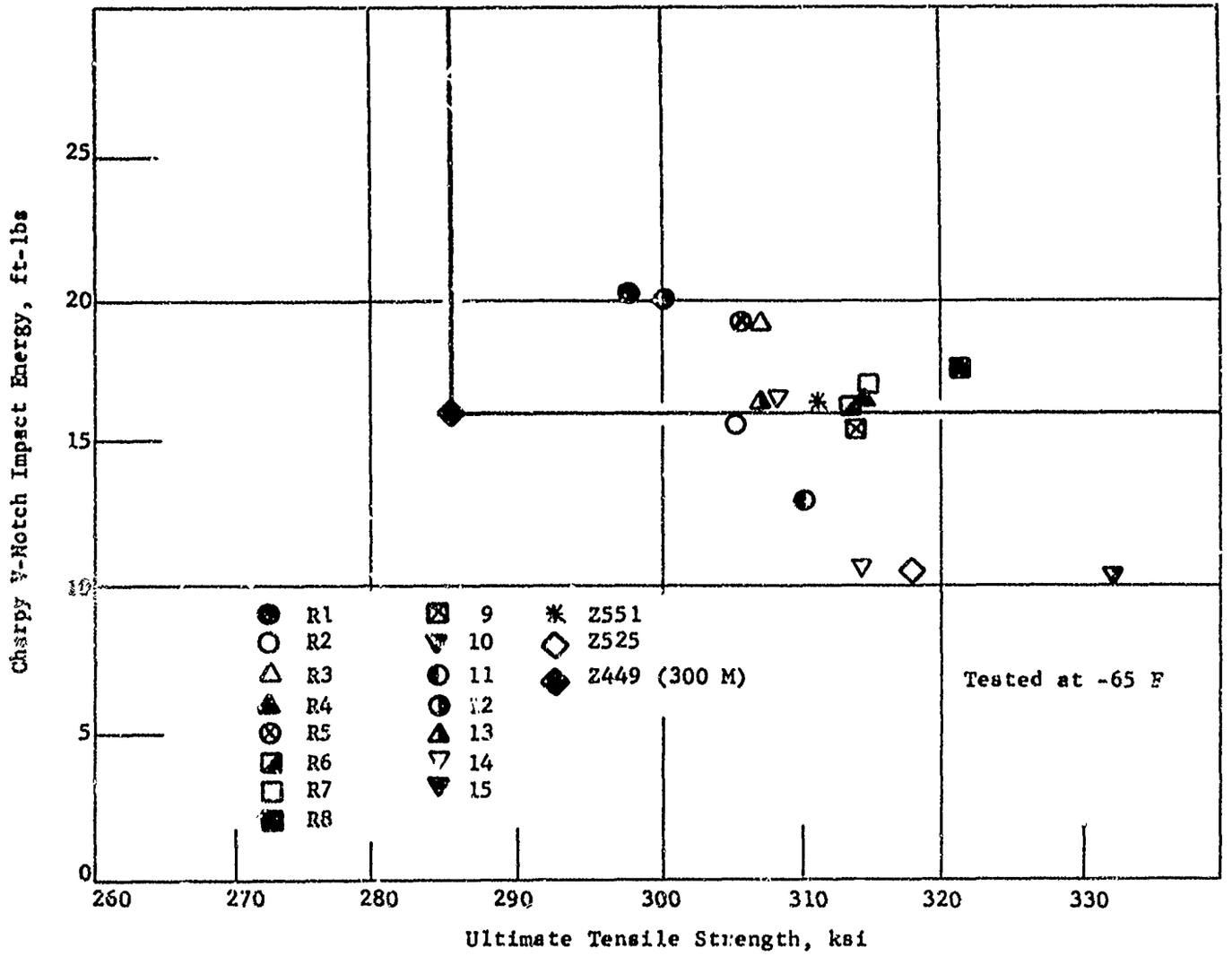

Figure 43. Strength-Toughness Relationships for Ni-Cr-Mo-Si-V Martensitic Steels Tested at -65 F

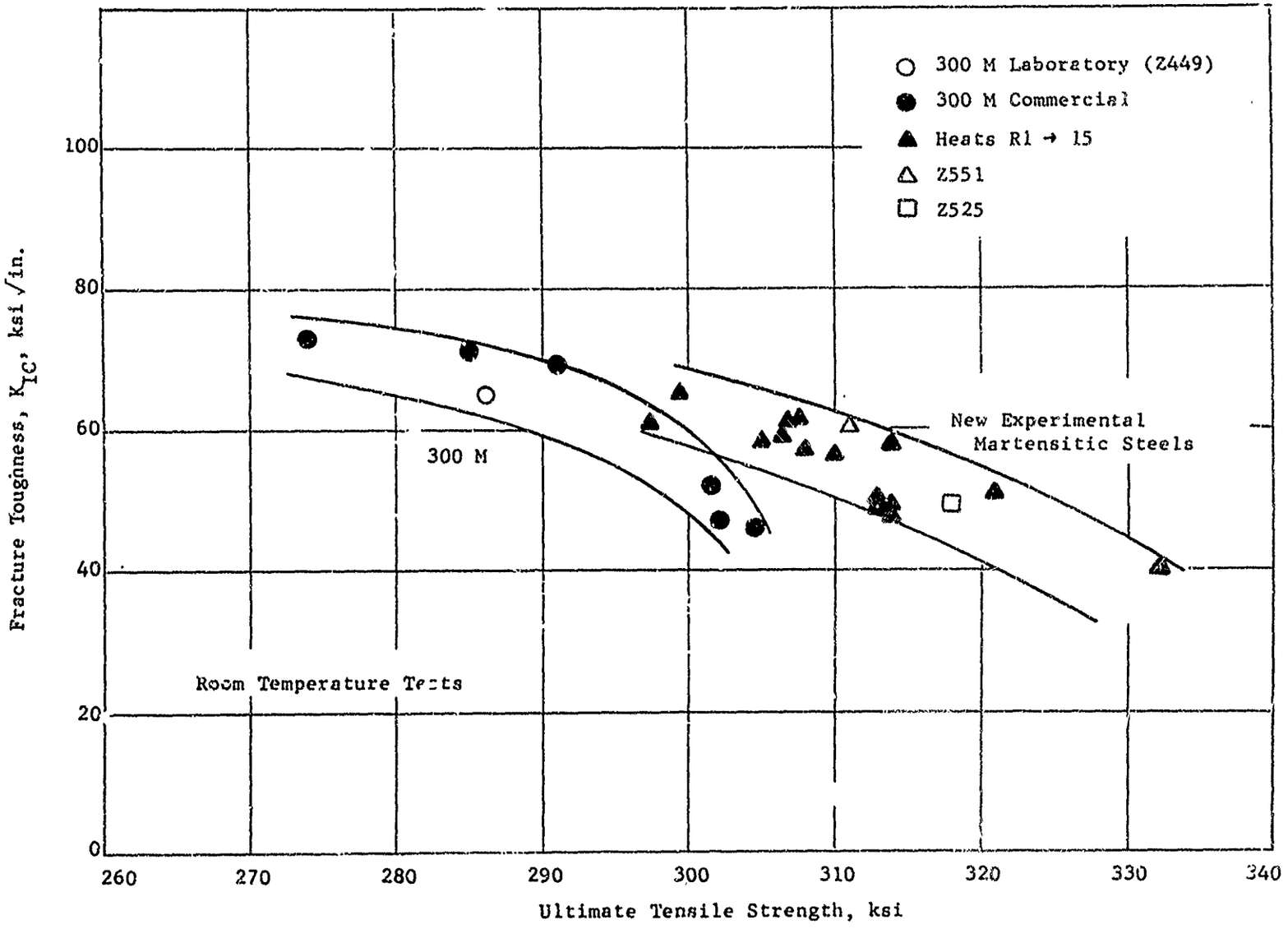

Figure 44. Tensile Strength-Fracture Toughness Relationships for Experimental Low Alloy Martensitic Steels Compared to 300 M Steel

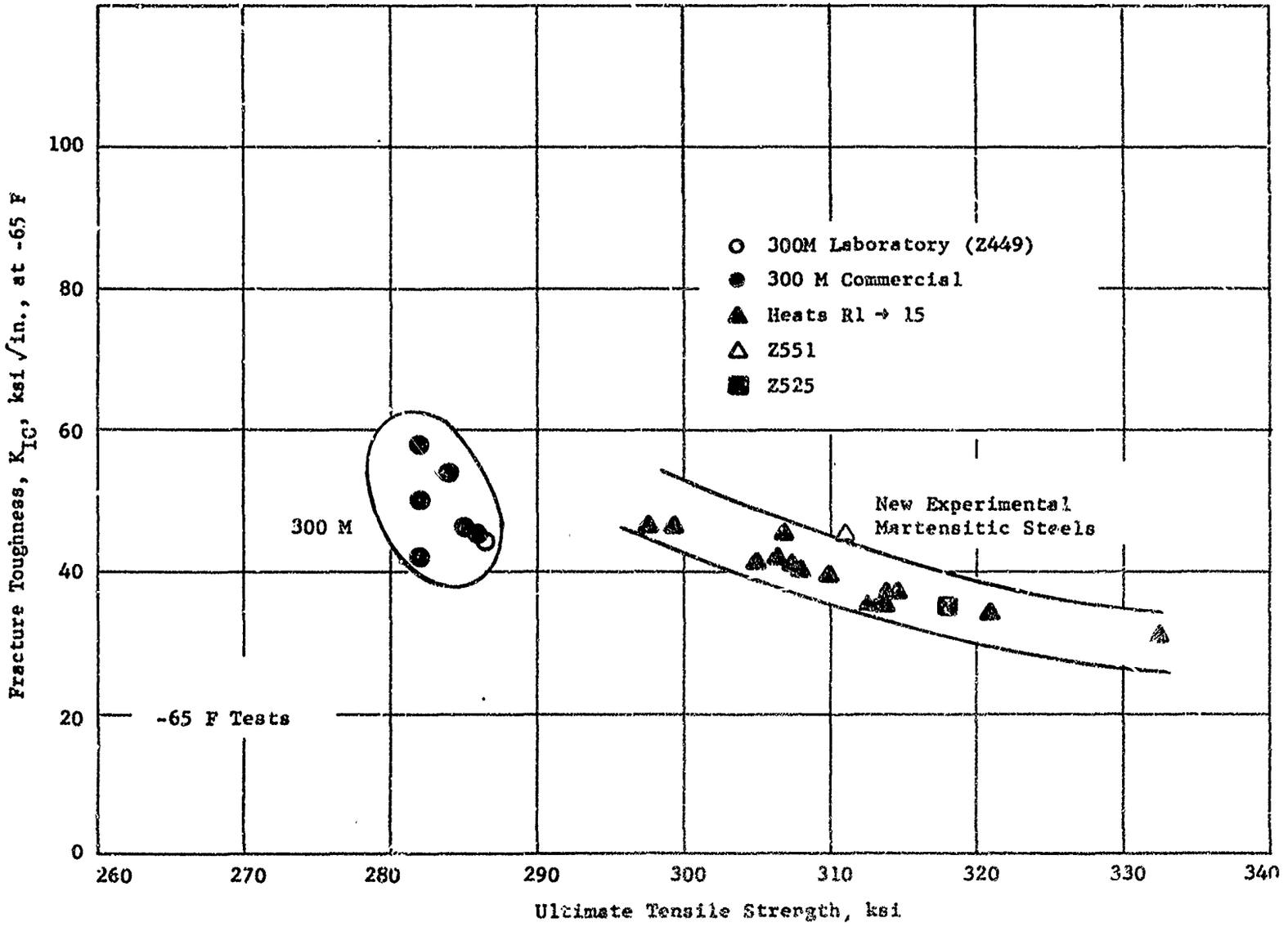

Figure 45. Tensile Strength-Fracture Toughness Relationships for Experimental Low Alloy Martensitic Steels Compared to 300 M Steel

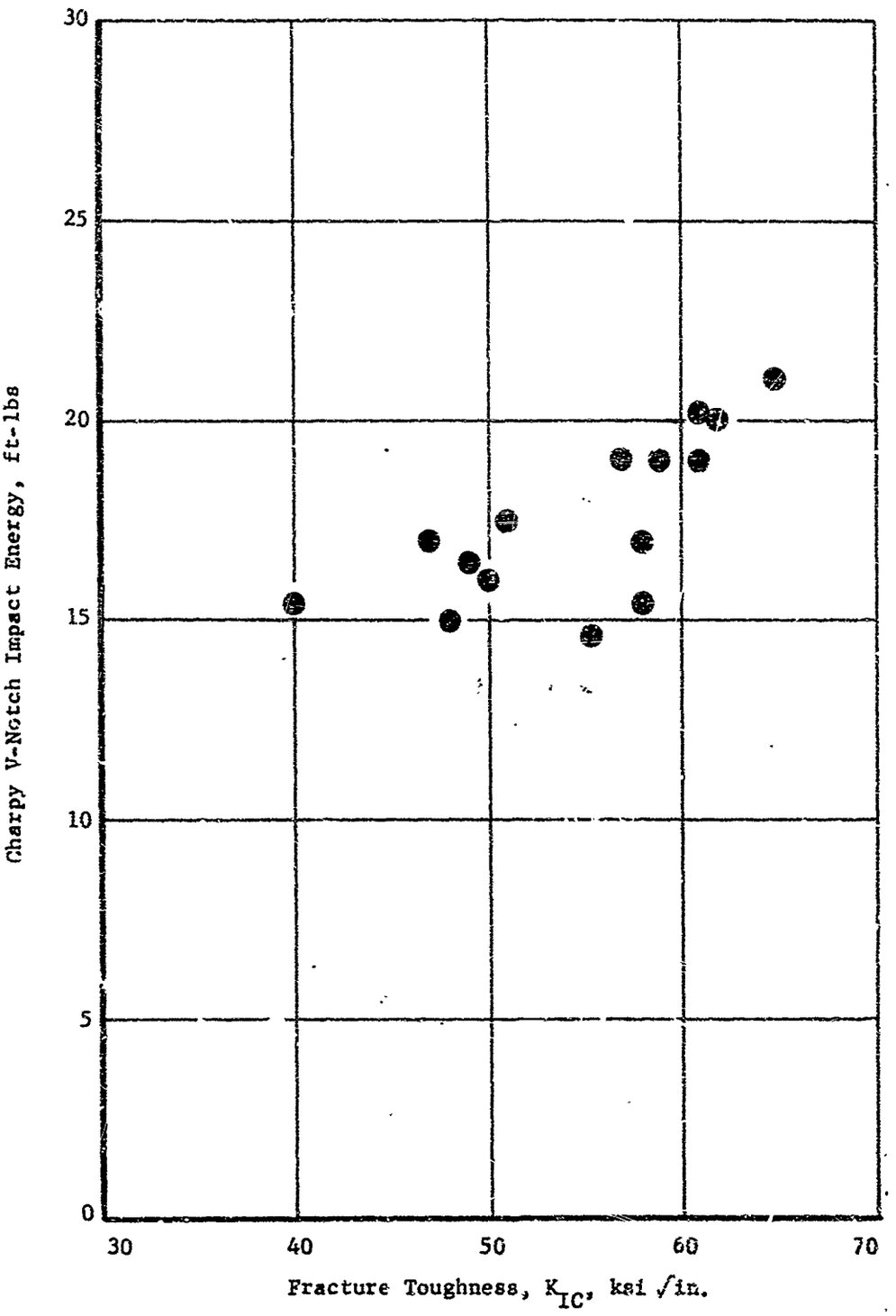

Figure 46. Comparison of Fracture Toughness and Charpy Impact Energy Values for Heats R 1 through 15

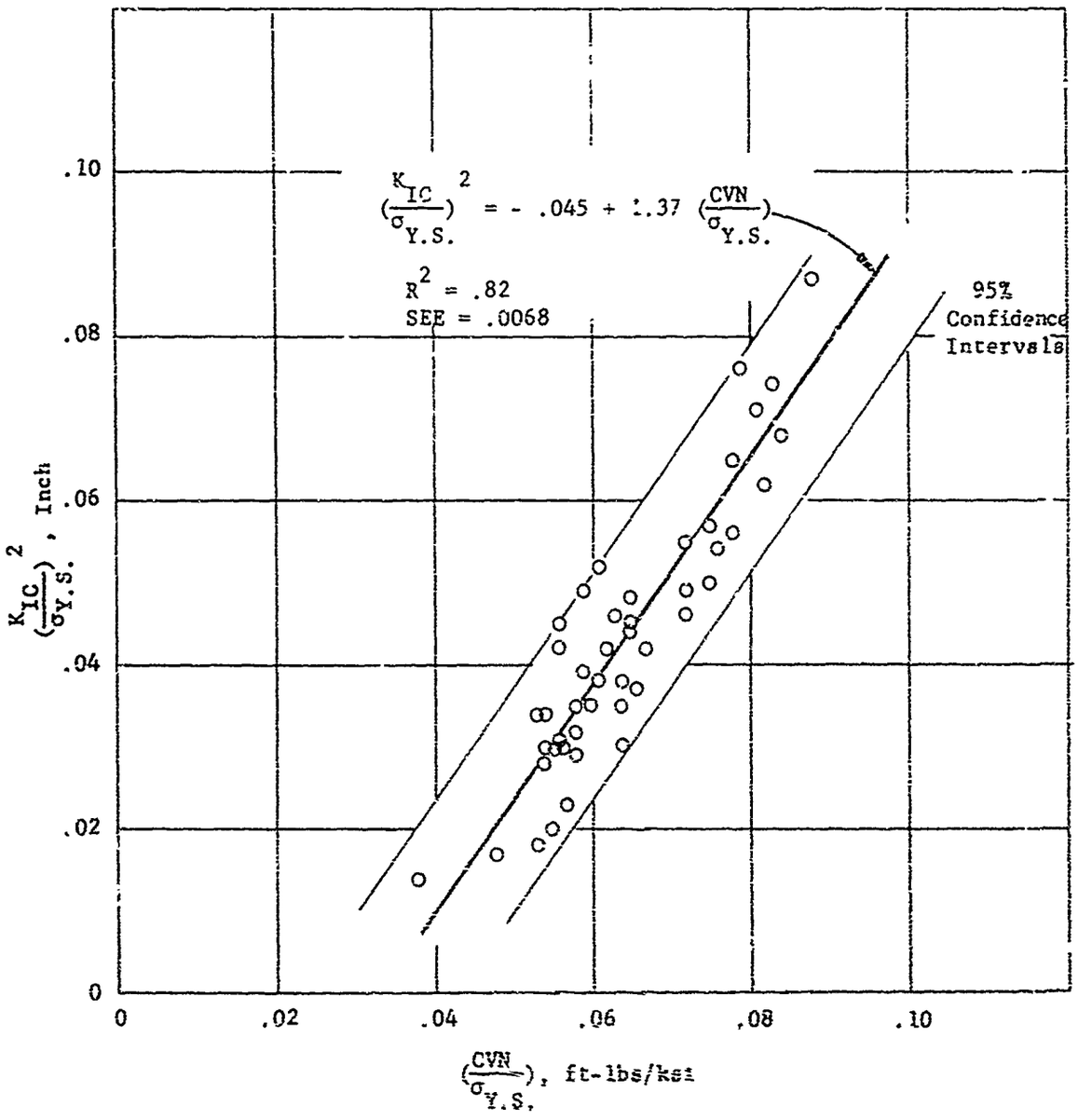

Figure 47. Relation Between Room Temperature K_{IC} and CVN Values for Low Alloy Ultra-High Strength Martensitic Steels

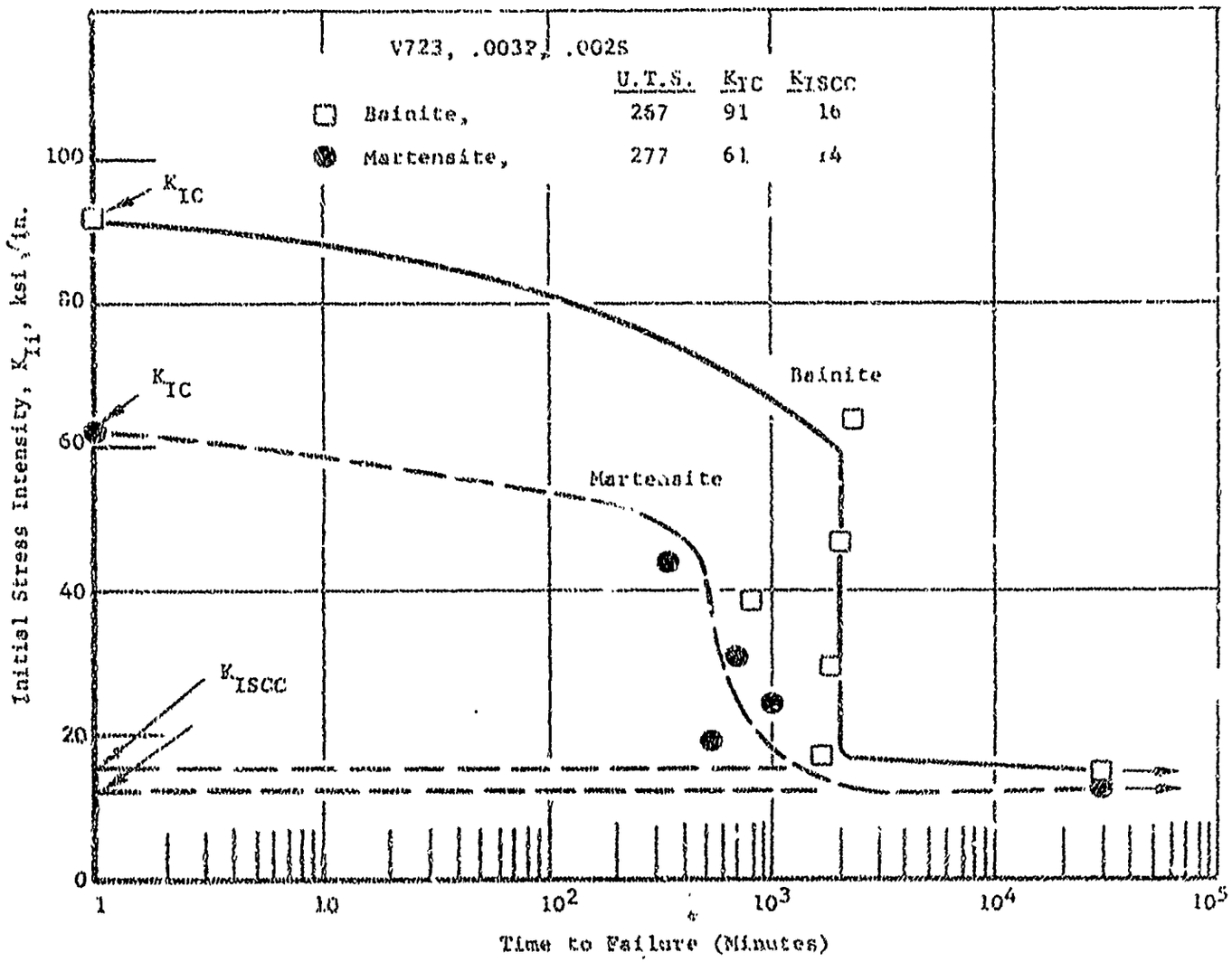

Figure 48. Stress Corrosion Behavior of 9-4-45 Steel with .003 P and .002 S

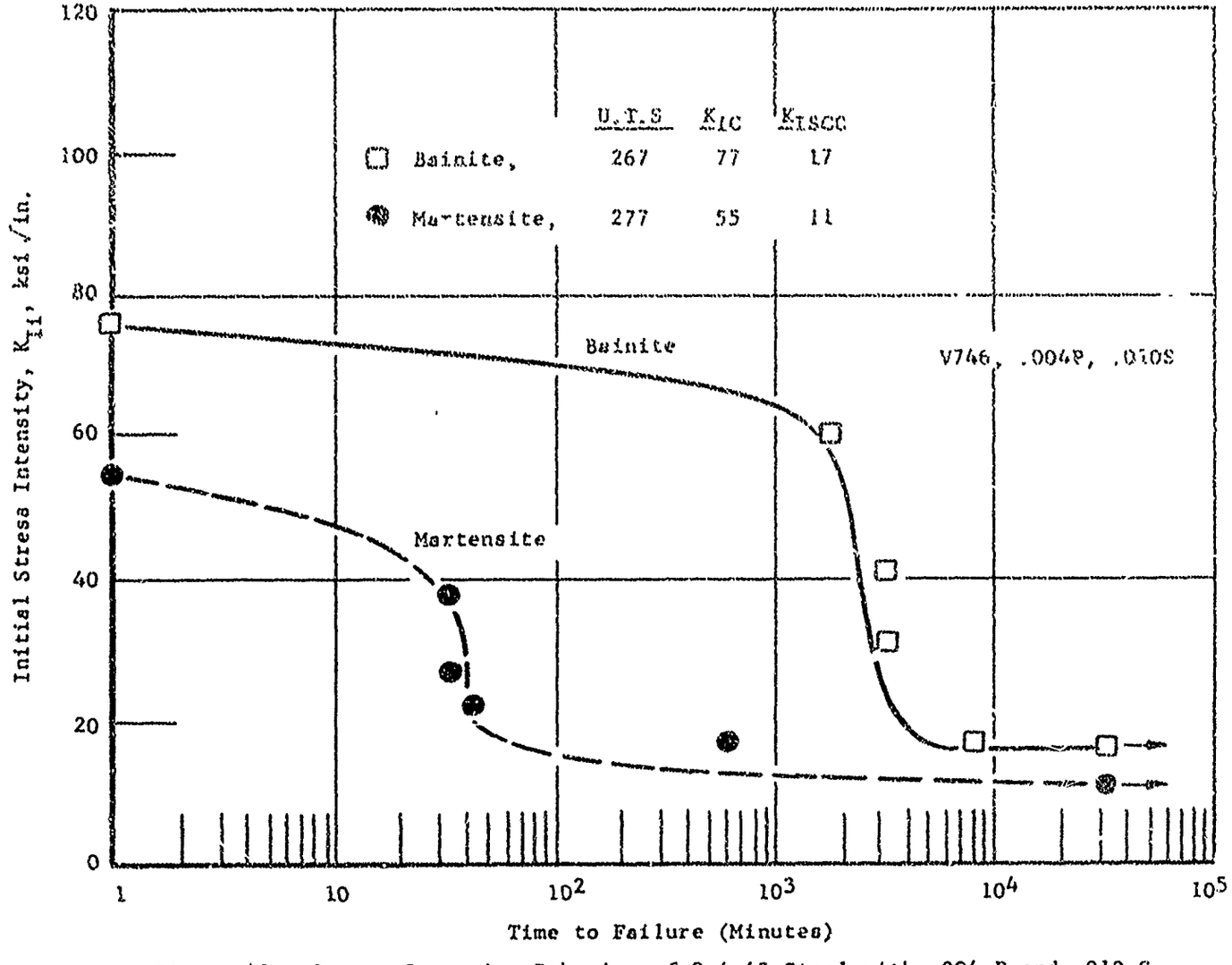

Figure 49. Stress Corrosion Behavior of 9-4-45 Steel with .004 P and .010 S

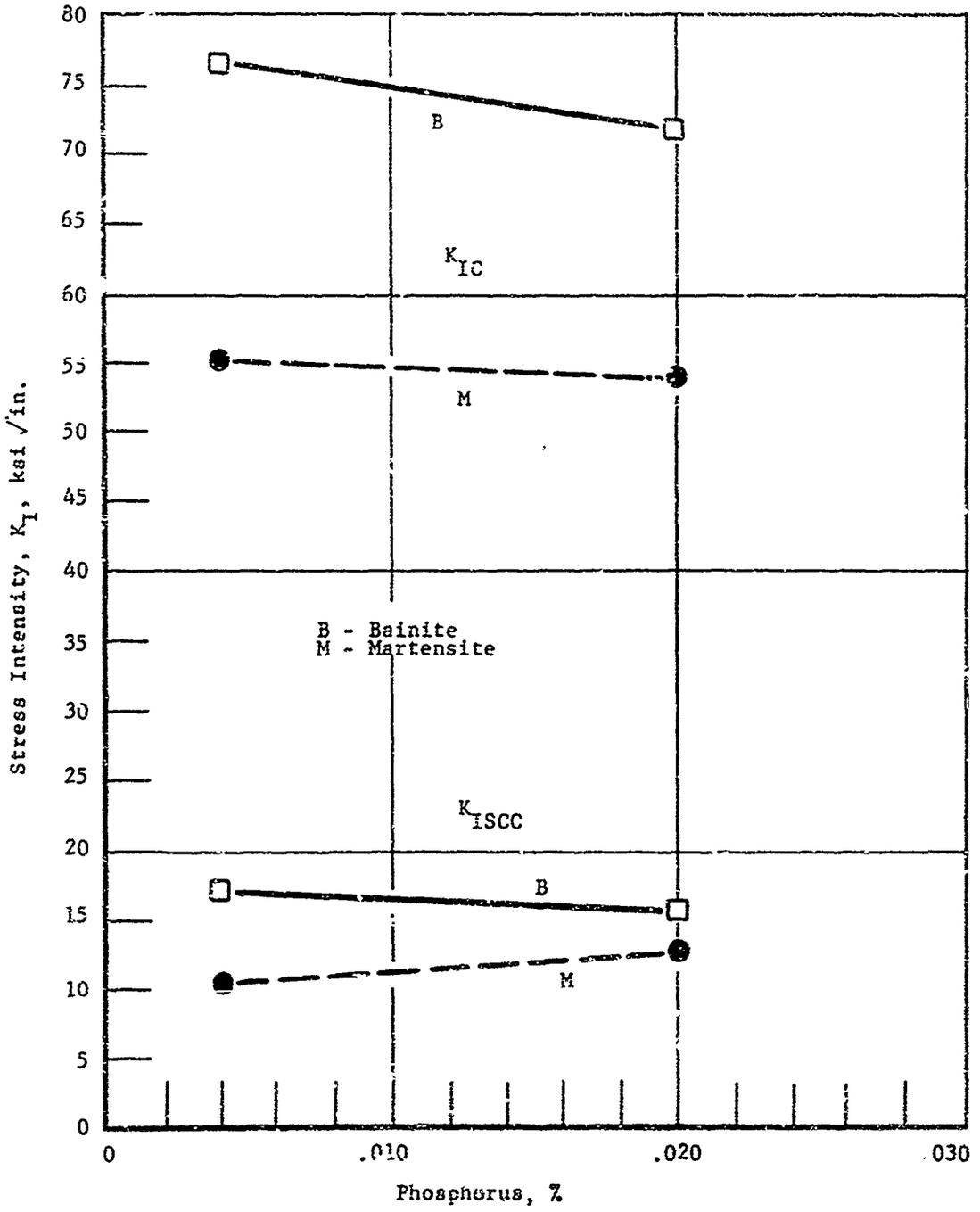

Figure 50. Effect of Phosphorus Content on K_{IC} and K_{ISCC} for 9-4-45 Steel

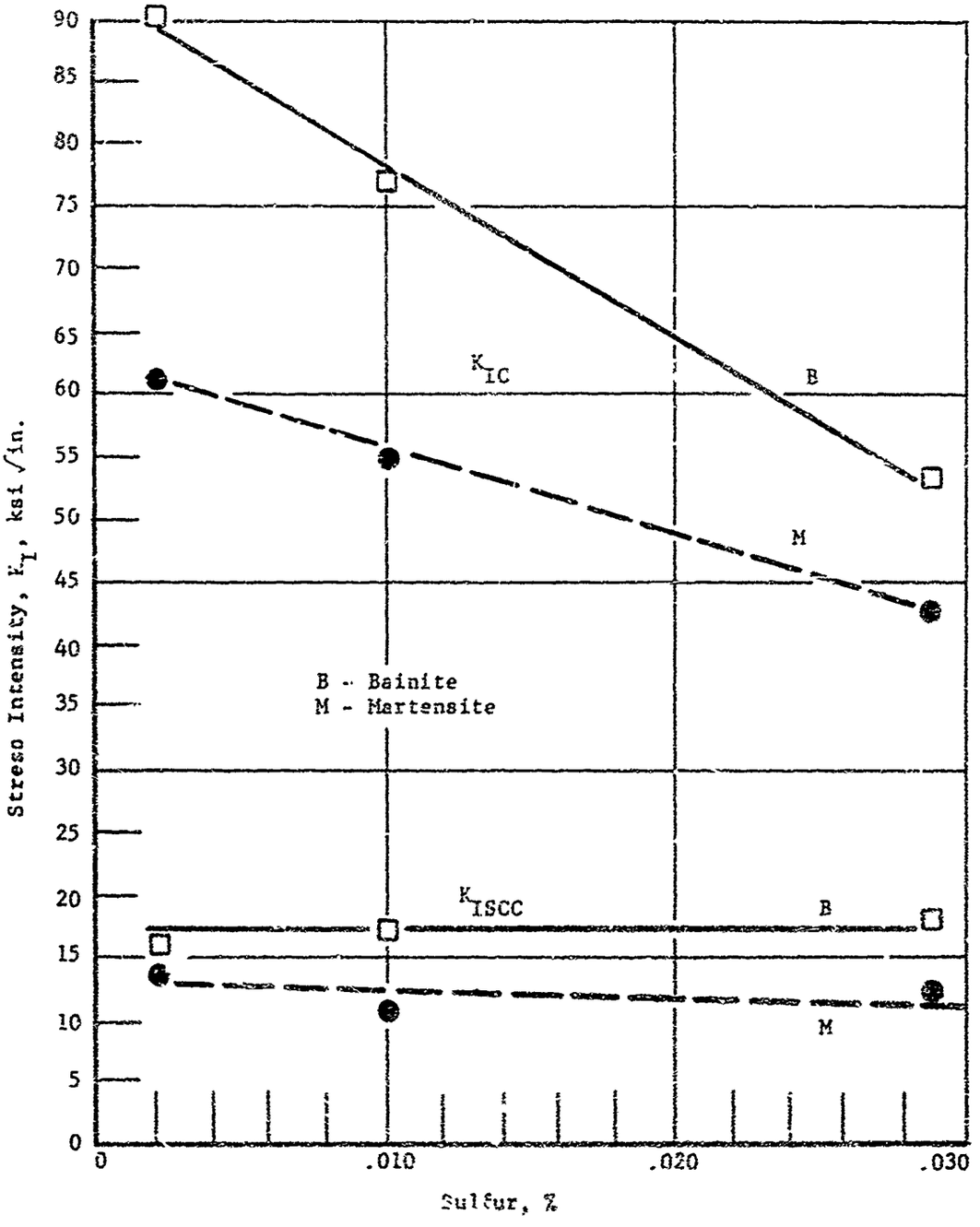

Figure 51. Effect of Sulfur Content on K_{IC} and K_{ISCC} for 9-4-45 Steel

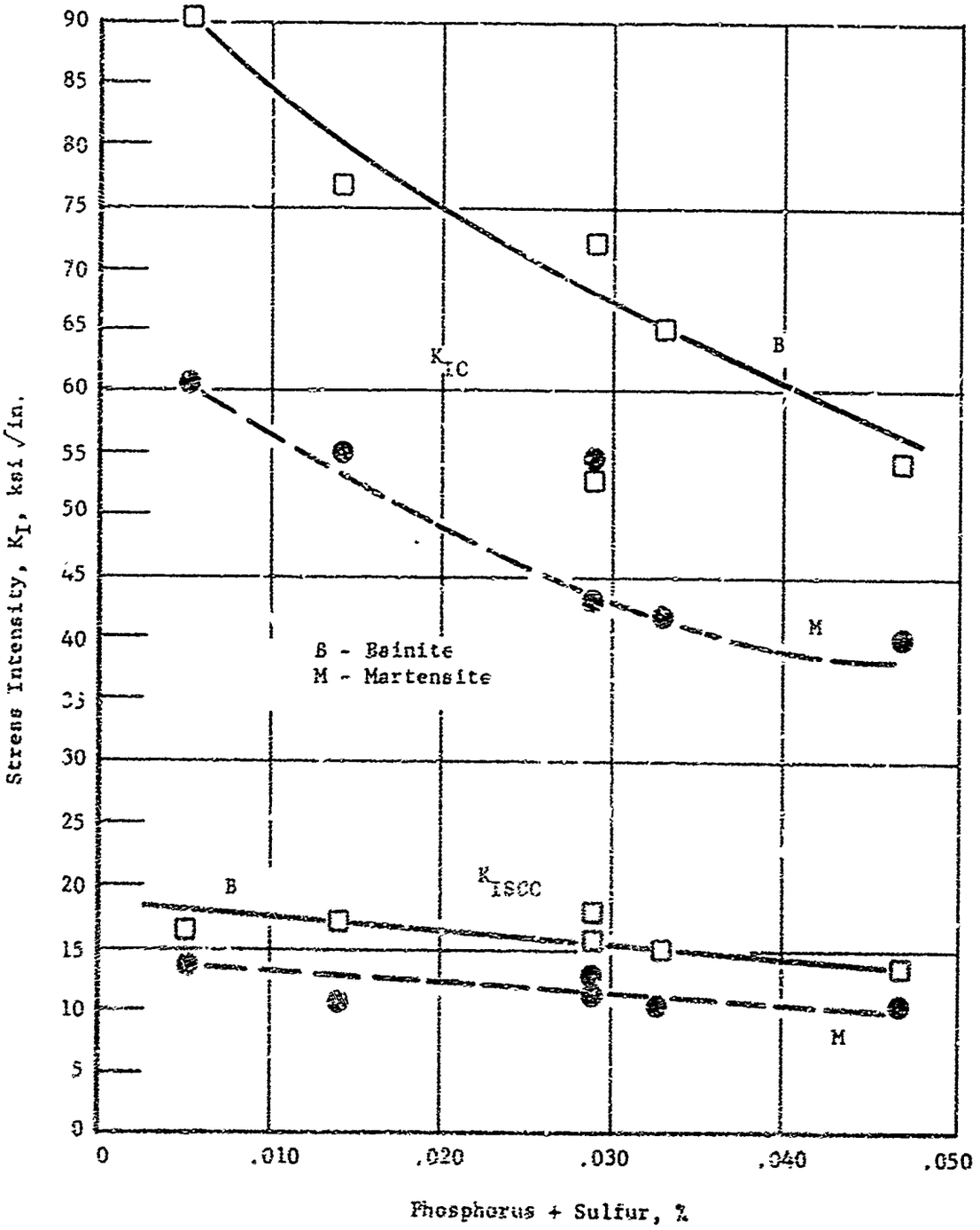

Figure 52. Effect of Phosphorus Plus Sulfur Content on K_{IC} and K_{ISCC} for 9-4-45 Steel

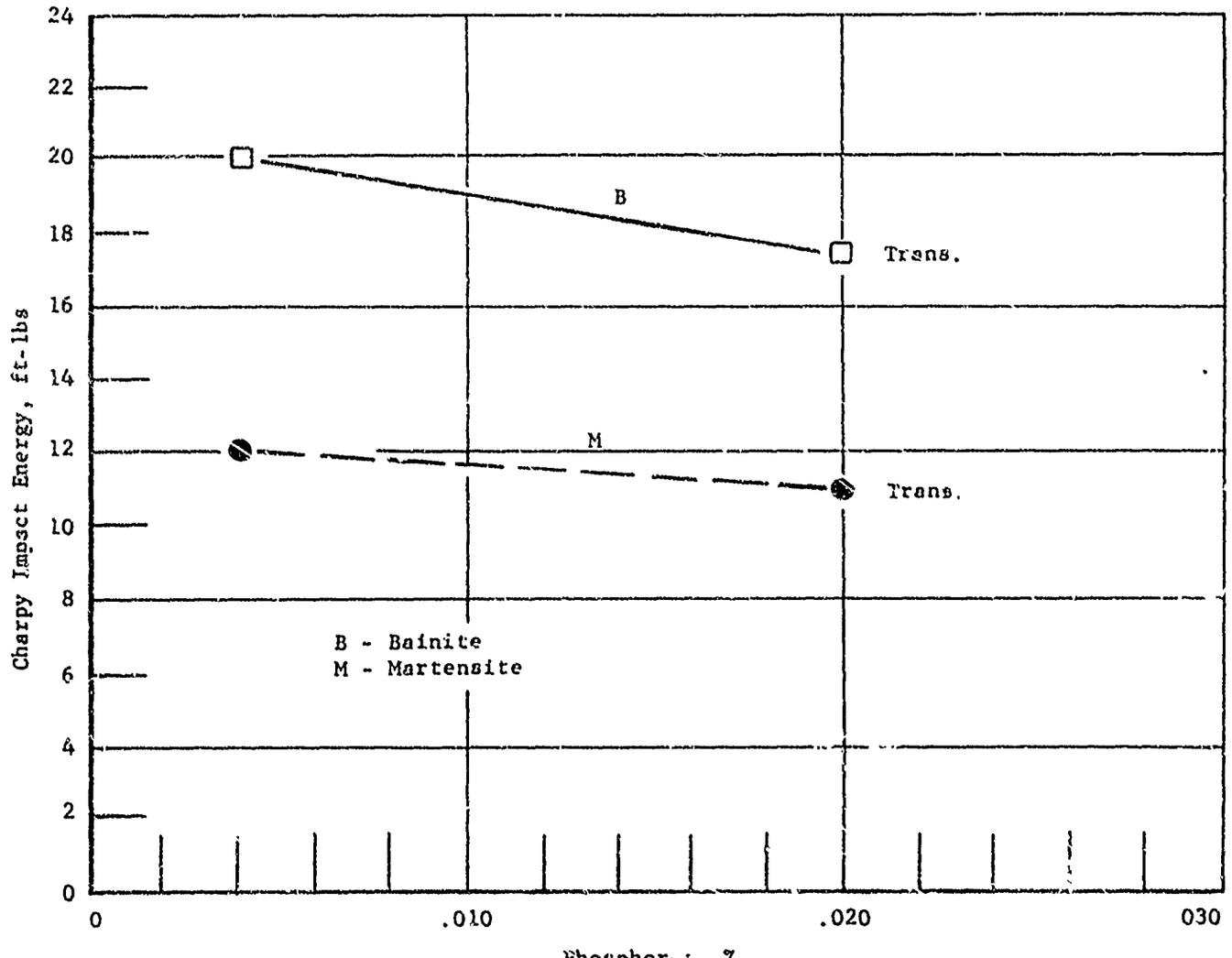

Figure 53. Impact Properties of 9-4-45 Steel as a Function of Phosphorus Content

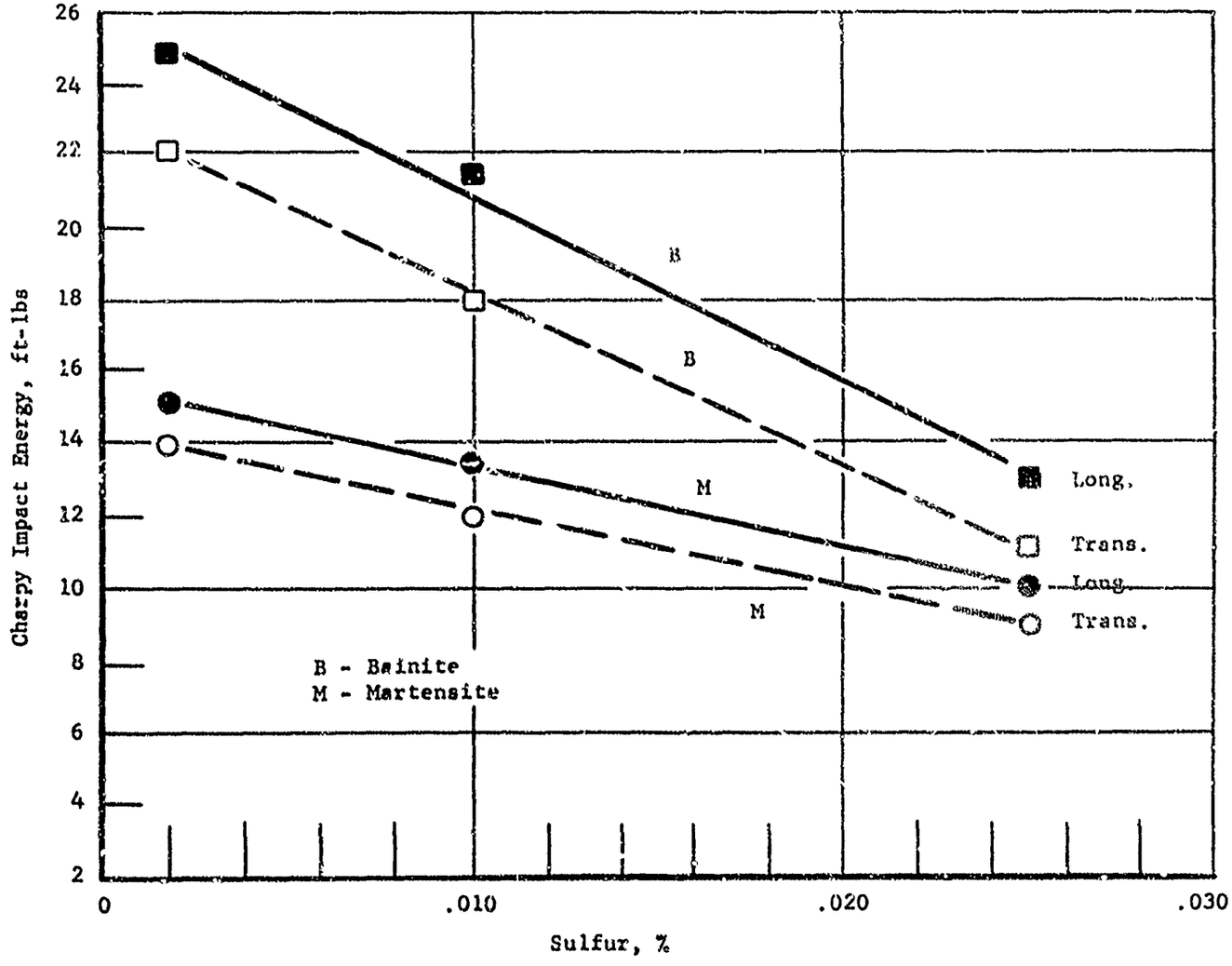

Figure 54. Impact Properties of 9-4-45 Steel as a Function of Sulfur Content

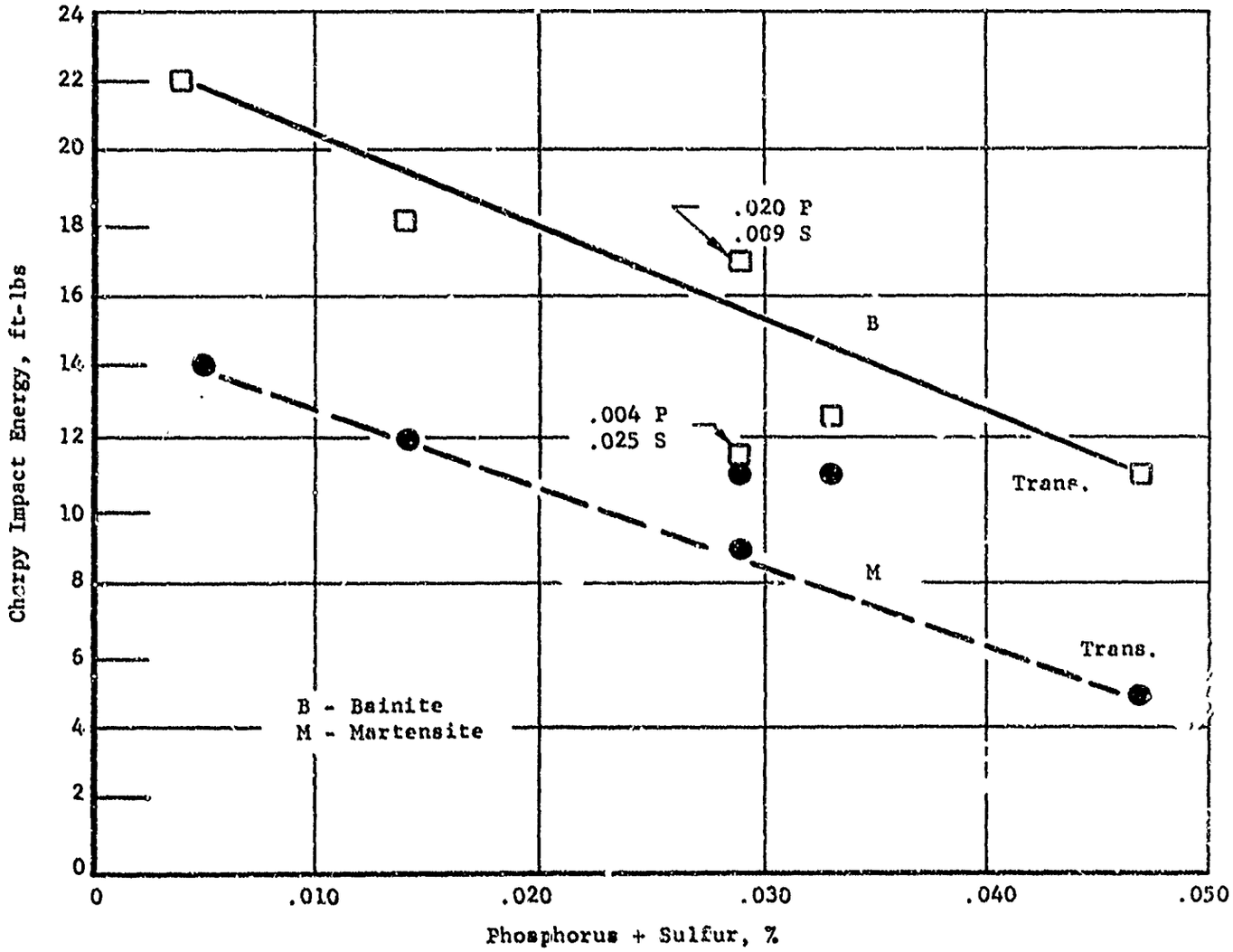

Figure 55. Impact Properties of 9-4-45 Steel as a Function of P + S Content

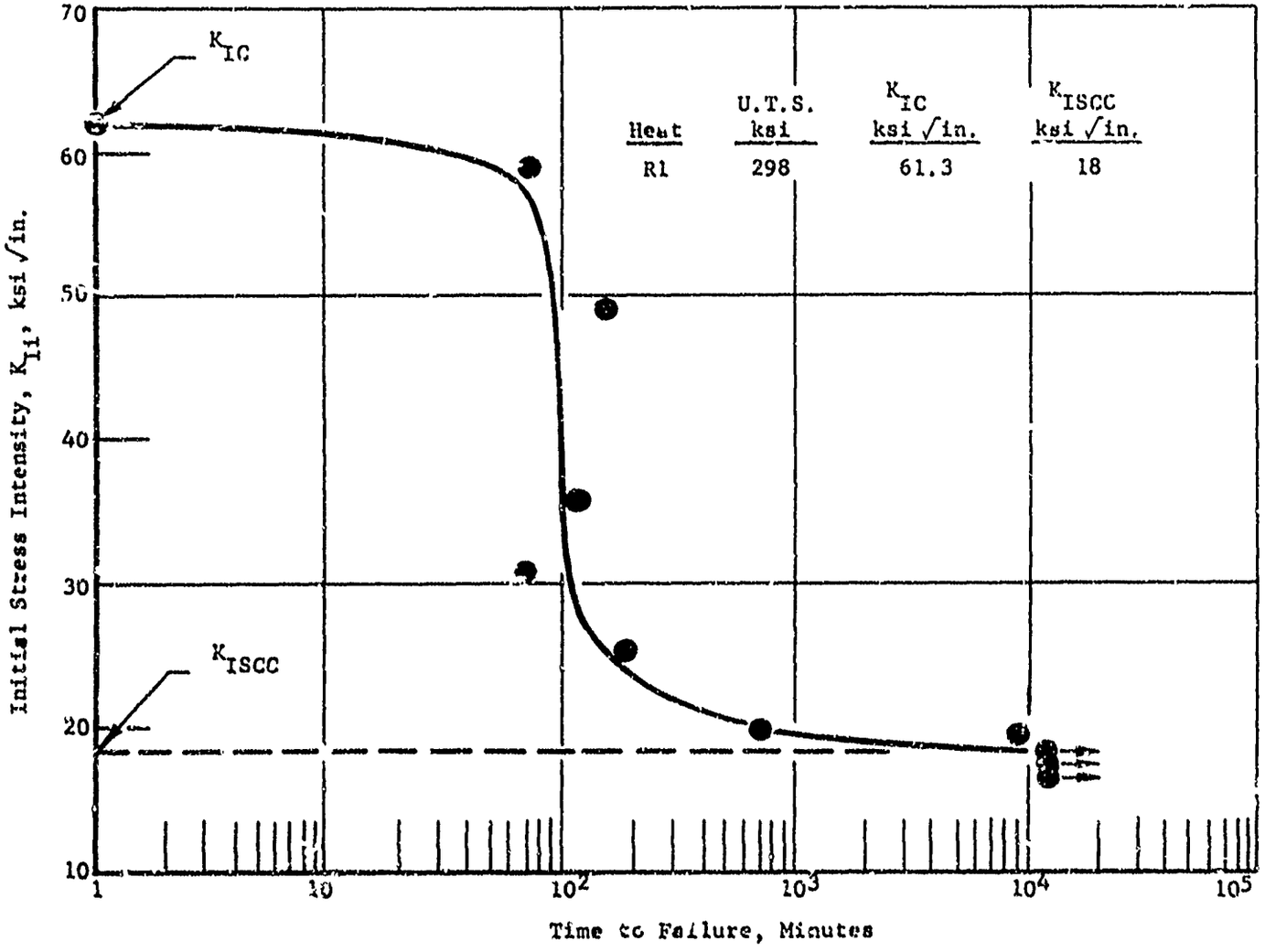

Figure 56. Stress Corrosion Curve for Heat R1

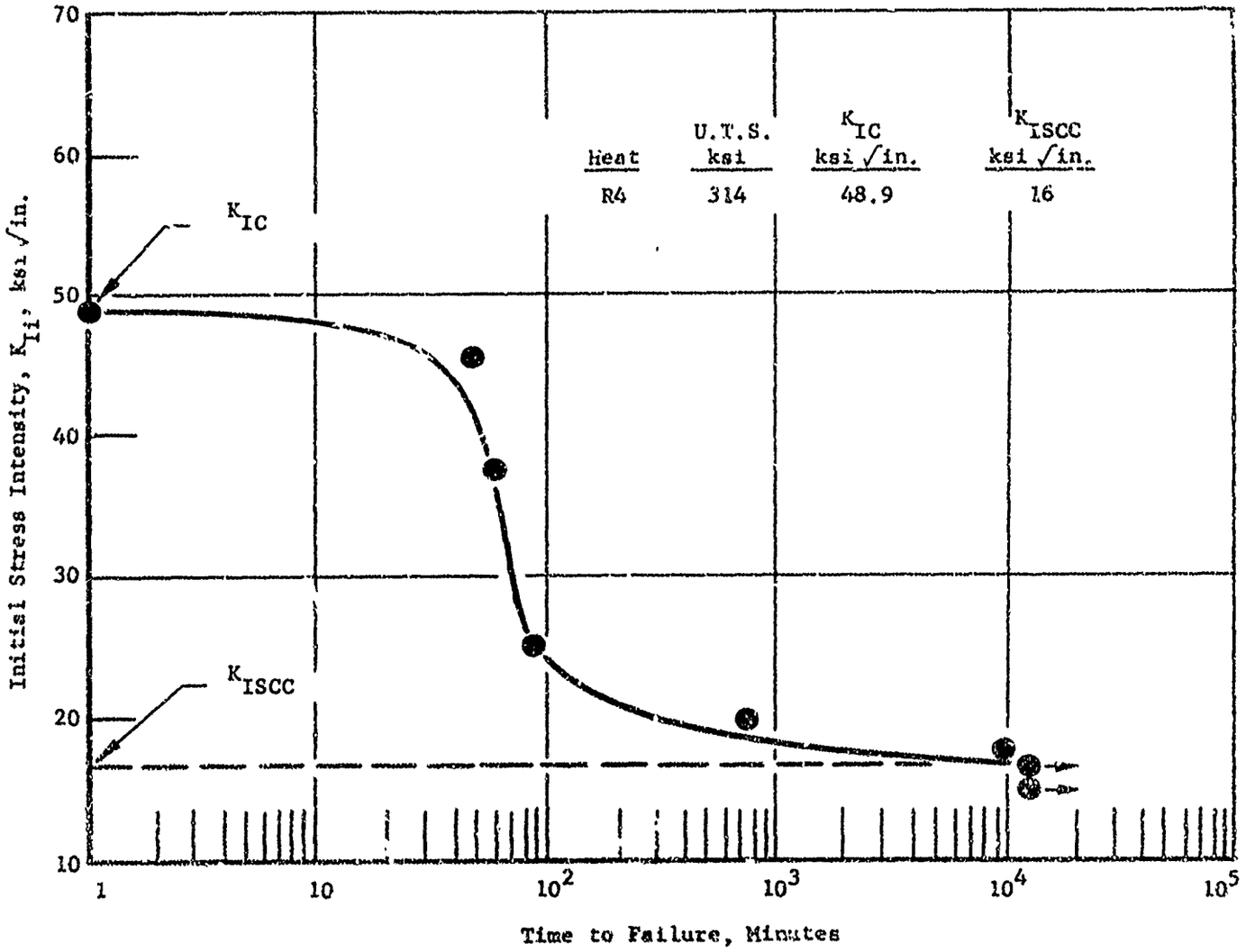

Figure 57. Stress Corrosion Curve for Heat R4

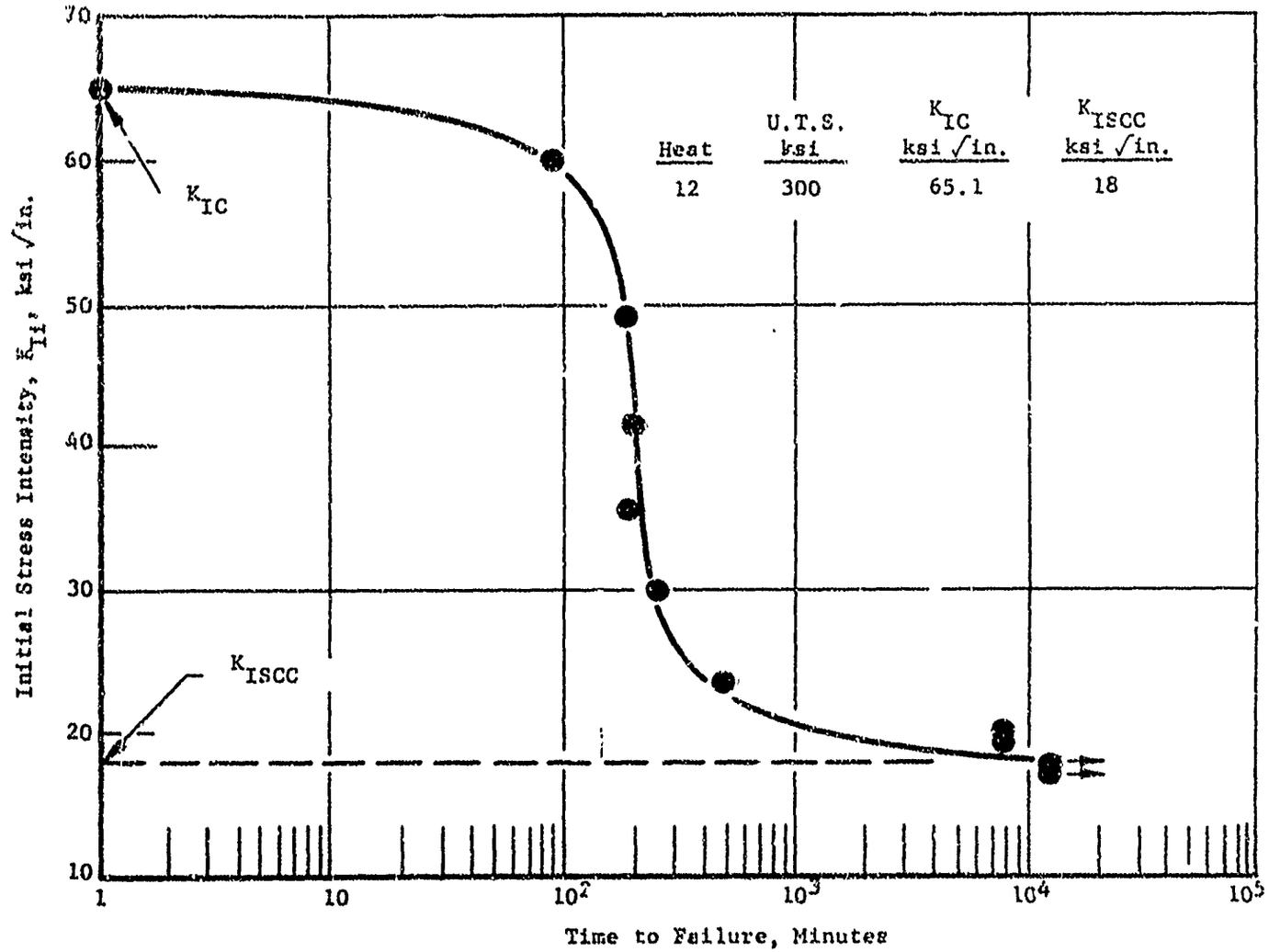

Figure 58. Stress Corrosion Curve for Heat 12

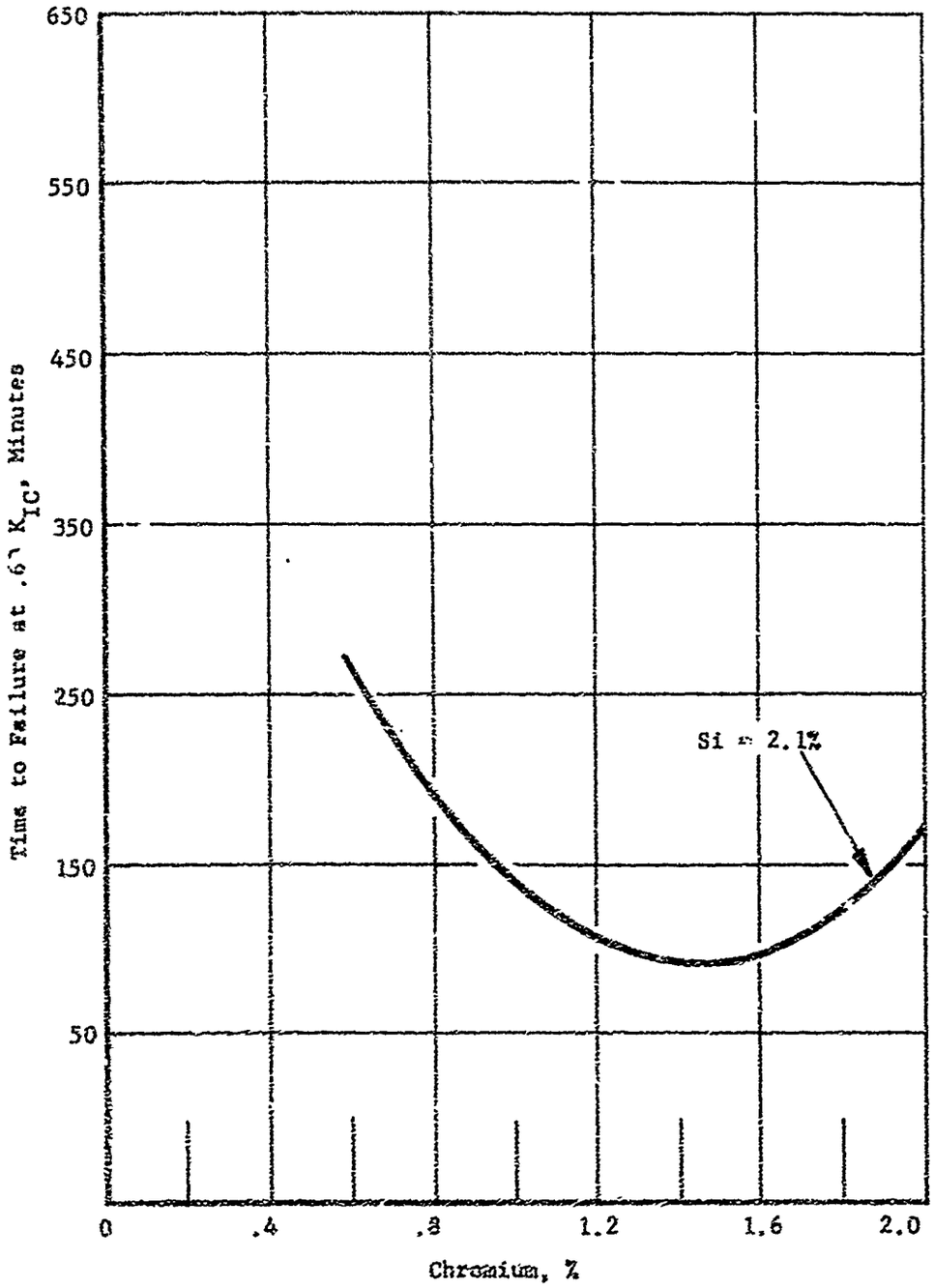

Figure 59. The Influence of Cr Content on Time to Failure at $K_{Ii} = 0.60\ K_{IC}$ for Ni-Cr-Mo-Si-V Martensitic Steels

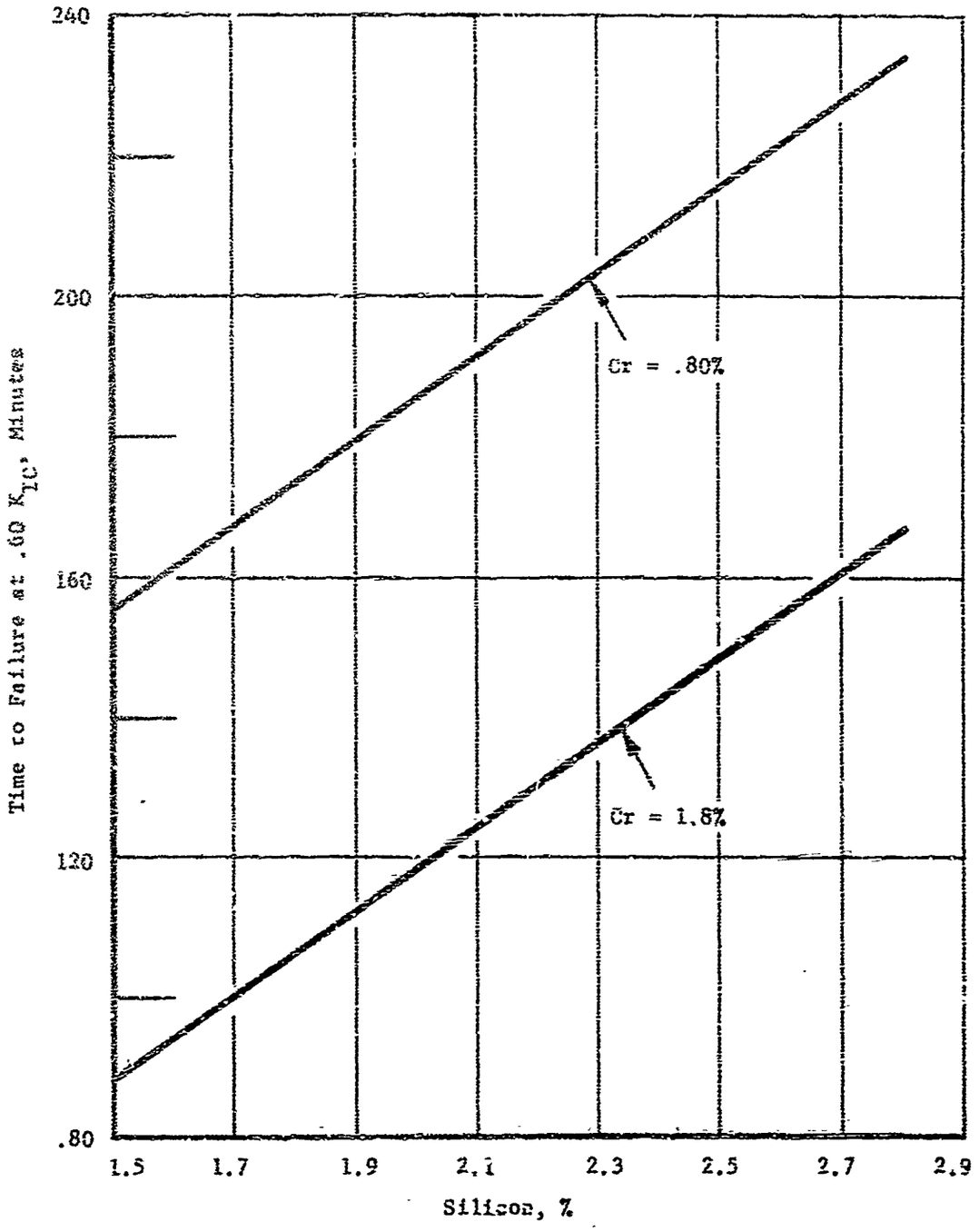

Figure 5. The Influence of Si Content on Time to Failure at $K_{Ii} = 0.60\ K_{Ic}$ for Ni-Cr-Mo-Si-V Martensitic Steels

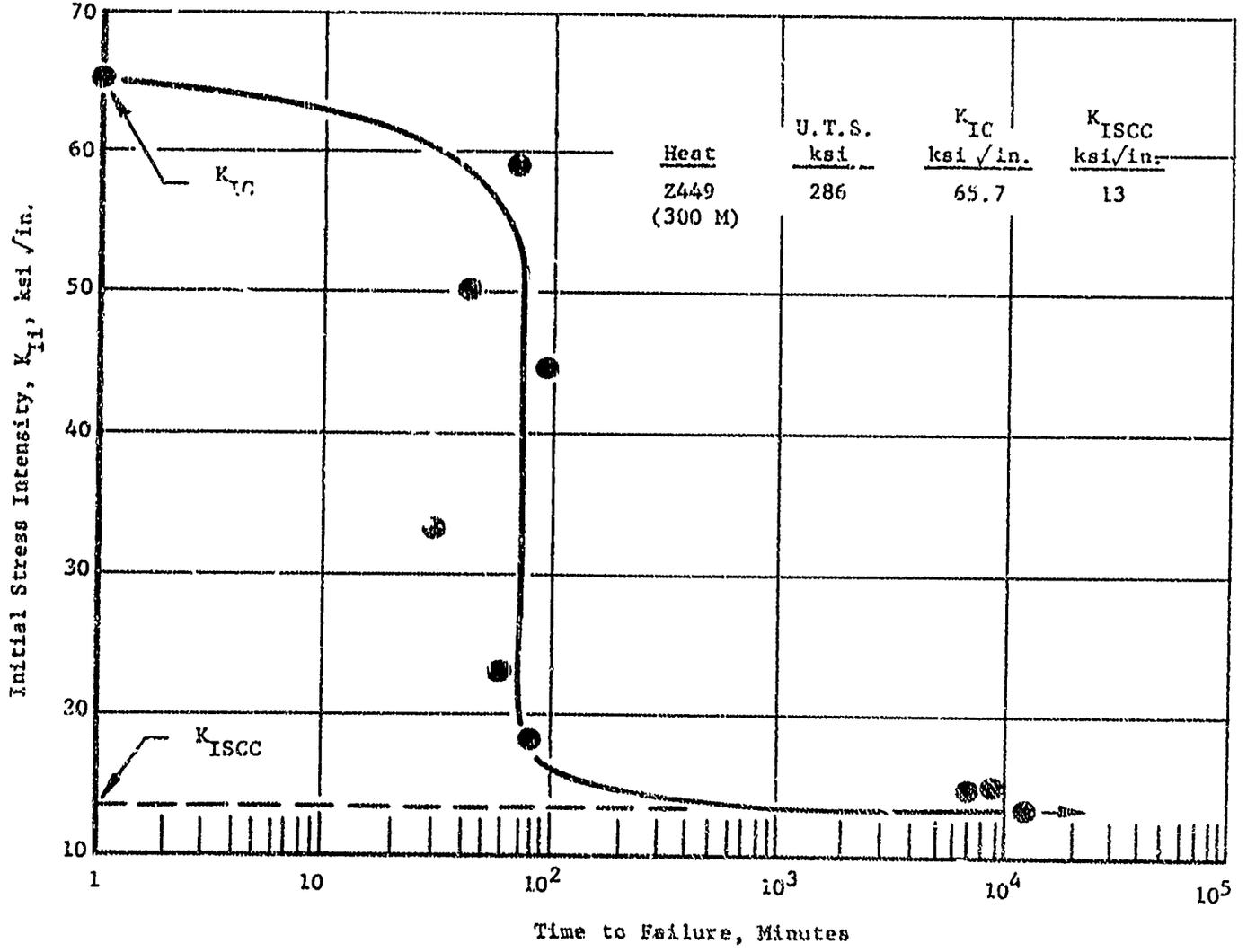

Figure 61. Stress Corrosion Curve for VIM Heat Z449 (300 M)

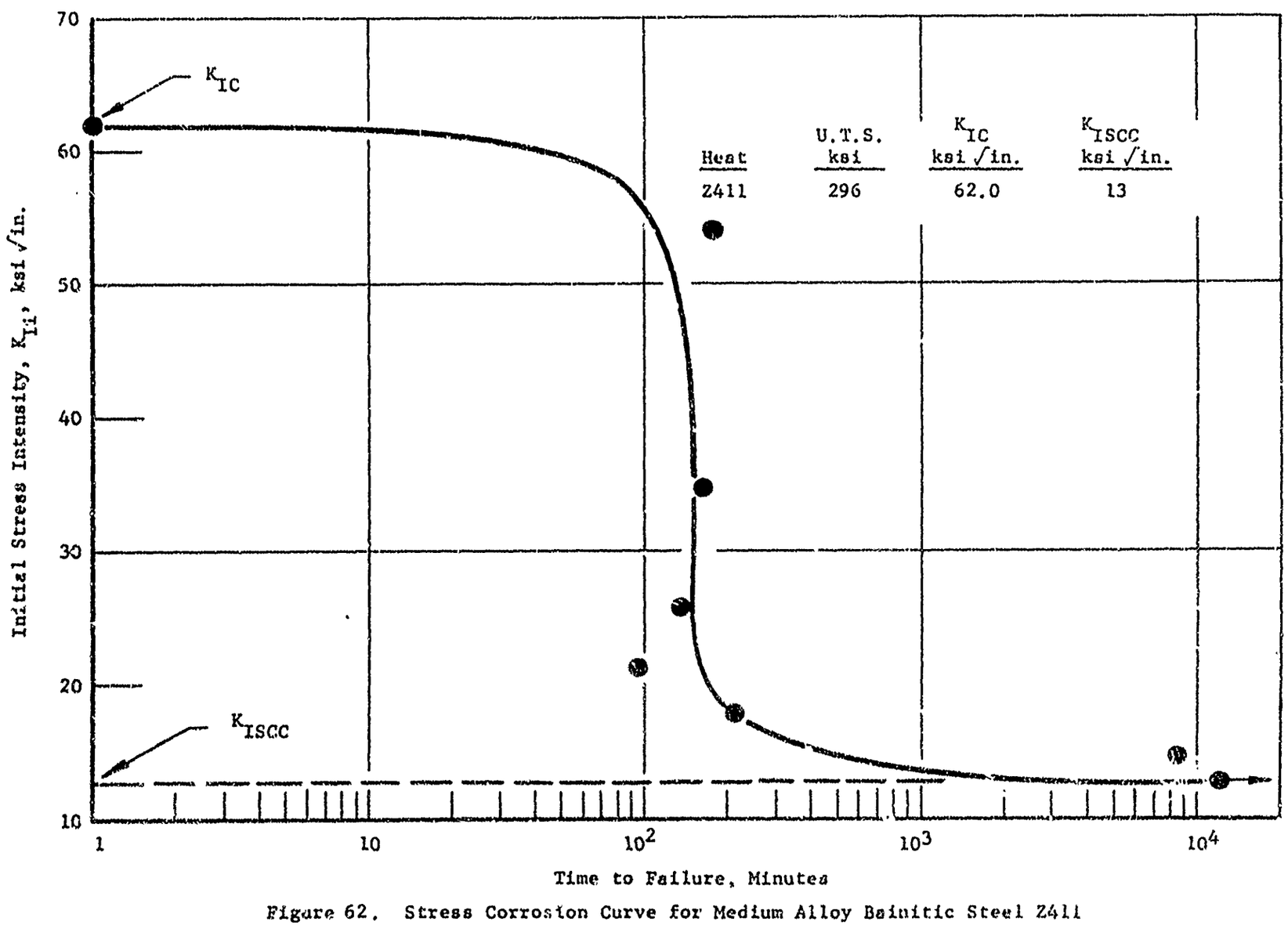

Figure 62. Stress Corrosion Curve for Medium Alloy Bainitic Steel Z411

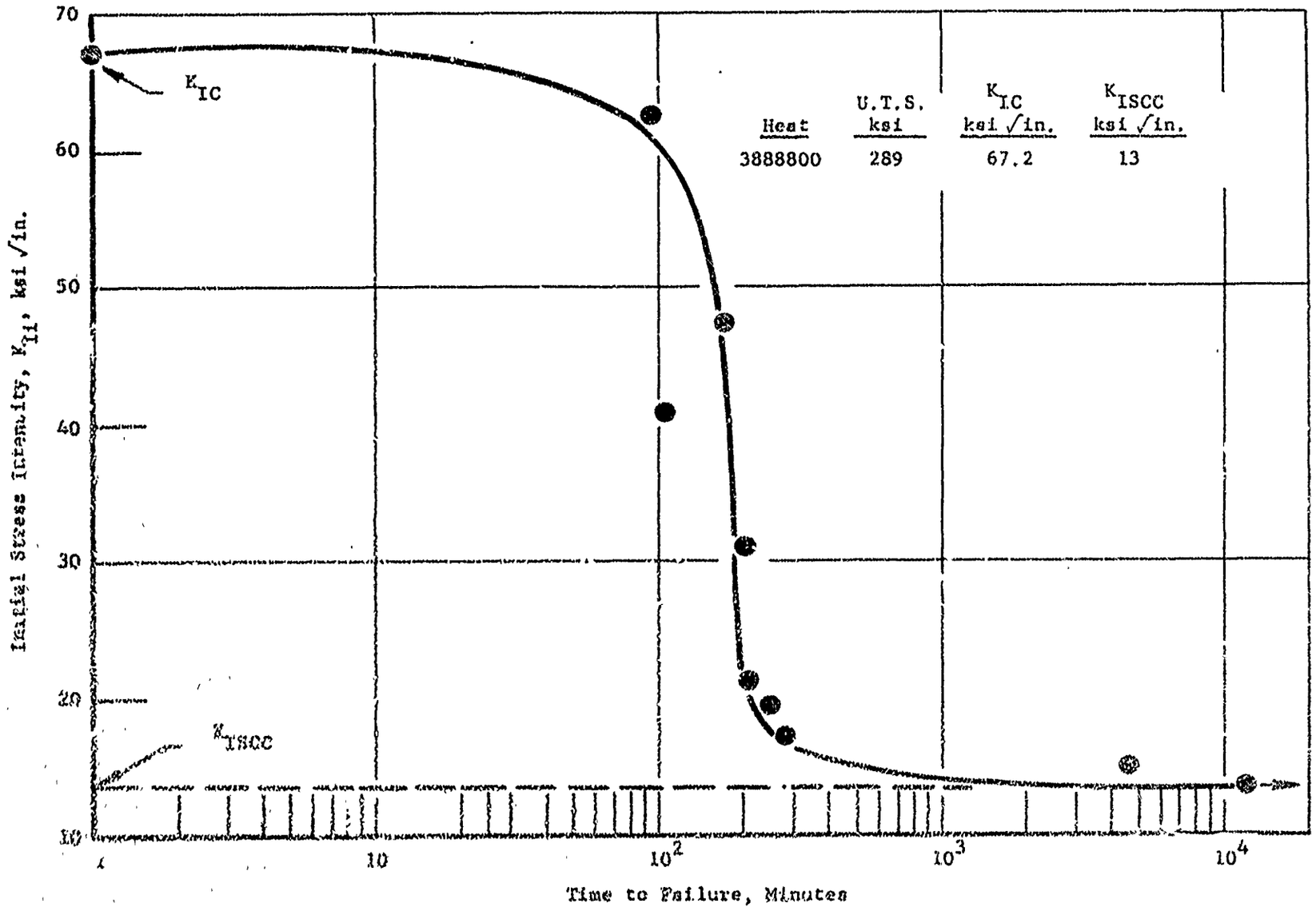

Figure 63. Stress Corrosion Curve for Medium Alloy Bainitic Steel VAR Heat 3888800

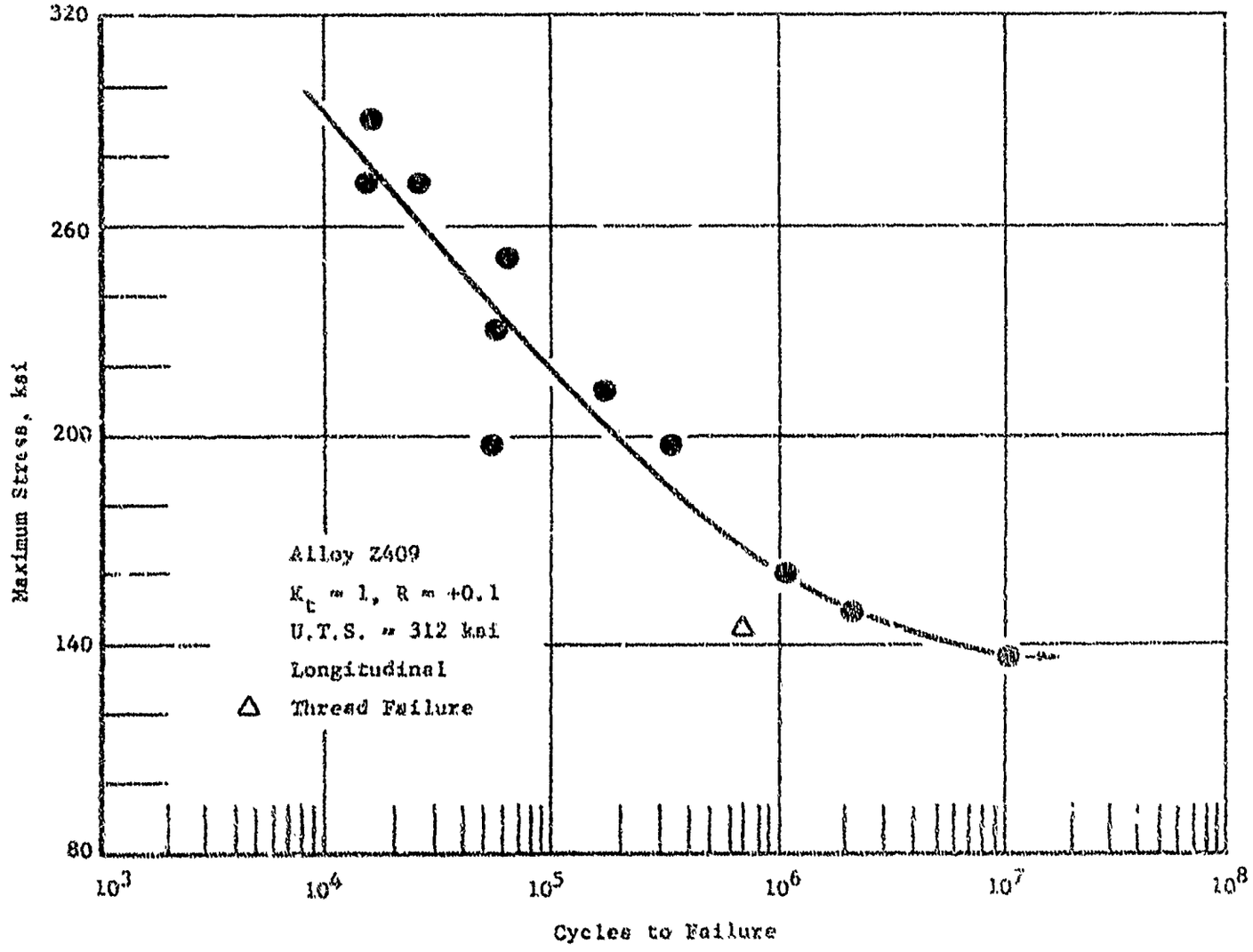

Figure 64. S-N Curve for Martensitic Alloy Z409 (VIM)

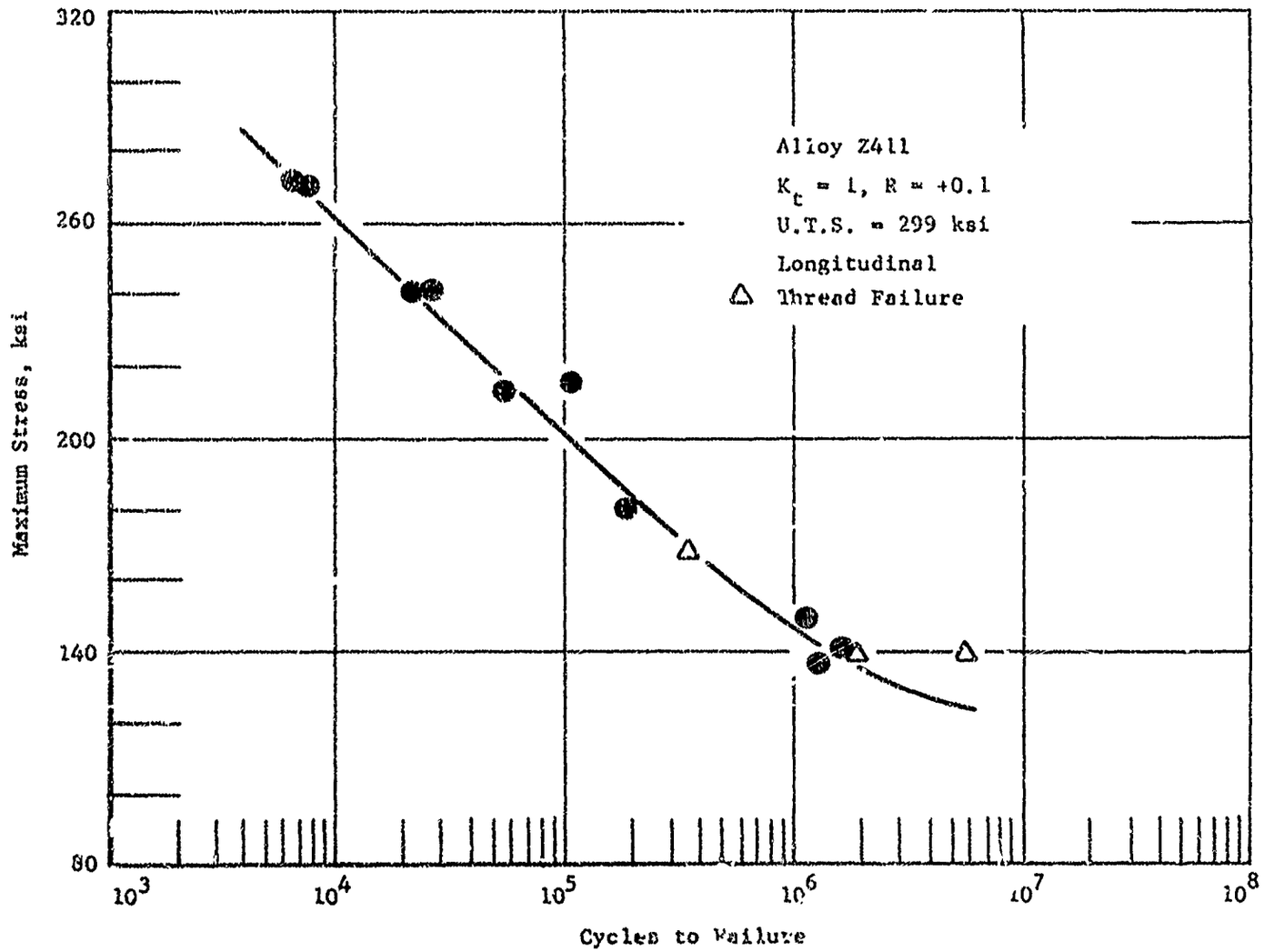

Figure 65. S-N Curve for Bainitic Alloy Z411 (VIM)

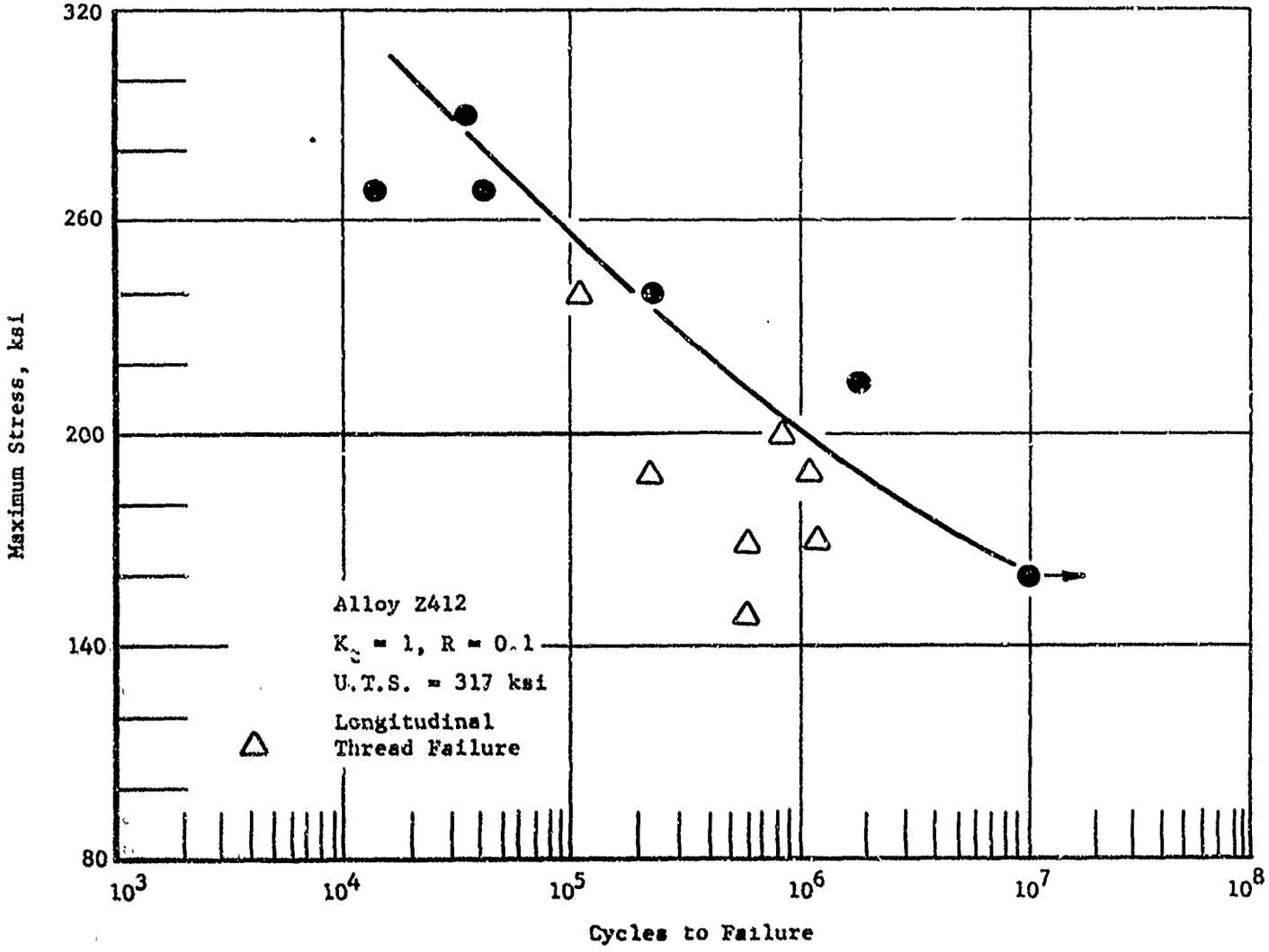

Figure 66. S-N Curve for Bainitic Alloy Z412 (VIM)

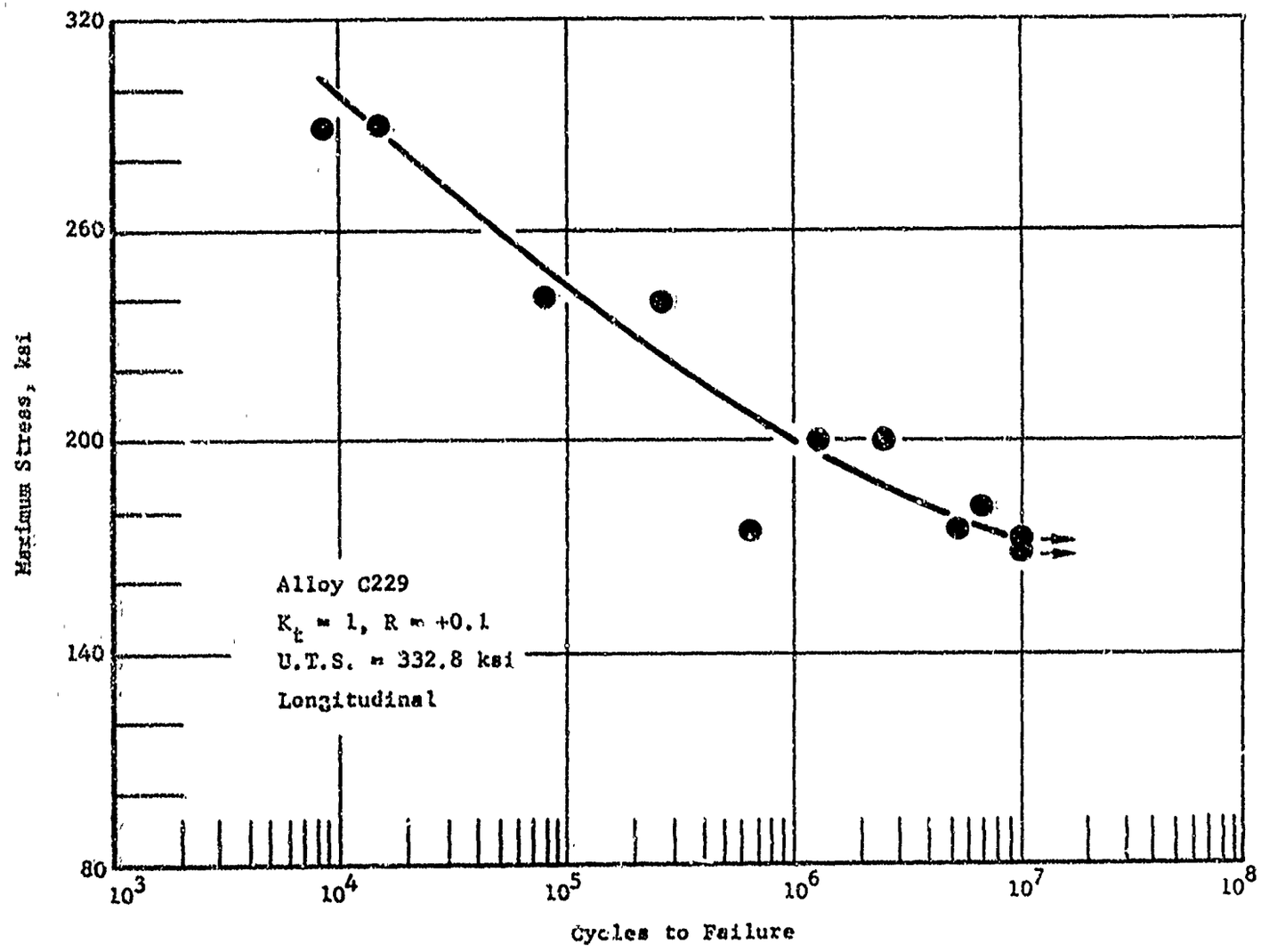

Figure 67. S-N Curve for Martensitic Alloy C229 (ESR)

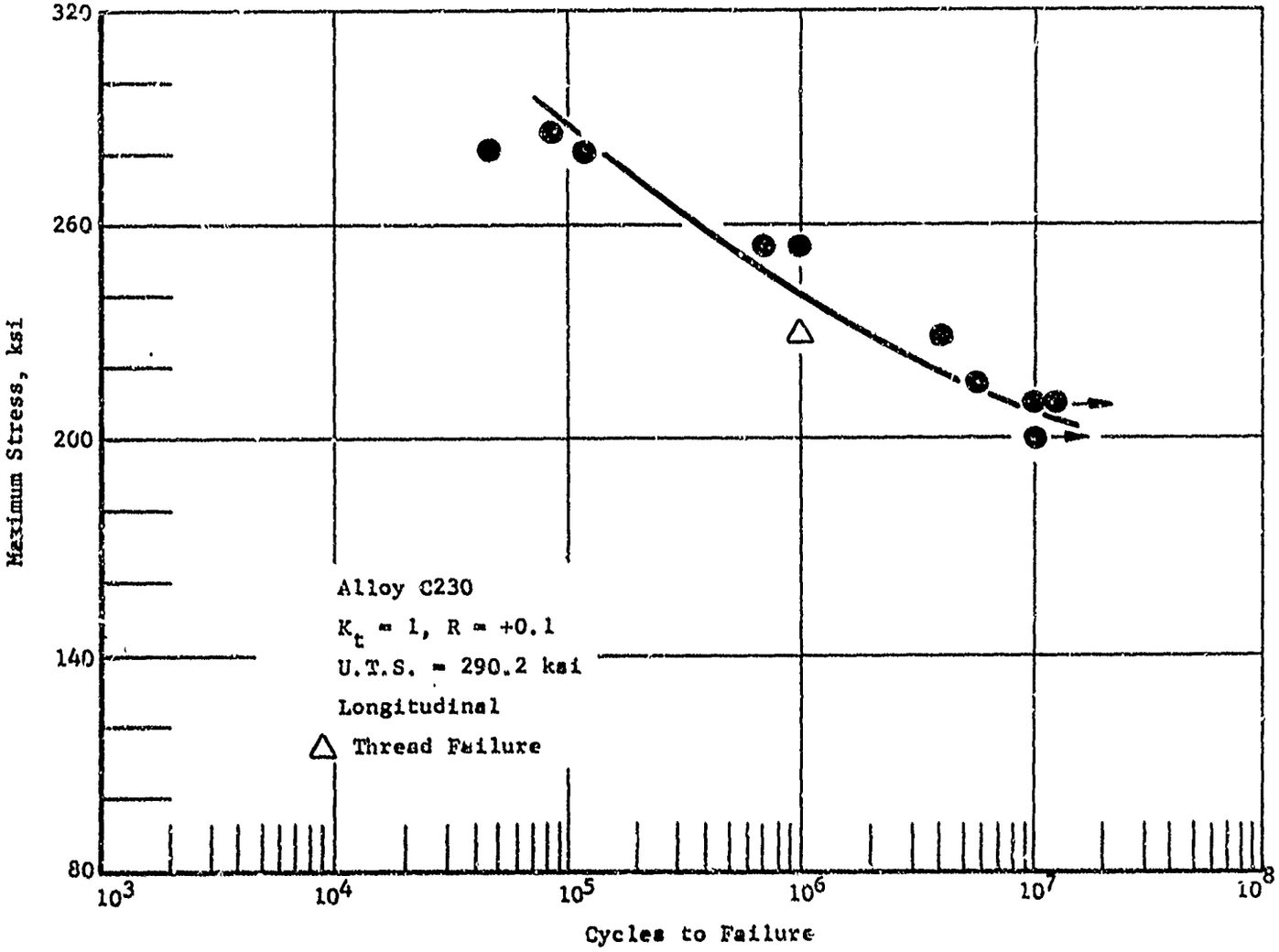

Figure 68. S-N Curve for Bainitic Alloy C230 (ESR)

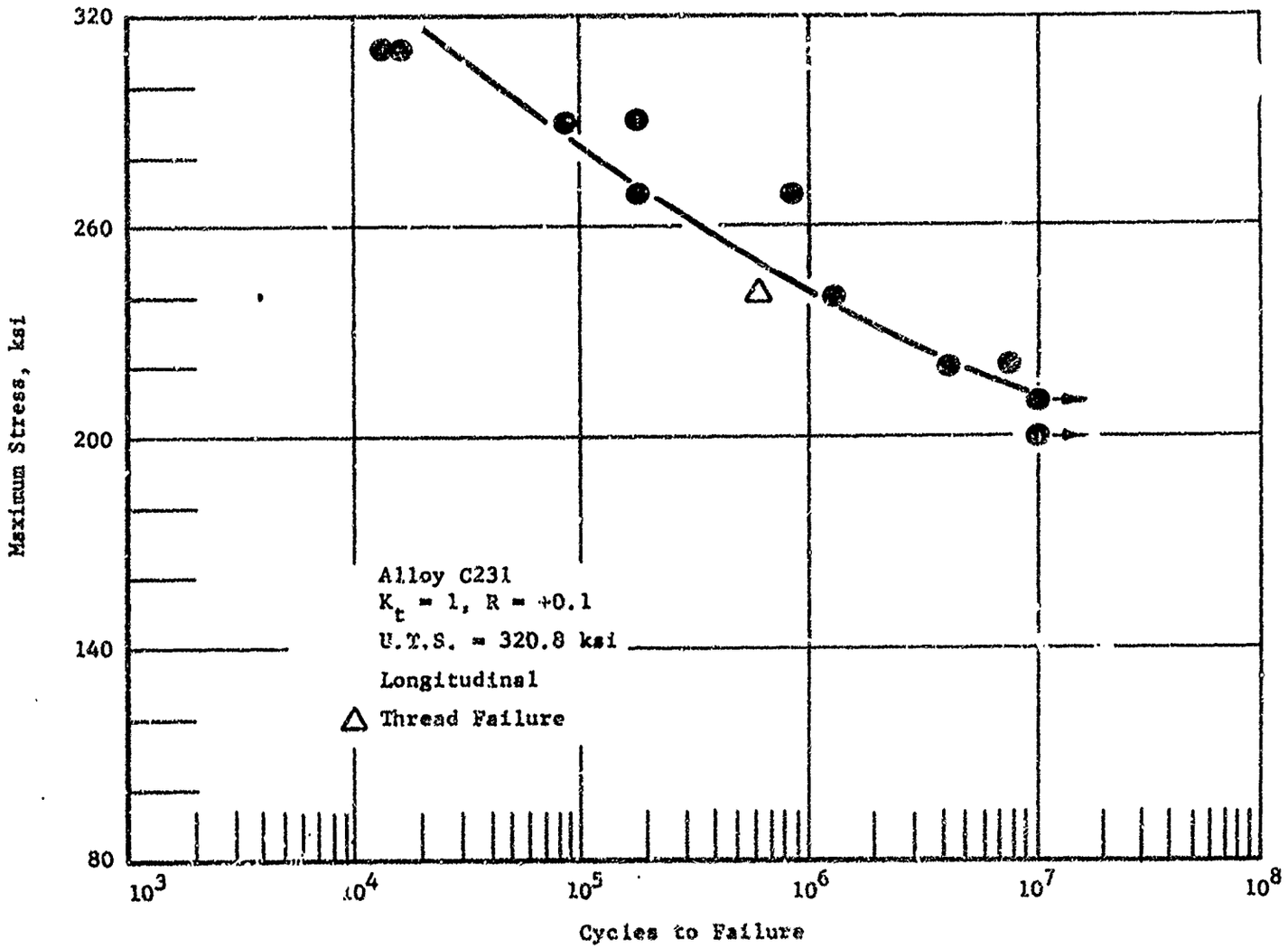

Figure 69. S-N Curve for Bainitic Alloy C231 (ESR)

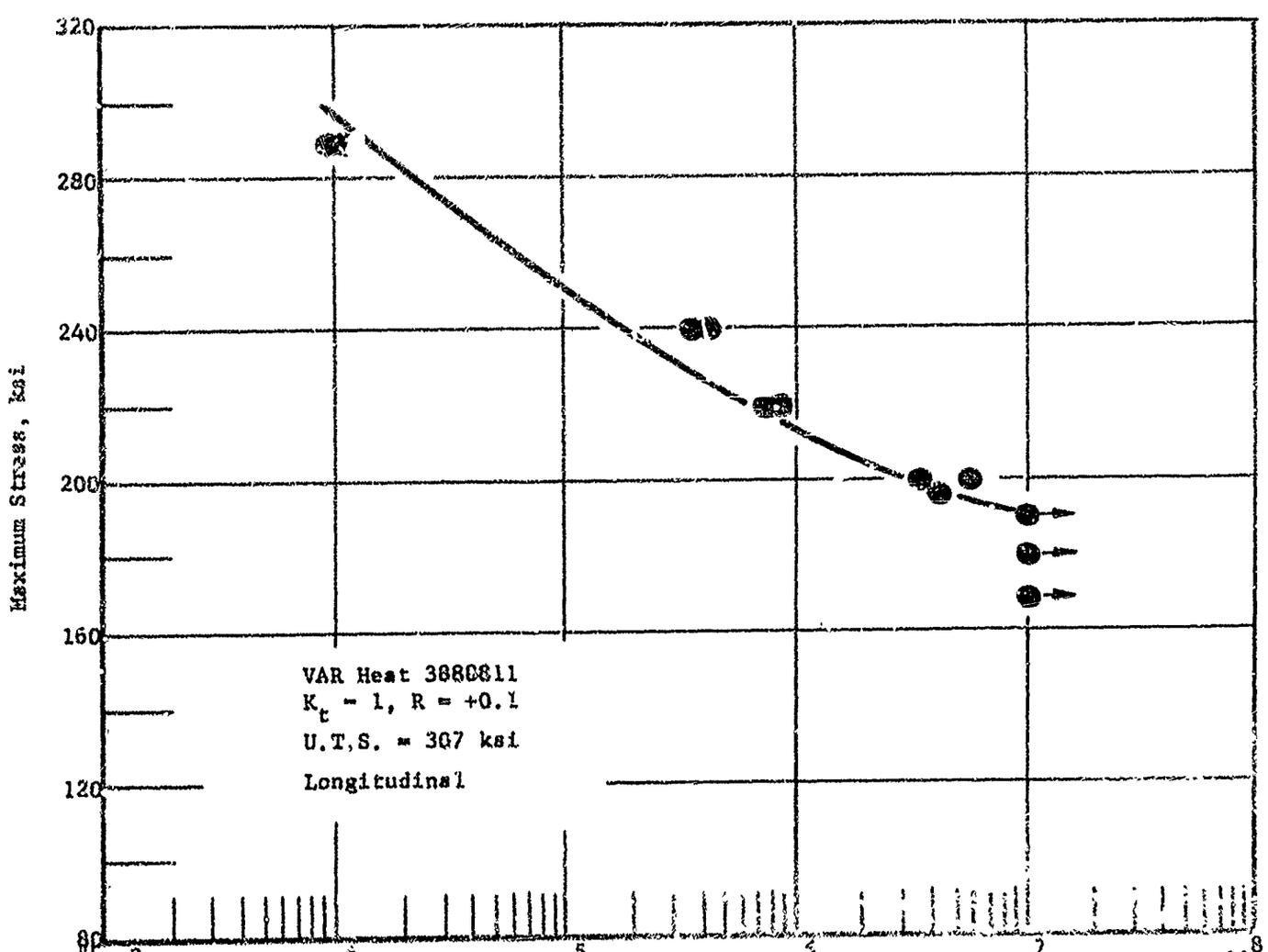

Figure 70. S-N Curve for Martensitic Alloy 3880811 (VAR)

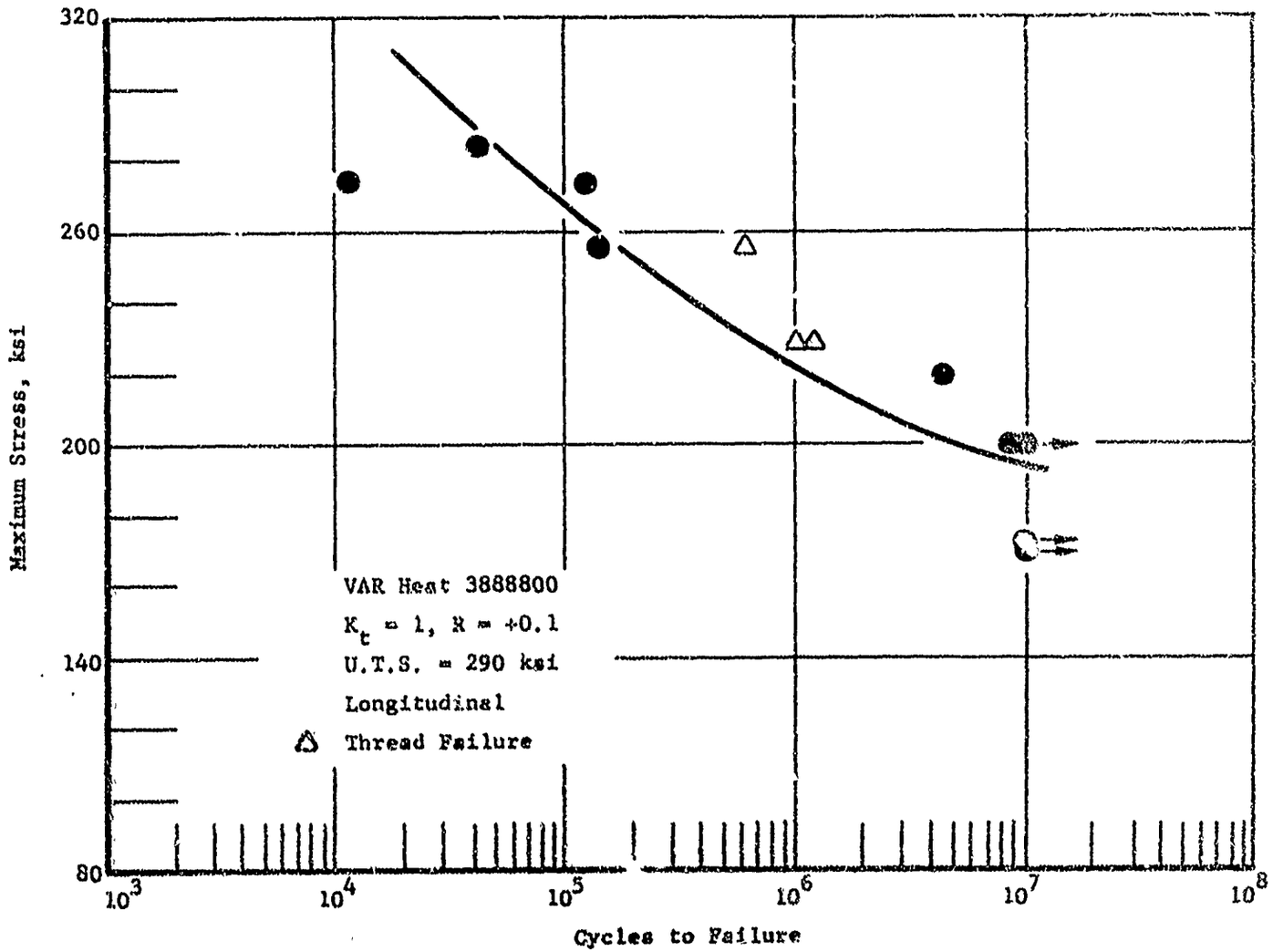

Figure 71. S-N Curve for Bainitic Alloy 3888800 (VAR)

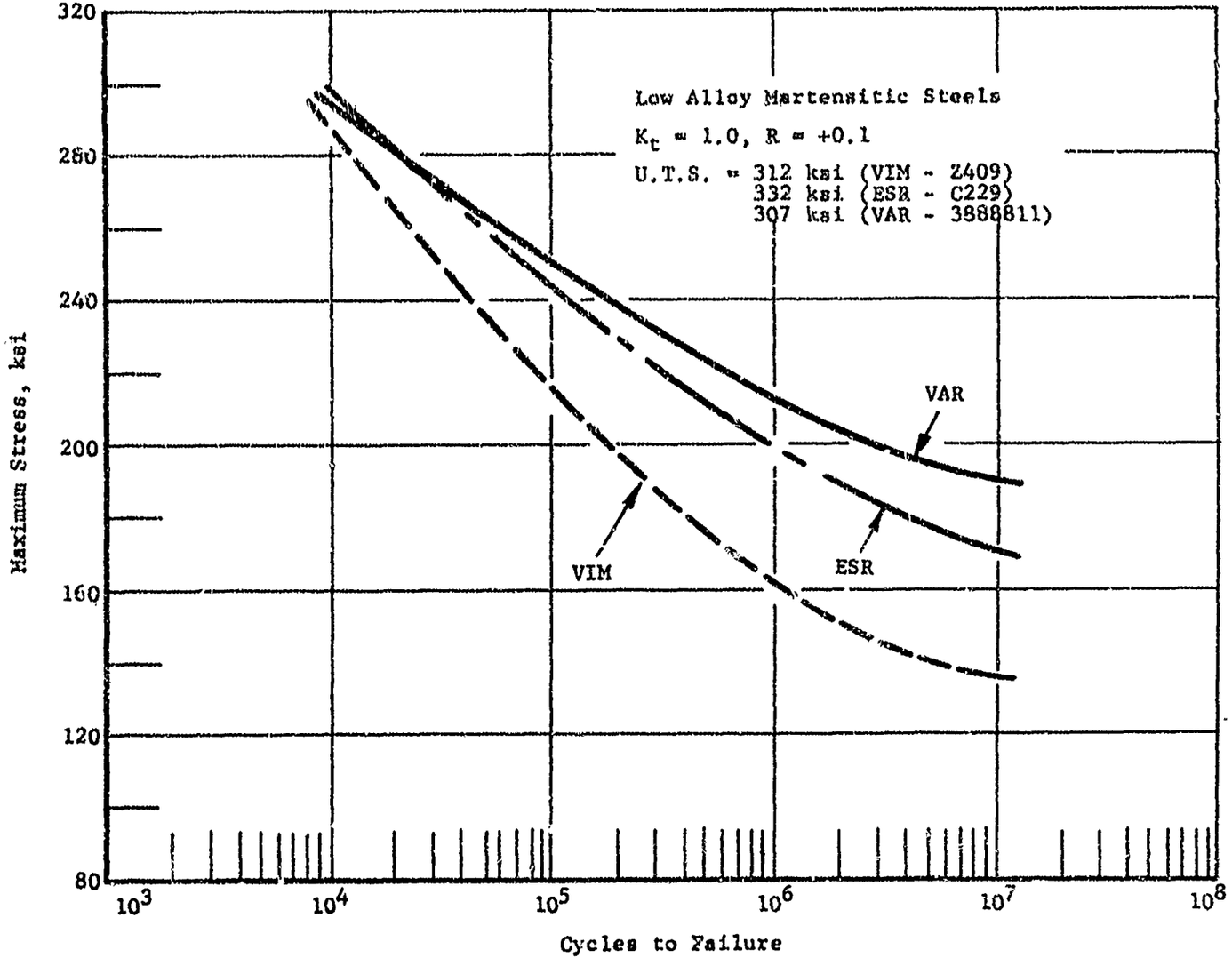

Figure 72. Comparison of S-N Curves for ESR, VIM, and VAR Low Alloy Martensitic Steels

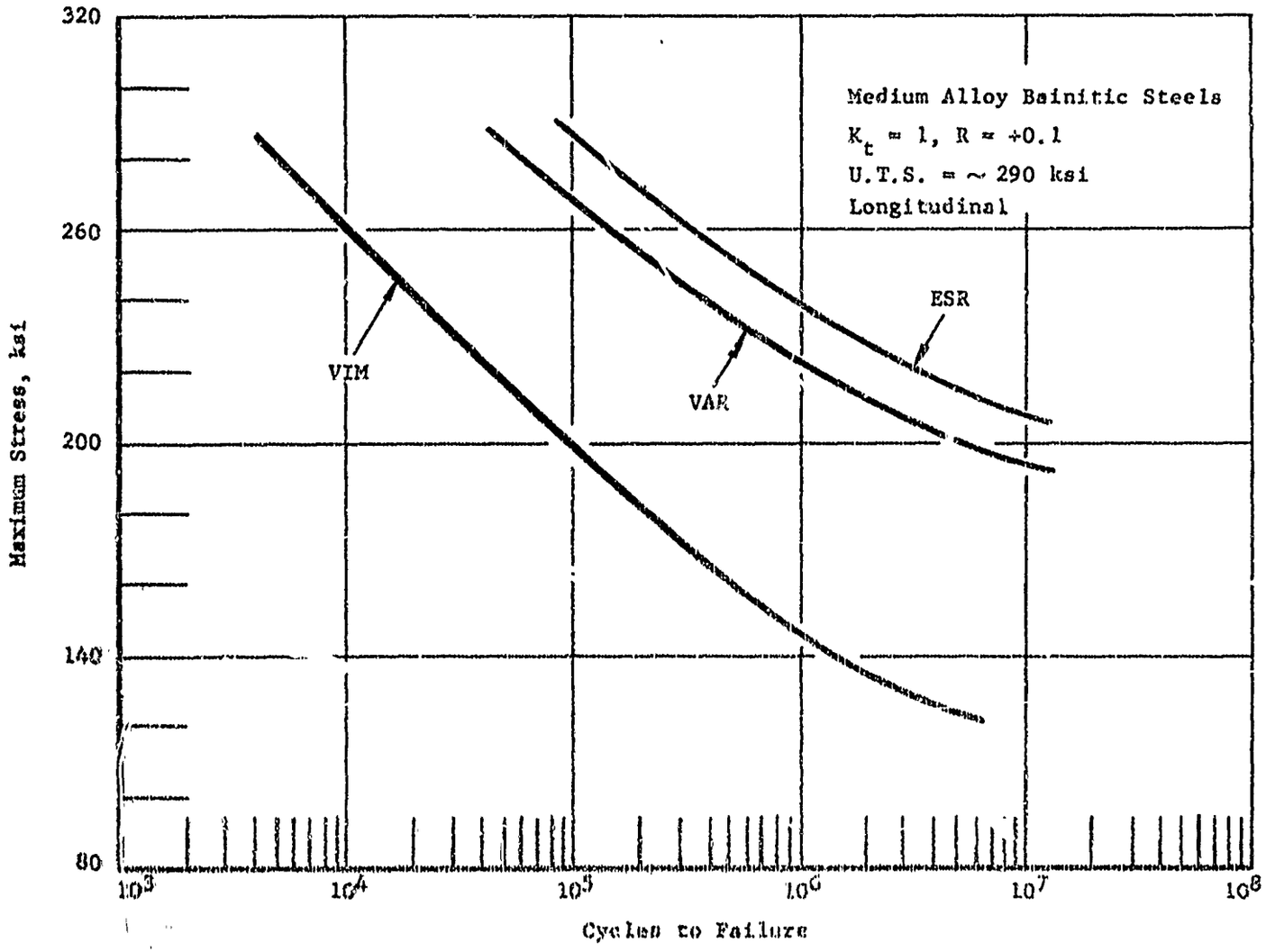

Figure 73. Comparison of S-N Curves for ESR (C230), VIM (Z411), and VAR (3888800) Medium Alloy Bainitic Steels

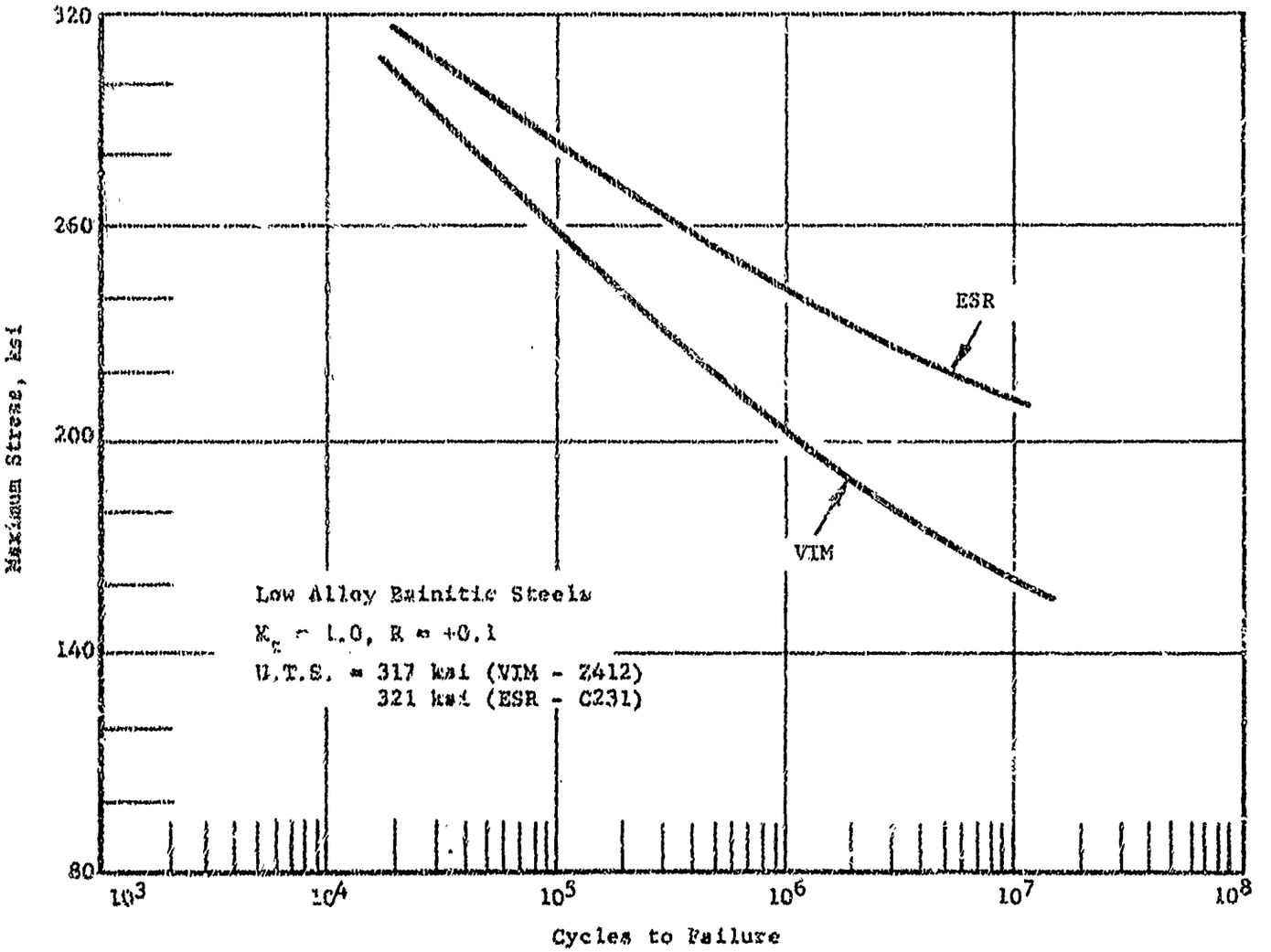

Figure 74. Comparison of S-N Curves for ESR and VIM Low Alloy Bainitic Steels

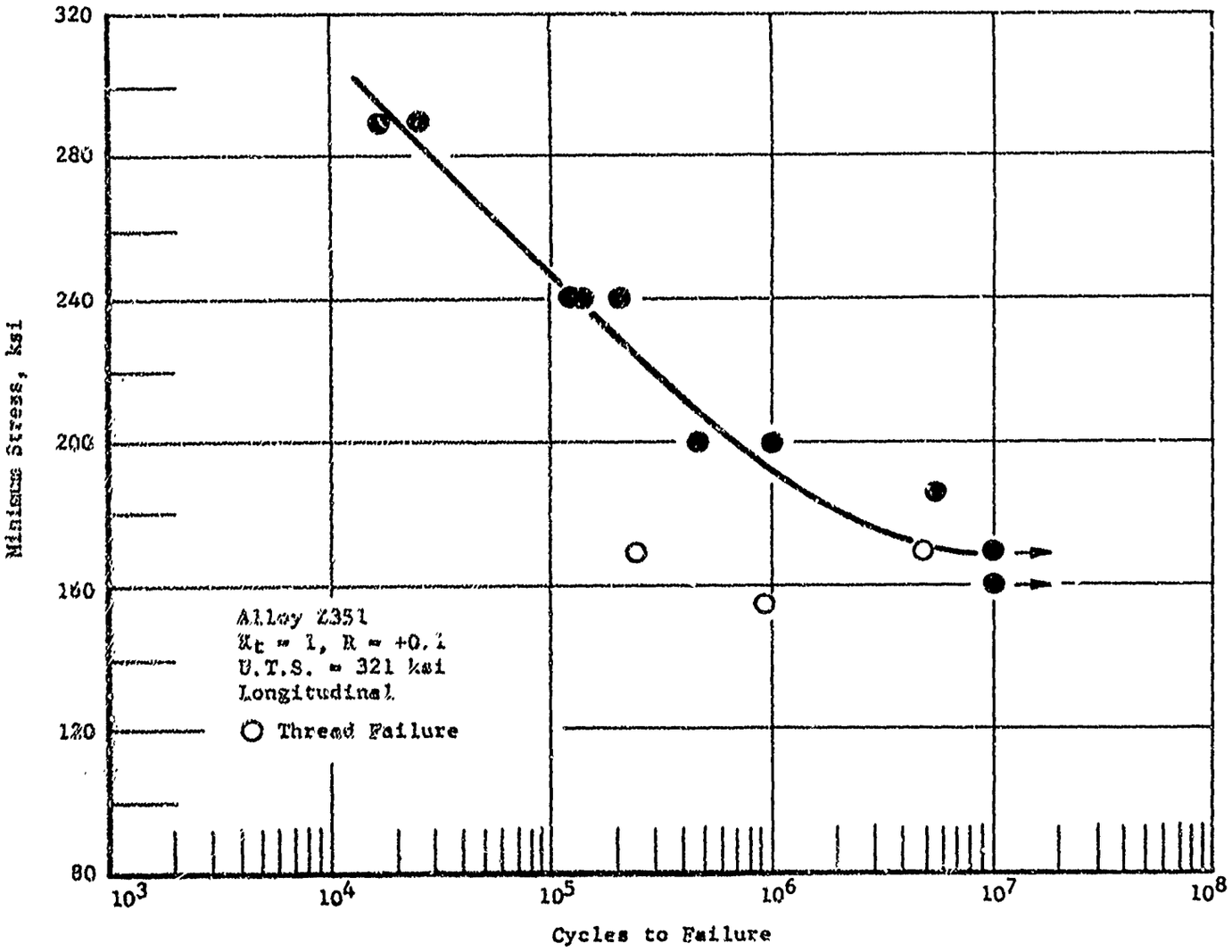

Figure 75. S-N Curve for Martensitic Alloy Z351 (VIM), Longitudinal

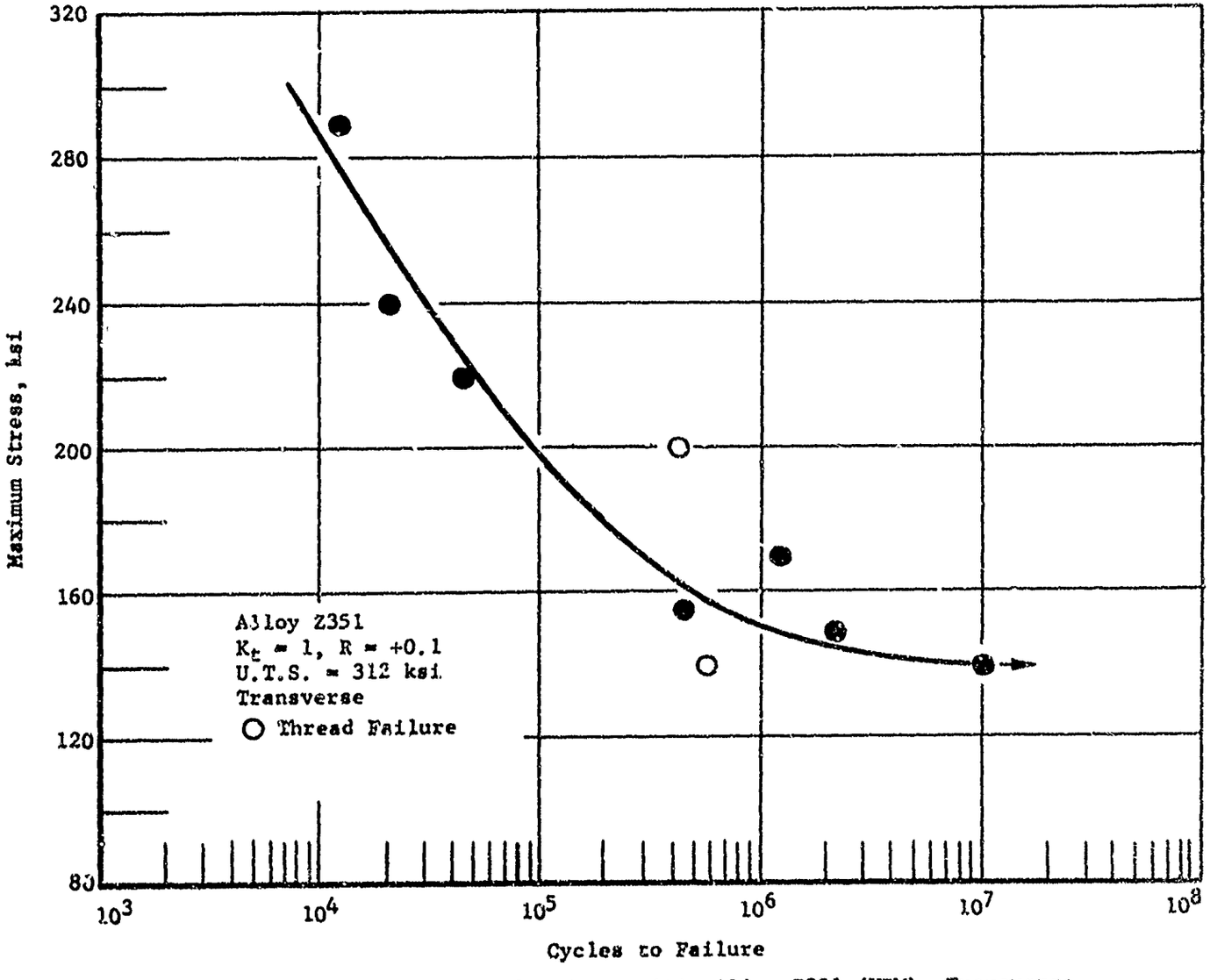

Figure 76. S-N Curve for Martensitic Alloy Z351 (VIM), Transverse

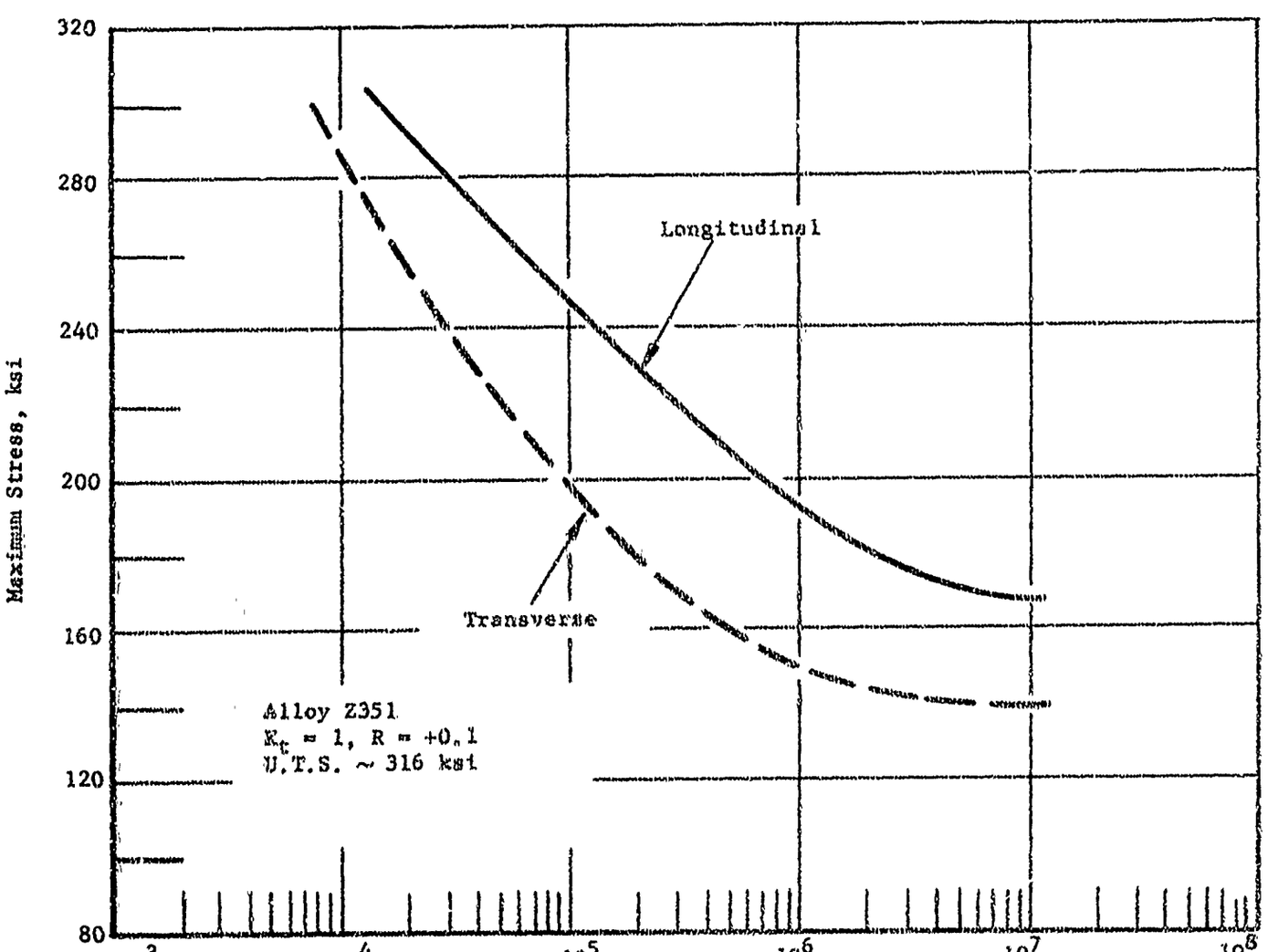

Figure 77. Longitudinal and Transverse Fatigue Strengths for Martensitic Alloy Z351 (VIM)

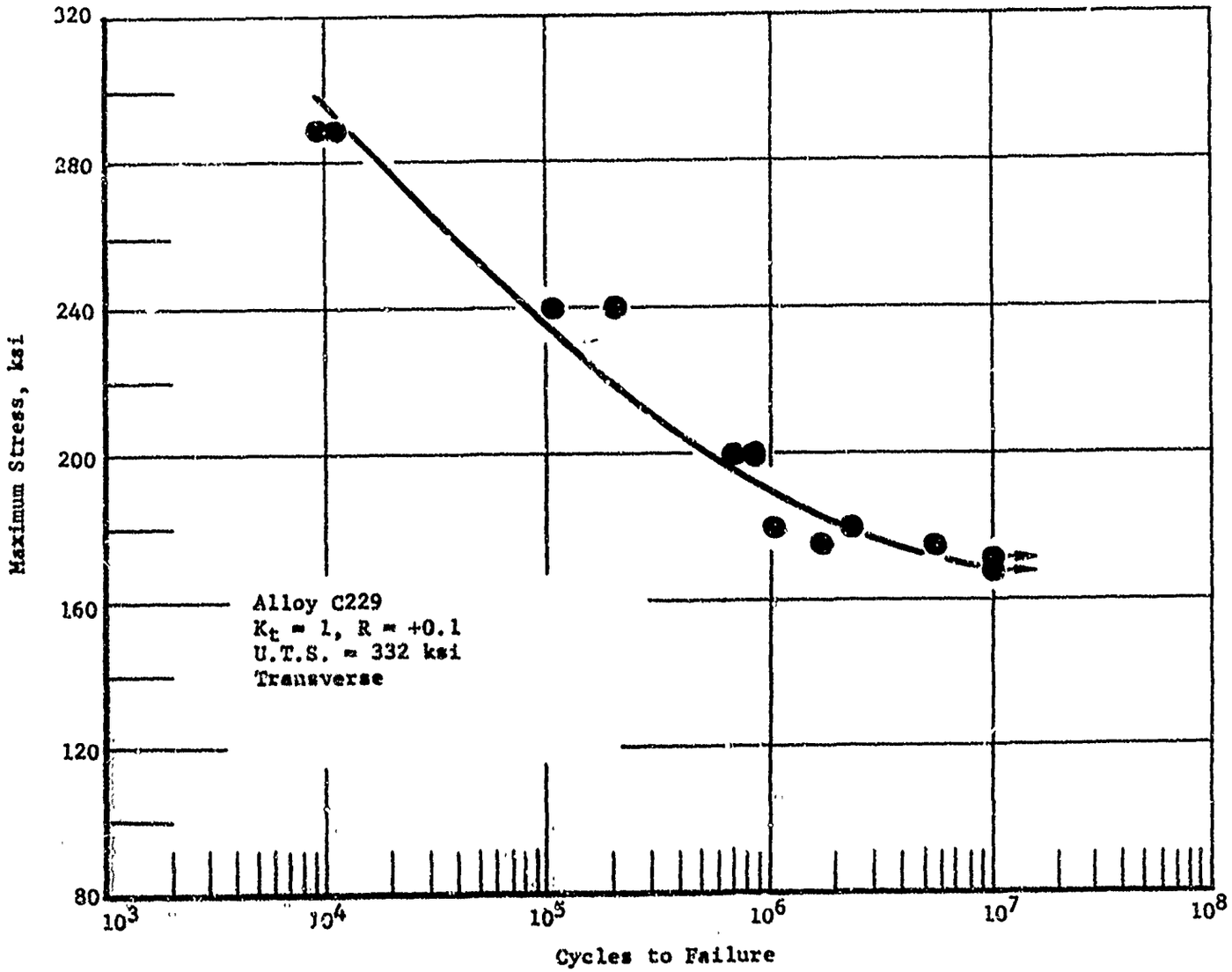

Figure 78. S-N Curve for Martensitic Alloy C229 (ESR), Transverse

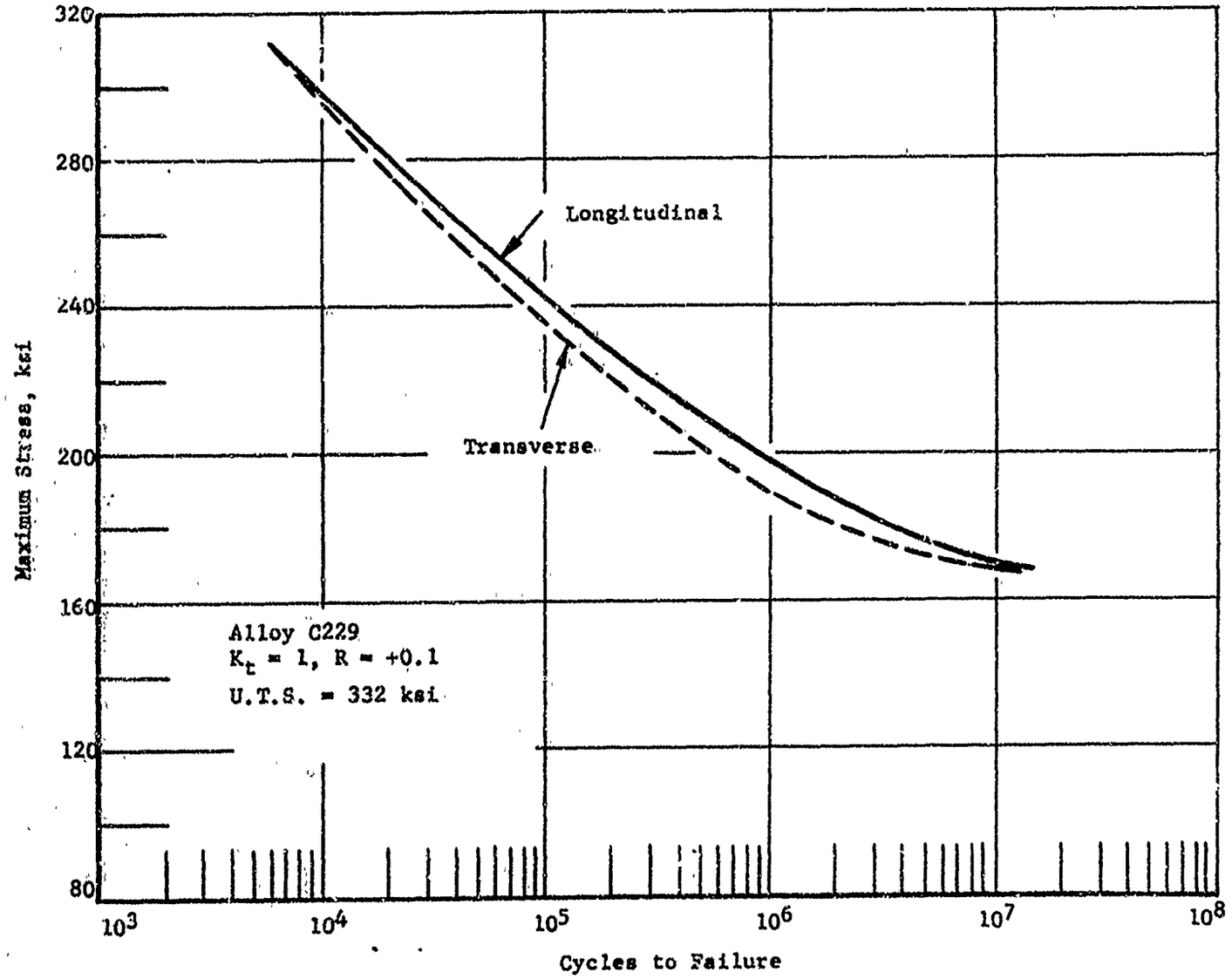

Figure 79. Longitudinal and Transverse Fatigue Strengths for Martensitic Alloy C229 (ESR)

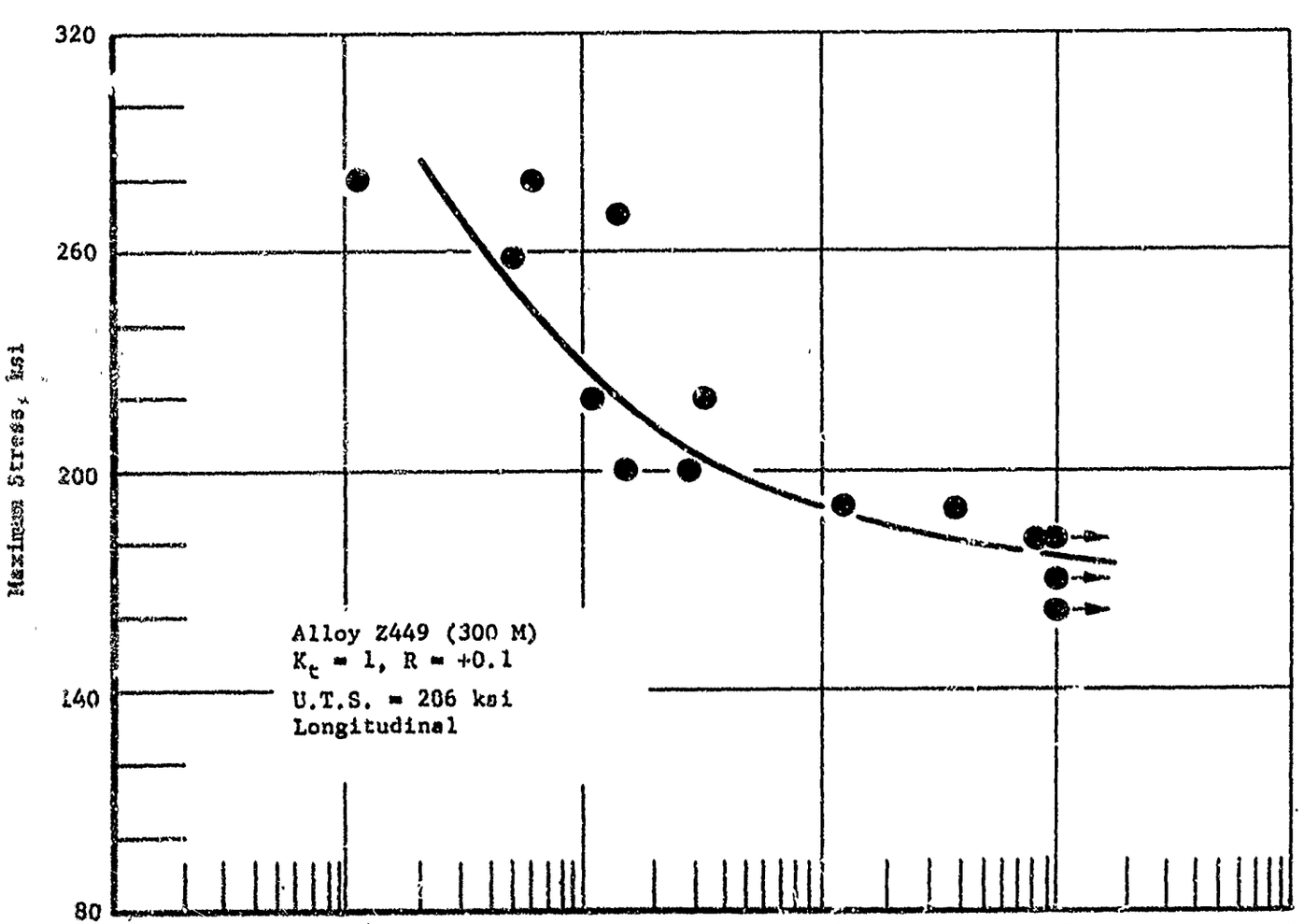

Figure 80. S-N Curve for 300 M Steel (Alloy Z449-VIM)

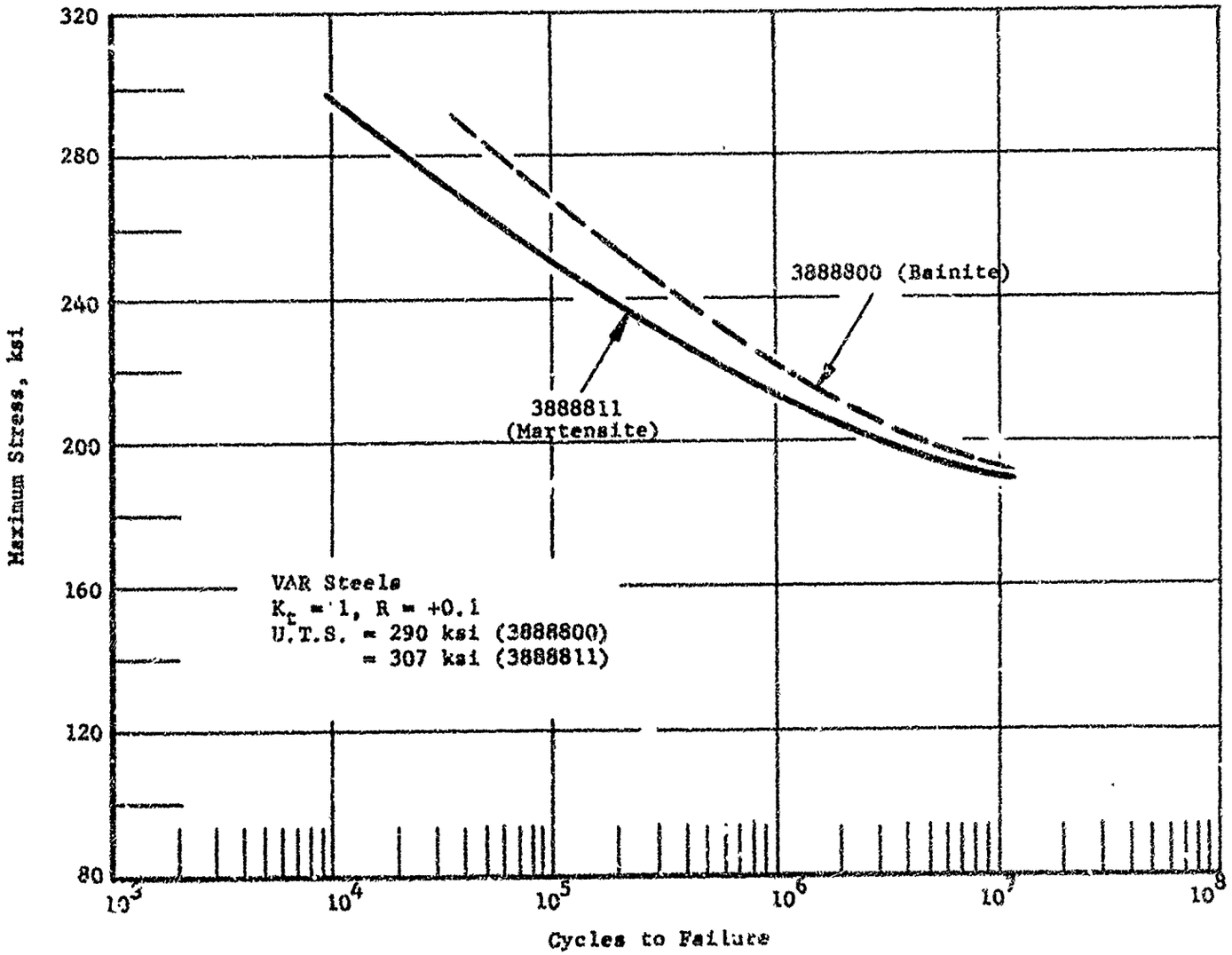

Figure 81. Fatigue Properties of VAR Experimental Bainitic (3888800) and Martensitic (3888811) Steels

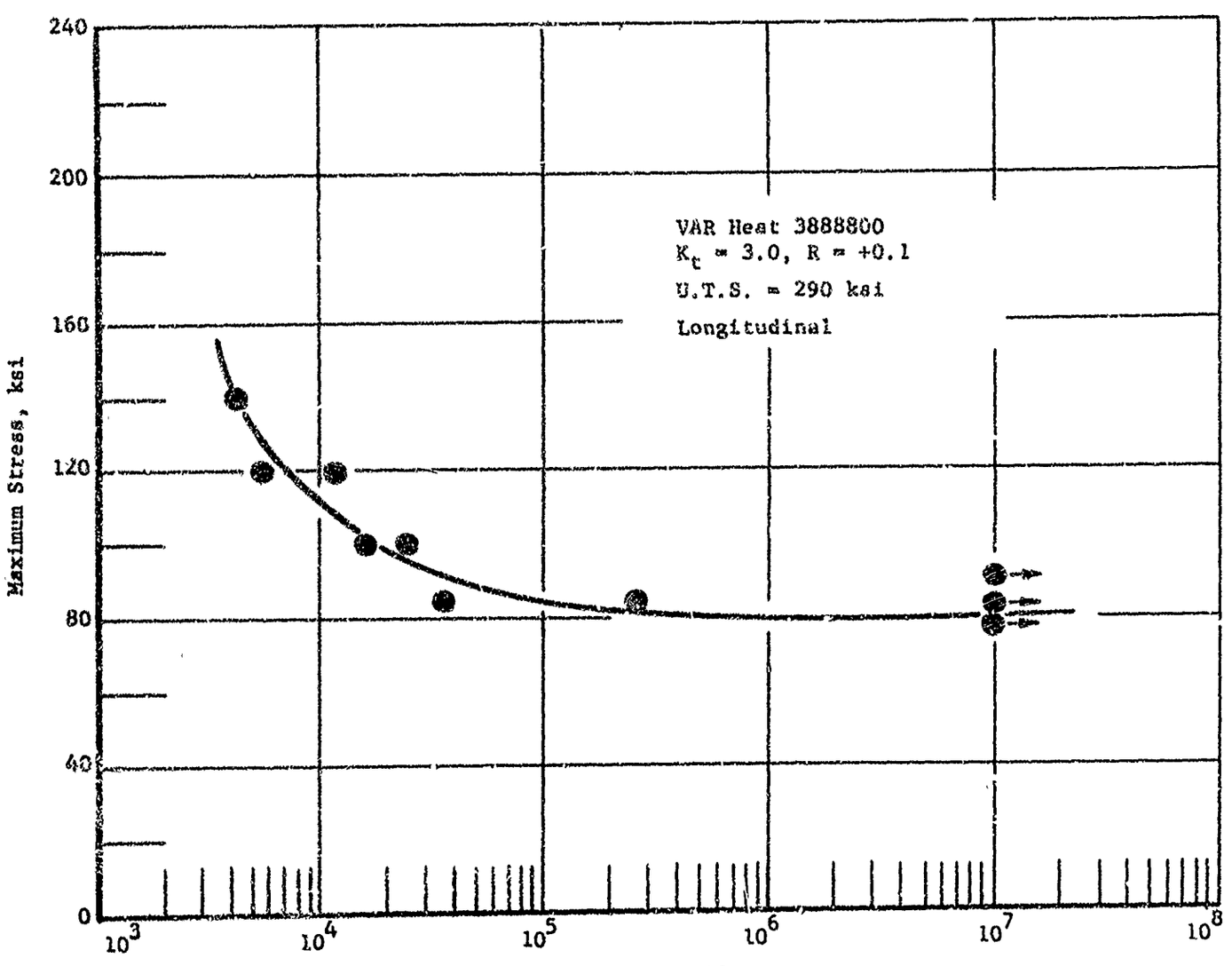

Figure 82. S-N Curve for Notched Specimens (K_t = 3.0) of bainitic Alloy 3888800 (VAR)

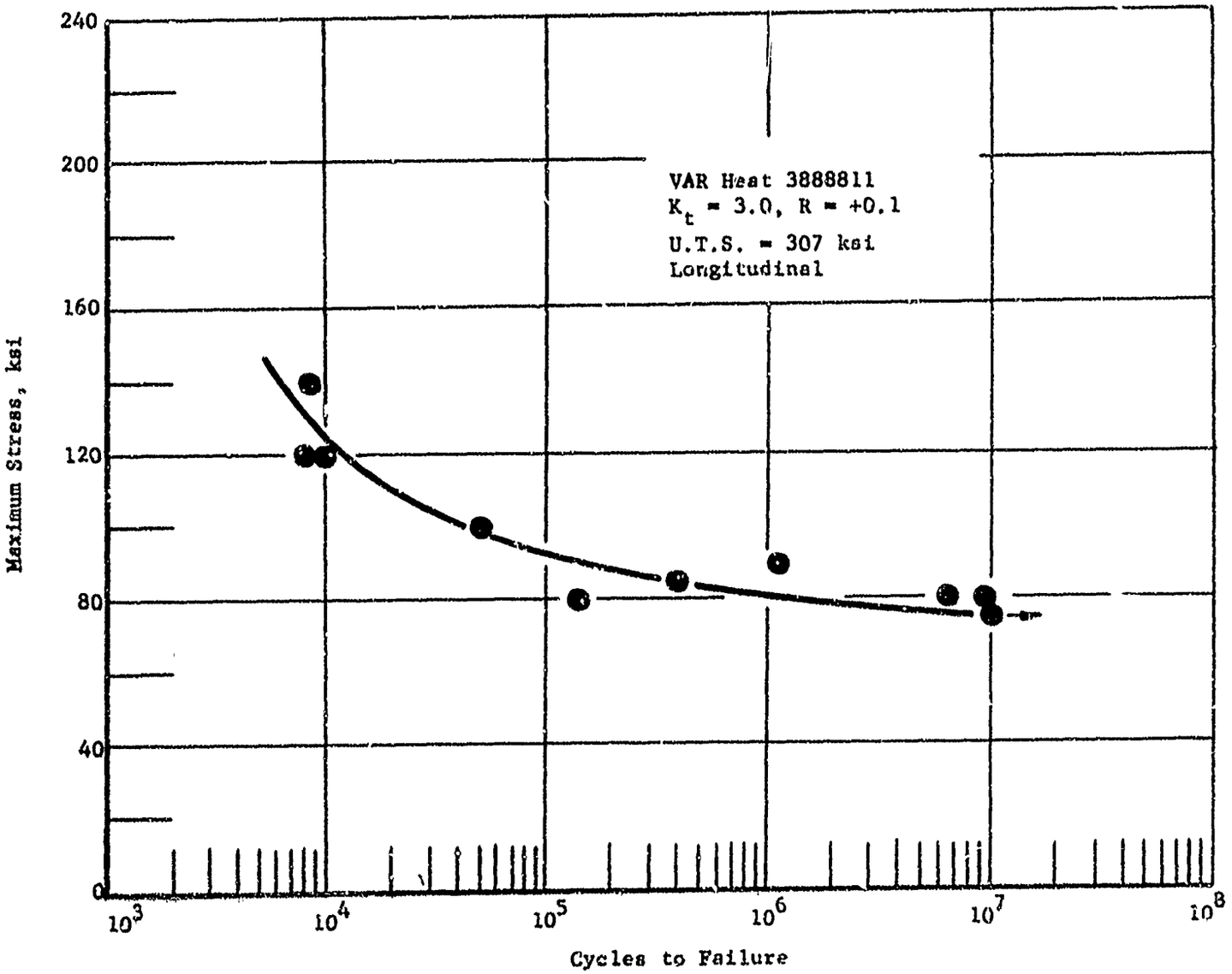

Figure 83. S-N Curve for Notched Specimens (K_t = 3.0) of Martensitic Alloy 3888811 (VAR)

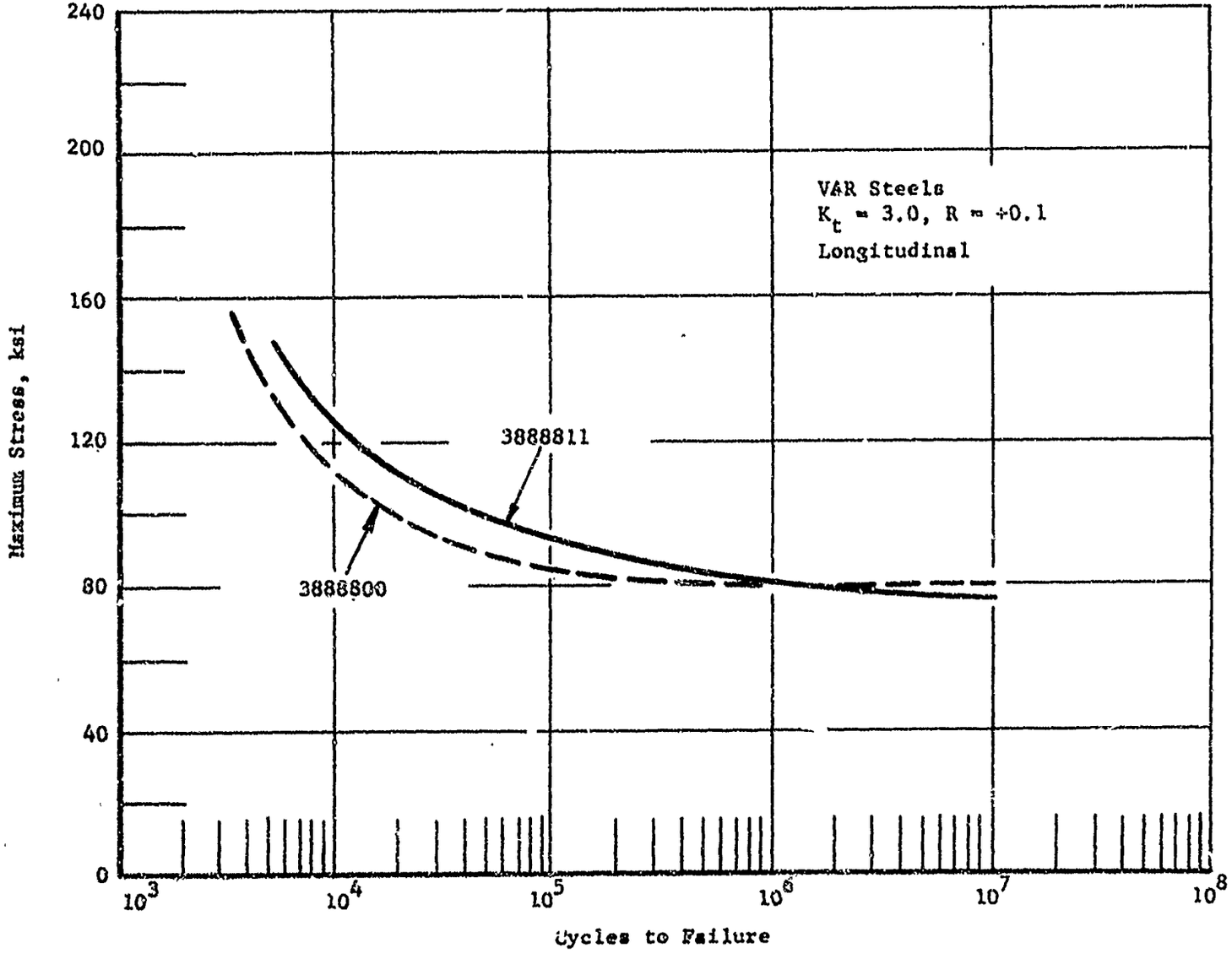

Figure 84. Comparison Notch (K_t = 3.0) S-N Curves for Bainitic Alloy 3888800 and Martensitic Alloy 3888811

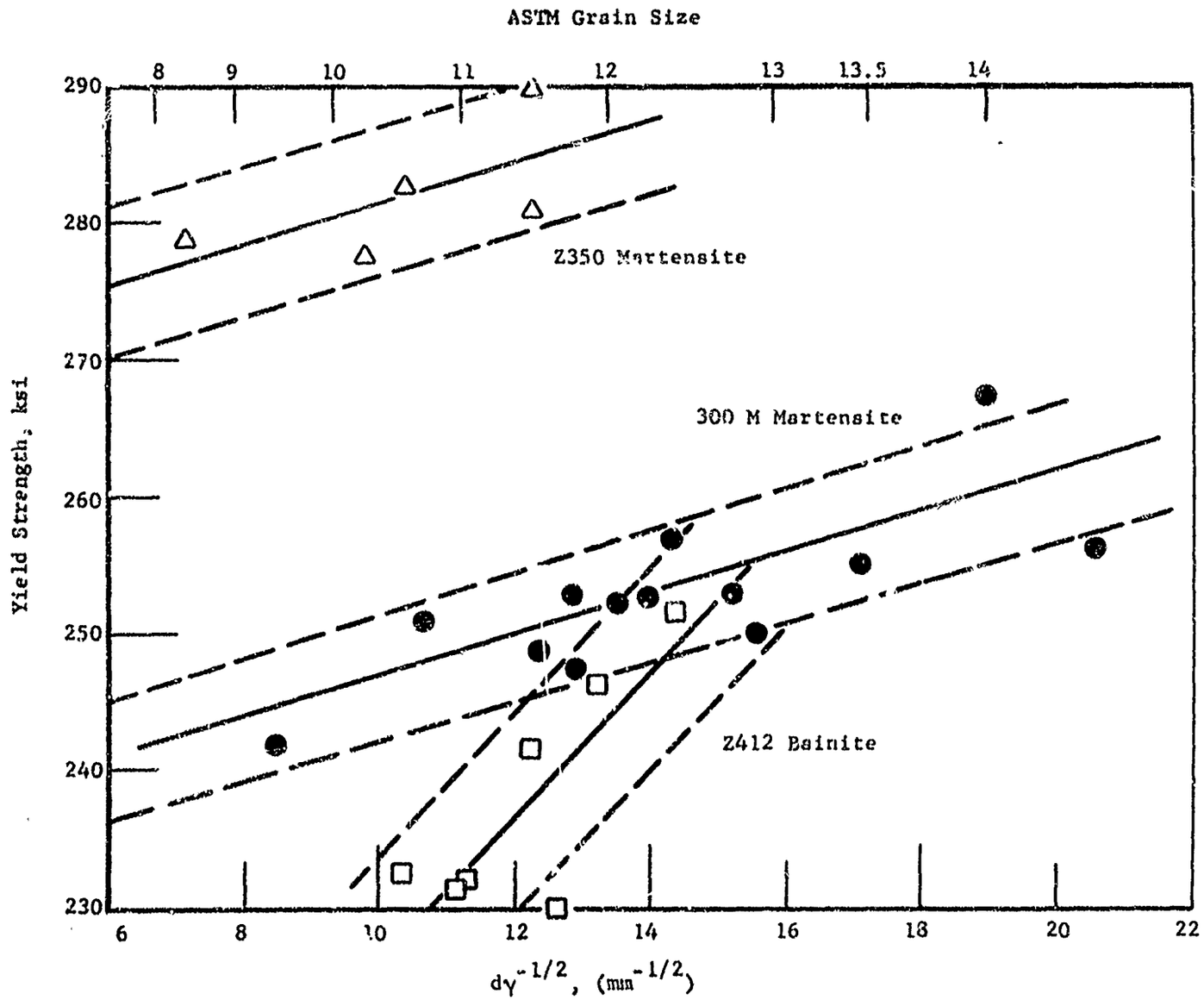

Figure 85. Hall-Petch Plot of Yield Strength Versus (Prior Austenite Grain Size)$^{-1/2}$ for Thermal-Mechanically Processed Bainitic and Martensitic Steels

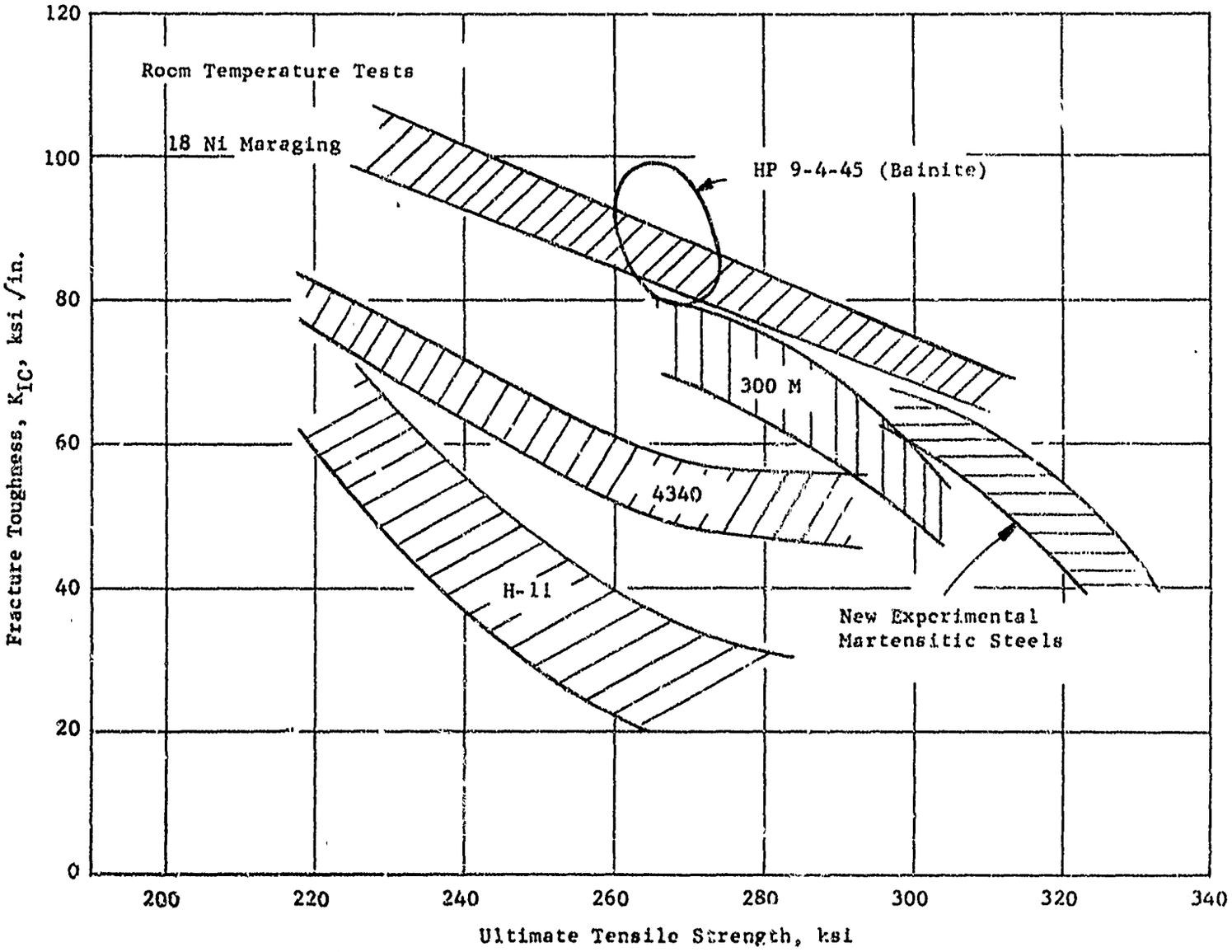

Figure 86. Comparison of Fracture Toughness Properties of the New Low Alloy Martensitic Steels with Commercial High Strength Steels

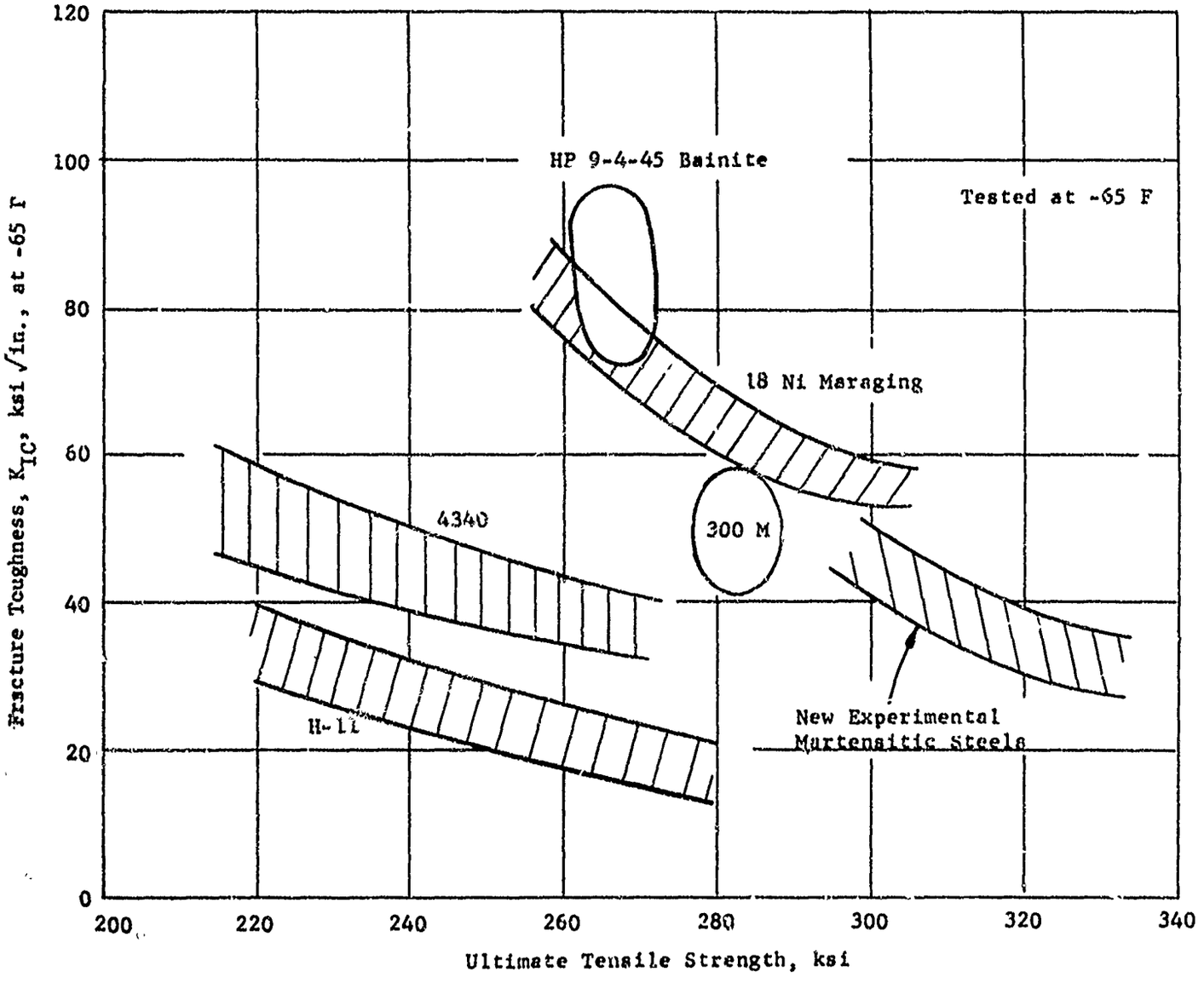

Figure 87. Comparison of Fracture Toughness Properties, at -65 F, of the New Low Alloy Martensitic Steels with Commercial High Strength Steels

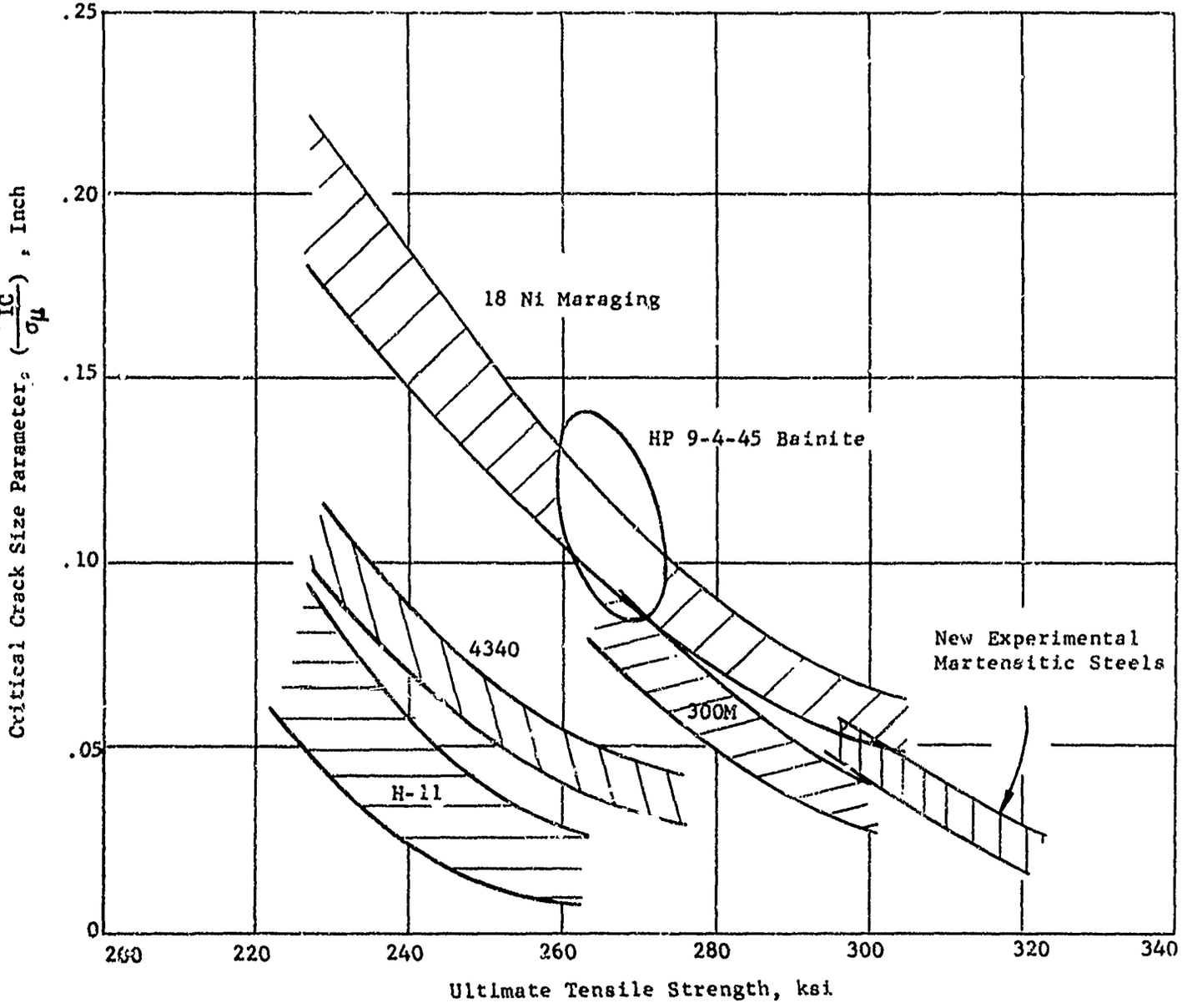

Figure 88. Comparison of Critical Crack Sizes of the New Low Alloy Martensitic Steels with Commercial High Strength Steels

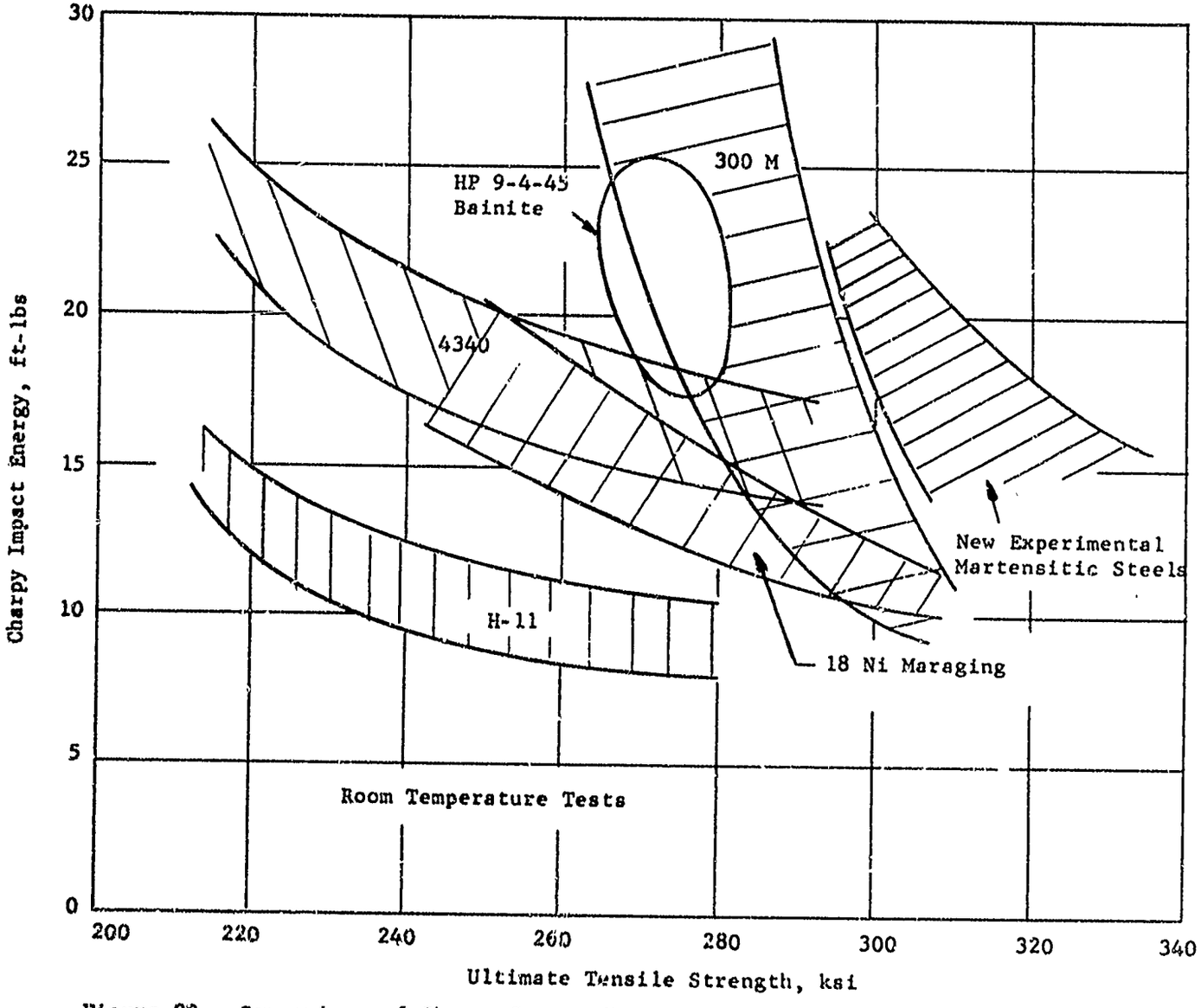

Figure 89. Comparison of Charpy Impact Energy Values of the New Experimental Martensitic Steels with Commercial High Strength Steels

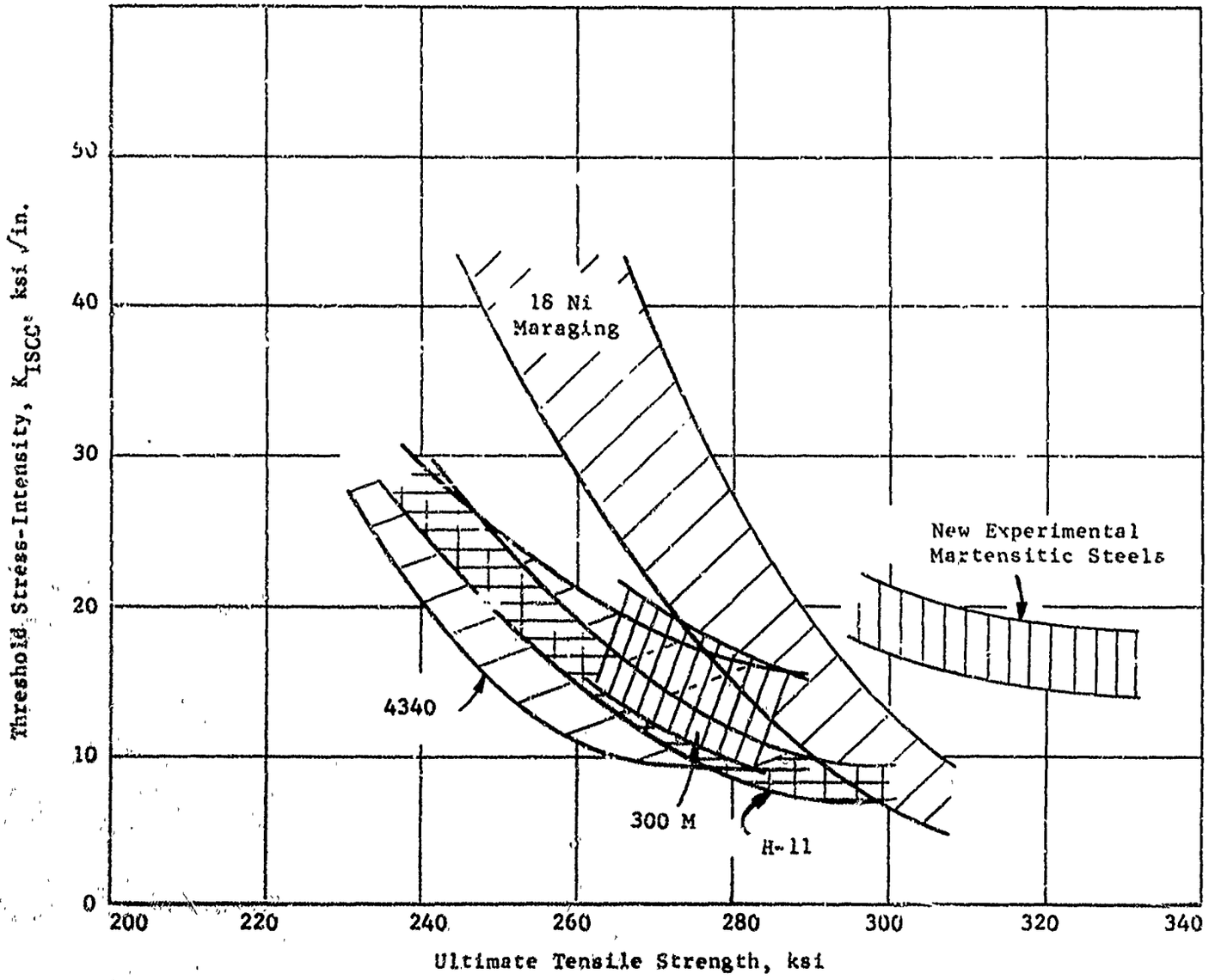

Figure 90. Comparison of SCC Threshold Stress Intensity Values (K_{ISCC}) of Experimental Martensitic Steels with Commercial High Strength Steels

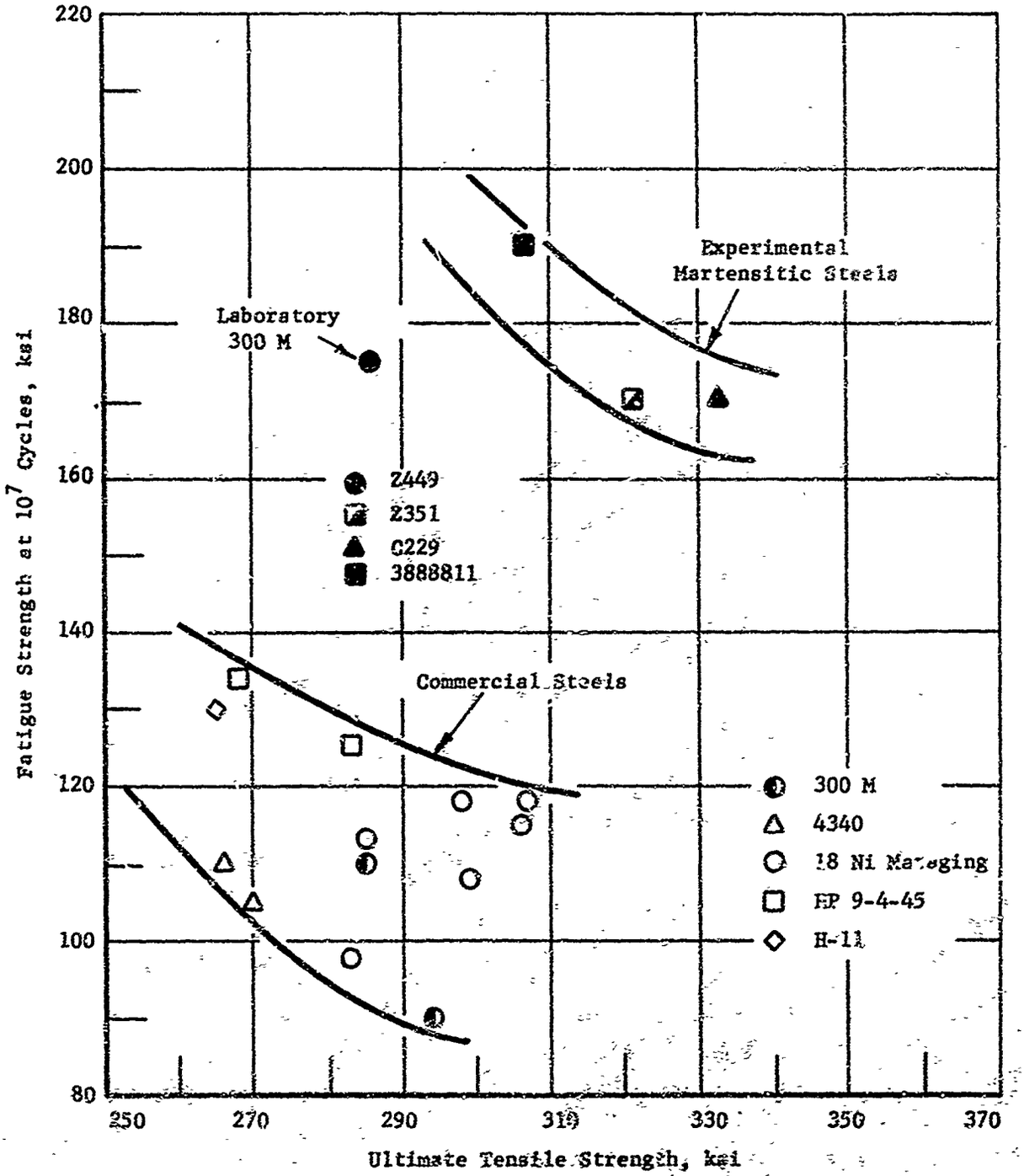

Figure 91. Comparison of the Unnotch 10^7 Cycle Fatigue Strengths of Experimental Martensitic Steels with Commercial High Strength Steels for R Values of +0.06 or +0.10

UNCLASSIFIED
Security Classification

DOCUMENT CONTROL DATA - R & D

(Security classification of title, body of abstract and indexing annotation must be entered when the overall report is classified)

1. ORIGINATING ACTIVITY (Corporate author)
Republic Steel Corporation
Research Center
Independence, Ohio 44131

2a. REPORT SECURITY CLASSIFICATION
Unclassified

2b. GROUP

3. REPORT TITLE
Development of an Improved Ultra-High Strength Steel for Forged Aircraft Components

4. DESCRIPTIVE NOTES (Type of report and inclusive dates)
Final Technical Report 1 May 1969 through 31 December 1970

5. AUTHOR(S) (First name, middle initial, last name)
Ault, R. T.
Ward, G. M.
Bercolo, R. P.

6. REPORT DATE
February 1971

7a. TOTAL NO. OF PAGES
159

7b. NO. OF REFS
46

8a. CONTRACT OR GRANT NO.
F33615-69-C-1638 NEW

b. PROJECT NO.
7351

c. Task No. 735105

d.

9a. ORIGINATOR'S REPORT NUMBER(S)

9b. OTHER REPORT NO(S) (Any other numbers that may be assigned this report)
AFML TR-71-27

10. DISTRIBUTION STATEMENT This document is subject to special export controls and each transmittal to foreign governments or foreign nationals may be made only with prior approval of the Air Force Materials Laboratory, LL, Wright-Patterson Air Force Base, Ohio 45433.

11. SUPPLEMENTARY NOTES

12. SPONSORING MILITARY ACTIVITY
Air Force Materials Laboratory
Air Force Systems Command
Wright-Patterson AFB, Ohio 45433

13. ABSTRACT

The objective of this program was to develop an ultra-high strength steel in the 300 to 320 ksi ultimate tensile strength range, with improved fatigue strength, fracture toughness, and stress corrosion resistance for greater reliability in forged landing gear components. Alloy development studies were conducted on two bainitic alloy systems and two martensitic alloy systems in order to develop the best combination of mechanical properties at tensile strength levels in excess of 300,000 psi. Of the four alloy systems investigated, steels from the low alloy, medium carbon Ni-Cr-Mo-Si-V martensitic system developed the best combination of fracture toughness, fatigue strength and stress corrosion cracking resistance. A martensitic alloy was developed which achieves the following average longitudinal, room temperature properties based on laboratory sized heats: Y.S. = 268 ksi, U.T.S. = 311 ksi, El. = 12%, R.A. = 44%, CVN = 20 ft-lbs, K_{IC} = 60 ksi $\sqrt{in.}$, K_{ISCC} = 17 ksi $\sqrt{in.}$, unnotch fatigue strength at 10^7 cycles of 170 ksi, and a notch (K_t = 3.0) fatigue strength of 80 ksi.

"This abstract is subject to special export controls, and each transmittal to foreign governments or foreign nations may be made only with prior approval of the Air Force Materials Laboratory, LL, Wright-Patterson Air Force Base, Ohio 45433."

DD FORM 1 NOV 68 1473

UNCLASSIFIED
Security Classification

14. KEY WORDS	LINK A		LINK B		LINK C	
	ROLE	WT	ROLE	WT	ROLE	WT
High Strength Steels						
Martensitic						
Bainitic						
Fracture Toughness						
Stress Corrosion						
Fatigue						